Spring 1990

Synthesis and complexation studies of cyclohexane-based tripodands

John Damon Peabody
University of New Hampshire, Durham

Order Number 9027436

Synthesis and complexation studies of cyclohexane-based tripodands

Peabody, John Damon, III, Ph.D.

University of New Hampshire, 1990

U·M·I

300 N. Zeeb Rd.
Ann Arbor, MI 48106

SYNTHESIS AND COMPLEXATION STUDIES OF CYCLOHEXANE-BASED TRIPODANDS

BY

John D. Peabody III

BS, Trinity College (Hartford) 1983

DISSERTATION

Submitted to the University of New Hampshire
in Partial Fulfillment of
the Requirements for the Degree of

Doctor of Philosophy

in

Chemistry

May, 1990

This dissertation has been examined and approved.

Gary R. Weisman

Dissertation director, Gary R. Weisman, Associate Professor of Chemistry

Kenneth K. Andersen

Kenneth K. Andersen, Professor of Chemistry

Paul R. Jones

Paul R. Jones, Professor of Chemistry

Edward H. Wong

Edward H. Wong, Professor of Chemistry

T. Taylor Eighmy

T. Taylor Eighmy, Research Assistant Professor of Civil Engineering

May 3, 1990

Date

DEDICATION

This dissertation is dedicated to the memory of Virginia Boyd Peabody and to my father and two brothers.

ACKNOWLEDGEMENTS

I would like to thank Gary Weisman for providing excellent guidance and assistance in this endeavor. I am indebted to my friends and the U.N.H. chemistry department staff for their encouragement and patience. I would like to thank the National Science Foundation and the University of New Hampshire for the financial support provided for my research. I thank all my family members for the sacrifices they have made in order to help me through this period in my life.

TABLE OF CONTENTS

DEDICATION..... iii

ACKNOWLEDGMENTS..... iv

TABLE OF CONTENTS..... v

LIST OF FIGURES..... vii

LIST OF TABLES..... x

ABSTRACT..... xii

I. INTRODUCTION..... 1

II. HISTORICAL..... 8

III. RESULTS AND DISCUSSION..... 15

Syntheses

(1,3,5-tripodands) General..... 15

Tosylates..... 16

Alkylation Reactions..... 17

Solvomercuration-Demercuration..... 19

Oxidation with CrO_3-$(py)_2$ Complex..... 20

(1,2,3)-tripodands General..... 22

Akylation with Tosylates..... 23

Hydrogenation with Rh/Al_2O_3..... 25

Complexation Studies

^1H NMR Complexation Studies..... 27

^{13}C NMR Complexation Studies..... 39

Experiments with Other Salts..... 57

Miscellaneous NMR Complexation Studies..... 62

III. RESULTS AND DISCUSSION (contd.)

Determination of Complexation Constants from 13-C NMR Titration Studies..... 66

Determination of Relative Complexation Constants from Competition Studies..... 78

^{13}C T_1 Relaxation Studies..... 105

IV. EXPERIMENTAL..... 122

General Experimental..... 122

Syntheses..... 127

Physical Organic Procedures..... 141

V. APPENDICES..... 151

A. Data Tables, Titration Plots, and Curve Fits for 13-C Titration Experiments..... 152

B. Derivation of Equations for Competition Studies..... 160

C. Data Tables for Competition Experiments..... 165

D. Data Tables, Plots, and Curve Fits for T_1 Experiments..... 167

E. Tabulated Results for NOE Measurements..... 179

F. Discussion of Tentative Chemical Shift Assignments..... 180

G. Spectra for Compounds..... 181

H. ^1H NMR Complexation Experiment Spectra.. 196

I. ^{13}C NMR Competition Experiment Spectra.. 208

LIST OF REFFERENCES..... 220

List of Figures

Number		Page #
1	"Nitrogen-pivot Lariat Ether".....	3
2	Coronand Capable of Chiral Recognition...	3
3	[2.2.1] Cryptate.....	4
4	"Spherand".....	5
5	cis-Inositol Binding Sites.....	8
6	1 (dicyclohexyl cryptand).....	9
7	Hydrogenation of a cyclophane.....	9
8	Partial aaa and aea structures.....	9
9	Complexation of the first "Venus Flytrap" (3 + Na^+).....	10
10	Complexation of 1,2,3-Venus Flytrap 4...	11
11	1,3-dipodand 5.....	12
12	Complexation of 1,3-dipodands.....	13
13	Complexation of 1,4-dipodands.....	13
14	Complexation of "Flipped out ionophores".	14
15	Synthesis of cis,cis-1,3,5-Tripodands....	15
16	Synthesis of Tosylates.....	16
17	Synthesis of Glycol Ether Tripodands.....	17
18	Synthesis of Cis,cis-1,3,5-Tris-(1,5-dioxaheptyl)cyclohexane (12).....	18
19	Synthesis of Cis,cis-1,3,5-Tris-(1-oxa-3-propenyl)cyclohexane (13).....	19
20	Solvomercuration-Demercuration.....	20
21	Synthesis of Cis,cis-1,3,5-Tris-(3-keto-1-oxabutyl)cyclohexane (17).....	21
22	Synthetic Scheme for 1,2,3-tripodands....	22

List of Figures (contd)

Number		Page #
23	Cis,cis,cis-Methyl-3,4,5-Tris-(1,4-dioxapentyl)cyclohexane carboxylate (**19**)...	23
24	Synthesis of Methyl-3,4,5-Tris-(1,4-dioxapentyl)benzoate (**20**).....	24
25	Attempted Hydrogenation of **20**.....	25
26	Complexation induced ring inversion.....	27
27	^{1}H NMR Spectra (0-5 ppm region) Complexation of **11** with Na^+.....	31
28	Complex Conformation of (1,3,5-Subst.) Cyclohexane Ring.....	32
29	^{1}H NMR Spectra (0-5 ppm region) Complexation of **17** with Na^+.....	34
30	Plot of Sodium tetraphenylborate Solubilized vs Equilibration Time (**12**)...	36
31	^{1}H NMR Spectrum of partially complexed **12** after 216 hrs of equilibration with excess $NaBPh_4$ in $CDCl_3$.....	38
32	Equatorial/axial methoxycyclohexane conformers.....	40
33	EQ/AX Methyldecanols.....	41
34	C^{β}-C^{γ} Bond Elongation.....	42
35	1,3-diaxial interaction.....	43
36	1,3-diaxial (g^+g^-).....	44
37	γ-anti substitution (g^+a).....	44
38	Hyperconjugative Mechanism.....	45
39	EQ/AX Methyldecanols.....	45
40	Numbering Scheme for Ligands **3** and **4**.....	47
41	Numbering Scheme for **11, 15, 17, and 12**..	48
42	Numbering Scheme for **21**.....	55
43	Pentacyclo-tetracosatetraene.....	60

List of Figures (contd)

Number		Page #
44	Tripod type open-chain cryptand.....	60
45	18-Crown-6 (22), [2.2.2.]Cryptand (23) Dibenzo-18-Crown-6 (24).....	65
46	Types of hexa-coordinate binding (11A and 11B).....	73
47	Numbering Scheme, 3, 25, 26, 21, 12, 4, 6	83
48	Favored Conformation of DME.....	97
49	Favored Conformation of DMP.....	97
50	Triaxial conformation of 12.....	99
51	Relaxation Time-parameter relationships..	108
52	Diphenylacetylene.....	111
53	Hemimellitene.....	112
54	Carbon Numbering Scheme.....	114
55	Triaxial Confromation of Na^+-3.....	118

List of Tables

Number		Page #
1	Yields of Tosylates Synthesized.....	16
2	Reaction Yields for Alkylations.....	18
3	Methods for Alkylation of Triphenols.....	24
4	Precedents for Hydrogenation of **20**.....	26
5	^{1}H NMR Complexation Results for **11, 15, 21, 17, and 12**.....	30
6	Limiting ^{13}C NMR chemical shifts for **3**; **3**-Na^{+} and **4**; **4**-Na^{+} in $CDCl_3$.....	47
7	^{13}C Limiting Chemical Shifts for **11** and **11**-Na^{+} in $CDCl_3$.....	49
8	^{13}C Limiting Chemical Shifts for **15** and **15**-Na^{+} in $CDCl_3$.....	50
9	^{13}C Limiting Chemical Shifts for **17** and **17**-Na^{+} in $CDCl_3$.....	51
10	^{13}C Limiting Chemical Shifts for **12** and **12**-Na^{+} in $CDCl_3$.....	53
11	^{13}C Limiting Chemical Shifts for **21** and **21**-Na^{+} in $CDCl_3$.....	56
12	Complexation Results for Various Ligands and Salts.....	57
13	^{13}C NMR Chemical Shift Results from Complexation of **3** with NaI in $CDCl_3$.....	59
14	^{1}H & ^{13}C NMR Results from Complexation of 18-Crown-6 (**22**) with $NaBPh_4$ in DMK-d_6.	63
15	^{13}C NMR Chemical Shifts for the Competition between **3** & **22** with $NaBPh_4$ in DMK-d_6.....	64
16	Stability constants for Na^{+}-complexes of **11** and **3** in DMK-d_6.....	69

Number		Page #
17	Results from Attempted Titration Experiments with $KBPh_4$ in DMK-d_6.....	69
18	Gutmann Donor Numbers (DN) and Acceptor Numbers (AN) for Selected Solvents.....	75
19	Competition Results.....	82
20	Other Competition Results.....	83
21	Competition Results for **25** & 3.....	84
22	Competition Results for **26** & 3.....	86
23	Competition Results for **21** & **4**.....	88
24	Competition Results for **25** & 4.....	90
25	Competition Results for **25** & **4**.....	91
26	Competition Results for **12** & **4**.....	92
27	Competition Results for **12** & **3**.....	95
28	Competition Results for **12** & **6** (3:1:1)..	100
29	Competition Results for **12** & **6** (6:1:1)..	102
30	NOE Result for **3**.....	115
31	NOE Result for Na^+-3.....	115
32	Titration Data Table [11]=02688M.....	152
33	TitrationDataTable[11]=0.2813M.....	153
34	TitrationDataTable[3]=0.2690M.....	153
35	TitrationDataTable[3]=0.2898M.....	154
36	TitrationDataTable[3]=0.4804M.....	154
37	Competition Peak Area Data.....	165
38	Competition Shift Data.....	166
39	Relaxation Time Data (3).....	168
40	Relaxation Time Data (Na^+-3).....	168
41	^{13}C-NOE Results (3).....	179
42	^{13}C-NOE Results (Na^+-3).....	179

ABSTRACT

SYNTHESIS AND COMPLEXATION STUDIES

OF CYCLOHEXANE-BASED TRIPODANDS

by

John D. Peabody III

University of New Hampshire, May, 1990

The present work has been concerned with the design and synthesis of cyclohexane-based polypodands and physico-chemical studies of the corresponding podates formed by complexation of alkali metal ions. Of particular interest has been the drastic conformational biasing of the back-bone ligand structure which is associated with the complexation process.

A number of new tripodand ligands (**11**, **12**, **13**, **15**, & **17**) have been synthesized. The methodology central to these syntheses has been the alkylation of the cyclohexanetriol with the "podal" tosylates (or alkyl halide). Some of the final synthetic targets were arrived at by subsequent functional group conversions.

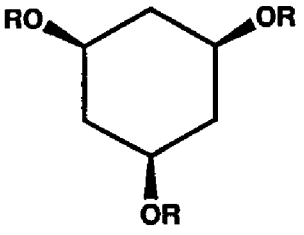

3 R = $CH_2CH_2OCH_3$
11 R = $CH_2CH_2OCH_2CH_20CH_3$
12 R = $CH_2CH_2CH_2OCH_3$
13 R = $CH_2CH{=}CH_2$
15 R = $CH_2CH(CH_3)0CH_3$
17 R = $CH_2(CO)CH_3$

^{1}H and ^{13}C NMR studies were conducted to determine the ability of these ligands to complex $NaBPh_4$ (as well as some other metal salts) in $CDCl_3$. The relative complex stability constants for some of these ligands (with $NaBPh_4$ in $CDCl_3$) were determined by ^{13}C NMR competition studies and compared. Complexation constants for **11** and **3** with $NaPBh_4$ in acetone-d_6 were obtained by ^{13}C NMR Titrations. ^{13}C-T_1 relaxation times were used to study the motional dynamics of uncomplexed and Na^+-complexed **3** in $CDCl_3$.

In general, the complexation of cyclohexane-base tripodands involves a relatively well defined reorientation of ligand to a complex conformation having a cavity with convergent binding sites. Complexation of sodium by **3** in $CDCl_3$ involves an induced cyclohexane ring inversion that organizes the oxygen donor sites in the podal groups. Hexacoordination with the sodium cation removes conformational flexibility. The overall molecular reorientational mobility of the ligand increases upon complex formation and has been rationalized in terms of a compact spherical complex geometry that rotates freely in solution.

I. INTRODUCTION

The field of "host-guest chemistry", also referred to as "supramolecular chemistry", has blossomed in the last 20 years and has seen major contributions from work conducted by Cram [1] and Lehn [2]. The results, reported by Pedersen in 1967, for complexation of alkali metal ions by crown ethers is commonly cited as the first introduction to this area of chemistry [3]. Comprehensive discussions of the concepts, terminology, definitions and the many recent developments are contained in a number of reviews of the journal literature [4-6]. The present discussion will start with a review of basic concepts and end by considering some of the prior results obtained in our laboratories.

Host-guest chemistry:

Host-guest systems or "complexes" as defined by Cram "are composed of two or more molecules or ions held together in unique structural relationships by electrostatic forces other than those of full covalent bonds" [1]. The electrostatic forces include hydrogen bonding, ion pairing, pi-acid-pi-base interactions, metal ion to ligand attractions and Van der Waals attractive forces [7]. The "host" component of a complex by definition contains binding sites that converge on and envelop the corresponding "guest" component, which can be a molecule or ion. Complexes, hosts, and guests are also referred to as

"supermolecules", "molecular receptors" and "substrates", respectively, by researchers influenced by terminology developed by Lehn [8] for describing supramolecular chemistry or "chemistry beyond the molecule". This latter set of terms resembles the nomenclature associated with biological chemistry (eg. receptor sites, enzymes, substrates, inhibitors, and cofactors). In our laboratories we have primarily adopted the former system although host molecules are often referred to as polydentate ligands.

Crown Ethers:

The novelty of crown ethers is that they combine the complexing ability of macrocyclic antibiotics (eg. valinomycin) with the chemical stability of the ether functions. Specifically, they were the first neutral organics to bind alkali ions strongly [9]. This has made them useful as catalysts for organic synthesis (eg. saponification of esters by KOH)[10].

Investigations involving coronands (modified crown ethers) have themselves led to new areas of study in the realm of host-guest chemistry. "Lariat ethers", a class of hosts (Fig. 1) designed by Gokel *et. al.* [11] for complexation of cations have exhibited dynamic properties [12] of monocyclic crown ethers and some of the enhanced binding character of the less dynamic cryptands [13]. Work with these compounds has also shed light on aspects of "complexation induced conformational biasing" of the ligand, which has been of primary interest in our

laboratories [14].

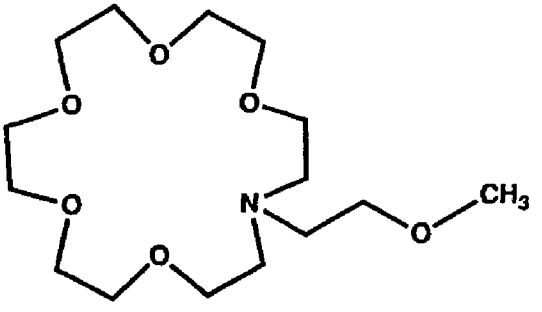

Nitrogen-pivot Lariat Ether

Figure 1:

Coronands have also been designed for the purpose of chiral recognition in complexation and ultimately used for the resolution of racemic amino acid (or ester) salt mixtures [15].

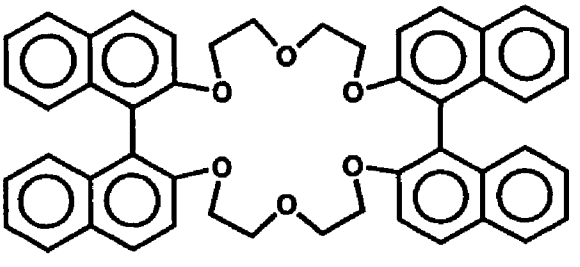

Figure 2: Coronand Capable of Chiral Recognition

Cryptands:

In 1969, reports were published on the design, synthesis and binding properties of a new class of hosts, known as "cryptands" (Fig. 3) [16]. In general, macrobicyclic cryptands have much stronger cation binding properties than simple crown ethers (or lariat ethers). This has been rationalized in terms of the "cryptate effect" which relates cation selectivity and complex stability to a structurally determined three-dimensional spheroidal cavity with convergent binding sites in the complexed host [2]. Cryptands have utility for anion activation and cation transport [16].

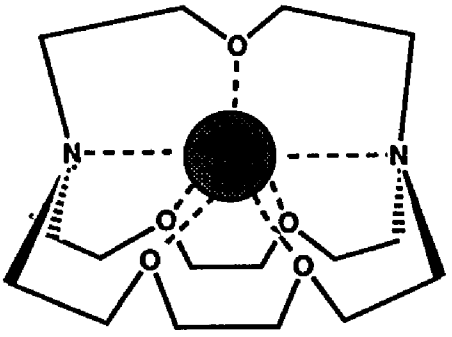

[2.2.1] Cryptate

Figure 3:

Spherands:

The family of ligands known as "spherands" (Fig. 4) provides a completely enforced spherical cavity with convergent binding sites which are shielded from solvation [17]. The complexation of a cation by a spherand results in the formation of the "spheraplex" and does not involve

conformationally biasing or desolvation of the uncomplexed ligand. Spherands have exhibited the stongest and most selective cation binding properties of synthetic hosts developed in the last twenty years [18]. This has been attributed to the "principle of preorganization" [19] which states that "the more highly hosts and guests are organized for binding and low solvation prior to their complexation, the more stable will be their complexes."

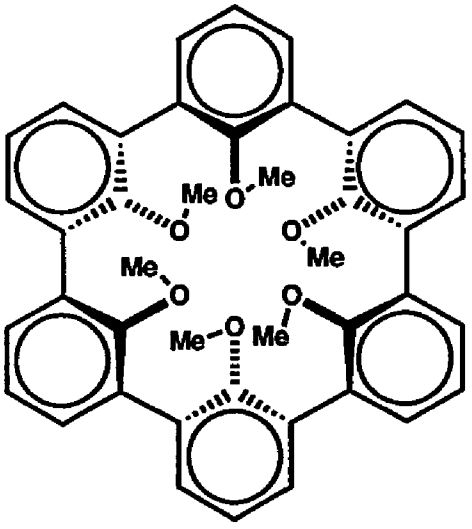

Figure 4: **Spherand**

Podands:

The conformationally flexible open-chain counterparts to crown ethers are known as "podands" [20]. These ligands typically exhibit weaker and less selective cation binding properties than their macrocyclic analogs. This has been rationalized in terms of a "macrocyclic effect" which is akin to the "cryptate effect" (or macrobicyclic effect) and is partly entropic in origin [21]. When considering

commercial applications podands are simpler and more economical to synthesize than macrocyclic ligands.

For the series, podands, coronands, cryptands and spherands, there is a general trend of increasing cation-complex stability and selectivity which is readily explained by the "principle of preorganization" [1]. A parallel and opposite trend is one of decreasing conformational flexibility and dynamic properties of these synthetic hosts. Built-in flexibility is of great importance to biological receptor-substrate interactions and the processes of exchange, regulation, cooperativity and allostery [2]. Understanding these dynamic properties and incorporating them into synthetic host-guest systems still remain formidable challenges to host-guest chemists. Towards this end, computer-assisted molecular design methods have been developed which allow researchers to consider dynamic and static features of host-guest systems [22].

Many other host systems such as cryptaspherands, hemispherands, cavitands, carcerands, cyclophanes, speleands, cyclointercalands and cryptophanes have been developed and are capable of binding many other types of guests in addition to metal ions (e.g. anions, salts, charged and uncharged organic substrates) [1,2].

In our laboratories, we have been concerned with the design and synthesis of cyclohexane-based polypodands and physico-chemical studies of the corresponding podates formed by complexation of alkali metal ions. Of particular interest is the drastic conformational biasing of the backbone ligand structure which is associated with the complexation process.

II. HISTORICAL

Angyal reported in 1974 that cis-inositol was capable of forming weak 1:1 and 2:1 metal:inositol complexes with metal ions [23]. The all-cis configuration of the six hydroxyls provides two types of binding site arrangements each having three hydroxyl groups. There are three equivalent arrangements of axial-equatorial-axial (aea) hydroxyls and one triaxial (aaa) arrangement (See Figure 5).

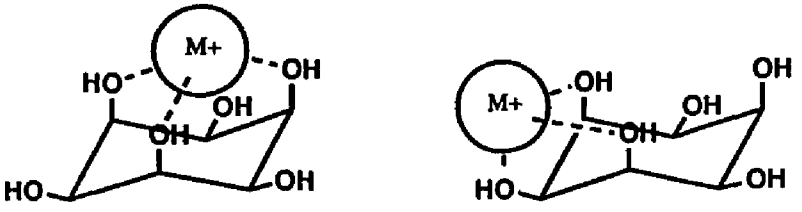

Figure 5: cis-Inositol Binding Sites.

One of the first attempts to utilize a 1,3,5-triaxial substituent arrangement in a polyether host-guest system was only partially successful [24]. The proposed synthesis of the cryptand 1 was never completed since preliminary investigations showed that the model cyclophane could only be partially hydrogenated to the hemicyclophane type structure (See figure 6).

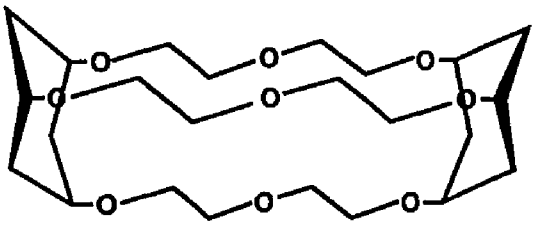

1

Figure 6:

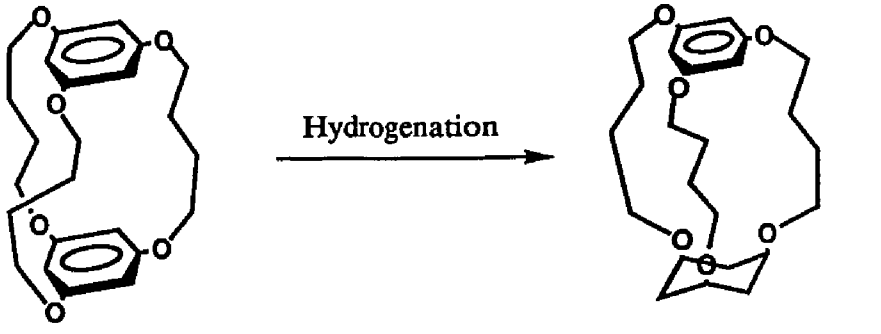

Cyclophane **Hemicyclophane**

Figure 7: Hydrogenation of a Cyclophane

Weisman had independently recognized that the partial structures **2A** and **2B** could be used in the design of dynamic host-guest systems [25].

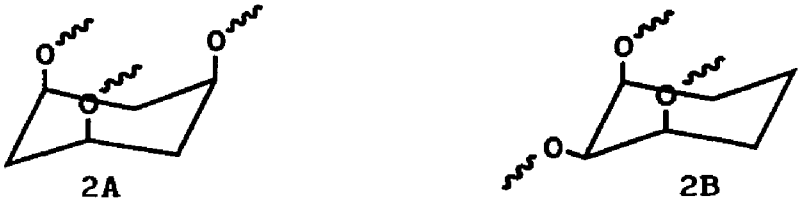

2A 2B

Figure 8: Partial aaa and aea Structures

The first prototype synthesized and studied by the Weisman group was the 1,3,5-tripodand **3**. Complexation with Na^+ was found to occur via drastic biasing of the cyclohexane ring

from a mixture of triequatorial conformations to a triaxial conformation [26] with stabilization of the ag±a gauche conformation of the 1,4-dioxa unit (-O-CH_2-CH_2-O-) [27]. The lowest energy conformation of the tripodate has six converging oxygen binding sites that hexacoordinate with the sodium ion [28].

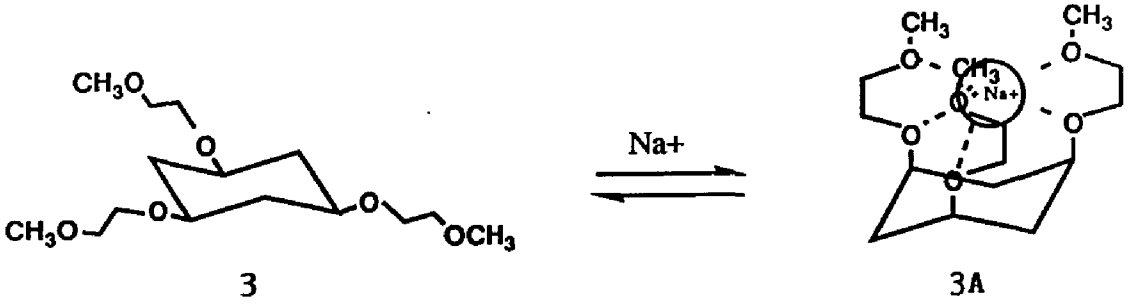

3 3A

Figure 9: Complexation of the First "Venus Flytrap"

Ligand 3 and similar synthetic analogs designed in our laboratories are commonly referred to as "Venus Flytraps". The figurative analogy to the carnivorous Venus Flytrap plant (Dionaea muscipula) illustrates the defined topographical changes believed to occur in these ligands upon complexation. Venus Flytrap plants are found in nature only on the coastal plain of North and South Carolina, and trap their prey when it lands on the inner surface between two opposing leaf halves which then snap shut [29]. The Venus Flytrap can distinguish between live prey and inanimate objects, such as twigs and small pebbles that may fall on the plant. The ability of our molecular

"Venus Flytrap" 3 to complex sodium but reject potassium ions in acetone has been attributed to the limited size of the podate cavity [30].

The first 1,2,3-tripodand 4 was synthesized by T.A. Pascarella and its complexing ability compared with that of 3 [30]. Complexation of 4 is also enabled by a cyclohexane ring inversion which sets up an axial-equatorial-axial substituent arrangement.

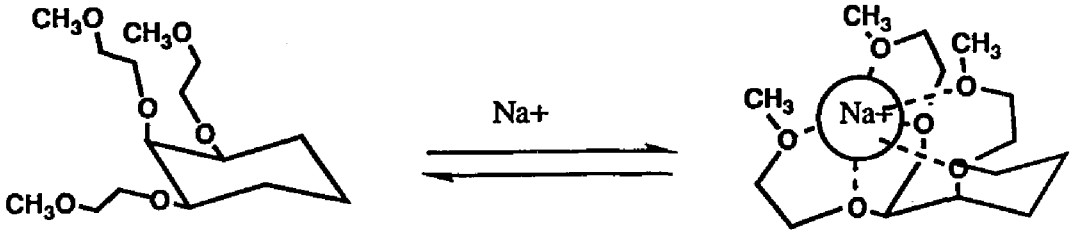

4 4A

Figure 10: Complexation of 1,2,3-Venus Flytrap

Complexation constants for $NaBPh_4$ in the nonpolar solvent $CDCl_3$ appeared to be roughly equal for 3 and 4 with lower limits for absolute values on the order of 10^7 M^{-1}. Neither ligand could be shown to complex $KBPh_4$ in $CDCl_3$ and this has been ascribed to the extreme insolubility of $KBPh_4$ in $CDCl_3$. Podand 4 was found to complex $KBPh_4$ in acetone with a complexation constant on the order of 10^2 M^{-1} [30]. Molecular mechanics calculations indicate that complexation should also stabilize the ag+a (or ag-a) gauche conformation of the 1,4-dioxa unit ($-O-CH_2-CH_2-O-$) [27,28,30].

Studies with the 1,3-dipodand **5** have shown the ligand to form some 2:1 ligand-sodium salt complex in a $CDCl_3$ solution [30]. Complexation constants (for 1:1 ligand-metal ratio) could not be determined for **5**, due to complications from 2:1 complexation in $CDCl_3$ and due to the weak binding properties of the ligand in acetone. It is important to note that **5** only has four oxygen binding sites which precludes the formation of a 1:1 ligand-metal hexacoordinate complex.

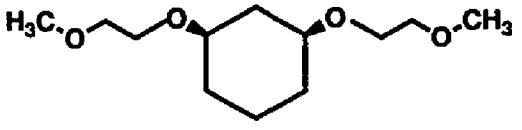

Figure 11: 1,3-Dipodand **5**

Additional studies conducted by S.M. Shirodkar [31] with two new 1,3-dipodands (**6** and **7**) demonstrated that the binding power of the system could be enhanced by increasing the numbers of binding sites (to allow hexacoordination) and by sterically biasing the ring conformation so that the aa-conformations are stabilized relative to ee-conformations. It has been shown that **6** is biased towards the ee conformation until complexation with sodium in an aprotic solvent induces a ring inversion to give the aa conformation [31b].

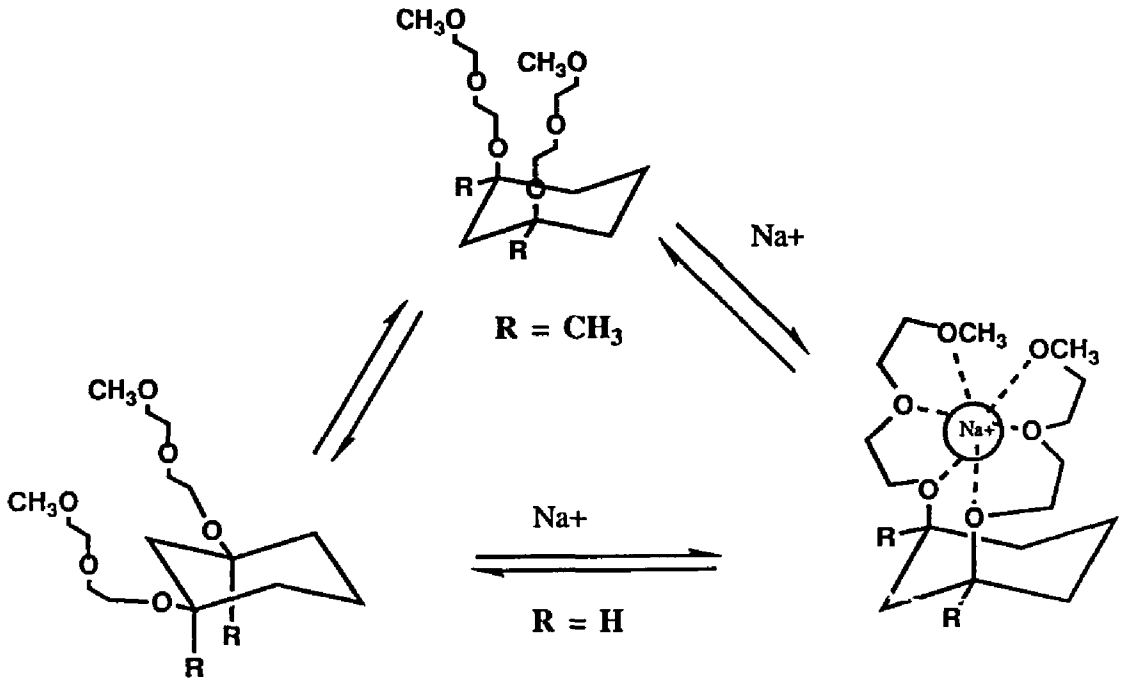

Figure 12: Complexation of 1,3-Dipodands

Attempts to bias the 1,4-dipodand 8intoa twist-boat conformation by complexation with various metal ions were unsuccessful [31a]. This has been rationalized in terms of destabilizing torsional strain from the eclipsing interactions in the complex conformation which cannot be overcome by the free energy of complexation [31a].

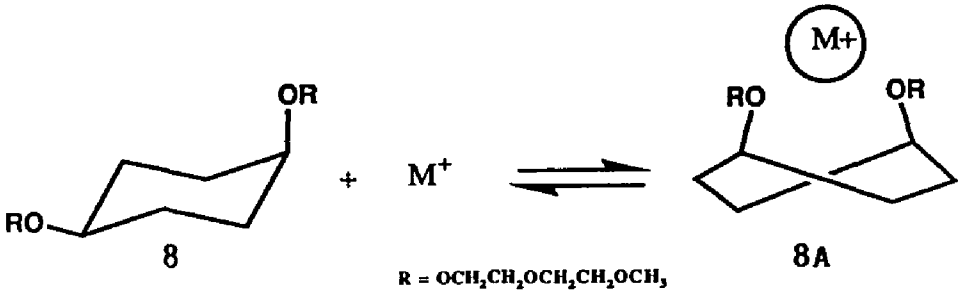

Figure 13: Complexation of 1,4-Dipodand

No cyclohexane-based 1,2-dipodands have been studied in our laboratories. However, recent work has been conducted in this area by Raban et. al.who have referred to these compounds as "flipped out ionophores" [32].

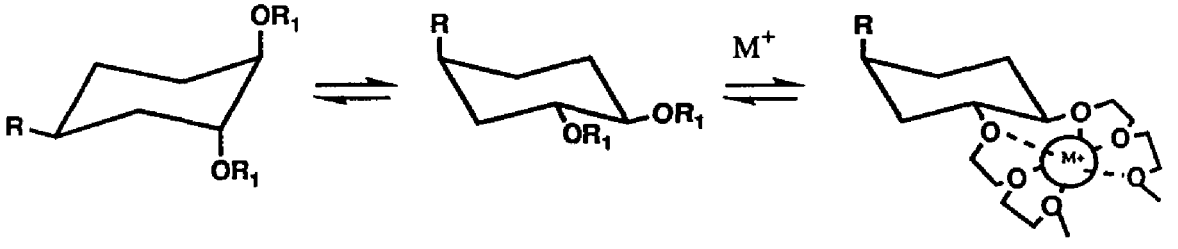

Figure 14: Complexation of "Flipped Out Ionophores"

The present dissertation will consider the synthesis of some new 1,3,5-tripodands and related physicochemical characterization of complexing abilities with metal ions. A major partof this work has dealt with the measurement of relative complexation constants for 1,3,5-, 1,2,3-, and 1,3-polypodand hosts synthesized in our laboratories. The first use of ^{13}C-T_1 (spin-lattice relaxation times) as a probe of molecular mobility in investigation of the complexation process for 1,3,5-tripodand 3 will also be discussed.

III. RESULTS AND DISCUSSION

Synthesis

(1,3,5-tripodands) General Synthetic Scheme:

The general synthetic scheme used in our laboratories for the synthesis cis,cis-1,3,5-tripodands is shown in Figure 15.

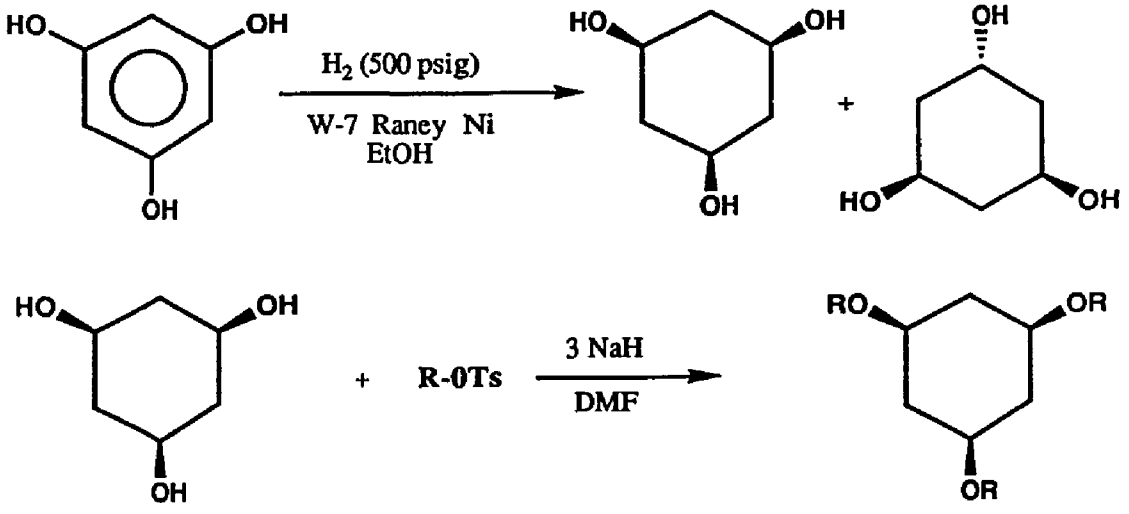

Figure 15: Synthesis of cis,cis-1,3,5-Tripodands

Since our synthetic objective was to attempt the synthesis ofanumber of tripodands using the general schemeabove, a large scale synthesis of the cis,cis-1,3,5-cyclohexanetriol precursor (from hydrogenation of 120 grams of the commercially available phloroglucinol) was conducted according to the procedure described by S. C.-Ho and G.

Caywood [33] based upon the procedure of Stetter and Steinacker [34]. The desired triol was isolated and purified by recrystallization from hot ethanol.

Synthesis of Tosylates:

All tosylates were prepared from the corresponding commercially available alcohols and tosyl chloride according to a standard method [35].

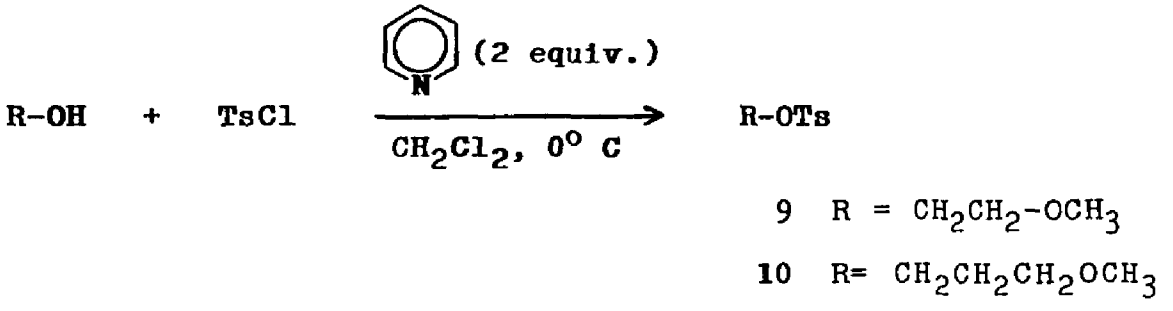

Figure 16: Synthesis of Tosylates

Table 1 contains a list of the tosylates prepared and used in subsequently described alkylation reactions.

Table 1: Yields for Tosylates Synthesized.

Tosylate Synthesized	Alcohol Precursor	% Yield
1,4-dioxapentyl Tosylate(**9**)	$CH_3OCH_2CH_2OH$	84
1,4,7-Trioxaoctyl Tosylate[a]	$CH_3(OCH_2CH_2)_2OH$	86
1,5-Dioxaheptyl Tosylate(**10**)	$CH_3CH_2OCH_2CH_2CH_2OH$	85

a- Synthesized by D. Gronbeck

Alkylation reactions:

The first new synthetic target was the cis,cis-1,3,5-tris-(1,4,7-trioxaoctyl)cyclohexane (**11**) analog. The synthesis and characterization of **11** was found to be straightforward using the scheme shown in Figure 17 below. The mineral oil (contained in the NaH dispersion) was removed in both procedures by extraction after the reactions were complete. extraction. After stripping off solvents, the crude reaction product **11** formed a two-phase system with the mineral oil which allowed for direct separation. A number of extractions with hexane had to be performed and for this reason subsequent preparations usually employed the pre-removal of the mineral oil from the NaH dispersion with n-hexane washings in order to simplify the work-up. Crude product oil was purified by column chromatography followed by bulb-to-bulb vacuum distillation.

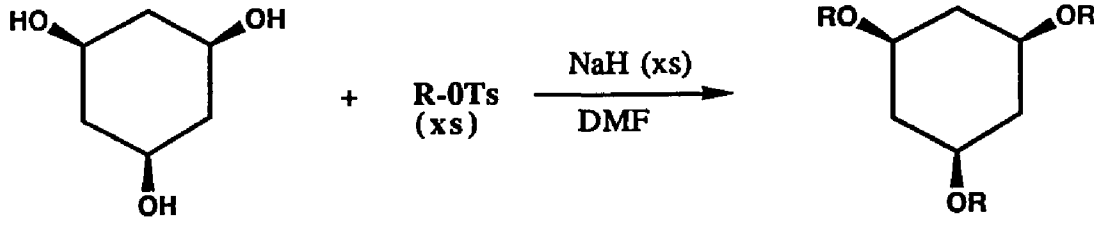

3 R = $-CH_2CH_2OCH_3$

11 R = $-(CH_2CH_2)_2OCH_3$

Figure 17: Synthesis of Glycol Ether Tripodands

The synthesis of cis,cis-tris-(1,5-dioxaheptyl)cyclohexane (**12**) (Figure 18) was in part due to the availability of the precursor alcohol (the 3-methoxypropanol was not

commercially available). The NaH was pre-washed to remove mineral oil and a larger excess of the tosylate was used to promote complete alkylation of the starting triol substrate.

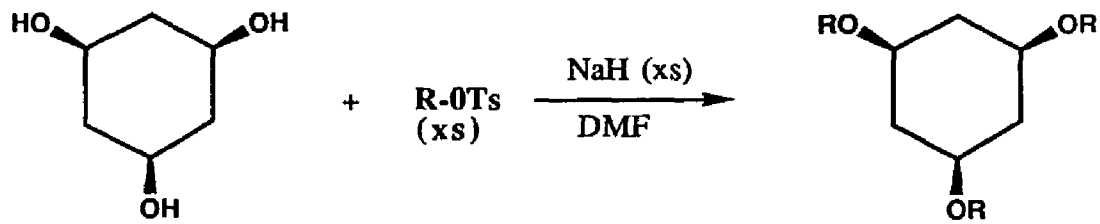

12 R = $-CH_2CH_2CH_2OCH_2CH_3$

Figure 18: Synthesis of Cis,cis-1,3,5-Tris-(1,5-dioxaheptyl)cyclohexane

Table 2 contains the list of some of the reaction yields and the corresponding equivalents of alkylating agent used.

Table 2: Reaction Yields for the Alkylation of cis,cis-1,3,5-cyclohexanetriol with Tosylates.

Product Tripodand	# Equivalents (Alkyl. agent)	Reaction Time (days)	Yield (%)
3	3.7	6	37
11	4.4	3	54
12	6.0	10	77

The synthesis of cis,cis-tris-(1-oxa-3-butenyl)cyclohexane (13) was modeled after the method described by Arndt et. al. for the preparation of cyclohexyl allyl ether [36]. The overall yield of isolated trisubstituted product was 51%. It is believed that this type reaction is catalysed by I^- (Finkelstein conditions.)

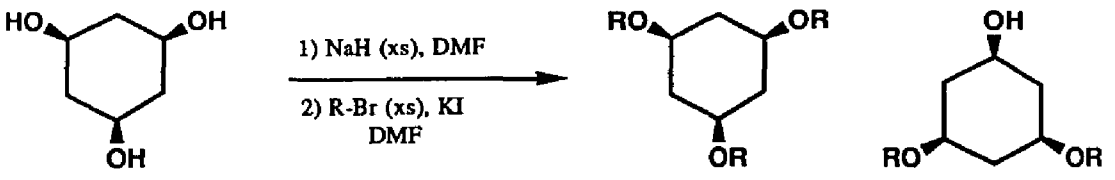

R = $-CH_2CH=CH_2$ **13** **14**

(Minor by-product)

Figure 19: Synthesis of Cis,cis-1,3,5-Tris-(1-oxa-3-butenyl)cyclohexane

Solvomercuration-Demercuration:

The cis,cis-1,3,5-Tris-(3-methyl-1,4-dioxapentyl)cyclohexane (**15**) was prepared using a synthetic method described by Brown et. al. for the synthesis of ethers by overall Markovnikov addition of alcohols to olefinic substrates [37]. After purification by consecutive column and flash-column chromatography the product **15** appeared as a clear colorless oil which gave one spot on TLC and was fully characterized by spectral analysis. The lack of formation of an anti-Markovnikov addition product confirms the very regioselective nature of addition to the carbon-carbon double bonds. Intuitively, it seemed unlikely that this reaction could have proceeded to give a single pair of enantiomers. NMR complexation studies subsequently revealed that compound **15** was in fact a mixture of all the possible stereoisomers (see section starting on p.39).

Cis,cis-1,3,5-Tris-(3-hydroxy-1-oxabutyl)cyclohexane (**16**) was prepared similarly [38] by substituting a 50/50H_2O-THF

mixture for the alcohol solvent previously used. The crude triol **16** (84% yield) was a clear yellow oil whose IR and NMR spectra were consistent with the proposed product constitutional structure. Triol **16** was assumed to be a stereoisomeric mixture and was oxidized with $CrO_3(py)_2$ complex without further purification.

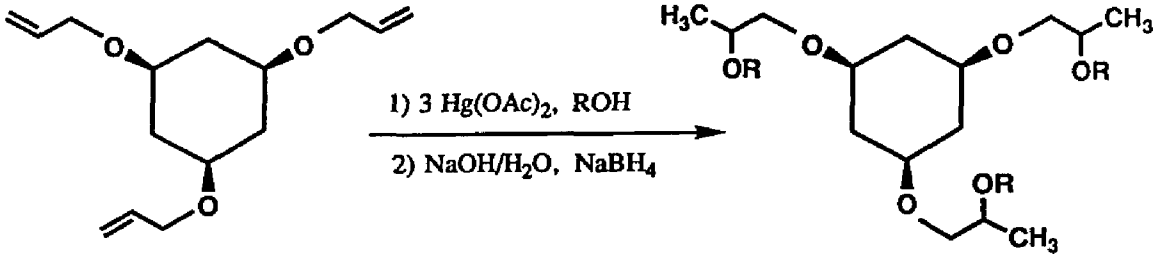

13 **15** R = CH_3

16 R = H

Figure 20: Solvomercuration-Demercuration of **13** to Produce the Corresponding Methyl Ether **15** and the Triol **16**.

Oxidation with CrO_3-Pyridine Complex:

Early applications of the CrO_3-pyridine complex for oxidation of acid-labile compounds employed a pyridine medium [39] which often presented technical difficulties for the isolation of products. The oxidation of our secondary alcohol **16** to the corresponding triketone **17** was accomplished in a methylene chloride solvent system according to the method of Collins *et al*. [40]. The $CrO_3(py)_2$ reagent was prepared by a standard procedure [41]

and used in a 6:1 mole-ratio (complex to alcohol functional groups). The final product yield was 30% which corresponds to approximately a 67% conversion of each hydroxyl position in the starting material. Future considerations for improving the yield are a longer reaction time, a larger excess of complex, and running the reaction at a lower temperature in a suspension of phosphorous pentoxide. In general, technique is a critical factor for obtaining optimum oxidation efficiencies, since the complex is extremely hydrophilic and readily hydrated.

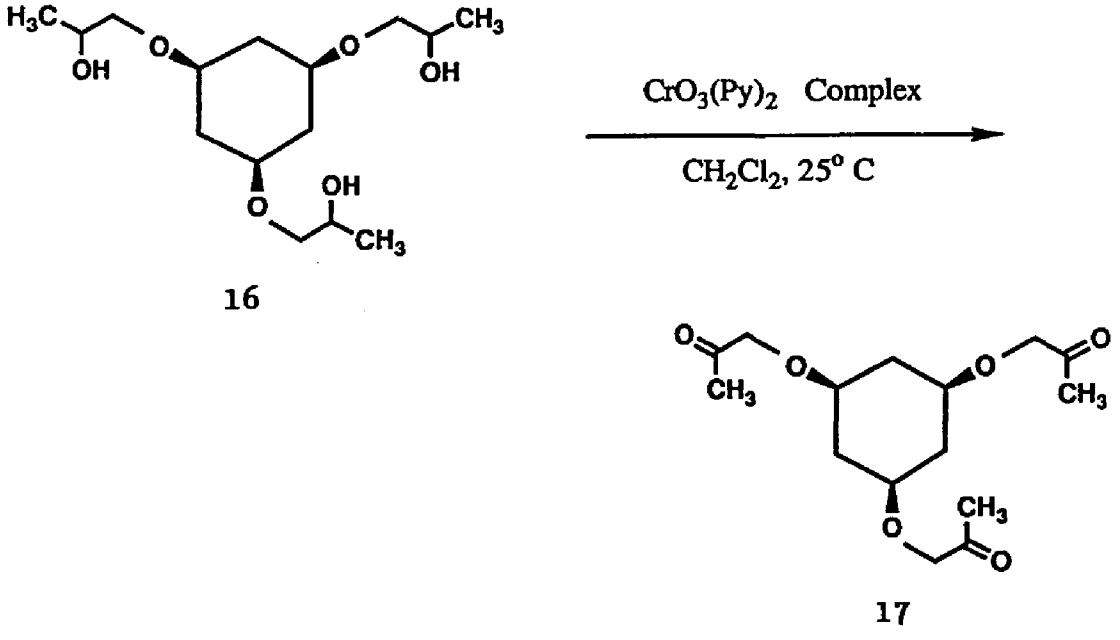

Figure 21: Synthesis of Cis,cis-1,3,5-Tris-(3-keto-1-oxabutyl)cyclohexane (17).

(1,2,3-Tripodands) General Synthetic Scheme:

The general synthetic scheme used in our laboratories for the synthesis of cis,cis-1,2,3-Tripodands is shown in Figure 22 [42].

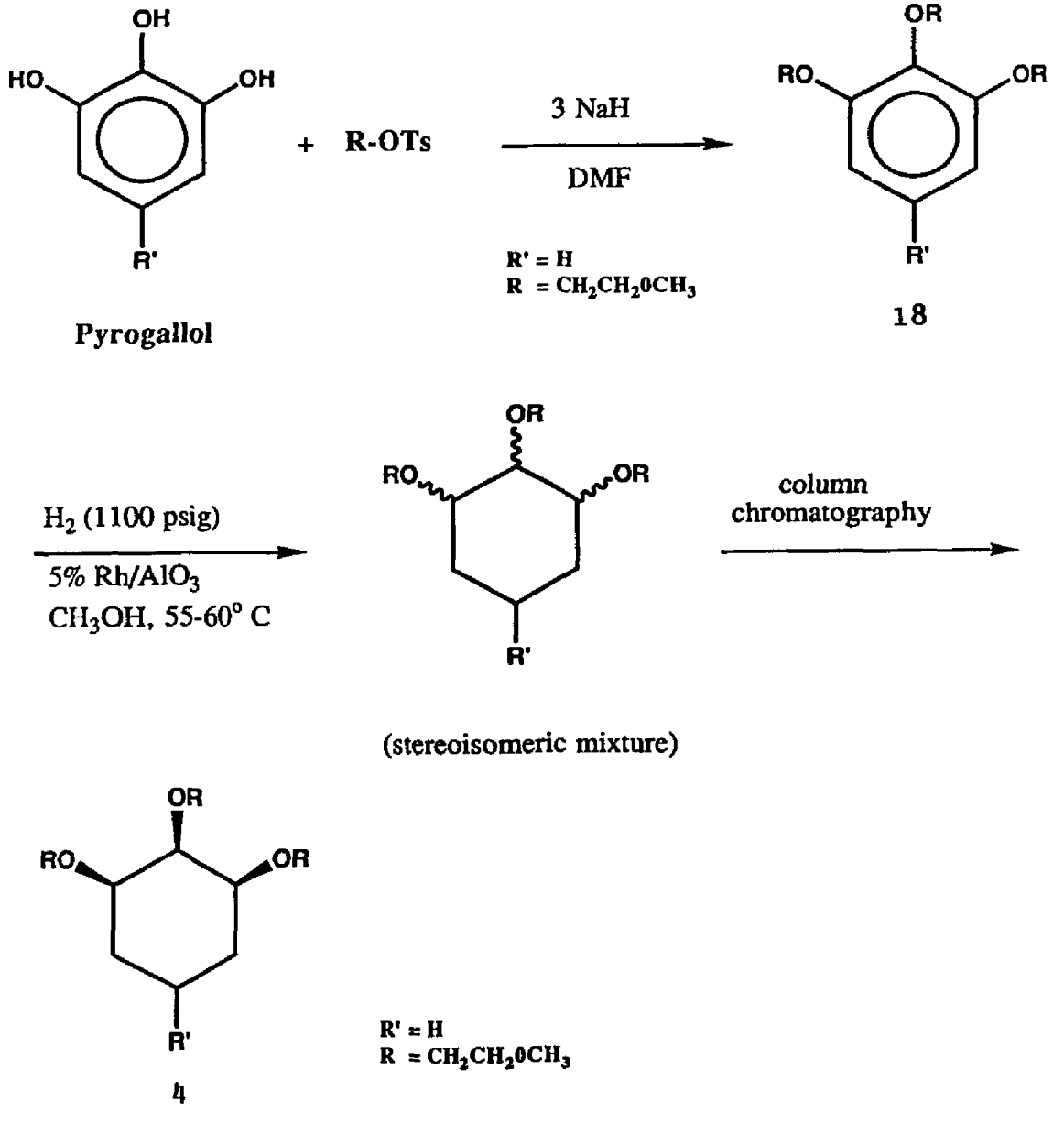

Figure 22: Synthetic Scheme for cis,cis-1,2,3-Tris-(1,4-dioxapentyl)cyclohexane.

Attempts to use a similar synthetic route for the preparation of the tripodand analog cis,cis,cis-Methyl-3,4,5-tris-(1,4-dioxapentyl)cyclohexane-carboxylate (**19**) were marginally successful.

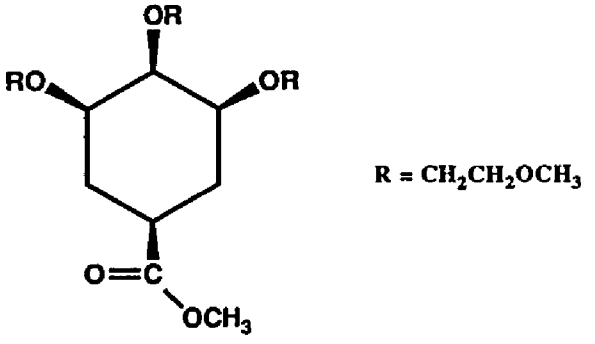

19 R = $CH_2CH_2OCH_3$

Figure 23: Cis,cis,cis-Methyl-3,4,5-Tris-(1,4-diooxapentyl) cyclohexane carboxylate.

Alkylation with Tosylates:

Two methods were described by Pascarella [42] for the alkylation of the triol, pyrogallol. The first procedure used K_2CO_3 in acetone, under reflux, while the second utilized NaH in DMF at 70° C as reaction conditions. The latter was found to be the method of choice due to higher yields of the desired product and the absence of the unsymmetrical dialkylated product (which had to be separated by careful column chromatography).

A hybrid of the above procedures was used to effect a relatively efficient alkylation of the 3,4,5-triol, methyl gallate (Figure 24).

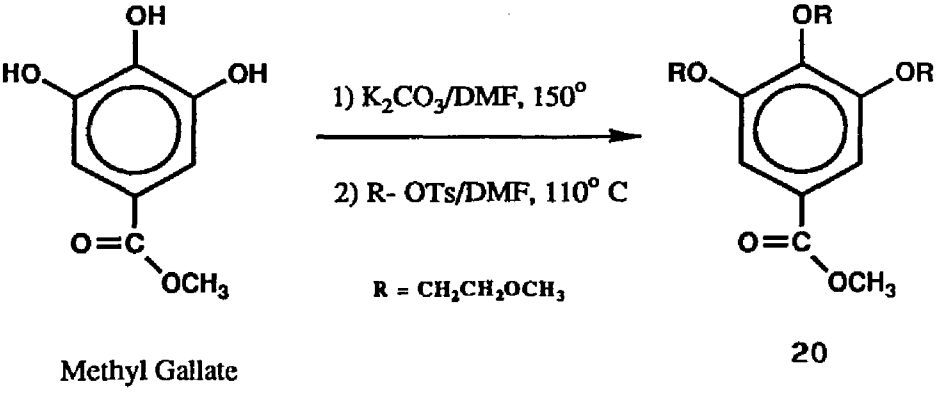

Figure 24: Synthesis of Methyl 3,4,5-Tris-(1,4-dioxapentyl)-benzoate (20).

Table 3 contains a list of reaction conditions used and the corresponding yields of fully alkylated products.

Table 3: Methods for Alkylation of Triols with Tosylates.

Triphenol	Reaction Conditions[a]	Yield (%)
Pyrogallol	K_2CO_3,Acetone,reflux	45[b]
Pyrogallol	NaH,DMF, 70° C	69[b]
Methyl Gallate	K_2CO_3,DMF,110-150° C	85

a- Alkylating reagent = $CH_3OCH_2CH_2$-OTs
b- Synthetic work conducted by T. Pascarella [42]

The isolation of purified 20 was simple and only involved a one-plate distillation of crude extract which yielded pure material that was fully characterized by spectral and elemental analysis.

Hydrogenation with Rh/Al_2O_3:

Repeated attempts to hydrogenate the substituted methyl gallate substrate (**20**) failed. The primary conditions used were 5% Rh/Al_2O_3 catalyst in methanol at 65° C with 1200 psig of H_2 (Figure 25). After work-up of reaction mixtures, spectroscopy indicated that little to no reaction had occurred. Recovered starting material in some cases appeared to be contaminated with a very minor organic impurity. Attempts to isolate this minor impurity by column chromatography were hampered by significant band broadening and tailing of **20**.

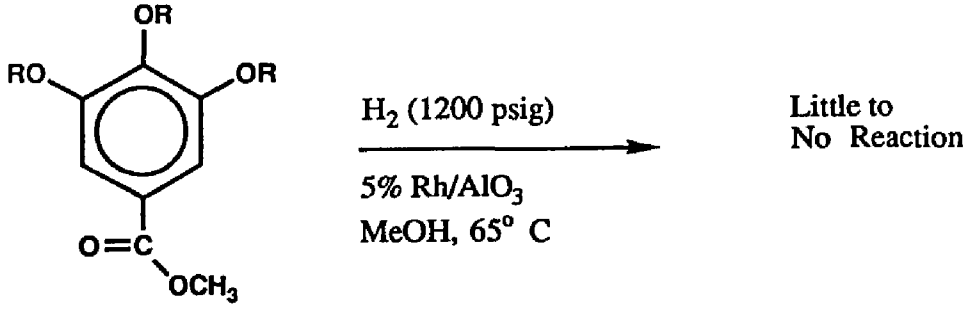

20 R = $CH_2CH_2OCH_3$

Figure 25: Attempted Hydrogenationof Methyl 3,4,5-Tris-(1,4-dioxapentyl)benzoate.

Table 4 contains a list of precedents that indicate that the attempted hydrogenation is possible. Catalyst poisoning (eg. by surfactants) must also be considered as a possible explanation for low yields. For this reason the subsequent attempts of the hydrogenation were conducted with

additional measures to preclude contamination or poisoning of the catalyst by the solvent, substrate, or reaction vessel and glassware. All that may be needed for the future synthesis of **19** is a hydrogenation apparatus capable of higher reaction pressures (> 2000 psig).

Table 4: Precedents for the Hydrogenation of 20 with 5% Rh/Al_2O_3 to the Hexahydro-product.

Substrate	Reaction Conditions	Yield (%)
Gallic Acid[a]	5% Rh/Al_2O_3, 95% EtOH H_2 (2500 psig), 75° C, 4-8 hr.	40-45[b]
Pyrogallol	5% Rh/Al_2O_3, 95% EtOH H_2 (3000 psig), 55-60° C, 20 min.	48[b]
18	5% Rh/Al_2O_3, MeOH H_2 (1100 psig), 55-60° C, 24 hr.	39[c]

a- gallic acid = 3,4,5-trihydroxy benzoic acid
b- data obtained from literature reference [43].
c- synthetic work conducted by T. Pascarella [42].

Standard ^{1}H NMR Complexation Studies

The first physical organic experiment which was typically run on a new host system was aimed at qualitatively establishing basic complexing ability for sodium ion. In these experiments, the host is combined with slightly more than one equivalent of $NaBPh_4$ in the relatively nonpolar solvent $CDCl_3$ [44]. The solubility of $NaBPh_4$ in $CDCl_3$ has been shown to be 1.24×10^{-6} M by atomic absorption analysis [45]. Since the inherent solubility of the salt is effectively negligible, the solubilization of one equivalent of the metal salt indicates the formation of a 1:1 complex. This has been found to be the typical result for good tripodand ligands synthesised in our laboratories.

In addition to physically observing the dissolution of one equivalent of $NaBPh_4$, the experiment is monitored by ^{1}H NMR. Because of the drastic conformational biasing of the ligand upon complexation, a significant change in the chemical shifts and coupling constants of the protons is to be expected. The clearest change is actually observed for the cyclohexane ring protons. This can be explained by the ring inversion necessary to reorganize oxygen donor atoms around the sodium cation to form the complex (see Figure 26).

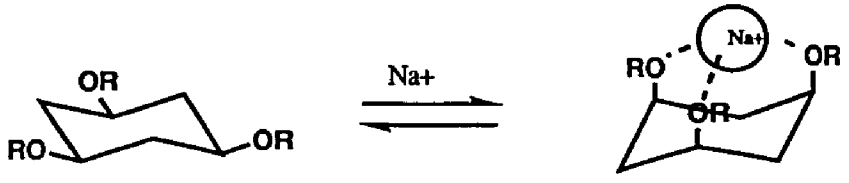

Figure 26: Complexation Induced Ring Inversion

The fraction of total host complexed (FTHC) is determined from relative ^1H NMR integrated intensity measurements. This is possible because the aromatic BPh_4^- anion resonances are downfield and well separated from the aliphatic host resonances. When the solvent is $CDCl_3$ any salt resonances observed correspond only to complexed material since any uncomplexed salt is in very low concentration due to low solubility and is not normally detectable by ^1H NMR. After the integrated signals of host and guest have been normalized by dividing by the appropriate number of protons, the fraction of total host complexed (FTHC) is given simply by the normalized guest integration divided by the normalized host integration (Equation 1).

$$FTHC = \frac{\text{Norm. } I_{(guest)}}{\text{Norm. } I_{(host)}} = \frac{\dfrac{I_{(guest)}}{\#\text{ H's (guest)}}}{\dfrac{I_{(host)}}{\#\text{ H's (host)}}} \qquad (1)$$

where: $FTHC$ = Fraction Total Host Complexed
I = ^1H NMR Integration
#H's = number of Hydrogens in molecular formula

The stability constant or lower limit on the stability constant of the $NaBPh_4$-ligand complex in $CDCl_3$ can be obtained from a variation [46] of the solid/liquid two-phase method of Reinhoudt and De Jong [47]. Complex stability is expressed in terms of the observed (ion-pair) stability

constant, K_{obs}^{ip} (Equation 3) for the complexation equilibrium [48] (Equation 2).

$$L + M^+X^- \rightleftharpoons (ML^+)X^- \qquad (2)$$

$$K_{obs}^{ip} = \frac{[(ML^+)X^-]}{[L][M^+X^-]} \qquad (3)$$

where: L = ligand or host molecule
M^+X^- = ion paired metal salt
$(ML^+)X^-$ = ligand/metal cation complex ion paired with counter-anion

Since excess solid $NaBPh_4$ is present, the value of $[M^+X^-]$ is assumed to be equal to the solubility of the salt in pure $CDCl_3$, which has been established by atomic absorption/emission analysis [49]. The ratio of $[(ML^+)X^-]/[L]$ is calculated (Equation 4) from the FTHC value obtained from the relative integrated intensity measurements of host versus guest proton resonances.

$$\frac{[(ML^+)X^-]}{[L]} = \frac{FTHC}{(1 - FTHC)} \qquad (4)$$

Equation (3) can then be used to calculate the K_{obs}^{ip}. The corresponding value for the free energy of complexation, ΔG^o can be calculated using equation (5).

$$\Delta G^o = -RT \ln K_{obs}^{ip} \qquad (5)$$

For very good ligands in $CDCl_3$, only lower limits for the K_{obs}^{ip} can be calculated. The error associated with ^1H NMR integrations makes it impossible to measure the percentage of complex in the 95-100% range with enough precision to allow determination of high K_{obs}^{ip} values. Results from this "standard" complexation of $NaBPh_4$ in $CDCl_3$ by host molecules **11**, **15**, **21**, **17**, and 12 are shown in Table 5.

Table 5: ^1H NMR Complexation Results in $CDCl_3$.

Ligand	FTHC[a]	$[(ML^+)X^-]/[L]$	K_{obs}^{ip} (M^{-1})	$-\Delta G^o_{300}$ (kcal/mol)
11	0.992±0.014	> ~ 20	> 1.6×10^7	> 9.9
15[b]	0.958±0.016	> ~ 20	> 1.6×10^7	> 9.9
21[c]	1.028±0.013	> ~ 20	> 1.6×10^7	> 9.9
17	ppt[de]	------	----------	-----
12	0.480±0.008[f]	0.941±0.02	$(7.58\pm0.16)\times10^5$	8.07±0.17

a: Errors represent one standard deviation.
b: Compound isolated as a mixture of diastereomers.
c: Synthetic and NMR work conducted by D. Gronbeck (1986)
d: When the host was combined with 1.11 equivalents of salt the complex precipitated from solution.
e: This type of experiment is only valid for systems in which a 1:1 ligand:metal complex is formed and all the equilibrium components remain in solution.
f: Assumes 1:1 complexation.

Tripodands **11**, **15** and **21** all solubilize one equivalent of salt to give 1:1 host/guest complexes in $CDCl_3$. Because they are very good ligands in this non-polar solvent, only lower limits for the K_{obs}^{ip} can be calculated. The results are similar to those obtained for **3** [50]. The relative

Figure 27: ^1H NMR Spectra (0-5 ppm region) for complexed, partially complexed and uncomplexed material for **11** with $NaBPh_4$ in $CDCl_3$.

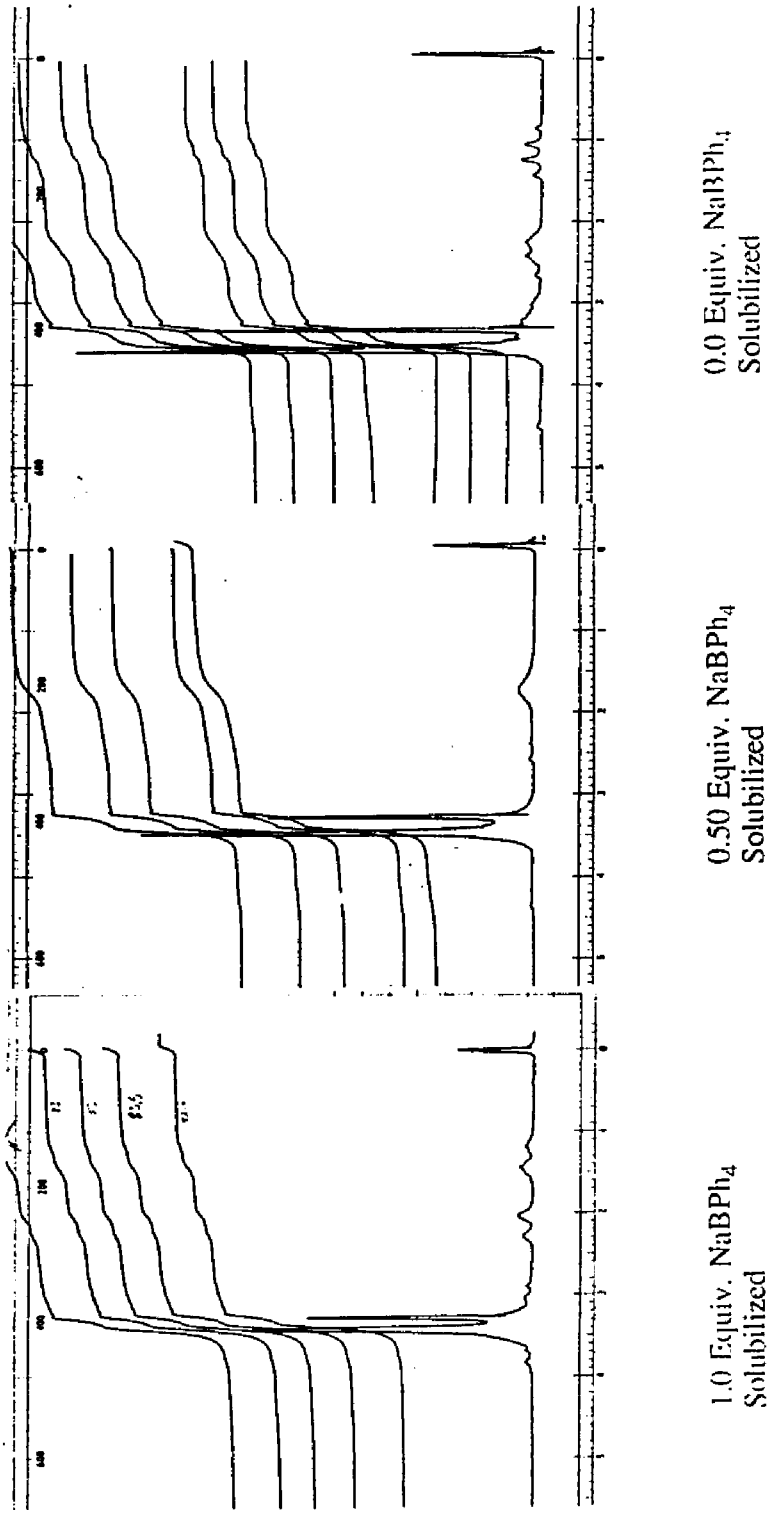

complexing abilities of these hosts in $CDCl_3$ can not be determined by this method.

The ^1H NMR spectrum for uncomplexed **11**shows an overlapping doublet of triplets (which appears as a quartet) for the axial methylene ring protons (1.20 ppm) and a doublet of multiplets (which appears as a broadened doublet) for the equatorial methylene protons (2.40 ppm).

When there is a 50/50 mixture of complexed and uncomplexed material the same two geminal ring protons appear as a single exchange-broadened resonance (~1.8 ppm) due to signal averaging. For fully complexed **11**a second order spectrum is observed. The ^1H NMR spectrum shows a dt and dm at 1.30 and 2.10 for axial and equatorial ring protons, H_1 and H_2 respectively.

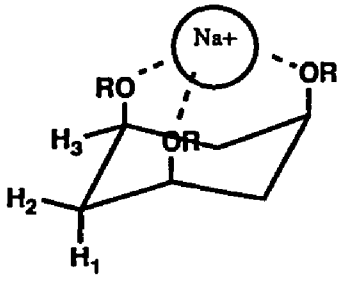

Figure 28: Complex Conformation of (1,3,5-Subst.) Cyclohexane Ring

Similar splitting patterns and chemical shifts were observed for **21** for uncomplexed, 50% complexed and fully complexed material (see Fig. 42, p.55 for structure).

The ring inversion associated with the complexation phenomenon interconverts the axial and equatorial positions of geminal ring protons. The axial ring proton is

upfield of the equatorial proton in both complexed and uncomplexed host [51] consistent with the normal situation in cyclohexanes. The ring methine peak is usually obscured by other peaks (eg. for podal CH_2's and CH_3) for most of our 1,3,5-(substituted) host systems. Assuming the ring inversion rate is proportional to the exchange rate, then the complexation-decomplexation kinetics of **11** and **21** appear to be fast relative to the ^1H NMR time scale under the conditions of these experiments (ie. at these concentrations, 0.1-0.4 M).

The spectrum of the 50/50 (complexed/uncomplexed) mixture **15** did not show a single broad peak for the ring methylene protons. The 0-3 ppm region actually looked like the 100 % complex spectrum superimposed on the 0 % complexed spectrum. This can be explained in terms of a slow exchange rate for Na^+ transfer that is unable to average the protons of free host and complex on the NMR time scale. This result may qualitatively indicate **15** to be a stonger ligand than **11**and **21**, since exchange rates are often lower for stronger ligands.

Combining **17** initially in a 3:1 ratio with $NaBPh_4$ in $CDCl_3$ resulted in complete solubilization of the salt and a single broadened peak for the methyl resonance at 2.03 ppm (see Figure 29).

Figure 29: ^1H NMR Complexation Spectra (0-5 ppm region) for **17** with $NaBPh_4$ in $CDCl_3$.

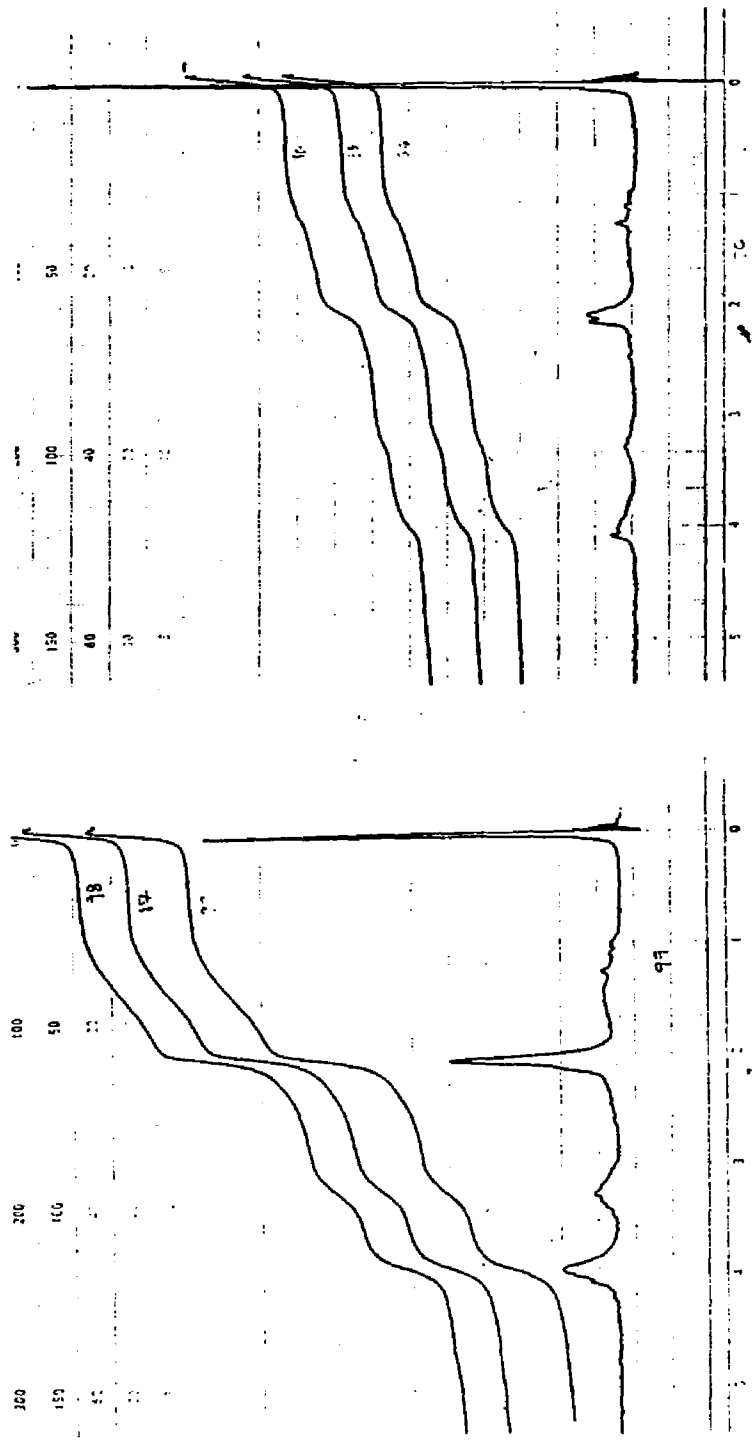

1.1 Equiv. $NaBPh_4$
Added/ with Formation
Precipitate

0.368 Equiv. $NaBPh_4$
Solubilized/ No Formation
Precipitate

When 1.11 equivalents of $NaBPh_4$ was combined with **17** in $CDCl_3$, a precipitate formed in the nmr tube. From the integration data it appeared that approximately 40% of the host remained in solution in a 3:1 ratio with solubilized salt, with the methyl resonance appearing as a broad pair of singlets (separated by 4 Hz) at approximately 2.10 ppm. For two-phase systems, where the host-guest complex precipitates from the solution, the standard assumptions cannot be made for the calculation of the stability constant for the complex in solution. No definite conclusion can be drawn concerning the molecularity of the host-guest complex. The observation of two peaks in the methyl resonance region corresponded to a lower sample concentration of host and guest due to precipitate formation relative to the sample that had a single broadened peak. One explanation for this is concentration dependent complexation-decomplexation kinetics which determine whether or not chemical shifts for uncomplexed and complexed material are averaged on the NMR time scale. This supports the idea that exchange occurs partially or possibly completely by a bimolecular process in a nonpolar solvent such as $CDCl_3$. Attempts to conduct the experiment in more polar solvents, such as acetone and acetonitrile, failed to produce clear results due to the weaker complexing ability of the host in these solvents (see section starting on p. 57 for discussion).

Host 12 did not solubilize a full equivalent of $NaBPh_4$ into $CDCl_3$, but almost half of an equivalent (0.48 eq) after the sample had been allowed to equilibrate for 216 hours. A plotof salt solubilized versus equilibration time indicated that the complexation process approached a limiting value of 0.50 equivalent as time went to infinity.

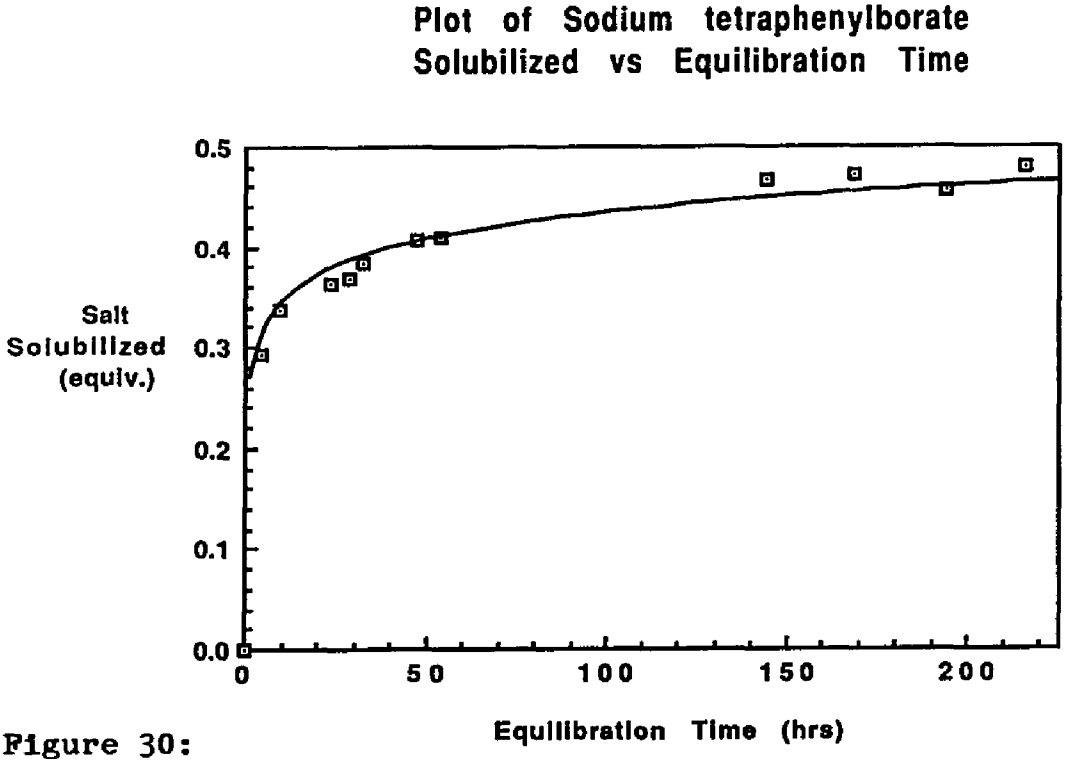

Figure 30:

This result seems to point towards the existence of a 2:1 host-guest complex. It is theoretically possible that this host could be forming a 1:1 complex that is in equilibrium with uncomplexed material. If this is the case, the stability constant and the free energy of complexation can be calculated using equations 6 & 7.

Calculation of a stability constant for a 1:1 complex of host **12** in $CDCl_3$:

$$K_{obs}^{1p} = [(ML^+)X^-]/\}[L][M^+X^-]\dagger \qquad (6)$$
$$= (0.941)/(1.24 \times 10^{-6}\ M)$$
$$= 7.58 \times 10^5\ M^{-1}$$

Calculation of the free energy of complexation for host **12** in $CDCl_3$:

$$\Delta G_{300}^{o} = -RT \ln K_{obs}^{1p} \qquad (7)$$
$$= -(1.9872\ cal/mol*K^o)(300\ K^o)\ \ln(7.58 \times 10^5)$$
$$= -8.07\ kcal/mol$$

The duration of the equilibration time is limited by slow decomposition of the salt. Attempts to speed the establishment of an equilibrium by sonicating and heating the sample were compromised by the formation of decomposition products and insoluble components. The results, at best, indicate a limited complexing ability for host **12**. The molecularity of complex and degree of complexing ability remain undetermined. (For further discussion of the complexation of this ligand refer to sections starting on p.39 and 78.)

Figure 31: ^1H NMR Spectrum of partially complexed **12** after 216 hours of equilibration with excess $NaBPh_4$ in $CDCl_3$.

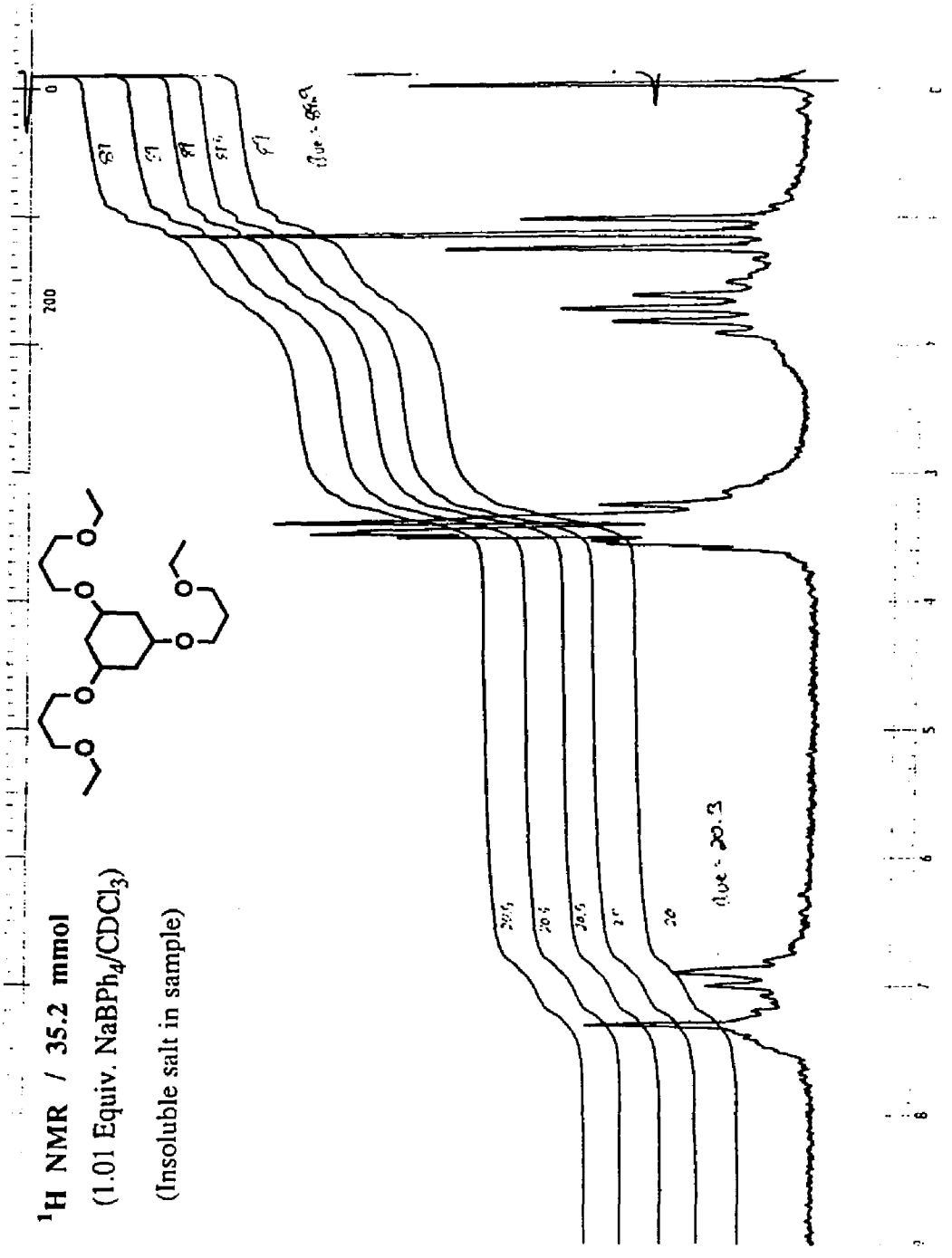

Standard ^{13}C NMR Complexation Studies

The development of pulsed-Fourier transform NMR with multinuclear capability has been crucial for the stereochemical analysis of systems for which well established ^{1}H NMR techniques provided equivocal and difficult-to-interpret data [52]. In our laboratories one of the standard applications of ^{13}C NMR spectroscopy has been for the characterization of newly synthesized hosts and the determination of corresponding chemical shifts of the metal cation complexes of these hosts in $CDCl_3$. Often these experiments have been conducted concomitantly with the previously described ^{1}H NMR experiments (p. 27) since the same samples can be used. These "standard" ^{13}C NMR experiments also provide data for conformational analysis of the host-guest system as well as create a foundation for competition experiments between hosts (See p. 78).

We use the ^{13}C NMR chemical shift changes to monitor complexation phenomena. All of our cyclohexane-based host systems undergo ring inversion upon complexation with a metal cation. The ring conformation significantly affects the observed chemical shifts of the ring carbons [53].

Because ^{13}C NMR (paramagnetic) shifts are much more sensitive to structure than ^{1}H NMR (diamagnetic) shifts, the interpretation of chemical shifts is more intricate and useful. It is for this reason that a meaningful discussion of our ^{13}C NMR results can not be given without a prerequisite minimum consideration of some basic aspects of

^{13}C data interpretation related to our host-guest systems. The existing body of empirical data indicates that ^{13}C shifts are subject to a variety of structural influences, some of which are not fully understood. Studies on substituent effects have helped identify some of these structural influences [54].

α-Effects:

Work with cyclohexane derivatives has shown in general that alpha hydrogen substitution with other substituents (eg. $-CH_3$, -OH, OMe) tends to shift ^{13}C signals downfield with the effect being larger for equatorial substituents than for axial [55]. Inductive effects through sigma bonds are commonly invoked as the rationalization for this type of substituent-induced chemical shift. The α-effect for the equatorial conformation of methoxy cyclohexanes is typically 4-5 ppm greater than that observed for the axial conformation [56].

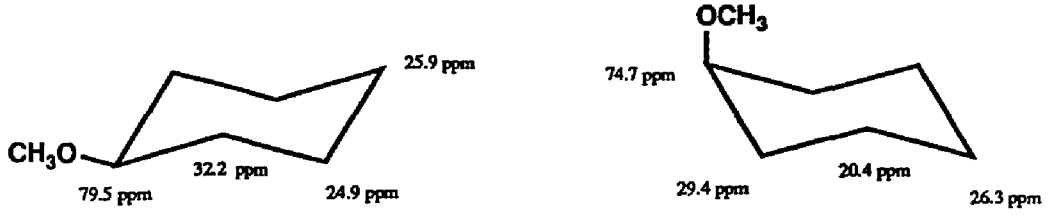

Figure 32: Equatorial/axial Methoxycyclohexane Conformers.

The stereochemical dependence of the observed a-effect has been rationalized in terms of syn-diaxial steric interactions involving hydrogens on the carbons γ-gauche to

the substituent [57]. It is important to note that not all syn-diaxial interactions result in upfield shift of the α-carbon position relative to to the same position in corresponding equatorial isomer (see Figure)[58].

Figure 33: Equatorial/axial Methyldacanols

β-Effects:

Substitution on the cyclohexane ring causes the β-position to be shifted downfield for both the equatorial and the axial conformational isomers. The inductive effect transmitted through sigma bonds is thought to be significantly diminished at the β-carbon position [59]. For axial methoxy cyclohexane the β-carbon has a chemical shift that is 2-3 ppm upfield of the corresponding β-carbon shift in the equatorial conformational isomer (See Figure 32) [60]. Earlier results obtained from the study of the effects of methyl and hydroxyl substituents prompted Roberts and co-workers to propose that steric interactions with an axial substituent cause bond elongation which results in the shielding of the β-carbon position (Figure 34) [61].

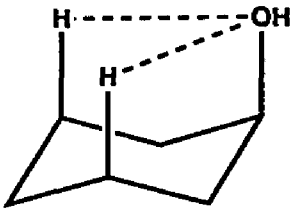

Figure 34: $C^{\beta}-C^{\gamma}$ Bond Elongation

However this theory has been questioned since molecular force field calculations on androstanols have indicated no such bond elongation [62]. Recently, Whitsell and Mark have correlated the difference in chemical shifts for equatorial and axial isomers (at the α and β positions) with the number of anti-vicinal H-H interactions [63].

γ-Effects:

In general, substitution on the cyclohexane ring causes an upfield shift at the γ-position. The magnitude of the upfield shift depends on the stereochemical orientation of the substituent. Axial substituents are gauche with respect to the γ-carbon position and usually give the largest upfield shift (γ-gauche effect). For methoxycyclohexane the γ-^{13}C resonances of the axial isomer are shifted upfield 4-5 ppm relative to those of the equatorial isomer (see Figure 32) [64].

The controversial "Grant-Cheney approach" explains the γ-gauche effect in terms of steric compression from the 1,3 diaxial interactions between the hydrogens on the γ-carbons and the substituent attached to the a-carbon. It has been proposed that a negative charge flux towards the γ-carbon

(from the axial ^{1}H) polarizes the C^{γ}-H bond and causes a general electron-orbital expansion (for γ-^{13}C which increases paramagnetic shielding) that shields the γ-carbon [65]. This type of rationale has also been used in an attempt to explain the (axial vs. equatorial) a-substituent effects [66].

Thermodynamic studies involving the measurement of ΔG^{o}'s (Axial-Equatorial) for mono-substituted cyclohexanes indicate that there is no direct correlation between the effective size of the substituent and the magnitude of shielding at the γ-position and that the often cited shielding mechanism through steric compression cannot be a dominant factor in the observed γ-gauche effects [67]. Some critics have questioned the existence of any diamagnetic upfield shift of steric origin and believe that the γ-gauche effect is really due to the removal of 1,3-diaxial hydrogen-hydrogen interactions as a result of substitution (See Figure 35) [68].

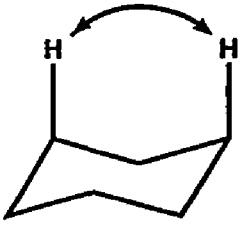

Figure 35: 1,3-Diaxial H-H Interaction

The traditional γ-gauche effect (involving an upfield shift) is significantly attenuated when it is a part of a 1,3-diaxial ($g^{+}g^{-}$) interaction (see Figure 36) [69]. In

spite of the large amount of empirical data accumulated on the γ-gauche effect, a good mechanistic interpretation of this substituent effect has remained elusive.

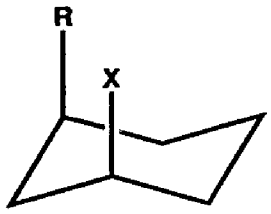

Figure 36: 1,3-Diaxial (g^+g^-)

The γ-anti effects are even less well understood than the γ-gauche effects and result sometimes in an upfield shift and sometimes in a downfield shift [70].

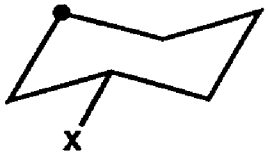

Figure 37: γ-Anti Substitution (g^+a)

The transmission mechanism seems to rely in part on the electronegativity of the substituent [71]. In most cases equatorial mono-substituted (second row heteroatoms, X=N,O,F) cyclohexanes have upfield γ-shifts which are smaller than the corresponding γ-gauche effects. It has been proposed that a hyperconjugative mechanism (see Figure 38) is responsible for this upfield γ-anti shift [72].

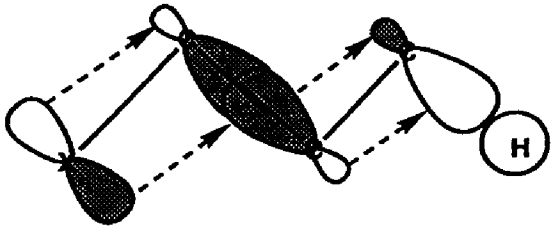

Figure 38: Hyperconjugative Mechanism

δ-effects:

These effects tend to be small and usually are obscured by the larger substituent effects described above. The major exception to this trend occurs when the substituent and the δ-carbon are syn-diaxial (g^+g^-) to each other (see Figure 39)[73].

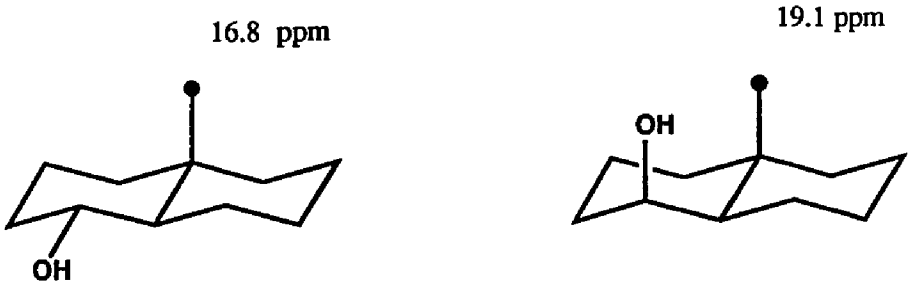

Figure 39: Equatorial/Axial Methyldecanols

The axial-OH substituent for 10-methyl-trans-decanol shifts the δ-methyl resonance downfield 3-4 ppm relative to the equatorial-OH isomer [74]. This result is inconsistent with the Grant-Cheney approach and actually supports the theory that steric compression from 1,3-diaxial interaction leads to deshielding [75].

Long-Range Effects:

These effects are very small and are only significant in those situations in which geometrical distortions of the molecular framework change the nonbonded internuclear distances or the substituent introduced is particularly effective at exerting long-range through-space effects. Our research involves drastic conformational biasing of the host molecules upon complexation which inevitablely changes spatial relationships. One of our complexed host molecules clearly exhibited long-range effects which allowed the differentiation of chiral centers that were chemical shift equivalent in the uncomplexed host (see below).

Obviously the study of simple mono- and di-substituted cyclohexanes can only give us insight into some of the more basic interactions that exist in poly-substituted systems. Conformational studies have been conducted on more highly substituted compounds, such as inositols and their O-methylated derivatives [76]. Substituent effects on cholestanols and androstanols have also been examined [77].

All uncomplexed cis,cis-1,3,5-trisubstituted cyclohexane host molecules exist predominantly in thermodynamically favored tri-equatorial conformations. To complex a prospective guest ion efficiently, the host must undergo a ring inversion to a tri-axial conformation either prior to or during the course of complexation. Chemical shift changes are observed for most of the carbon nuclei upon complexation, but it has been found that the ring

methylene group exhibits an especially large upfield shift of ~-7 ppm [78]. cis,cis-1,2,3-trisubstituted host **4**, which also undergoes a ring inversion upon complexation, exhibits similar but different chemical shifts. Limiting ^{13}C chemical shifts for ligands **3** and **4** in $CDCl_3$ are given in Table 6 (see Figure 40 for cyclohexane ring numbering schemes).

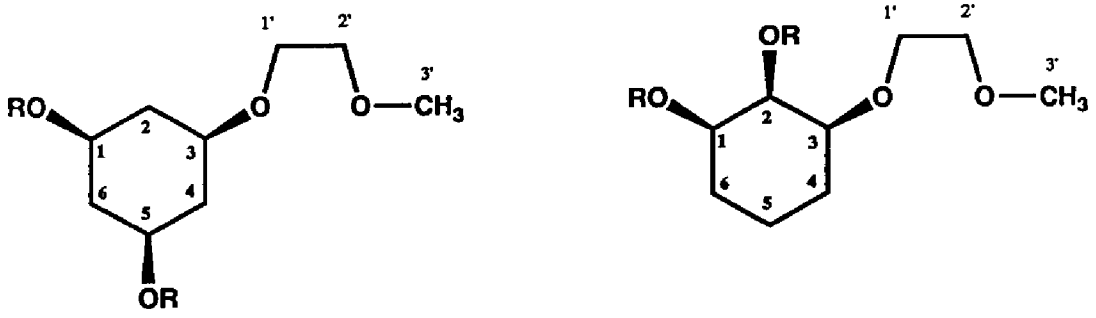

Figure 40: -------Numbering Scheme for Ligands **3** and **4**------

Table 6: Limiting ^{13}C NMR chemical shifts for cyclohexane ring resonances in ligands **3** and **4** in $CDCl_3$.

Ligand #	Carbon #	Free Ligand (ppm)	$NaBPh_4$ Complex (ppm)	$\Delta\delta^c$ (ppm)
3				
	1,3,5	73.84	73.73	-0.11
	2,4,6	38.08	30.82	-7.3
4				
	1,3	80.3[b]	74.4	-5.9
	2	76.5[b]	75.8	-0.7
	4,6	25.4	26.4	1.0
	5	20.5	13.5	-7.0

a- Data taken from T. Pascarella Thesis, pg 24-25.
b- Chemical shift assignments confirmed by G.R. Weisman
c- chemical shift change (complex-free ligand).

Small complexation-induced chemical shift changes give useful but qualitative information about the complexation

process since they have greater relative errors associated with their measurement. Selected cyclohexane-ring carbon resonances in our trisubsituted ligands exhibit large complexation-induced chemical shift changes, making these resonances particularly useful for monitoring the complexation process. ^{13}C NMR chemical shifts for the ring carbons of some new hosts and their corresponding 1:1 $NaBPh_4$ complexesin $CDCl_3$ are given in Tables 7-11. Slightly more than one equivalent of salt was used to ensure saturation of each system. The results presented here confirm the large and relatively well-defined conformational changes expected upon complexation of our hosts with metal-ions.

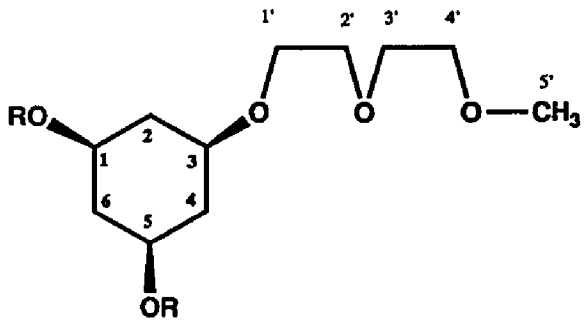

11

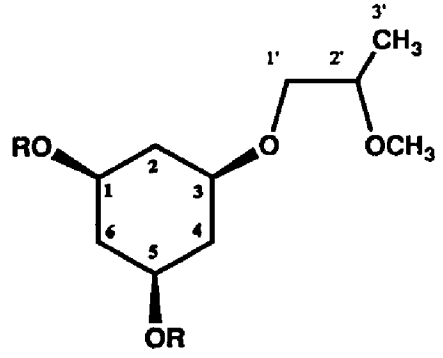

15

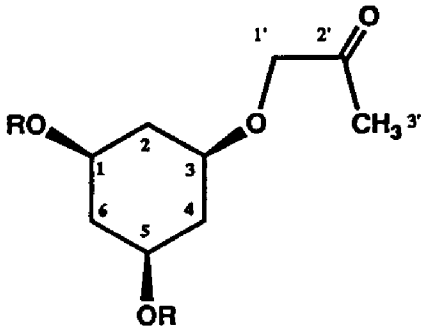

17

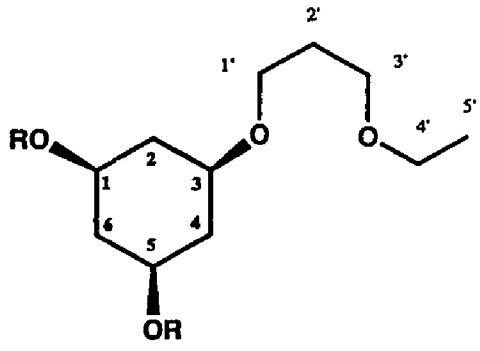

12

Figure 41: -----Numbering Scheme for 1,3,5-VFT Ligands-----

Table 7: ^{13}C Limiting Chemical Shifts/**11** in $CDCl_3$.

Carbon #	Free Ligand (ppm)	$NaBPh_4$ Complex (ppm)	$\Delta\delta^a$ (ppm)
1,3,5	73.75	73.61	-0.14
2,4,6	38.17	31.48	-6.69
1'[b]	67.83	68.02	+0.19
2'[b]	71.98	70.95	-1.03
3'[b]	70.56	69.26	-1.30
4'[b]	70.88	69.45	-1.43
5'	58.92	58.85	-0.07

a- change in chemical shift (complex-free ligand).
b- chemical shift assignments are tentative.

The results obtained for **11** are consistent with previous results obtained for **3** [79]. The largest complexation-induced chemical shift change observed is for the ring methylene carbon, -6.69 ppm. This has been rationalized in terms of the cyclohexane ring inversion and substituent effects discussed previously, and is confirmation of the drastic conformational biasing necessary to reorganize the ligand donor atoms to form a cavity capable of encapsulating the guest cation.

It is interesting to note that the large complexation-induced chemical shift does fall short of -7.3 ppm , the value obtained for **3**. In fact, the -6.69 ppm shift is almost identical to the value of -6.70 ppm obtained for a similar system containing an additional ethyleneoxy unit in each ligating arm [80].

Table 8: ^{13}C Limiting Chemical Shifts/**15** in $CDCl_3$.

Carbon #	Free Ligand (ppm)	$NaBPh_4$ Complex (ppm)	$\Delta\delta^a$ (ppm)
1,3,5	73.94	73.74	-0.20
2,4,6	38.18	30.89	-7.29
		30.69	-7.49
		30.50	-7.68
1'	72.18	72.44	+0.26
		72.05	-0.13
		71.92	-0.26
2'	76.15	76.02	-0.13
		75.89	-0.26
		75.63	-.051
3'	16.58	14.76	-1.82
		14.57	-2.01
4'	56.77	56.51	-0.26
		56.32	-0.45
		56.19	-0.58
		55.73	-1.04

a- change in chemical shift (complex-free ligand).

Prior to running the ^{13}C NMR complexation experiment for host **15** there was no direct experimental evidence that substantiated our belief that the compound isolated was a mixture composed of two diastereomerically related enantiomeric pairs (RRR,SSS and RRS,SSR).

Due to accidental chemical shift equivalence only six carbon resonances were observed for uncomplexed material. Complexation-induced removal of accidental chemical shift equivalence (isochrony) for some carbon resonances resulted in the observation of separate chemical shifts for different host isomers. This result can be explained in terms of

long-range effects that only become significant in the complexed host. Complexation-induced ring inversion alters the intramolecular spatial relationships of the ligating arms and effectively increases the interaction between stereocenters. The ring methylene in complexed **15** is shifted upfield approximately -7.4 ppm relative to uncomplexed material.

Table 9: ^{13}C Limiting Chemical Shifts/**17** in $CDCl_3$.

Carbon #	Free Ligand (ppm)	Partially[a] Complexed (ppm)	$\Delta\delta$[d] (ppm)
1,3,5	73.88	74.27	+0.39
2,4,6	37.59	~37.4[bc] ~30.4	-0.2 -7.2
1'	73.68	73.55[b]	-0.13
2'	206.54	206.99[b]	+0.45
3'	26.34	26.21	-0.13

a- 0.368 eq. $NaBPh_4$ solubilized by host.
b-Significant line broadening.
c-This resonance may be broadened due to slow exchange with a carbon resonance at ~30.0 ppm which has almost completely been broadened into the baseline.
d- chemical shift change (complex-free ligand)

The "standard" NMR complexation experiment with host**17** could not be completed due to the limited solubility of the host-guest complex in $CDCl_3$. The spectrum of partially complexed material (solubilization of 0.368 equiv. $NaBPh_4$) showed two very exchange-broadened peaks at 37.4 and 30.4 ppm, which correspond to the ring methylenes in uncomplexed

and complexed host,respectively. Exchange is slow on the ^{13}C NMR time scale for **3**, which is also true for the new host systems discussed previously. Thus, separate sets of chemical shifts are observed for mixtures containing both complexed and uncomplexed material. The broadening of the methylene resonances in **17** is due to faster complexation/decomplexation kinetics. Attempts to measure relative peak areas by integration produced only a qualitative ratio of free host to complex. In spite of the large errors associated with the integration of very broad peaks with a low S/N ratio, the experimental value obtained for % complex (37%) indicates that all the salt added was complexed via drastic conformational biasing of the ligand. The faster exchange kinetics may be a manifestation of weaker complex stability relative to **3** and other hosts that exhibit slower exchange rates.

Table 10: ^{13}C Limiting Chemical Shifts/12 in $CDCl_3$.

Carbon #	Free Ligand (ppm)	Partially[a] Complexed (ppm)	$\Delta\delta^c$ (ppm)
1,3,5	73.42	73.49	+0.07
2,4,6	38.37	35.96[b]	-2.41
1'	67.44	68.02	+0.58
2'	30.59	30.37	-0.22
3'	66.14	(66.92)	+0.78
4'	65.42	(66.33)	+0.91
5'	15.15	15.02	-0.13

a- The sample was allowed to equilibrate for over 9 days; undissolved salt still remained and resonances associated with decomposition of the salt also appeared.
b- significant line broading
c- change in chemical shift (complex-free ligand).

Since the 1,3,5(HOMO) system **12** only solubilized half of an equivalent of $NaBPh_4$ in $CDCl_3$ it was not possible to obtain the limiting chemical shifts for a 1:1 ligand/salt complex. In the presence of excess $NaBPh_4$ no precipitation of complex was observed. The ring methylene signals for complexed and uncomplexed material appeared as a single chemical-shift averaged peak at 35.96 ppm. This represents a complexation-induced upfield shift of -2.4 ppm.

Based on the assumption that the limiting chemical shift change is approximately -7.0 ppm, the data suggest that 34% of the host in solution is in the triaxial conformation. The chemical shift averaged signal for the ring methylene is broadened due to an intermediate exchange

rate relative to the NMR time scale. Thus the exchange rate is even faster than that for the 1,3,5(keto) system. The use of higher-field NMR (90 MHz) in conjunction with decreased sample concentration failed to resolve the signals for complexed and uncomplexed material. A low temperature experiment was not attempted. In the absence of a limiting complex chemical shift in $CDCl_3$, the magnitude of the complexation-induced upfield shift cannot be used to measure the percentage of complex in equilibrium with free ligand.

The results do confirm that the solubilization of 0.5 equivalents of $NaBPh_4$ significantly affects ligand conformation via a dynamic complexation process. The faster exchange kinetics observed are also consistent with an apparently weaker complex stability.

It is unclear from the ^1H and ^{13}C NMR results whether a 2:1 host-guest complex and/or a 1:1 complex is formed. The ^1H NMR integration results show that solubilization of $NaBPh_4$ approaches a limiting value of approximately 0.5 equivalents after 9 days of equilibration. The ^1H NMR spectrum (of 12 with 0.5 equiv $NaBPh_4$ solubilized, see Figure 31, p. 38) rules out the posibility of the host being biased 100% to the triaxial (or the triequatorial) conformation. This only indicates the possibility of a 2:1 (ligand:metal) complex with only one ligand biased to the triaxial conformation. The ^{13}C NMR result only confirms the existence of a dynamic complexation process involving biased and unbiased ligand conformations. Preliminary experiments aimed at determining the concentration dependence of the

complexation process have been complicated by the need for long sample equilibration times and limited sample stability.

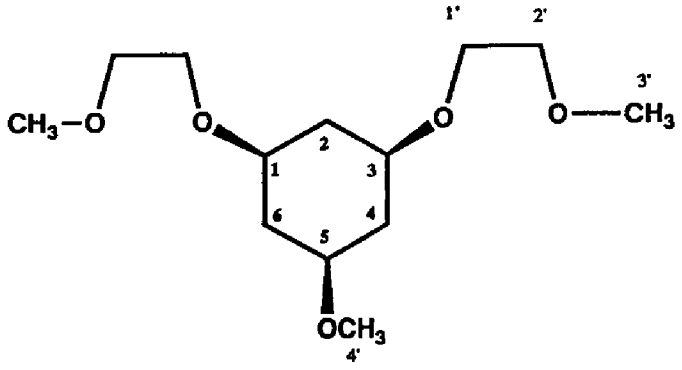

Figure 42: ----- Numbering Scheme for 21 ------

The data from experimental work conducted with D. Gronbeck [81]for ligand 21 has been included for future reference in relation to competition experiments discussed later. From Figure 42, it can be seen that host 21 is a simple analog of 3 in which the polyether arm at C-5 has been replaced by a methoxy group.

The substitution removes the C_3 axis of symmetry and makes the ring methylene positions, C-2 and C-4,6 chemical shift nonequivalent (also for ring methines, C-1,3 and C-5). The tentative chemical shift assignments of these resonances for uncomplexed and complexed 21 are based in part on relative ^{13}C peak intensities (see Table 11 below).

Table 11: ^{13}C Limiting Chemical Shifts/21 in $CDCl_3$.

Carbon #	Free Ligand[b] (ppm)	$NaBPh_4$[c] Complex (ppm)	$\Delta\delta$ (ppm)
1,3[d]	73.88	73.49	-0.39
5[d]	74.72	75.11	+0.39
2[d]	38.04	31.34	-6.70
4,6[d]	37.78	30.63	-7.15
1'	72.25	71.66	-0.59
2'	67.70	67.31	-0.39
3'	59.11	59.24	+0.13
4'	55.93	57.75	+1.82

a: Synthetic work and sample prep. conducted by D. Gronbeck (1986).
b: NMR spectrum obtained by J. Peabody.
c: NMR spectrum obtained by S. Shirodkar.
d: Chemical shift assignments are tentative and based in part on relative peak intensities.

A single chemical shift averaged spectrum is observed for a 2:1 ligand/salt mixture. The exchange broadened overlapping ring methylene resonances qualitatively show that the exchange rate is similar to that of 1,3,5(HOMO) **12** and much faster than that observed for **3**. The exchange kinetics may be a manifestation of diminished complex stability for **21** due to a smaller number of oxygen donor atoms relative to **3**.

Experiments with Other Salts

One of the original aims of this research was to determine the complexing abilities of the cyclohexane-based tripodands for more than one type of cation in the nonpolar solvent $CDCl_3$. It was originally hoped that complexation of tetraphenylborate salts (eg. Li^+, Na^+, K^+, Rb^+, Cs^+, NH_4^+) could be studied by the two-phase ^1H NMR technique. Unfortunately the extreme insolubility of many tetraphenylborate salts in $CDCl_3$ led to low complexation constants [82]. The results of some complexation experiments with miscellaneous salts (Table 12) are followed by a brief discussion.

Table 12: Complexation Results for Various Ligands and Salts in a number of solvents.

Ligand	Salt	Solvent	Comments
3	NH_4^+,Picrate	$CDCl_3$	No Complexation-^1H NMR
3	NH_4^+,Picrate	CD_3CN	No Complexation-^1H NMR
3	NH_4^+,SCN^-	$CDCl_3$	No Complexation-^1H NMR
3	NH_4^+,SCN^-	CD_3CN	No Complexation-^1H NMR
3	$NaBF_4$	$CDCl_3$	No Complexation-^1H NMR
3	NaI	$CDCl_3$	1:1 Complex formed
17	NaI	$CDCl_3$	Some Complexation with rapid decomposition.
13	Ag^+,Triflate	$CDCl_3$	No Complexation-^1H NMR
13	Ag^+,Triflate	Mixture[a]	No Complexation-^1H NMR
3	Ag^+,Triflate	MeOH-d4	Some Complexation with rapidsample decomp.

a- solvent mixture composed of DMK-d6 and $CDCl_3$

Complexation of $KBPh_4$:

The relevant complexation studies are discussed at the end of the section starting on p.66.

Complexation of Ammonium Salts:

The ring ^1H NMR shifts in the ligand 3 were used to monitor the experiments. No complexation was observed with ammonium picrate or ammonium thiocyanate. In the latter case the salt was observed to dissolve when the solvent was CD_3CN, but no complexation was detected.

Complexation of $NaBF_4$:

Proton NMR studies indicated no complexation of $NaBF_4$ by 3 in $CDCl_3$. By visual inspection of the sample, there appeared to be no solubilization of the salt.

Complexation of NaI:

Ligand 3 solubilized a full equivalent of NaI in $CDCl_3$. The ^1H NMR of the ligand changed upon addition of salt in a manner characteristic of complex formation. Since there were no protons in the salt to integrate, ^{13}C NMR chemical shift changes in the ligand were used to measure the degree of complexation. The ^{13}C NMR results are given in Table 13.

Table 13: ^{13}C NMR Chemical Shift Results from Complexation of **3** with NaI in $CDCl_3$.

Carbon Resonance in **3**	No salt Added (ppm)	Excess Salt (ppm)	Chemical Shift Change (ppm)
C-1,3,5	73.9	74.0	0.1
C-2,4,6	38.0	31.7	-6.3
C-1'[a]	67.7	68.0	0.3
C-2'[a]	70.3	72.1	1.8
C-3'	59.1	59.5	0.1

a- Chemical shift assignments are tentative.

The limiting chemical shifts for the NaI complex are very similar to those for the $NaPBh_4$ complex. This indicates the formation of a similar 1:1 complex in $CDCl_3$ even though this could not be shown quantitatively since there were no protons signals for measuring the amount of salt solubilized.

Attempts to complex NaI with the triketone ligand **17** in $CDCl_3$ resulted in rapid decomposition of the sample (presumably -iodination) which hindered the measurement of the degree of complexation by NMR.

Complexation of Silver Triflate:

McMurry et al. have shown that a pentacyclo-tetracosatetraene (Figure 43) formed a stable crystalline Ag^+-olefin complex in THF, whose square planar geometry was confirmed by x-ray crystal analysis [83a]. Given this and other literature precedents for complexation of Ag^+ [83], the complexation of our allyl ether with silver triflate was attempted.

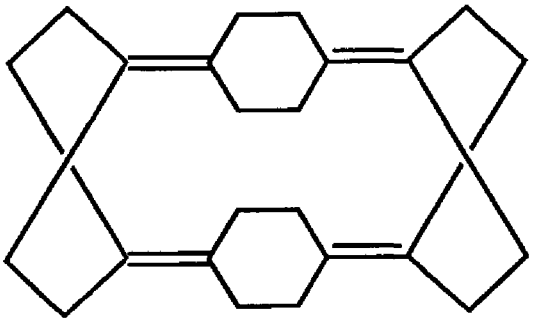

Figure 43: Pentacyclo-tetracosatraene

There was no indication by ^1H NMR that there was any complexation of silver ion by our allyl ether ligand 13 in $CDCl_3$ or a $CDCl_3$/DMK-d6 solvent mixture. In the latter case the salt was solubilized, but no complexation was observed. In order to complex Ag^+ it may be necessary to have a more rigid backbone structure that enforces a more desirable orientation and positioning if the olefinic binding sites.

Specific Ag^+ ion binding and transport properties of tripod type open-chain cryptands (Figure 44) have been demonstrated [84]. The similarity of these ligands to our oxygen ether tripodands prompted us to attempt the complexation of silver triflate with ligand 3.

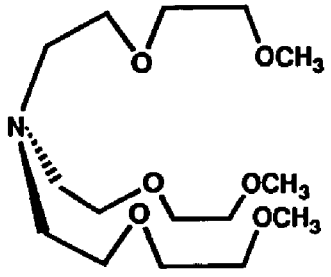

Figure 44: Tripod type open-chain cryptand

Using ^{13}C NMR chemical shifts in the ligand 3, some complexation was observed of silver ion in MeOH-d_4. Unfortunately rapid decomposition of the sample hampered the quantitation of the degree of complexation or the determination of exchange dynamics of the complexation process relative to the NMR time scale. The sample stability appears to be compromised by Lewis acid (eg. silver ion) catalyzed elimination in the ligand.

Miscellaneous NMR Complexation Studies:

Another objective in our laboratories was to compare the complexing ability of some known ligands with that of our cis,cis-1,3,5-tris-(dioxapentyl) cyclohexane (3). Some preliminary investigations were conducted with $NaBPh_4$ and ligands such as 18-crown-6 (22), [2.2.2] cryptand (23), and dibenzo-18-crown-6 (24).

Some of our initial attempts to run 1:1:1 competition experiments [85] in $CDCl_3$ failed due to precipitate formation when the ligands and salt were combined.

Complexation of 18-crown-6:

The first attempts to complex $NaBPh_4$ in $CDCl_3$ with 18-crown-6 (22) were conducted by T. Pascarella [86]. Using the two phase ^1H NMR method (p.27) it was concluded that there was no solubilization of salt and thus that 22 did not complex sodium ion in $CDCl_3$. A comparison of proton integrations of host and the reference TMS in a repeat of this experiment indicated that an insoluble complex had actually formed and precipitated upon addition of salt to the ligand solution.

The experiment was repeated in acetone and monitored by ^1H & ^{13}C NMR chemical shift changes in the ligand. The results for the addition of 1, 2 and 3 equivalents of salt are given in Table 14.

Table 14: ^{1}H & ^{13}C NMR Results from the Complexation of 18-crown-6 (22) with $NaBPh_4$ in Acetone-d6.

# Equiv. $NaBPh_4$	^{1}H δ (ppm)	^{1}H Δδ (ppm)	^{13}C δ (ppm)	^{13}C Δδ (ppm)
0	3.63		71.27	
1	3.56	-0.07	70.04	-1.23
2	3.51	-0.12	69.91	-1.36
3	3.43	-0.20	69.78	-1.49

The addition of the first equivalant of $NaBPh_4$ results in the largest complexation induced chemical shift change (for the ^{13}C nucleus). This indicates the initial formation of a 1:1 ligand:metal complex. The chemical shift changes observed upon addition of the second and third equivalents of salt are probably the result of polarity effects.

Competition Between 3 & 23:

Our initial attempt to run a ^{13}C NMR (1:1:1) competition experiment between 3, and [2.2.2.]cryptand (23) for $NaBPh_4$ in $CDCl_3$ failed due to precipitate formation upon sample preparation. The one equivalent of the salt was initially solubilized with one equivalent of 3 in $CDCl_3$. The introduction of the cryptand induced immediate precipitation of what is no doubt a cryptate complex of $NaBPh_4$. This is similar to the result obtained with the complexation of 18-crown-6 (22) in $CDCl_3$.

Competition Between 3 & 22:

Again, our initial attempts to run a ^{13}C NMR competition experiment between 3, and 22 for $NaBPh_4$ in $CDCl_3$

failed due to precipitate formation upon sample preparation and as a result the same conclusions were drawn. The solvent was changed to acetone-d6, which prevented precipitation of complex and the 1:1:1 and 1:1:2 (2 equiv. $NaBPh_4$) competitions were monitored by chemical shift changes in both ligands. (Table 15)

Table 15: ^{13}C NMR Chemical Shifts for the Competition between 3 & 22 with $NaBPh_4$ in Acetone-d6.

Conditions	Tripodand (3) C-2,4,6 (ppm)	18-Cr-6 (22) (ppm)
Uncomplexed	39.34	71.27[4]
1:1 complex	30.84[a]	70.04[b]
1:1:1 Compet.	38.76	70.04
1:1:2 Compet	33.75	69.97

a- base on a limiting chemical shift change of -8.50 ppm determined by titration experiment.
b- not a limiting chemical shift, but that observed for a 1:1 ligand:metal solution ratio.

The results show that the first equivalent of $NaBPh_4$ added was entirely complexed by the crown ether (22) and that the second equivalent added was then complexed by the tripodand ligand (3). Thus, in comparison, 22 is a much better complexer of sodium ion in acetone than ligand 3. The large difference in complexing abilities of these ligands obviates the calculation of relative stability constants from observed chemical shift changes.

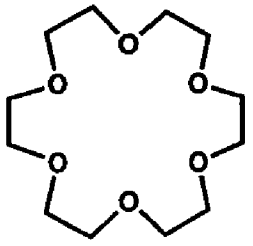

18-Crown-6

22

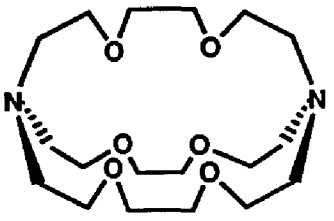

[2.2.2.] Cryptand

23

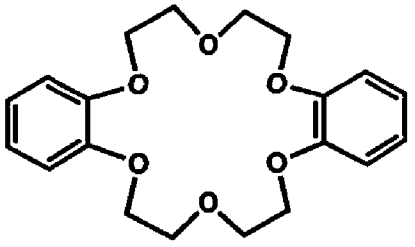

Dibenzo-18-Crown-6

24

Figure 45:

Competition Between 3 & 24:

The ^{13}C NMR (1:2:1) competition experiment in $CDCl_3$ with 3, dibenzo-18-crown-6 (24) and $NaBPh_4$ resulted in complexation of at least 90% of the single equivalent of salt by the crown ether ligand (24).

In general the results show the sodium-tripodate complex (Na^+-3) is less stable than corresponding crown ether complexes (Na^+-22 & Na^+-24) and no doubt less stable than the cryptate (Na^+-23).

Determination of Complexation Constants from ^{13}C NMR Titration Studies

General Theory

The association constant, K, for 1:1 complex formation can be determined from a titration experiment. The prerequisite conditions for making the determination is the existence of a spectral parameter or other measurable quantity that changes as a function of the extent of complexation and sufficient solubilities of host, guest, and complex in the solvent chosen. A number of useful NMR techniques have been developed for the evaluation of stability constants [87-89]. Since work done in our group by Pascarella [90] has fully documented the details related to the determination of complexation constants using ^{13}C NMR chemical shift changes for cyclohexane based tripodands with sodium ion in acetone, only the more salient features necessary for understanding the titration experiment will be considered in the following discussion.

For tripodand complexation of $NaBPh_4$ in acetone, the kinetics of ligand exchange (or cation exchange) are fast on the ^1H and ^{13}C NMR time scales; separate chemical shifts for complexed and uncomplexed material are not typically observed [91]. For a given nucleus, the result of the exchange process is a single time-averaged peak whose chemical shift represents a weighted average between the limiting chemical shifts for uncomplexed and complexed material. The change in chemical shift of time-averaged

peaks may serve as the spectral parameter monitored during a titration experiment.

Determination of K_{obs}^{ip}

The thermodynamics of complex formation are quantitated in terms of an observed (ion-paired) association constant, K_{obs}^{ip}, which is used to calculate the free energy of complexation, ΔG^{o}. An NMR experiment is conducted by titrating a solution of host with guest salt until the solubility limit of the solution for the salt is reached and/or no further chemical shift changes are observed (saturation point) for the system. A plot of the measured ^{13}C chemical shift changes $\Delta\delta_{obs}$ $(\delta_{obs}-\delta_{L})$ versus [guest]/[host] is made. The titration curve is generated by fitting the titration function, T (Equation 8) to the plot using a non-linear iterative least-squares analysis of the data (see Experimental Section).

$$T = |\delta_{obs}-\delta_{L}| = 0.5B\{(1+A+X)-[(1+A+X)^{2}-4X]^{1/2}\} \qquad (8)$$

where: $A = \dfrac{1}{K[L]_{T}}$ $\quad B = |\delta_{ML}-\delta_{L}|$ $\quad X = \dfrac{[M^{+}]_{T}}{[L]_{T}}$

$[L]_{T}$ = Total ligand conc.

$[M^{+}]_{T}$ = Total metal ion conc.

This curve fitting procedure yields values for K_{obs} and $\Delta\delta_{ML}-\Delta\delta_{L}$ (see Appendix A for plots).

The procedure has limitations and is only applicable

to host systems that are saturated (fully complexed) at the solubility limit for the salt in the solvent chosen. The results are based on the assumption of a 1:1 complexation ratio. Under fast-exchange conditions, it is not possible to distinguish between 1:1 and 2:1 (ligand/salt) complexation using ^{13}C NMR chemical shifts. At higher salt concentrations medium polarity effects can induce small but observable chemical shift changes that are not directly a result of or related to complex formation and the attendant conformational biasing of the ligand. Thus the overall observed parameter change ($\Delta\delta_{obs}$) used to measure the degree of complex formation in the experiment must be larger than the typical changes associated with the background medium polarity effects.

The K_{obs}^{ip} and corresponding ΔG^{o}_{300K} values were obtained by titrations of ligands 11 and 3 [92] with $NaBPh_4$ in acetone. Each experiment was conducted at constant ligand concentration by adding aliquots of salt. The effect of initial starting concentration as well as the number of titration points was examined. Attempts to measure stability constants for analogous $KBPh_4$ complexes were unsuccessful since the salt solubility limits were reached before the saturation points (i.e. no further chemical shift changes observed). This is due to the low inherent solubility of the salt in acetone. Tables of chemical shift data, titration plots, and various types of curve fits for each experiment are displayed in the Appendix A. Stability

constants for podands **11** and **3** are listed in Table 16.

Table 16: Stability Constants for $NaBPh_4$ Tripodand Complexes with **11** and **3** in Acetone-d_6.

Podand	[L] (M)	# points (on plot)	$-\Delta\delta^{a}_{ML^+-L}$ (ppm)	log K^{ip}_{obs} (M^{-1})	$-\Delta G^{o}_{300K}$ (kcal/mol)
11	0.2688	21	6.86	1.30	1.79
11	0.2813	7	6.55	1.59	2.19
3	0.2690	23	8.58	1.36	1.86
3	0.2898	7	8.25	1.62	2.22
3	0.4805	5	8.09	1.81	2.48
3[b]	0.84	6	7.77	2.2	3.0

a: Limiting ^{13}C chemical shift change (for C-2,4,6) obtained from curve fit.
b: Measurement made by T. Pascarella [90,p. 39].

Table 17: Results from Attempted Titration Experiments with $KBPh_4$ in Acetone-d_6.

Podand	[L] (M)	# points (on plot)	$-\Delta\delta^{a}_{obs}$ (ppm)	Solubility Limit [$NaBPh_4$]/[Ligand]
11	0.1167	4	1.43[b]	<1.25
3	0.1095	4	0.46[b]	<1.25
3[c]			0.54[b]	≈1.25

a: Total observed ^{13}C chemical shift change (for C-2,4,6).
b: Too small to permit calculation of K value.
c: Measurement made by T. Pascarella [90,p. 39].

Increasing the number of data points for a given titration corresponded to a poorer curve fit. More points should better define the titration plot but in practice also increased the systematic errors. A poor curve fit is a reflection of the inadequacies in the mathematical model and/or in the experimental methodology.

The position of each data point on a titration plot is partially determined by the summation of systematic errors up to that point. Possible sources of error come from weighing and adding the titrant to the NMR tube, not to mention the possible errors due to solvent evaporation and/or contamination by water vapor from the repeated exposure of the sample to air. Taking more points means making more additions and thus must amplify the amount of systematic error introduced to a system as it approaches the saturation point. The results from our experiments show a negative correlation between the number of data points and a curve fit for the titration plot. The specific nature of the systematic errors that cause this effect is not immediately apparent.

Varying the initial concentration of ligand clearly affected the results. The titration data for 3 ([L] = 0.2898, 0.4805, and 0.84 M) in Table 16 suggests that initial concentration has a direct relationship of the magnitude of the observed stability constant and an inverse relationship of the calculated limiting chemical shift change for C-2,4,6 (See Equations 9 & 10).

$$[L]_i \sim K_{obs}^{ip} \quad (9)$$

$$[L]_i \sim 1/|\Delta\delta_{ML^+-L}| \quad (10)$$

where: $[L]_i$= initial ligand concentration.

Ideally, the K_{obs}^{ip} for 1:1 complex formation should not be dependent on ligand concentration. The deviation from theoretical expectations is most readily explained in terms of systematic errors. At higher total ligand concentrations, the saturation point for the titration is reached sooner relative to a titration of a more dilute ligand solution. The more dilute the ligand solution, the greater the total amount of $NaBPh_4$ that must be added to force the reaction to completion. For our titrations at lower total ligand concentration there appeared to be a pronounced polarity effect towards the end of the titrations (at higher salt concentration) that continued to shift the observed carbon resonances (after the saturation point was reached). This would explain the lack of a plateau in the corresponding titration plots, abnormally high limiting chemical shifts, and abnormally low K_{obs}^{ip}'s.

Compound **11** contains nine oxygen donor sites versus the six in the original model tripodand **3**. Thermodynamic studies done on oligoethylene glycol ethers show that stability constants and the selectivity ratios, $K_{(K)}/K_{(Na)}$ increase with the number of coordinating sites on the ligand [93]. Compound **11** was designed with the intent to test the effect of additional oxygen donor sites on complexing

ability and ion selectivity relative to the original model tripodand **3**. The stability constants for the $NaBPh_4$ complexes in acetone for **3** (K^{ip}_{obs} = 42 M^{-1} for [L] = 0.29 M) and **11** (K_{obs} = 39 M^{-1} for [L] = 0.28 M) are almost equal. The additional donor sites in **11** appear to have a relatively small effect on the complex stability. Analysis of CPK [Corey-Pauling-Koltun] molecular models indicates that the cavity formed by **11** is more than sufficient to accommodate the cation diameter for sodium. One possible conclusion is that the analogous six donor sites in axial-11A (Fig.46 below) provide an adequate cavity for sodium and that the three additional oxygen donor sites are not utilized in the complex. The limiting ^{13}C chemical shift change, $|\Delta\delta_{ML^+-L}|$ (C-2,4,6) for **11** falls short of the value for **3** by approximately 1.7 ppm. This result is inconsistent with the previous results obtained for $CDCl_3$ solutions. The larger cavity provided by axial-**11** may allow for cation migration between different sets of oxygen donor sites (See Fig.46). An explanation for the lower limiting $|\Delta\delta_{ML^+-L}|$ observed is that a less constricted complex conformation leads to an alteration of substituent effects and thus the limiting chemical shifts for the complex. The different substitution on the cyclohexane ring for **11** and **3** does not affect the uncomplexed chemical shifts (for [L] $\simeq$ 0.269 $\pm$ 0.0002 M, C-2,4,6 = 39.279 ppm for both ligands).

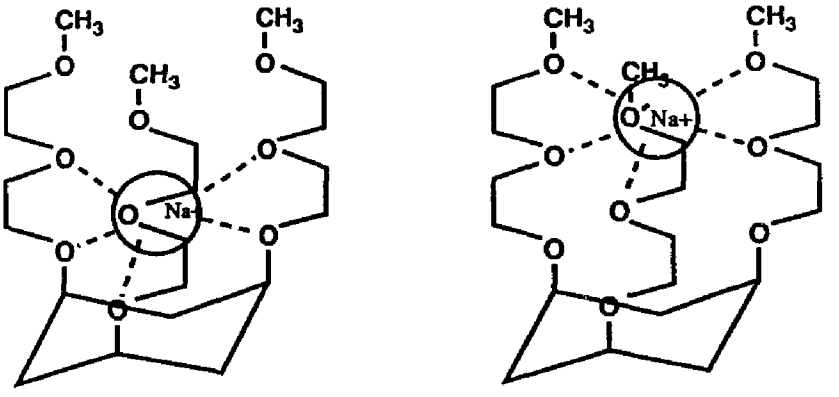

11A 11B

Figure 46. Types of hexa-coordinate binding.

Attempts to measure the stability constants for $KBPh_4$ complexes in acetone were unsuccessful (Table 17). Ligands 11 and 3 appear to be poor potassium complexers. For both systems the solubility limit of the salt in the solvent was reached before the saturation point (i.e. no further change in chemical shifts observed). In each case, the $\Delta\delta_{obs}$ was too low to permit the calculation of a K^{ip}_{obs}.

The total observed chemical shift change in tripodand 3 of -0.46 ppm (for C-2,4,6) corroborates the result obtained by T. Pascarella [90,p. 39], and the conclusion that insertionof a K^+ ion into the sodium-sized cavity leads to unfavorable ligand strain and a low complexation constant. It was anticipated that the additional oxygen-donor sites and the larger cavity size provided by axial-11 might result in a greate- K^+ association constant in acetone. Even though the K^{ip}_{obs} could not be calculated, the total $\Delta\delta_{obs}$ of -1.43 ppm is almost three-fold greater than the value for 3 This upfield shift is outside the typical range

associated with solution polarity effects and thus must be a manifestation of the conformational biasing induced by the complexation process. The results can be rationalized in terms of tripodand **11** having a larger K^+ association constant than 3 but this interpretation is speculative since the limiting chemical shift, (ie. that of the complex) is unknown.

The stability contants in acetone-d_6 for ligands **11** and 3 with $NaBPh_4$ are five orders of magnitude smaller than the lower limit values obtained with $CHCl_3$ as the solvent.

For many years the solution structures of aqueous and nonaqueous electrolyte solutions have been interpreted mainly by the electrostatic theory. Complex stabilities in solution can be understood better by using the "Donor-Acceptor Approach" [94] to molecular interactions. Solvents are characterized in terms of empirically derived donor numbers (DN) and acceptor numbers (AN). Attention must be paid to the specific solvent effects associated with each species in the solution equilibrium. The coordination process can be viewed as a competition between ligand and solvent molecules for the metal cation [94,p. 165]. Donor numbers reflect the ability of a solvent (or solutes) to participate in the solvation of a cation. Acetone is a much better donor (DN = 17.0) than chloroform, which has a negligible donicity [94,p. 20]. Even though the donicity of the ligand is unknown, the donor nature of a polyether arm segment can be approximated from a similar solvent system, such as dimethoxyethane (DN = 20)(note-this assumes that the

ligand can adopt an appropriate conformation). Thus in acetone there is considerable solvent-ligand competition for solvation of the cation which lowers the observed association constants relative to those in chloroform.

Table 18: Gutmann Donor (DN) and Acceptor (AN) Numbers for Selected Solvents.

Solvent	DN[a]	AN[a]
Chloroform	--	23.1
Acetone (DMK)	17.0	12.5
Dimethoxyethane (DME)	20[b]	10.2
Tetrahydrofuran (THF)	20.0	8.0
Diethyl ether	19.2	3.9
Ethanol	20[b]	37.1
Water	18.0	54.8
Nitromethane	2.7	20.5
Acetonitrile	14.1	19.3

a: Reference [94], p. 20, 29.
b: Donor numbers indicated by indirect method.

The acceptor properties of the solvent will also affect the position of the complexation equilibrium [95]. Acetone behaves as a weaker acceptor (AN = 12.5) in contrast to chloroform (AN = 23.1) and is only slightly stronger than the approximated ligand acceptor ability (AN = 10.2, dimethoxyethane). Chloroform should solvate the BPh_4^- counter anion better than acetone or the ligand and result in a more stable (ion-paired) solution complex. In general the effective differences in solvation of the BPh_4^- are

relatively small due to its lipophilic nature and large size.

Acetone can be viewed as a "homoselective" solvent that has similar donor and acceptor properties that allow it to solvate both cations and anions [96] Both chloroform and our ligands are "heteroselective" in nature and tend to only solvate one component of a binary electrolyte [97]. A ligand-chloroform solution results in a synergistic enhancement of the complexation constant relative to an analogous acetone solution.

The proposed order of acceptor properties for a selected number of cations is [98].

$$Me_4N^+ < Cs^+ < Rb^+ < K^+ < Na^+ < Li^+$$

Because potassium is a weaker acceptor than sodium, the specific free enthalpy of solvation is less negative (more negative for sodium). A less negative free enthalpy of solvation may partially explain the insolubility of $KBPh_4$ in chloroform which precluded the measurement of stability constants by Pascarella [90,p. 20]. A number of alternative solvents that would increase salt solubility without compromising acceptor properties could be tested in future experiments . Both nitromethane (DN = 2.7, AN = 20.5) and acetonitrile (DN = 14.1, AN = 19.3) appear to be good trial candidates which may have advantages over chloroform and acetone. Results from experiments conducted in these solvents could also lead to a better understanding of

preferential solvation and specific solvent-solute interactions affecting complex stability.

The complexation studies done on ligand **11** show that increasing the number of oxygen donor sites and the size of the complexation cavity resulted in an increased $K_{(K^+)}/K_{(Na^+)}$ selectivity ratio. For conformationally flexible ligands that can easily accommodate either cation, less favorable specific solvent effects (solute-solvent interactions from solvation of metal ions, and their tripodate complexes) associated with potassium ions appear to bias the selectivity towards sodium.

Determination of Relative Complexation Constants from Competition Studies

General Theory

The relative complexing abilities of some of our ligands in $CDCl_3$ have been quantified from competition experiments. The solubilization of a limited amount of salt (M^+X^-) by a binary host solution results in competing complexation equilibria (equations 11 and 12) that contribute to the overall equilibrium reaction represented by equation (13).

$$M^+X^- + L_1 \overset{K_1}{\rightleftharpoons} (ML_1^+)X^- \qquad (11)$$

$$M^+X^- + L_2 \overset{K_2}{\rightleftharpoons} (ML_2^+)X^- \qquad (12)$$

$$(ML_2^+)X^- + L_1 \overset{K_{1\&2}}{\rightleftharpoons} (ML_1^+)X^- + L_2 \qquad (13)$$

Where: L_1 and L_2 = ligands

For simplicity, the subsequent discussion will consider the typical competition experiment in which solution components (L_1:L_2:M^+X^-) are in a 1:1:1 molar ratio. The observed (ion-paired) equilibruim constant, $K^{ip}_{1\&2}$ for the competition reaction (14) can be measured and used to calculate the free energy of competition, $\Delta G^{\circ}_{1\&2}$ (15).

$$K^{ip}_{1\&2} = \frac{[(ML_1^+)X^-][L_2]}{[(ML_2^+)X^-][L_1]} \qquad (14)$$

$$\Delta G^{o}_{1\&2} = -RT \ln K^{ip}_{1\&2} \qquad (15)$$

The thermodynamic result from a competition reaction is directly related to the component stability constants (K_1 and K_2) and free energies of complexation (ΔG^{o}_1 and ΔG^{o}_2) according to equations (16) and (17) respectively (see Appendix B for derivations).

$$K_{1\&2} = K_{rel} = \frac{K_1}{K_2} \qquad (16)$$

$$\Delta G^{o}_{1\&2} = \Delta G^{o}_1 - \Delta G^{o}_2 \qquad (17)$$

Determination of Relative Complexation Equilibrium Constants.

For the determination of $K^{ip}_{1\&2}$ (or K_{rel}) it is only necessary to quantitate the fraction of total host complexed (FTHC) for one of the host components. The FTHC for the other host can be obtained by difference if it is assumed that essentially all of the salt in solution is complexed.

$$FTHC_1 = \frac{[ML_1^+]}{[L_1]_T} \qquad (18)$$

Where: $[ML_1^+]$ = concentration of complexed ligand.

$[L_1]_T$ = total ligand concentration.

When the kinetics of the complexation process are fast on the NMR time scale, the ^{13}C chemical shifts represent population-weighted averages for fully complexed and uncomplexed ligand. For a chosen ^{13}C nucleus of ligand 1, the observed chemical shift change for the competition ($\Delta\delta_{obs}$) and the maximum possible chemical shift change ($\Delta\delta_{max}$) [99] are used to calculate the FTHC (equation 19).

$$FTHC_1 = \frac{\Delta\delta_{obs}}{\Delta\delta_{max}} = \frac{|\delta_{obs} - \delta_L|}{|\delta_{ML} - \delta_L|} \qquad (19)$$

where: $\Delta\delta_{obs}$ = the observed chemical shift change of ligand 1 for the experiment.

$\Delta\delta_{max}$ = the value for the limiting chemical shift change for ligand 1 obtain other complexation experiments (see p.39).

For a slow exchange situation, separate peaks are observed for uncomplexed and complexed material, and relative peak areas [100] obtained from integrations can be used to calculate the FTHC (equation 20).

$$FTHC = \frac{I_{ML}^+}{I_L + I_{ML}^+} \qquad (20)$$

where: I_{ML}^+ = Integration of carbon resonance in complex

I_L = Integration of carbon resonance in free ligand

In a 1:1:1 competition there is only one equivalent of salt for two equivalents of host. Due to the low solubility of $NaBPh_4$ in $CDCl_3$ (1.24×10^{-6} M)[101], the fraction of salt not solubilized by one host must by default be

solubilized by the other host. Thus by difference (see Equation 21), the measured value for the fraction of total host complexed for ligand 1 ($FTHC_1$) can be used to calculate the fraction of total host complexed for ligand 2 ($FTHC_2$).

$$FTHC_2 = (1 - FTHC_1) \tag{21}$$

where: $FTHC_2$ = value obtained by difference.

$FTHC_1$ = value derived empirically (see equation 18).

The ratio of complexed to uncomplexed host for each host component in the competition experiment can be calculated using Equation (22).

$$\frac{[(ML^+)X^-]}{[L]} = \frac{FTHC}{(1 - FTHC)} \tag{22}$$

Appropriate substitution of the ratios into equation (14) will give the $K_{1\&2}^{ip}$ value for the competition reaction (13). The calculations for a 1:1:1 competition can be greatly simplified by using equation (23) or (24). (See Appendix B for derivations.)

$$K_{1\&2}^{ip} = \frac{(FTHC_1)^2}{(FTHC_2)^2} \tag{23}$$

$$K_{1\&2}^{ip} = \left|\frac{[ML_1^+]}{[L_1]}\right|^2 = \left|\frac{[L_2]}{[ML_2^+]}\right|^2 \tag{24}$$

Limitations

The competition experiment can not accurately measure the relative complexing abilities for compounds that have K's that differ by more than 3 orders of magnitude. Sometimes, two compounds cannot be directly compared by this method due to ambiguous and/or overlapping chemical shifts.

Results:

The tabulated results for all competition experiments between cyclohexane-based podands for $NaBPh_4$ in $CDCl_3$ are given in Table 19.

Table 19: Results from Competition Experiments with Tripodands and $NaBPh_4$ in $CDCl_3$.

Ligands (L_1/L_2)	Component Monitored	K_1/K_2[a]		$\Delta\Delta G^{o}_{300K}$ (kcal/mol)	
25 & 3	25	2.55	±0.27	-0.56	±0.06
26 & 3	26	<(0.002)		>(+3.7)	
21 & 4	21 & 4	0.006	±0.002	+3.1	±0.2
25 & 4	25 & 4	3.34	±0.27	-0.72	±0.05
12 & 4	4	0.02	±0.03	+2.3	±0.5
12 & 3	12	0.007	±0.003	+2.9	±0.2
12 & 6	6	7.2 ± 1.7 (x 10^{-4})		+4.3	±0.2[b]

a- Estimate of error obtained by propogation of error from chemical shift measurements.
b- Estimate or error based on a population standard deviation.

The structures and appropriate numbering schemes for the polypodand ligands referred to in the subsequent discussion are given in Figure 47.

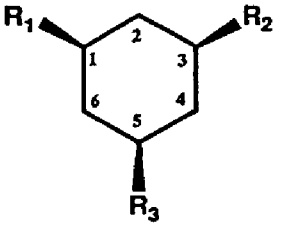

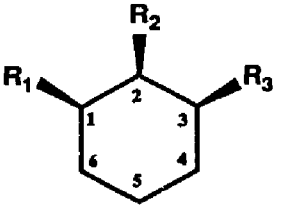

3: R's = OCH_2CH_2-OMe

25: R's = $OCH_2CH_2(CH_3)_2$-OMe

26: R's = $OCH_2CH_2(CH_3)_2$-OiPr

21: R_1 = OMe
$R_{2\&3}$ = OCH_2CH_2-OMe

12: R's = $OCH_2CH_2CH_2$-OEt

4: R's = OCH_2CH_2-OMe

6: $R_{1\&3}$ = OCH_2CH_2-OMe
R_2 ≡ H

Figure 47: Structures and Numbering Schemes for Ligands used in Competition experiments.

Some important results obtained by other coworkers are included in Table 20.

Table 20: Results from Competition Experiments Conducted by Other Co-workers for $NaBPh_4$ in $CDCl_3$.

Ligands (L_1/L_2)	Component Monitored	K_1/K_2	$\Delta\Delta G^{\circ}_{300K}$ (kcal/mol)
4 & 3	4 & 3	1.004	0.00238[a]
6 & 3	6	0.143	1.14[b]

a- Data obtained from T.Pascarella Thesis [102]
b- Data obtained from S.Shirodkar Thesis [103]

25 & 3 Competition

From competition experiments it was found that tripodand 25 has an average complex stability constant that is 2.55 times greater than that of tripodand 3. Both ligands have sufficiently slow complexation-decomplexation kinetics in $CDCl_3$ that separate sets of peaks were observed for complexed and uncomplexed ligands. Thus, changes in chemical shifts could not be used to monitor this particular experiment. Integrated peak areas for the gem-dimethyl resonances in uncomplexed and complexed 25 were used to obtain the $[ML^+]/[L]$ ratio [100], which was then used to calculate K_{rel}. (Equation 14 can only be use for a 1:1:1 competition.) Results are shown in Table 21 (see Appendix C for integration data).

Table 21: ^{13}C NMR Results from Competition Experiments with 25 versus 3 and $NaBPh_4$ in $CDCl_3$.

Competition[a] Ratio (25:3:$NaBPh_4$)	$\frac{[ML^+]}{[L]}$[b]	$\frac{K_{25}}{K_3}$	Log $K_{25\&3}$	$\Delta\Delta G_{300}^{o}$ (Kcal/mol)
1:0.5:1	2.820	2.57	0.410	-0.563
1:1:1	1.578	2.49	0.396	-0.544[c]
1:1.5:1	2.343	2.59	0.414	-0.568
Mean Values		2.55	0.407[d]	-0.558[e]

a- [3] = 0.098 M, 0.210 M, and 0.204 M, respectively.
b- Ratio obtained for tripodand 25 fromrelative digital integrations of gem-dimethyl peak areas.
c- Result from second run of 1:1:1 competition (see Appendix C).
d- Population Standard deviation, $\pm$0.008.
e- Population Standard deviation, $\pm$0.010.

The competition experiment was run three times using different ligand ratios (**21**:**3**:$NaBPh_4$ = 1:0.5:1, 1:1:1, and 1:1.5:1). The average $K^{ip}_{25\&3}$ (K_{rel}) = 2.55 obtained from these experiments indicates that the gem-dimethyl groups enhance the complexing ability of the tripodand system. The results can be explained in terms of a "gem-dimethyl effect," in which steric interactions associated with the gem-dimethyl groups favorably bias the conformation of the glycol ether arms relative to the unbiased ligand. Conformational analysis of smaller molecules (eg. dimethoxyethane and gem-dimethyl-dimethoxyethane) by molecular mechanics methods indicates that the C-C bond in glycol ethers is enthalpically gauche-favored, and that the gem-dimethyl analogs are even more enthalpically biased [104]. The "gem-dimethyl effect" also ultimately results in a more favorable entropy term for complexation of **25** versus ligand **3**.

Attempts to use ^{13}C peak heights to approximate peak areas produced inconsistent results and gross errors in the evaluation of $[ML^+]/[L]$ ratios. Nothing was gained by decreasing the NMR spectral width parameter. The increase in the point-to-point resolution did not significantly improve the accuracy of the peak height approximation of areas, while attendant spectral foldover hampered the use of digital integrations to measure peak areas.

26 & 3 Competition

The 1:1:1 competition result can only be viewed qualitatively since the sample of tripodand **26** was known to be slighty impure. In spite of the limitation placed on the experiment by sample impurity, we can surmise that **26** competes poorly against **3** for a limited amount of $NaBPh_4$.

Table 22: ^{13}C NMR Chemical Shifts from a Competition Experiment between Tripodands **26** and **3**, for $NaBPh_4$ in $CDCl_3$.

Carbon Resonance	Uncomplexed **26** (ppm)	Complexed[a] **26** (ppm)	$\Delta\delta_{max}$ (ppm)	Competition[b] (1:1:1) (**26**:**3**:Salt)
C-2,4,6	38.17	31.61	-6.57	38.17[d]
Gem-dimethyl (ethyleneoxy)	25.04	(25.43)[c]	0.39	25.04
Gem-dimethyl (isopropyl)	23.93	(21.98)[c]	-1.95	23.93

note - The sample of **26** used was not absolutely pure.
a- in the presence of excess salt, these chemical shift averaged peaks were still exchange broadened, [**26**] = 0.269 M.
b- [**26**] = [**3**] = 0.168 M.
c- chemical shift assignment tentative.
d- overlapping chemical shift with uncomplexed **3**.

Tripodand **26** exhibited chemical shift averaged peaks for complexed and uncomplexed material due to intermediate to fast exchange kinetics relative to the ^{13}C NMR timescale (20 MHz). Selected chemical shifts shown in Table 22 indicate that there is no complexed **26** for the 1:1:1 competition. It was not possible to use ^{13}C resonances in **3** to monitor the experiment due to overlapping chemical shifts with **26**. Thus only a lower limit can placed on the relative

complexing abilities of these two hosts. A conservative estimate is $K^{ip}_{26\&3} < 0.002$.

It is important to note that there is no direct connection between equilibrium thermodynamics and exchange kinetics. Nevertheless, using the "Hammond Postulate" [105] it is possible to qualitatively correlate the driving force for a given reaction with the position of the transition state along the reaction coordinate. In general we have found that faster exchange kinetics quite often correlate with weaker complexation. Thus, in addition to the thermodynamic result, the fast exchange kinetics for ligand 26 (in relation to ligand 25) implies a less stable complex too.

Substitution with terminal isopropoxy groups (iPrO-) on the oligoether arms in ligand **26** disfavors complexation relative to the methoxy substituted analog, **25**. We hypothesize that mutual steric repulsion of the bulky iPrO- groups in the triaxial complex of 26 will destabilize the complex making the reaction enthalpically less favorable.

21 & 4 Competition

Ligand **21** has averaged ^{13}C NMR spectra for mixtures of uncomplexed and complexed material due to fast exchange kinetics. It has been shown [106] that a 50/50 mixture of complexed and uncomplexed ligand **4** has averaged peaks for each set of carbon resonances except for the C-5 resonance, which has two broadened peaks 7.0 ppm apart. However, under the conditions of the competition experiment with ligands 21

and **4**, there appeared to be only one chemical shift averaged peak corresponding to the C-5 resonance in **4**. The experiment thus can be monitored from observed chemical shift changes in both host molecules. Table 23 contains the results for selected ^{13}C nuclei for the 1:1:1 competition experiment. (See Appendix C for specific chemical shifts.)

Table 23: ^{13}C NMR Results for a 1:1:1 Competition with **21** and **4** for $NaBPh_4$ in $CDCl_3$ ([**21**] = [**4**] = 0.100 M).

Carbon Resonance	Compet. $\Delta\delta_{obs}$ (ppm)	Limit. $\Delta\delta_{max}$ (ppm)	FTHC[a]	$\frac{K_{21}}{K_4}$	$\Delta\Delta G^{o}_{300}$ (Kcal/mol)
Ligand **4**					
C-5	-6.50[b]	-7.01[c]	0.927	0.0062	3.03
C-1,3	-5.33	-5.87[c]	0.908	0.0102	2.73
Ligand **21**					
C-2	-0.46	-6.70[de]	0.0680	0.00532	3.12
C-4,6	-0.39	-7.15[de]	0.0545	0.00333	3.40
C-4'	0.13	1.82[de]	0.0714	0.00592	3.05
Mean Values				0.00619[f]	3.07[g]

a- Fraction Total Host Complexed.
b- C-5 resonance appears to be chemical shift averaged with competition conditions.
c- Limiting chemical shifts measured Tom Pascarella.
d- Sample preparation by Dana Gronbeck.
e- NMR spectrum run by Shailaja Shirodkar.
f- Population Standard deviation, ±0.0025.
g- Population Standard deviation, ±0.21 Kcal/mole.

Calculation of the fraction of total host complexed (FTHC) for each host (using equation 19) shows that approximately 90% of the $NaBPh_4$ is complexed by **4**, which leaves the remaining 10% to be complexed by **21**. The relative complexation constant, $K^{1p}_{21\&4}$ was calculated using

equation (23). The observed deviation of the results can be accounted for by experimental error (with sample preparation/ digital resolution of the NMR spectrometer). The complex stability constant for **4** is at least 2 orders of magnitude greater than that for tripodand **21**, which translates into a free energy difference of at least 3.1 Kcal/mole for the competition reaction.

It can be concluded from this competition study that the cavity formed by tripodand **4** with six oxygen donor sites binds sodium ion much better than the cavity formed with five donor sites in **21**. The lower complex stability for **21** is thus due to the shorter ligating arm (i.e. the methoxy group) and the inability of the ligand to form a hexacoordinate complex with sodium.

25 & 4 Competition

It was possible to monitor the experiment using both chemical shift changes and relative integration data. The results from measuring relative peak areas for uncomplexed and complexed 25 for two different resonances is given in Table 24.

Table 24: ^{13}C NMR Results from Relative Peak Area Analysis for the 1:1:1 Competition Experiments with 25 versus 4 and $NaBPh_4$ in $CDCl_3$ ([25] = [4] = 0.0406).

Carbon Resonance (Ligand 25)	$\frac{[ML^+]^a}{[L]}$	$\frac{K_{25}}{K_4}$	Log $K^{ip}_{25\&4}$	$\Delta\Delta G^{o}_{300}$ (Kcal/mol)
C-2,4,6	1.857	3.45	0.538	-0.738
Gem-dimethyls	1.861	3.46	0.539	-0.741

a- Ratio obtained by relative digital integration of ^{13}C NMR peaks.

The existence of two unobscured pairs of resonances in 25 provided a means of establishing the accuracy of using digitally integrated ^{13}C NMR peak areas for measuring the $[ML^+]/[L]$ ratio [100]. The result from using the C-2,4,6 resonance, which could not be evaluated in a previously discussed competition (with 25 and 3), is consistent with the result obtained for the gem-dimethyl resonance.

The results from monitoring chemical shift changes in tripodand 4 are given in Table 25. Only one resonance could be used, since the others were either not observed (due to severe exchange broadening) or had chemical shift changes too small to allow accurate quantification of the FTHC.

Table 25: ^{13}C NMR Chemical Shift Results for the 1:1:1 Competition with 25 and 4 for $NaBPh_4$ in $CDCl_3$ ([25] = [4] = 0.0406).

Carbon Resonance (Ligand 4)	Compet. $\Delta\delta_{obs}$ (ppm)	Limit. $\Delta\delta_{max}$ (ppm)	FTHC[a]	Log $K^{ip}_{25\&4}$	$\Delta\Delta G^{o}_{300}$ (Kcal/mol)
C-1,3	-3.77	-5.87	0.642	0.509	-0.699
C-4,6	-0.48[b]	-1.0	0.52	-----	-----
C-5	----[c]	-7.01	----	-----	-----

a- Fraction Total Host Complexed
b- Chemical shift change too small to be measured accurately.
c- Not observed (chemical shift exchange broadened into baseline).

The assignment of the exchange-broadened C-1,3chemical shift was not obvious due to its close proximity to other resonances. The chemical shift changes for the C-4,6 were too small to be measured accurately. Under the conditions of this competition experiment, the C-5 resonance in 4 was not observed due to extreme exchange broadening. Nevertheless, the average result from the peak area analysis of 25 ($K^{ip}_{25\&4}$ = 3.45), is within experimental error of the value of $K^{ip}_{25\&4}$ = 3.23 calculated from chemical shift changes in 4. In conclusion, the $K^{ip}_{25\&4}$ = 3.34 $\pm$ 0.27 ($\Delta\Delta G^{o}_{300}$ = -0.72 $\pm$ 0.05 Kcal/mole).

12 & 4 Competition

In theory, both ligands should exhibit observable time averaged chemical shifts for complexed and uncomplexed material that can be used to follow the competition reaction. From Table 26, it can be seen that the results from the experiment were less than adequate for quantifying the relative complexing abilities of tripodands **12** and **4**.

Table 26: ^{13}C NMR Chemical Shift Results for the 1:1:1 Competition with **12** and **4** for $NaBPh_4$ in $CDCl_3$ ([12] = [2] = 0.765 M).

Carbon Resonance	Compet. $\Delta\delta_{obs}$ (ppm)	Limit. $\Delta\delta_{max}$ (ppm)	FTHC[a]	Log $K^{ip}_{12\&4}$	$\Delta\Delta G^{o}_{300}$ (Kcal/mol)
Ligand **4**					
C-1,3	----[b]	-5.87	----	-----	-----
C-4,6	-0.87[c]d	-1.0	0.87[d]	-1.7	+2.3
Ligand **12**					
C-2,4,6	+0.06[e]	-2.40[f]	----	-----	-----

a- Fraction Total Host Complexed
b- Not observed (chemical shift exchange broadened into base line).
c- Chemical shift differences too small to be measured accurately.
d- SD = ±0.088 (from propogation of error of ±0.06551 ppm.) Calculated value for K_{12}/K_4 = 0.02 ±0.03.
e- The abnormal positive shift could be due to the point to point error associated with the digital resolution for 6000 Hz (spectal width) ^{13}C NMR spectrum.
f- Limiting shift for 1:0.5 ligand/salt mixture.

It has been demonstrated [107] that the complexation of $NaBPh_4$ by **4** in $CDCl_3$ normally involves intermediate to rapid exchange kinetics that average only some of the ^{13}C NMR chemical shifts for uncomplexed and complexed material (eg.

C-5 is not averaged normally). In light of the result from the competition between **21** and **4**, it was hoped that both C-5 and C-1,3 resonances could be used to monitor FTHC of **4** in a competition experiment with **12**. Unfortunately this has not been possible, despite many trials, due to unanticipated complexation exchange kinetics for tripodand **4**. The lack of an observed C-5 resonance is probably due to extreme line broadening. In this case, it is not clear whether the C-1,3 resonance is absent because of line broadening or obscured by chemical shift equivalence with a solvent peak. A chemical shift change was measured for the C-4,6 resonance, but unfortunately the complexation-induced chemical shift change for this resonance is small and cannot be used to accurately quantify the FTHC for **4**. Based on the digital resolution of the spectrometer and the possible propagation of error, the relative complexation constant was calculated to be $K^{ip}_{12\&4} = 0.02 \pm 0.03$.

Attempts to follow the experiment in an analogous manner by using the C-2,4,6 resonance in **12** also failed to produce any conclusive results. The unexpected positive $\Delta\delta_{obs}$ can be rationalized in terms of a relative intrumental error that completely negates a small upfield shift associated with any complexed **12**. The calculation of a negative FTHC is meaningless as far as evaluating relative complexing abilities.

At best, it can be surmised that $K^{ip}_{12\&4} < 0.05$ and the $\Delta\Delta G^{o}_{300} > +1.8$ Kcal/mole. The complexation of **12** involves the organization of more atoms relative to **4**. The

difference is accounted for in the propylenoxy linkages versus the ethylenoxy linkages in the arms of the respective tripodands. Thus entropy considerations appear to favor complex formation with 4. The geometry of the cavity formed by the ligand as well as enthalpy considerations may also favor complex formation with 4.

12 & 3 Competition

The 12 & 3 competition experiment was not conducted initially since it was known that there were no obvious methods for adequately following the competition reaction. After obtaining the less than definitive result from the 12 & 4 competition it became necessary to attempt the competition with hope of at least confirming the previously obtained qualitative result.

Relative peak area analysis for the C-2,4,6 resonance in 3 was not possible because of the close proximity of the chemical shift averaged C-2,4,6 resonance in 12. Thus it was necessary to rely on changes in chemical shift for the C-2,4,6 resonance in 12. As indicated previously, it was only possible to obtain a limiting complex chemical shift for a 1:0.5 ligand/salt mixture for 12 (due to limited solubilization of $NaBPh_4$ by the ligand). The results for the 1:1:1 and the 3:1:1 (12:3:$NaBPh_4$) competition experiments are given in Table 27.

Table 27: ^{13}C NMR Chemical Shift Results for Competition Experiments with **12** and **3** for $NaBPh_4$ in $CDCl_3$.

Compet.[a] Ratio (12:3:Salt)	Compet. $\Delta\delta_{obs}$ (ppm)	Limit. $\Delta\delta_{max}$ (ppm)	FTHC[b]	$\frac{K_{12}}{K_3}$	Log $K^{ip}_{12\&3}$	$\Delta-\Delta G^{o}_{300}$ (Kcal/mol)
1:1:1	-0.39	-2.40[c]	0.0811	0.00778[dh]	-2.11	+2.89[fh]
3:1:1	-0.13	-2.40[c]	0.0270	0.00245[eh]	-2.61	+3.58[gh]

a- C-2,4,6 resonance in **12** used to monitor experiment.
For (1:1:1 ratio) [**12**] = [**3**] = 0.146 M.
For (3:1:1 ratio) [**12**] = 0.259 and [**3**] = 0.086 M.
b- Fraction Total Host Complexed
c- Limiting shift for tripodand **12** for a 1:0.5 ligand/salt ratio.
d- Error = $\pm$0.00266
e- Error = $\pm$0.00130
f- Error = $\pm$ 0.10 Kcal/mole
g- Error = $\pm$ 0.25 Kcal/mole
h- Estimate of propogated error from chemical shift measurements.

There is more inherent precision in measuring the FTHC for a ligand component with a nucleus that exhibits a large $\Delta\delta_{max}$ than a nucleus that exhibits a smaller limiting chemical shift change upon complexation. A nucleus with a marginal $\Delta\delta_{max}$ had to be used for the **12** & **4** competition, which introduces a large degree of uncertainty in results. The C-2,4,6 resonance in **12** is not an ideal nucleus for measuring an FTHC, since it was experimentally impossible to measure directly the $\Delta\delta_{max}$ for 1:1 complex formation. One equivalent of tripodand **12** in $CDCl_3$ only solubilizes 0.50 equivalent of $NaBPh_4$ salt (see section-p.39) and results in a chemical shift change of -2.40 ppm for the C-2,4,6 resonance. If this chemical shift change corresponds to a 50/50 mixture of uncomplexed and complexed ligand (1:1

complex) then by extrapolation a 100% complexed ligand in solution would exhibit a -4.80 ppm (2 x -2.40 ppm) chemical shift change for the C-2,4,6 resonance in **12**. This approximate $\Delta\delta_{max}$ was used to compute the FTHC values for the competition. The result for the 1:1:1 competition has less error than that of the 3:1:1 competition because of the larger observed chemical shift change in the former.

Both **12** and 3 are 1,3,5-trisubstituted cyclohexane analogs, in which the only significant structural difference is a propylenoxy linkage versus an ethylenoxy linkage, repectively. Thus these experiments serve as a direct approach for studying the effects of the additional arm methylenes on the relative complexing ability of **12**.

The results indicate that the complexing ability of tripodand **12** is at least two orders of magnitude less than that of **3**. This substantiates the previous result for the **12** & 4 system. It is proposed that at least part of the diminished complexing ability related to the introduction of additional carbon units in the ligating arms is a manifestation of the unfavorable entropy requirements for organization of the molecular framework into a complex conformation.

The conformational analysis of large molecules is often difficult. For this reason it has been useful to consider the conformational analysis of smaller molecules such as 1,3 dimethoxypropane and 1,2 dimethoxyethane, which are representative of the polyether substitutuents in ligands **12** and 3 respectively. The favored conformation for the single

C-C bond in dimethoxyethane (DME) is gauche while the C-O bonds are anti-preferred (see Figure 48) [108a].

Figure 48. Favored Conformation of DME

The favored conformations for 1,3-dimethoxypropane (DMP) are ag^+g^+a (or ag^-g^-a) and aag^+a (aag^-a) (see below) [108a].

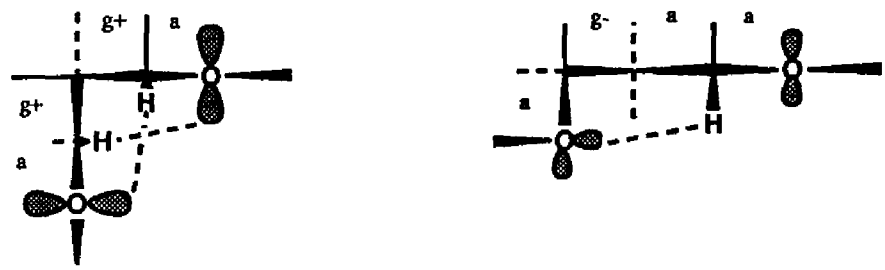

Figure 49. Favored Conformations for DMP

Analysis of CPK models shows that the probable uncomplexed conformations of the 1,5-dioxa grouping in 12 must be altered considerably in order to provide a cavity capable of binding sodium ion. An approximate $ag^{\pm}g^{\pm}a$

conformation of the ligating arms (with a triaxial cyclohexane ring conformation) yields a very large cavity not appropriate for Na^+, while the $aag^{\pm}a$ conformation has no cavity.

A less favored g^+g^- conformation must be adopted for the two internal O-C-C-C-O torsion angle bonds in the podal linkages in order to have an complex conformation capable of accommodating a sodium sized cation. It must be noted that low energy distortions of a non-rigid pure diamond lattice structure probably occur to adjust the cavity size to the particular cation.

This is quite different from complexation of ligand 3 which involves the conformational biasing of a 1,4-dioxa grouping in the ligating polyether arms. Fewer degrees of freedom are lost upon complexation of 3 (relative to 12), which probably makes the overall process entropically more favorable (or less unfavorable).

The favored gauche conformation for the 1,4-dioxa grouping (with a triaxial cyclohexane ring conformation) is suitable for forming a sodium sized binding site. Thus the complexation process is also favored enthalpically. Our results have been consistent with Dale's comparison and conformational analysis of 1,4-dioxa and 1,5-dioxa units in crown ethers [108b-c].

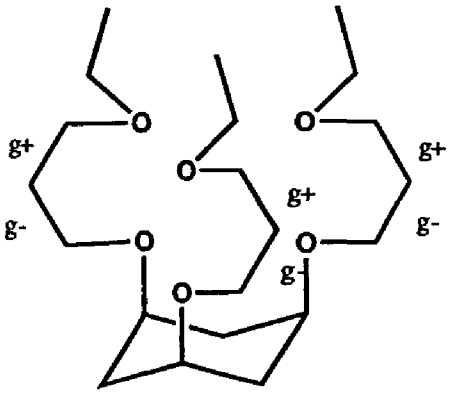

Figure 50: Triaxial Conformation for Ligand 12

It would be desirable to know the relative enthalpy and entropy contributions to the observed $\Delta\Delta G^{\circ}_{300}$ = 2.9 Kcal/mole for the 1:1:1 competition reaction. However, the attendant experimental difficulties place this out of our reach. It can be concluded that the substitution of arm ethyleneoxy units in our tripodand ligands with propylenoxy units adversely affects the thermodynamic stability of the $NaBPh_4$-ligand complex in $CDCl_3$.

Competition **12** & **6**

The relative complexation constant for the competition between **6** and **3** has been determined to be $K^{ip}_{7\&1} = 0.143$ (See Table 20) by S. Shirodkar via analogous ^{13}C NMR experiments [109]. In light of the apparent weaker complexing ability of **6** it was expected that $K^{ip}_{12\&6}$ could be measured more accurately than $K^{ip}_{12\&4}$ or $K^{ip}_{12\&3}$, and that the relative magnitudes would be $K^{ip}_{12\&4} \cong K^{ip}_{12\&3} < K^{ip}_{12\&6} < 1$. The results for the 3:1:1 and the 6:1:1 (**12**:**6**:$NaBPh_4$) competition experiments are given in Tables 28 and 29 respectively.

Table 28: ^{13}C NMR Chemical Shift Results for the 3:1:1 (**12**:**6**:$NaBPh_4$) Competition in $CDCl_3$ ([**12**] = 0.245 M & [**6**] = 0.081 M).

Carbon Resonance	Compet. $\Delta\delta_{obs}$ (ppm)	Limit. $\Delta\delta_{max}$ (ppm)	FTHC[a]	$\frac{K_{12}}{K_6}$	$\Delta\Delta G^{o}_{300}$ (Kcal/mol)
Ligand **6**[b]					
C-1,3	-1.88	-1.95[c]	0.964	4.51×10^{-4}	+4.59
C-2	-2.41	-2.54[c]	0.949	9.37×10^{-4}	+4.16
C-4,6	-3.97	-4.16[c]	0.954	7.41×10^{-4}	+4.30
C-5	-6.76	-7.09[c]	0.953	7.71×10^{-4}	+4.27
Mean Values				7.24×10^{-4}[d]	+4.33[e]
Ligand **12**					
C-2,4,6	-0.06	-2.40[f]	0.012	4.956×10^{-4}	+4.54

a- Fraction Total Host Complexed
b- Synthesis of **6** done by S. Shirodkar.
c- Limiting chemical determined by S. Shirodkar [109].
d- Population Standard Deviation, $\pm 1.74 \times 10^{-4}$
e- Population Standard Deviation, ± 0.16 Kcal/mole
f- Limiting shift for 1:0.5 ligand/salt mixture.

For the 3:1:1 competition it was possible to monitor resonances in both ligand components. The mean value of $K^{ip}_{12\&6}$ = 7.24 ± 1.74 (x 10^{-4}) obtained from following dipodand 6 should be more accurate than the single value corresponding to C-2,4,6 in tripodand 12. The larger limiting chemical shift changes coupled with the advantage of a statistical average tends to diminish the effect of instrumental error. Also the use of the C-2,4,6 resonance in 12 is based on two questionable assumptions: first, that tripodand 12 and $NaBPh_4$ primarily form a 1:1 complex; and second, that an experimental chemical shift change for a 1:0.5 ligand/salt mixture can be extrapolated to the chemical shift change for 1:1 complex formation.

The purpose of running the 6:1:1 (**12**:**6**:$NaBPh_4$) competition was to confirm the 3:1:1 result as well as obtain a more accurate value for $K^{ip}_{12\&6}$. It was anticipated that the increase in the relative molar concentration of the weaker complexer tripodand 12 would decrease the amount of complexed 6, which would translate into larger measured chemical shift differences (between $\Delta\delta_{obs}$'s and $\Delta\delta_{max}$'s for ligand 6) which would have less relative error. The 6:1:1 molar ratio also effectively eliminates the possibility for using the C-2,4,6 resonance in 12 since the expected chemical shift change is too small to be measured.

Table 29: ^{13}C NMR Chemical Shift Results for the 6:1:1 (12:6:$NaBPh_4$) Competition in $CDCl_3$ ([12] = 0.237 M & [6] = 0.073 M).

Carbon Resonance	Compet. $\Delta\delta_{obs}$ (ppm)	Limit. $\Delta\delta_{max}$ (ppm)	FTHC[a]	$\frac{K_{12}}{K_6}$	$\Delta\Delta G^{o}_{300}$ (Kcal/mol)
Ligand **6**[b]					
C-1,3	-1.90	-1.95[c]	0.974	1.13×10^{-4}	+5.42
C-2	-2.47	-2.54[c]	0.972	1.31×10^{-4}	+5.33
C-4,6	-4.09	-4.16[c]	0.983	4.81×10^{-5}	+5.93
C-5	-7.02	-7.09[c]	0.990	1.64×10^{-5}	+6.57
Mean Values				7.70×10^{-5}[d]	+5.81[e]
Ligand **12**					
C-2,4,6	-0.10[f]	-2.40[g]	-----[h]	----	----

a- Fraction Total Host Complexed
b- Synthesis of 6 done by S. Shirodkar.
c- Limiting chemical shifts obtained from S. Shirodkar Thesis [109].
d- Population Standard Deviation, $\pm 4.65 \times 10^{-5}$
e- Population Standard Deviation, ± 0.49 Kcal/mole
f- Expected value $\cong$ 0.03 ppm.
g- Limiting shift for 1:0.5 ligand/salt mixture (ligand **12**).
h- Too small to be measured.

In fact, the results indicate that the FTHC (Fraction Total Host Complexed) for dipodand 6 in the 6:1:1 competition is larger than the corresponding value in the 3:1:1 competition experiment. Instead of competing for salt more effectively, the increased relative concentration of tripodand **12** actually enhances the formation of complexed dipodand **6**. The most likely explanation for this uncharacteristic result is that the limiting chemical shifts used in previous experiments (1:1:1 competitions) are

invalid at high concentrations of ligand **12**. Another possibility is that at higher ligand concentrations the original assumption that primarily 1:1 complexation predominates may also be invalid. Nevertheless, the results still indicate that $K_{12}^{ip} < K_{6}^{ip}$.

Thecompetition results can be summarized in terms of a proposed relative order of stability constants (see Equation 25).

$$K_{12}^{ip} < K_{6}^{ip} < K_{3}^{ip} \cong K_{4}^{ip} \qquad (25)$$

The tripodands **3** and **4** are stronger complexers and have been demonstrated to form primarily 1:1 complexes with $NaBPh_4$ in both $CDCl_3$ and acetone solvents [110]. It has also been shown that dipodand **6** will form a 1:1 complex in $CDCl_3$ but is a weaker ligand than **3** [111]. Tripodand **12** is a still weaker ligand which complexes approximately half of an equivalent of salt in $CDCl_3$.

One rationalization for the **12** & **6** competition results is that in addition to 1:1 ligand/salt complexes, 2:1 and greater complex ratios are viable components of the competition reaction equilibrium. It is unlikely that rigid 2:1 complexes are formed in solution but rather 1:1 complexes are stabilized by association with free ligands with favorable solvent donor properties. These ligand

solvent properties can only become apparent when both components in a competition form less stable 1:1 complexes and when overall ligand concentrations are high.

In conclusion, it appears that the normal assumptions made about complexation stoichiometry for competition reactions between strong complexers do not apply to analogous reactions involving ligands having intermediate to weak complexing ability.

T_1(^{13}C NMR) Relaxation Studies

The use of ^{13}C longitudinal (spin-lattice) relaxation times (T_1's) has been found to be a useful probe of the dynamics and structure of macrocyclic complexes in solution [112-118]. This probe is directly applicable to the study of systems (such as our polypodands/polypodates) that involve complexation via conformational biasing of the ligand. One of the first applications of longitudinal relaxation times (T_1's) in the area of host-guest chemistry was for the study of the macrocylic antibiotics valinomycin and nonactin and the polyethers dicyclohexyl-18-crown-6 and dibenzo-18-crown-6 [119]. These compounds are all known to complex metal cations selectively and aid in ion transport across membranes. These early experiments illustrated the general utility of T_1 measurements for understanding complexation related conformational changes as well as for the elucidation of transport mechanisms. More recently, T_1's have been used to study the complexation of neutral molecules (eg. malononitrile) by crown ethers and study macrocyclic hosts exhibiting a high degree of preorganization of the molecular structure [120]. To date, ^{13}C longitudinal relaxation experiments have been used to monitor the conformational changes resulting from complexation by ligands such as podands [121], tetraazamacrocycles [122], crown [123] and lariat ethers [124], and cryptands [125].

General Theory

With the advent and application of Fourier transform methods to ^{13}C NMR, it was found that the ^{13}C nucleus is particularly suited to relaxation studies. Since carbon predominantly forms the backbone of organic molecular structures, the analysis of relaxation data is not complicated by intermolecular relaxation which is typical of experiments focusing on ^{1}H and ^{19}F nuclei. Under proton-decoupled conditions, each carbon resonance appears as a single spectral line whose longitudinal and transverse relaxation processes are governed by single exponential time constants (T_1 and T_2 respectively) [126]. The large chemical shift range in ^{13}C NMR facilitates the resolution of many individual carbons, providing more available sites at which to probe the motional behavior of complex molecular structures [116]. Due to the low natural abundance of ^{13}C, complications that would otherwise arise from ^{13}C-^{13}C dipolar interactions and the spin-diffusion phenomenon are eliminated, simplifying the interpretation of the relaxation data [116].

Longitudinal and transverse relaxation are often referred to in the literature as "spin-lattice" and "spin-spin" relaxation respectively, and correspond to T_1 and T_2 measurements. ^{13}C spin-relaxation measurements and their application to organic chemistry have been thoroughly reviewed in the literature [112-118]. The following discussion will mainly address spin-lattice relaxation by

the dipole-dipole mechanism and the relationship of the dipole-dipole T_1's (T_1^{DD}) to molecular dynamics.

Spin-lattice relaxation results from interaction between excited nuclear spins (in this case ^{13}C nuclei) and the liquid or solid lattice environment. By one or more mechanisms, involving fluctuating localized magnetic fields at or near the nucleus being relaxed, energy is transferred between the nuclear spins and the lattice so as to restore thermal equilibrium to the system. The spin-lattice relaxation rate [127] is governed by an exponential time constant (T_1) for the decay of spin excitation. The magnitude of a T_1 is dependent on the efficiency of energy transfer between the spin system and the lattice environment.

For organic substrates, ^{13}C spin-lattice relaxation usually occurs via the ^{13}C-^{1}H dipole-dipole mechanism (DD) [128]. Dipole-dipole relaxation is based on fluctuating local magnetic fields arising from the reorientation of neighboring magnetic nuclei relative to the external magnetic field B_o. The efficiency of energy transfer between a ^{13}C spin and the lattice is dependent on the number of attached ^{1}H nuclei and on molecular reorientation.

Assuming that the motional narrowing limit conditions apply [129], T_1^{DD}'s are directly related to the overall molecular mobility (tumbling) and specific motion (determined by internal degrees of freedom)(See Fig.51). For rigid molecules rotating isotropically, the molecular

motion can be described by a single rotational correlation time, τ_c [130]. The τ_c is a function of frictional and inertial effects [131] and is inversely proportional to the T_1^{DD} time.

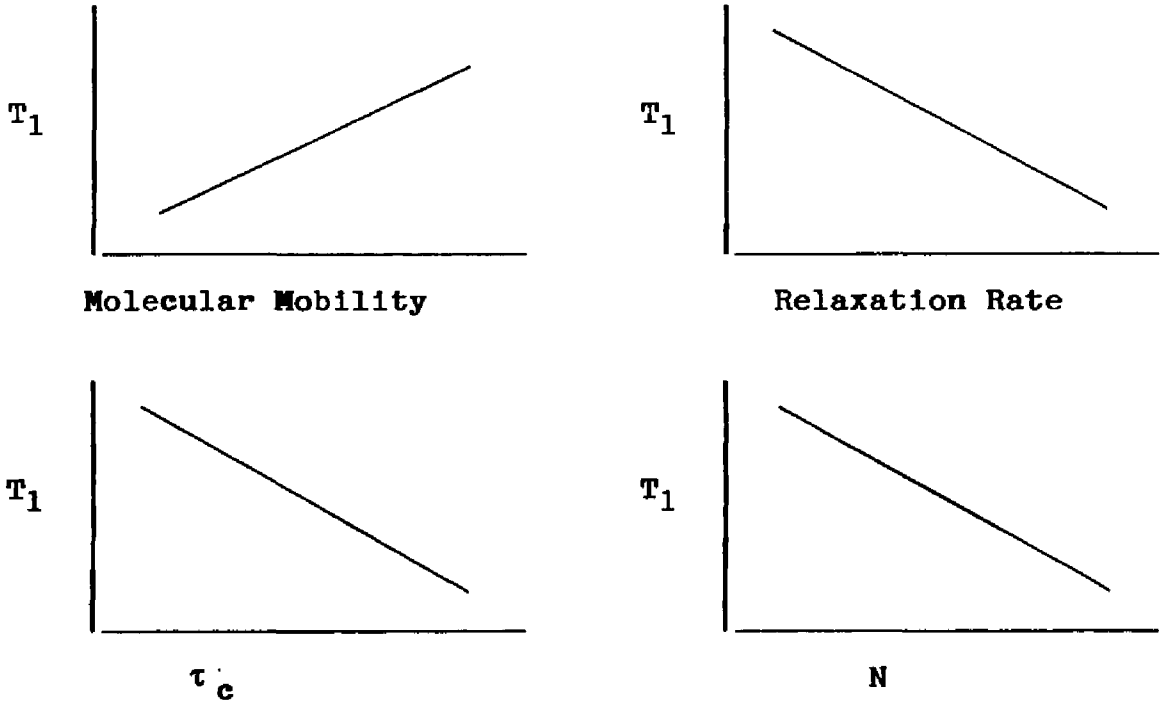

where:

T_1 = ^{13}C T_1^{DD} (Dipolar relaxation time measurement)

τ_c = Rotational Correlation time

N = Number of attached Hydrogens

Figure 51: Relationships between T_1 and Various Relaxation Parameters under Motional Narrowing Conditions.

Larger bulkier molecules tend to rotate more slowly and thus have large τ_c's. Slower molecular reorientation allows for greater spin-lattice interaction and more efficient energy transfer, which results in faster nuclear relaxation and shorter T_1^{DD}'s. For very small, rapidly rotating molecules

and very large, slowly rotating macromolecules and polymers (MW > 1000), the motional narrowing conditions are not satisfied and thus increased motion does not always result in increased spin-lattice relaxation times.

Non-isotropic motion resulting from conformational flexibility and/or anisotropic tumbling will also affect dipolar relaxation (and T_1^{DD}'s) and invalidates the characterization of molecular reorientation with a single correlation time, τ_c. In such situations, comparison of T_1^{DD}'s (discussed later) within a given molecular structure can confirm the presence of segmental and anisotropic motion.

Segmental Motion:

Conformational changes are the result of specific motion or segmental motion resulting from internal degrees of freedom in a molecular structure. In order to detect this non-isotropic motion with ^{13}C T_1^{DD} measurements, the segmental motion must equal or exceed the motion due to overall tumbling or Brownian motion [132]. The multiple degrees of freedom inherent in specific motion usually obviate quantitative theoretical representation by formulas. It has been demonstrated that for an aliphatic chain the T_1^{DD}'s of methylene carbons increase with increasing distance from the anchoring point [133]. Similar results are to be expected for polyethylene oxide ether chains, $(-CH_2CH_2O-)_n$. The use of ^{13}C relaxation times for the determination of the degree of side arm participation in

sodium complexation by carbon- and nitrogen-pivot lariat ethers illustrates their applicability to host-guest chemistry [134].

Anisotropic Tumbling

Unsymmetric molecules are susceptible to frictional, inertial, and electrostatic effects that result in anisotropic rotational diffusion and a preferred axis of rotation. Rotation around the C_2 axis running the length of the rod-shaped molecule, diphenyldiacetylene, is favored since the moment of inertia is lower than that for rotation around any other axis. Due to this rotational behavior the ortho and meta carbons in the phenyl rings have an increased molecular mobility and interact less with the lattice environment. The para carbons on the C_2 axis remain unaffected by this favored mode of rotation and thus have lower T_1^{DD} times (Fig. 52) [135]. The unusually large ratio of $T_1(\underline{o},\underline{m})/T_1(\underline{p}) = 5$ is a clear indication of anisotropic molecular reorientational mobility. The anisotropic motion may be quantitatively treated in terms of a rotational diffusion tensor [136] which replaces the single correlation time used to describe isotropic behavior [137], but a discussion of this treatment is beyond the scope of this section.

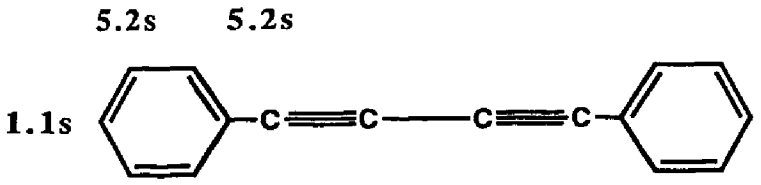

Diphenyldiacetylene

Figure 52:

Internal Rotation

Rapid internal rotation for methyl groups is another form of specific (anisotropic) motion that results in T_1^{DD} values being higher than would be expected for simple isotropic overall motion. In some instances methyl rotation can be so fast as to allow other relaxation mechanisms (spin-rotation) to compete with the dipolar relaxation of these nuclei [138]. It has been established that the T_1^{DD} for a methyl group acting as a free rotor is 9 times greater than the T_1^{DD} for a methyl in a completely locked orientation [139]. The contribution of internal rotational motion to the relaxation of methyl nuclei can be assessed from $T_1(CH_3):T_1(CH)$ ratios within a molcule. For a molecule exhibiting overall isotropic motion, a locked methyl group should relax three times faster than a methine carbon in the backbone structure of the molecule ($T_1(CH_3):T_1(CH)$ = 1:3.) The relaxation rates are simply proportional to the number of attached protons. A methyl acting as a free rotor will relax three times slower than a methine carbon in the same

molecule ($T_1(CH_3):T_1(CH)$ = 3:1). It is important to note, that methyl rotational mobility is not intrinsically affected by steric compression. [138]. This is illustrated by the T_1^{DD}'s for hemimellitene, which show that the more sterically perturbed 2-CH_3 has a greater mobility than the 1,3-CH_3 and essentially acts as a free rotor ($T_1(CH_3):T_1(CH)$ = 3:1) [140].

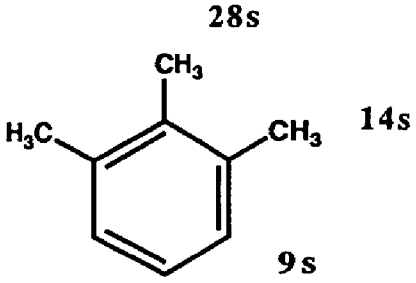

Figure 53: **Hemimellitene**

When comparing the molecular mobilities of CH_3, CH_2 and CH's it is useful to first multiply the T_1^{DD} times by the number of attached hydrogens to get the "NT_1^{DD}" values [141]. The ratio of NT_1^{DD}'s for $CH_3:CH_2:CH$ will be approximately 1:1:1 for a molecule if it is rotating isotropically and there is no specific anisotropic motion. Observed deviations from a 1:1:1 relationship of NT_1^{DD} values are a measure of the degree of motional anisotropy in a system. Because unequal molecular dimensions and conformational flexibility (as well as other factors) affect molecular dynamics and thus the dispersion of the NT_1^{DD} values, it is often difficult to pinpoint the specific origin of anisotropic behavior in some molecules.

Measuring NOE (Nuclear Overhouser Enhancement)

It is important to note that only T_1^{DD}'s are directly related to molecular mobility and thus useful for the study of molecular dynamics. Even though the ^{13}C-^{1}H dipole-dipole (DD) mechanism tends to dominate longitudinal relaxation in most molecules, this must be confirmed for each ^{13}C nucleus studied through nuclear Overhauser enhancement (NOE) measurements. In order to assume that $T_1^{(obs)} = T_1^{DD}$ and that relaxation is dominated by the DD mechanism, a 90% or better NOE must be observed. The assumption that a full NOE is to be expected whenever relaxation is dominated by the DD mechanism is not generally valid outside of the motional narrowing limits [142]. For our host systems (i.e. size and MW) the motional narrowing limits should apply.

Measurement of Podand and Podate T_1's

The ^{13}C-T_1^{DD} and NOE measurements made for uncomplexed and fully complexed podand 3 with $NaBPh_4$ in $CDCl_3$ are recorded in Tables 30 & 31. The T_1^{DD}'s were obtained by a standard inversion-recovery technique [143] on a JEOL FX-90Q spectrometer operating at 22.5 MHz, while the NOE measurements were made on a high field Bruker AM360 NMR spectrometer operating at 91 MHz [144].

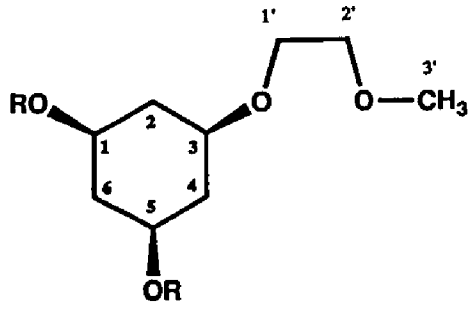

3

Figure 54: Carbon Numbering Scheme

Table 30: Results of ^{13}C-T_1^{DD} and NOE Measurements for Uncomplexed 3 in $CDCl_3$.

Carbon #	^{13}C-shift (ppm)	T_1^{DD}[a] (sec.)	% NOE[bc]	NT_1^{DD} (sec.)
C-1,3,5	73.75	1.2	96	1.2
C-2,4,6	37.98	0.5	92	1.0
C-1'	67.57[d]	1.4	103	2.8
C-2'	72.12[d]	2.1	102	4.2
C-3'	58.99	5.7	100	17.1

a- Estimated Standard deviation = ±8% (see ref. [134]).
b- Estimate of error ± 5%.
c- Fully decoupled (Full NOE) and gated decoupled (No NOE) ^{13}C NMR spectra obtained by K.S. Gallagher (UNH instrumentation).
d- Chemical shift assignments tentative [145].

Table 31: Results of ^{13}C-T_1^{DD} and NOE Measurements for Complexed 3 with $NaBPh_4$ in $CDCl_3$.

Carbon #	^{13}C-shift (ppm)	T_1^{DD}[a] (sec.)	% NOE[bc]	NT_1^{DD} (sec.)
C-1,3,5	73.55	1.7	90	1.7
C-2,4,6	30.70	(2.9)[e]	83	(5.8)[e]
C-1'	67.31[d]	1.3	92	2.6
C-2'	71.67[d]	1.2	92	2.4
C-3'	58.99	5.5	92	16.5

a- Estimated Standard deviation = ±8% (see ref. [134]).
b- Estimate of error ± 5%.
c- Fully decoupled (Full NOE) and gated decoupled (No NOE) ^{13}C NMR spectra obtained by K.S. Gallagher (UNH instrumentation).
d- Chemical shift assignments tentative [145].
e- Since NOE < 90%, the assumption that $T_1^{(obs)} = T_1^{DD}$ is no longer justified.

From the NT_1^{DD} values it is evident that the molecular mobility for uncomplexed tripodand 3 is not isotropic. The higher NT_1^{DD} values for the C-1', C-2' and C-3' carbons in the podal groups are probably a manifestation of specific (anisotropic) motion. Segmental motion for the podal methylenes should increase with distance from the anchor point on the cyclohexane ring. One conclusion that can be drawn is that the original tentative chemical shift assignments [145], C-1'= 67.57 ppm and C-2'= 72.12 ppm are in fact correct. The large NT_1^{DD} value for C-3' can be rationalized in terms of segmental motion and internal rotation of the methyl group.

The relaxation time results can be used to shed new light on the tentative chemical shift assignments [145] for the podal methylenes (C-1' & C-2') in Na^+-3. Indirectly the T_1^{DD} results for uncomplexed 3 indicate that C-1'= 67.31 ppm and C-2'= 71.67 ppm for the complex but ultimately the definitive assignments of these carbons must wait.

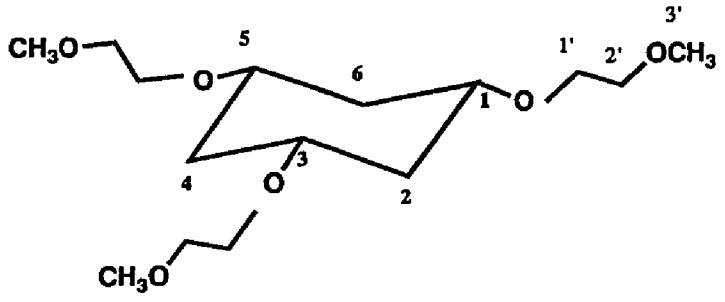

Figure 55: Triequatorial Conformation of Ligand 3

The triequatorial conformation of **3** is conducive to roughly isotropic reorientation for the cyclohexane ring and anisotropic behavior for the podal carbons. The latter is most likely due to specific motion (derived from the greater conformational flexibility of podal groups relative to the ring), rather than due to overall anisotropic tumbling. It is probably safe to assume that the overall rotational correlation time for **3** is comparatively long due to the extended ligand geometry which must sweep through more solvent upon rotation than a compact spherically shaped ligand.

The relaxation results seem to indicate that the sodium complex, Na^+-**3** rotates in a roughly in an isotropic manner. The reliability of the C-2,4,6 for monitoring molecular mobility in the complex is questionable since the observed NOE is less than 90%. If we assume the methyls act as free rotors, dividing the $NT_1^{DD}(CH_3\text{-free rotor})$ by a factor of nine should crudely compensate for the motional contribution from spin rotation to give $NT_1^{DD}(CH_3\text{-locked}) = 1.8$. This value along with the remaining three NT_1^{DD}'s indicates low overall anisotropic reorientational mobility in the complexed structure. The similar T_1^{DD}'s for the podal methylenes is consistent with a relatively rigid triaxial complex conformation. Complexation of sodium involves an induced cyclohexane ring inversion that organizes the oxygen donor sites in the podal groups. Hexacoordination with the sodium cation thus removes conformational flexibility. This is clearly reflected in the fact that all the podal T_1^{DD}'s

decrease from uncomplexed to complexed ligand. The ring methine NT_1^{DD}'s suggest that the overall molecular reorientational mobility increases upon complex formation. This can be rationalized in terms of a compact spherical complex geometry that rotates more freely in solution.

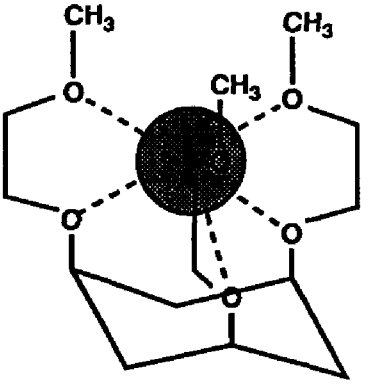

Figure 56: Triaxial Conformation of Na^+-3

The nature of the association between Na^+-3 and the BPh_4^- counter ion is still unclear. A free positively charged complex might be expected to be susceptible to electrostatic interaction with the solvent lattice, decreasing overall rotational mobility. An intimate ion pair would drastically increase the molecular mass of the complex relative to uncomplexed ligand and possibly introduce a preferred axis of rotation or center of inertia. Solvent separated ion pairing may sufficiently satisfy the electrostatic needs of the positively charged sodium complex without significantly affecting the overall reorientational

mobility but generally is not favored by a nonpolar solvent such as $CDCl_3$. Given the lipophilic nature of both ions it is conceivable that individual ion mobilities are not significantly restricted by contact ion pairing.

Other T_1 Relaxation Mechanisms

From the NOE result for the C-2,4,6 nucleus (Na^+-3) it must be concluded that $T_1^{(obs)} \neq T_1^{DD}$ and that this nucleus cannot be used to directly monitor molecular mobility. As indicated in the above discussion, a less than full NOE is expected when the DD mechanism does not dominate spin-lattice relaxation. Other spin-lattice relaxation mechanisms, such as spin-rotation (SR), chemical shift anisotropy (CSA) and scalar (SC) relaxation can contribute to the observed relaxation time, $T_1^{(obs)}$. Assuming the extreme spectral narrowing condition applies, T_1^{DD} can be calculated from the $T_1^{(obs)}$ and the measured NOEF (Nuclear Overhouser Enhancement Factor) using equation 26 [146].

$$T_1^{DD} = T_1^{(obs)} * \frac{1.98}{NOEF_{(obs)}} \qquad (26)$$

Thus the calculated T_1^{DD} and the corresponding NT_1^{DD} (for C-2,4,6 in Na^+-3) are 3.9 and 7.8 seconds, respectively. This represents a relatively large molecular mobility which we are unable to explain readily[147].

Any increase in the overall reorientation rate upon complex formation would also increase the mobilities of the

ring methines, which was not observed. We do not find interpretation of this result in terms of specific motional behavior on the part of the ring methylenes to be possible.

The introduction of a competing spin-lattice relaxation mechanism(s) is a result of (not the cause of) the increased mobility of the ring methylenes. Under our experimental conditions (low magnetic field, 22.5 MHz) it is unlikely that the CSA mechanism competes significantly with the DD mechanism [148].

The SR mechanism is most efficient for relaxation in small, rapidly tumbling molecules at higher temperatures or in the vapor phase [112, pg.137]. The SR mechanism usually operates at the expense of the DD mechanism. Increased molecular mobility always decreases the efficiency of the DD mechanism and if it increases the angular momentum it increases the efficiency of the SR mechanism. The fact that all the NOE's decreased upon complex formation can be rationalized by the increased efficiency of the SR mechanism. This is consistent with the idea that complex formation results in a more compact spherically shaped molecular structure which should have greater angular momentum and overall reorientational mobility. If the SR mechanism is more prevalent in the complexed ligand, it should affect all the nuclei equally, which still does not explain the result obtained for C-2,4,6 (in Na^+-3).

By the process of elimination, the only mechanism left to consider is the SC mechanism. This mechanism affects ^{13}C spin-lattice relaxation when either chemical exchange or

rapid quadrupolar relaxation of the spin-coupled nucleus prevails or electrons cause rapid modulation of the spin-spin (scalar) coupling between ^{13}C and another spin (nucleus or electron) [148]. The former situation may be operative in our ligands, since the complexation-decomplexation equilibrium can result in a rapid fluxional exchange of the proton positions on C-2,4,6.

In light of the intent and limitations of this experiment, the above discussion as it pertains to a mechanistic rationalization of spin-lattice relaxation must be viewed as hypothetical. Given future relaxation studies on this system, a better picture may be formulated of the particular mechanistic contributions to ^{13}C spin-lattice relaxation.

III. EXPERIMENTAL SECTION

General Experimental

Instrumentation:

^{1}H NMR Spectra were recorded on a Varian EM-360A continuous wave spectrometer. All chemical shifts are reported relative to the internal reference, $(CH_3)_4Si$.

^{13}C NMR (low field) Measurements were performed at 22.5 MHz on a JEOL FX90Q Fourier transform NMR spectrometer equipped with a quadrature phase detection system. All chemical shifts are reported relative to the internal reference, $(CH_3)_4Si$.

^{13}C NMR (high field) Spectra were obtained through the University Instrumentation Center at 91 MHz on a Bruker AM-360 fourier transform NMR spectometer. All chemical shifts are reported relative to the internal reference, $(CH_3)_4Si$.

Infrared Spectra were recorded on a Perkin-Elmer 283B grating infrared spectrometer. Absorptions were reported in wave numbers (cm^{-1}), with polystyrene (1601 cm^{-1}) as the calibration peak.

Low Resolution Mass Spectra were obtained through the University Instrumentation Center on a Perkin-Elmer Hitachi RMU-60 mass spectrometer.

High Resolution Mass Spectra were obtained from the Massachusetts Institute of Technology Mass Spectrometry Facility in Cambridge, Massachussetts.

CHN Analyses were obtained through the University Instrumentation Center on a Perkin-Elmer 240B elemental analyzer.

Hydrogenations were run in a Parr Series 4500 medium pressure hydrogenation apparatus.

Melting Points were recorded on a Thomas Hoover capillary melting point apparatus, and are uncorrected.

Solvents:

NMR: All deuterated solvents were used as obtained from Stohler Chemcals or Aldrich Chemical Company and stored over 3A molecular sieves.

Acetone: Reagent grade acetone was fractionally distilled from K_2CO_3 prior to use.

DMF: Dimethylformamide was vacuum distilled from CaH_2 and stored over molecular sieves.

THF: Tetrahydrofuran was freshly distilled from purple sodium benzophenone ketyl under a nitrogen atmosphere and used immediately.

CH_2Cl_2: Methylene chloride was distilled from CaH_2 and stored over molecular sieves.

n-Hexane was distilled from CaH_2 and stored over molecular sieves.

Pyridine was distilled from CaH_2 and stored over 3A molecular sieves.

Ethanol: Absolute ethanol was used without further purification and stored over molecular sieves.

Methanol for hydrogenations was J.T Baker spectrophotometric grade, used without further purification.

Anhydrous Ether: Baker Analyzed anhydrous ether was stored over sodium wire and used immediately.

Purified Ether: Baker Analyzed "purified" ether was used as obtained without further purification.

Column Chromatography Adsorbents:

Alumina: Baker Analyzed aluminum oxide powder "suitable for chromatography" was used as obtained from J.T. Baker Chemical Company.

Silica gel: 60-200 mesh Baker Analyzed silica gel "suitable for chromatography" was used as obtained from J.T. Baker Chemical Company.

Reagents:

cis,cis-1,3,5-cyclohexanetriol was prepared according to the method described by Caywood [150] as well as Steinacker and Stetter [151].

Methyl 3,4,5-trihydroxybenzoate was used as obtained from Aldrich Chemical Company.

1,4,7-trioxaoctyl-tosylate (2-(2-Methoxyethoxy)ethyl p-toluenesulfonate) was prepared by D.A. Gronbeck according to a variation of the method of Kyba et al. [152].

Cis,cis-1,2,3-Tris-(1,4-dioxapentyl)cyclohexane (4) was prepared by T. Pascarella [153a].

Cis-1,3-Bis-(1,4,7-trioxaoctyl)cyclohexane(6) was prepared by S. Shirodkar [154].

Allyl bromide was used as obtained from Aldrich Chemical Company.

2-Methoxyethanol was used as obtained from J.T. Baker Chemical Company.

3-Ethoxypropanol was used as obtained from Aldrich Chemical Company.

Sodium Hydride: NaH was obtained from Alfa Chemical Co. as a 57% dispersion in mineral oil. Mineral oil was removed prior to use by repeated washings with dry n-hexane under an N_2 atmosphere.

5% Rhodium on Alumina was used as obtained from the Aldrich Chemical Company.

Mercuric acetate ($Hg(OAc)_2$) was purchased from Aldrich Chemical Company and used without further purification.

$CrO_3(py)_2$ Complex: Chromium trioxide-pyridine complex was prepared according to the method of Dauben et al.[155]

Miscellaneous Chemicals

Tosyl Chloride (p-Toluenesulfonyl chloride) was used as obtained from Aldrich Chemical Company.

CrO_3 was obtained from Fisher Scientic and dried over P_2O_5 under reduced pressure.

$NaBPh_4$ (sodium tetraphenyl borate) was Baker Analyzed Rgt. (99.5%) as obtained from Aldrich Chemical Company.

$KBPh_4$ was prepared by T. Pascarella [153b].

Celite (Diatomaceous Earth Powder) was use as obtained from VWR Scientic Company.

Syntheses

2-Methoxyethyl p-toluenesulfonate (9)

Tosylate 9 [156] was prepared according to a variation of the method of Kyba *et al.* [152]. To an ice-cold 1.0 M solution of p-toluenesulfonyl chloride (190.65 g, 1.000 mol) in dry CH_2Cl_2 (1000 mL) was added an ice-cold solution of 2-methoxyethanol (76.096 g, 1.000 mol) and pyridine(158.20 g, 2.000 mol) in CH_2Cl_2 (1000 mL). The flask was tightly stoppered and stored at 10 °C for 5 days (at which time large pyridinium chloride crystals had formed). The cold reaction mixture was washed with ice-cold water (4x 250 mL) followed by ice-cold 10% aqueous HCl (2x 500 mL) to remove residual pyridine. All aqueous washes were combined and back-extracted with 250 mL of CH_2Cl_2. The original and back-extract organic phase were subsequently worked up separately. The original organic phase was washed with another 2x 500 mL of water before being dried over anhyd Na_2SO_4 for 24 h. The dry organic solution was vacuum filtered and the solvent was removed under reduced pressure to yield 180.36g of clear product oil **9**, which was combined with 13.52g of product obtained from the similar workup of the back-extract. The total reaction yield of 9 was 193.88 g (84%) which was used without further purification for subsequent alkylation reactions. The ^1H NMR spectrum of a sample of the product was consistent with the structure [Lit. 156]; ^1H NMR ($CDCl_3$, 60 MHz) δ 2.40 (s, 3H), 3.30 (s,

3H), 3.55 (t, 2H, J = 6 Hz), 4.16 (t, 2H, J = 6 Hz), 7.35-7.85 (m, 4H).

3-Ethoxypropyl p-toluenesulfonate (10)

Tosylate **10** [157] was prepared according to a variation of the method of Kyba et al. [152]. To an ice-cold 1.0 M solution of the p-toluenesulfonyl chloride (4.99 g, 26.2 mmol) in dry CH_2Cl_2 (26 mL) was added an ice-cold solution of the 3-ethoxypropanol (2.53 g, 24.3 mmol) and pyridine (4.30 g, 54.3 mmol) in CH_2Cl_2 (25 mL). The flask was tightly stoppered and stored at -10 °C for 5 days (at which time large pyridinium chloride crystals had formed). The cold reaction mixture was washed with ice-cold water (25 mL) followed by ice-cold 10% aq HCl (2 x 25 mL) to remove residual pyridine. All aqueous washes were combined and back-extracted with 25 mL of CH_2Cl_2. The original and back-extract organic phase were each washed with 25 mL of saturated aq NaCl before the organic layers were combined and dried together over anhyd Na_2SO_4 for 24 h. Na_2SO_4 was removed from the anhyd organic solution by vacuum filtration and the solvent was under reduced pressure removed to yield 5.35 (85%) of clear product oil **10**. This was used without further purification for subsequent alkylation reactions. The ^1H and ^{13}C NMR spectra of a sample of the product were consistent with the structure [Lit. 157]. ^1H NMR ($CDCl_3$, 60 MHz) δ 1.10 (t, 3H, J = 7 Hz), 1.89 (m, 2H), 2.40 (s, 3H), 3.32 (m, 4H), 4.15 (t, 2H, J = 6 Hz), 7.32-7.80 (m, 4H); ^{13}C NMR ($CDCl_3$, 22.5 MHz) δ_c 14.90, 21.40, 29.33, 65.62, 66.14,

67.70, 127.72, 129.68, 133.19, 144.50.

cis,cis-1,3,5-Tris-(1,4,7-trioxaoctyl)cyclohexane (11)

A 57% mineral oil dispersion of NaH (4.33 g)(102 mmol, NaH) was added to a 250 mL 3-neck round bottom flask fitted with a reflux condenser and a N_2 inlet. Dry DMF (30 mL) was added via syringe to the flask,and the suspension was stirred. A solution of cis,cis-1,3,5-trihydroxycyclohexane (3.37 g, 25.5 mmol) dissolved in 60 mL of dry DMF was added dropwise to the stirred NaH suspension. After H_2 evolution had ceased the solution was heated to 110°C for one hour, and allowed to cool to 80°C. 1,4,7-Trioxaoctyl tosylate [152] (28.46 g, 112.2 mmol) was then added in aliquots in DMF solution over a period of three days. The procedure involved the addition of approximately one equivalent of alkylating agent followed by heating, cooling, and subsequent addition of more NaH (ca. 1 equiv.) with heating and then cooling for 12 to 24 hours. Workup involved quenching excess NaH by the slow addition of 1 mL of H_2O. The reaction mixture was then suction filtered along with CH_2Cl_2 washings of the reaction flask. Solvents were removed under reduced pressure and the residue was redissolved in CH_2Cl_2. A white precipitate which remained insoluble was removed by filtration. The filtrate was concentrated under reduced pressure to give two phases: a clear upper mineral oil layer and a dark brown opaque lower product layer. The lower product layer was separated, extracted with 2 X 15 mL of H_2O, diluted with CH_2Cl_2, and

dried over anhydrous Na_2SO_4. The water washings were back extracted with CH_2Cl_2. The extract was also dried as above. After vacuum filtration to remove Na_2SO_4 the organic extracts were combined and the CH_2Cl_2 was removed under reduced pressure to yield 11.92 g of crude product. TLC analysis (neutral alumina, 1.5% (v/v) EtOH in CH_2Cl_2) showed three components, one of which (R_f = 0.21) was the most prominent. Column chromatography (200 g alumina, 1.5% (v/v) EtOH in CH_2Cl_2) of 3.05 g of crude product gave 2.52 g of the desired product **11** (clear light yellow oil, R_f = 0.21) which was contaminated with residual solvent. This chromatographed material was kugelrohr distilled (155-195°C, 0.75 mm Hg) to yield 1.51 g (3.44 mmol)(54% total calculated yield) of a clear colorless **11**: IR (NaCl, neat) 2960, 2890, 1460, 1260, 1200, 1120, 1025 cm^{-1}; ^1H NMR ($CDCl_3$, 60 MHz) δ 1.20 (dt, 3H, J = 12, 12 Hz, axial ring -C<u>H</u>$_2$-), 2.10-2.75 (m, 3H, equatorial ring -C<u>H</u>$_2$-), 3.28 (t of t, 3H, J = 12, 4 Hz, ring CH_2-C<u>H</u>(OR)-CH_2), 3.40 (s, 9H), 3.45-3.75 (m, 24H); ^{13}C NMR ($CDCl_3$, 22.5 MHz) δ_c 38.17, 58.91, 67.83, 70.56, 70.88, 71.99, 73.75; Mass Spectrum, m/z (Rel. Intensity) 139(1), 95(23), 94(36), 90(15), 89(20), 75(13), 73(15), 68(13), 67(10), 66(11), 60(15), 59(100), 58(50); Anal. Calcd. for $C_{21}H_{42}O_6$: C, 57.51; H, 9.65. Found: C, 57.47; H, 9.89.

<u>cis</u>,<u>cis</u>-1,3,5-Tris-(1,5-dioxaheptyl)cyclohexane (12)

A clean dry 100 mL 3-neck conical flask was fitted with a condenser, N_2 inlet, and a pressure equalizing

addition funnel. A stirring bar was added to the flask before the system was purged with N_2 and flame dried. Dry DMF (20 mL) was added via syringe to the flask, followed by direct addition using a glassine paper funnel of cis,cis-1,3,5-trihydroxy-cyclohexane (0.4253 g, 3.218 mmol). The solution was stirred while NaH powder (0.080 g, 3.33 mmol) was added slowly (to allow for controlled H_2 evolution). (The NaH powder was prepared by washing a 60% mineral oil dispersion with dry n-hexane washings. The residual n-hexane was removed under vacuum.) A solution of 1,5-dioxaheptyl tosylate (**10**) (4.985 g, 19.29 mmol) in DMF (20 mL) was placed in the addition funnel. Alternating additions of approximately one equivalent of alkylating agent and 1-2 equivalents NaH powder (total = 0.874 g, 36.4 mmol) were made over a period of 10 days, while stirring the reaction mixture under N_2. Excess NaH was quenched by pouring the reaction mixture into a 250 mL Erlenmeyer flask containing H_2O and ice. (Note: large concentrated quantities of NaH should be quenched carefully to prevent fires.) The aqueous DMF solution was then concentrated by rotary evaporation. The solid residue was taken up in 20 mL H_2O and extracted with (3 X 50 mL) CH_2Cl_2, the combined organic phases were dried over anhydrous Na_2SO_4 and the solvent was removed by rotary evaporation to give 1.08 g of a cloudy oil. Column chromatography (115 g alumina, purified Et_2O) followed by kugelrohr distillation (140-150 ^oC, 0.03 mm Hg) yielded 0.9655 g of clear colorless liquid [**12**] (77% total calculated yield): IR (NaCl, neat) 2970, 2940, 2860, 1460,

1440, 1370, 1350 cm^{-1}; ^1H NMR ($CDCl_3$, 60 MHz) δ 1.18 (t, 9H, J = 8 Hz, arm -C<u>H</u>$_3$), 1.20 (dt, 3H, J = 12, 12 Hz, axial ring -C<u>H</u>$_2$-), 1.79 (tt, 6H, J = 6, 6 Hz, arm CH_2-C<u>H</u>$_2$-CH_2), 2.10-2.50 (m, 3H, equatorial ring -C<u>H</u>$_2$-), 3.16 (tt, 3H, J = 12, 4 Hz, ring CH_2-C<u>H</u>(OR)-CH_2), 3.25-3.60 (m, 18H); ^{13}C NMR ($CDCl_3$, 22.5 MHz) δ_c 15.15, 30.50, 38.37, 65.42, 66.14, 67.44, 73.42; Mass Spectrum, m/z (Rel. Intensity) 390(M+, < 0.1), 305(10), 182(14), 157(12), 143(42), 105(54), 103(12), 97(20), 96(29), 95(29), 87(100), 86(41), 71(30), 59(95), 57(15); Anal. Calcd. for $C_{21}H_{42}O_6$: C, 64.58; H, 10.84. Found: C, 64.66; H, 11.07.

<u>cis</u>,<u>cis</u>-1,3,5-Tris-(1-oxa-3-butenyl)cyclohexane (13)

In a 100 mL, 3-necked, round bottom flask, fitted with a reflux condenser, and N_2 inlet tube, 1.79 g of 57% NaH/mineral oil dispersion was washed with dry n-hexane (3 X 10 mL) to remove the mineral oil. Residual hexane was removed under N_2 flow to leave a light gray NaH powder (1.02 g, 42.5 mmol), to which was added 15 mL of dry DMF. A solution of <u>cis</u>,<u>cis</u>-1,3,5-trihydroxycyclohexane (1.16 g, 8.77 mmol) in 25 mL of dry DMF was added dropwise to the stirred NaH suspension. After H_2 gas evolution had ceased, NaI (1.77 g, 10.6 mmol) was added to the reaction mixture followed by the dropwise addition of a solution of allyl bromide (2.50 mL, 3.49 g, 28.8 mmol) in 25 mL of DMF. The reaction mixture was stirred at room temperature for 12 h after which time excess NaH was quenched by dropwise addition of H_2O. The reaction mixture was then added to 50

mL of H_2O with stirring, followed by the addition of 150 mL of saturated aqueous NaCl. The solution was extracted with (3 X 60 mL) Et_2O, the combined extracts were dried over anhydrous Na_2SO_4, and solvent was removed by rotary evaporation to give 1.84 g of a yellow oil. The crude product was kugelrohr distilled (65-110°C, 0.03-0.04 mm Hg) to yield 1.74 g of a clear liquid. TLC analysis (neutral alumina/ 2.0% (v/v) EtOH in CH_2Cl_2) showed three components (R_f = 0.13, 0.78,and 0.93) with the intermediate component being most prominent. Column chromatography (200 g alumina, 1.5% (v/v) EtOH in CH_2Cl_2) of 1.29 g of the distilled material gave 1.13 g of clear colorless liquid [13] (51% total calculated yield): IR (NaCl, neat) 3080, 3005, 2940, 2910, 2860, 1645, 1460, 1420, 1380, 1350, 1280, 1235, 1120, 1070, 990, 915 cm^{-1}; ^1H NMR ($CDCl_3$, 60 MHz) δ 1.20 (q, 3H, J = 12 Hz, axial ring -C<u>H</u>$_2$-), 2.37 (d of t, 3H, J = 12, 4 Hz, equatorial ring -C<u>H</u>$_2$-), 3.25 (t of t, 3H, J = 12, 4 Hz, ring -C<u>H</u>(OR)-), 4.00 (d of t, 6H, J = 6, 1 Hz, allyl -C<u>H</u>$_2$-), 5.14 (d of m, 3H, J = 12 Hz, <u>cis</u> vinyl CH_2-CH=C<u>H</u>$_2$), 5.20 (d of m, 3H, J = 17 Hz, <u>trans</u> vinyl CH_2-CH=C<u>H</u>$_2$), 5.92 (ddt, 3H, J = 17, 12, 6 Hz, vinyl CH_2-C<u>H</u>=CH_2); ^{13}C NMR ($CDCl_3$, 22.5 MHz) δ_c 38.23, 69.32, 72,.63, 116.66, 135.13; Mass Spectrum, m/z (Rel. Intensity) 252(M^+, <0.1), 183(33), 153(23), 141(18), 139(13), 138(52), 137(14), 127(17), 120(11), 111(100), 97(92), 81(76), 69(57), 55(89); After an additional kugelrohr distillation (125-140°C, 0.03-0.05 mmHg) Anal. Calcd. for $C_{15}H_{24}O_3$: C, 71.39; H, 9.59. Found:

C, 71.22; H, 9.95.

cis,cis-3,5-Di(1-oxa-3-butenyl)cyclohexanol [14] was isolated as a by-product in the synthesis of cis,cis-1,3,5-tris-(1-oxa-3-pentenyl)cyclohexane [**13**]. The column chromatography of the 1.29 g of crude reaction product gave [**14**] as a clear colorless oil (0.09 g, 4.8% total calculated yield): (TLC, neutral alumina/ 2.0% (v/v)) R_f = 0.13; ^{1}H NMR ($CDCl_3$, 60 MHz) δ 1.26 (q, 3H, J = 12 Hz, axial ring $C\underline{H}_2$), 2.28 (d of t, 3H, J = 12, 4 Hz, equatorial ring $C\underline{H}_2$), 3.30 (t of t, 3H, J = 12, 4 Hz, ring -C<u>H</u>(-OR)), 2.57 (s, 1H, -O<u>H</u>), 3.99 (d of t, 4H, J = 6, 1 Hz, allyl $C\underline{H}_2$), 5.13 (d of m, 2H, J = 12, Hz, vinyl CH_2-CH=$C\underline{H}_2$), 5.20 (d of m, 2H, J = 17, Hz, vinyl CH_2-CH=$C\underline{H}_2$), 5.90 (ddt, 2H, J = 17, 12, 6 Hz, vinyl CH_2-C<u>H</u>=CH_2); ^{13}C NMR ($CDCl_3$, 22.5 MHz) δ_c 37.67, 41.03, 65.03, 69.32, 72.57, 116.79, 135.00.(No CH&N Anal.)

cis,cis-1,3,5-Tris-(3-methyl-1,4-dioxapentyl)cyclohexane (15).

To a 100 mL round bottom flask equipped with N_2 inlet tube and reflux condenser was added 3.44 g (10.8 mmol) $Hg(OAc)_2$ and 10 mL of anhydrous MeOH. A solution of cis,cis-1,3,5-tris-(1-oxa-3-propenyl)cyclohexane [**13**] (0.80 g, 3.17 mmol) in 10 mL of anhydrous MeOH was added and the reaction mixture was stirred for 20 min. The suspension turned into a thick slurry so that it was necessary to add an additional 10 mL of MeOH to facilitate stirring. The reduction of the organomercurial was effected by addition of 10 mL of 3 M

aqueous NaOH followed by 10 mL of 0.5 M $NaBH_4$ in 3 M aqueous NaOH. Upon addition of the $NaBH_4$ solution, a dark solid material (containing mercury metal) was observed to precipitate. The solution was stirred for 1 h before the solid ppt was allowed to settle. The supernatent was decanted and vacuum filtered through a Celite pad. The filtrate was saturated with NaCl and extracted 3 times with Et_2O (500 mL total). The combined Et_2O extracts were dried over anhydrous Na_2SO_4 and Et_2O was removed by rotary evaporation. Residual solvent was removed under high vacuum to yield 1.14 g of crude product, a clear light yellow liquid. At this point a small amount of salt precipitated from the oil so the sample was dissolved in $CHCl_3$ and filtered through a glass wool plug. Solvent was removed as described previously to yield 1.13 g of crude product. TLC analysis (neutral alumina, 1.5% (v/v) EtOH in CH_2Cl_2) showed one major component (R_f = 0.36) and two minor components (R_f = 0.17 and 0.07). Column chromatography (200 g alumina, 1.5 % (v/v) EtOH in CH_2Cl_2) followed by a second flash column chromatography (150 g alumina, same solvent system) of the 1.13 g of crude product gave 0.61 g of pure [**15**] (clear colorless oil, R_f = 0.36), shown later (via comlexation with $NaBPh_4$) to be a diastereomeric mixture (RRR/SSS and RRS/SSR) : IR (NaCl, neat) 2960, 2930, 2860, 2815, 1460, 1370, 1090 cm^{-1}; ^1H NMR ($CDCl_3$, 60 MHz) δ 1.10 (d, 9H, J = 6 Hz, arm $C\underline{H}_3$-CH), 1.20 (q, 3H, J = 12 Hz, axial ring -$C\underline{H}_2$-), 2.36 (d of t, 3H, J = 12, 4 Hz, equatorial ring -$C\underline{H}_2$-), 3.20 (t of t, 3H, J = 12, 4 Hz, ring -$C\underline{H}$(-OR), 3.39 (s, 9H, -O-$C\underline{H}_3$),

3.40 (m, 3H, -C<u>H</u>-CH_3), 3.40 (m, 6H, O-C<u>H_2</u>-CH); ^{13}C NMR ($CDCl_3$, 22.5 MHz) δ_c 16.58, 38.10, 56.77, 72.18, 73.94, 76.15; Mass Spectrum, m/z (Rel. Intensity) 348(M^+, <0.1), 94(25), 73(35), 59(100), 58(37).

<u>cis</u>,<u>cis</u>-1,3,5-Tris-(3-hydroxy-1-oxabutyl)cyclohexane (16)

A solution of $Hg(OAc)_2$ (5.35 g, 16.8 mmol) in 10 mL of H_2O and 10 mL of THF was stirred in a 100 mL 3-necked round bottom flask. To this was added a solution of 1.09 g (4.31 mmol) of <u>cis</u>,<u>cis</u>-1,3,5-tris-(1-oxa-3-propenyl)cyclohexane [13] in 5 mL of THF. The reaction solution remained bright yellow until the addition was complete, at which time it suddenly became colorless. The reaction mixture was stirred for a total of 10 min. before 20 mL of 3 M aqueous NaOH was added (solution turned yellow immediately), followed by the slow addition of 30 mL of 0.5 M $NaBH_4$ in 3 M aqueous NaOH, which caused mercury to precipitate immediately. The mercury was allowed to settle before the supernatent was filtered through fluted filter paper. The solid residue was washed with THF. The combined filtrates were saturated with NaCl and extracted five times with THF (total vol. = 400 mL). The THF extracts were rotary concentrated to give a residue that was redissolved in acetone. This produced a supernatant with a grey precipitate (probably mercury). The acetone solution was decanted and vacuum filtered through Celite and glass wool. The initial filtrate was cloudy but later became clear.

This was then rotary concentrated and traces of solvent were removed under high vacuum to give 1.11 g (3.62 mmol) of the crude diastereomeric mixture [16] (RRR/SSS and RRS/SSR)(84 % yield) as a clear yellow oil, which was carried on to compound [17] without further purification: IR (NaCl, neat) 3370, 2960, 2940, 2920, 2880, 1470, 1375, 1090 cm^{-1}; ^{1}H NMR (acetone-d_6, 60 MHz) δ 1.10 (m, 9H, CH(OH)-C<u>H</u>$_3$), 1.25 (m, 3H, axial ring -C<u>H</u>$_2$-), 2.40 (d of m, 3H, J = 12 Hz, equatorial ring -C<u>H</u>$_2$-), 2.92 (s, 3H, -O<u>H</u>), 3.2 (m, 3H, ring -C<u>H</u>-), 3.35 (d, 6H, J = 6 Hz, O-C<u>H</u>$_2$-CH), 3.8 (m, 3H, CH_2-C<u>H</u>(OH)-CH_3); ^{13}C NMR (acetone-d_6, 22.5 MHz) δ 20.03, 38.82, 66.79, 74.33, 75.11; Mass Spectrum, m/z (Rel. Intensity) 263(1), 156(11), 129(16), 115(22), 109(19), 108(15), 98(15), 97(19), 87(58), 81(21), 80(60), 71(15), 65(17), 64(16), 63(17), 59(100), 60(16), 58(23), 57(19).

<u>cis</u>,<u>cis</u>-1,3,5-Tris-(3-keto-1-oxabutyl)cyclohexane (17)

To a 500 mL, 3-necked, round bottom flask fitted with a reflux condenser and a N_2 inlet tube was added 2.72 g (7.59 mmol) of $CrO_3(py)_2$ complex [155] and 150 mL of dry CH_2Cl_2. The dark red solution was stirred under N_2 as 0.109 g (0.355 mmol) of <u>cis</u>,<u>cis</u>-1,3,5-tris-(3-hydroxy-1-oxabutyl)cyclohexane diastereomeric mixture [16] was added with 50 mL CH_2Cl_2 washings. The mixture, which immediately changed from a red to a orange-brown color, was stirred vigorously. After 15 min., excess $CrO_3(py)_2$ complex was destroyed by the addition of 20 mL of H_2O. The supernatant mixture was decanted and filtered before the aqueous and organic phases

were separated. Methylene chloride was removed from the organic phase by rotary evaporation to give crude product oil. TLC analysis (neutral alumina, 2.0% (v/v) EtOH in CH_2Cl_2) showed one major component (R_f = 0.32) and two minor components (R_f = 0.41 and 0.09). Column chromatography (100 g neutral alumina, 2.0% EtOH in CH_2Cl_2) of the crude product mixture gave 0.0315 g (0.1048 mmol) (30% total calculated yield) of the desired product [**17**] as a clear colorless oil: IR (NaCl, neat) 2930, 2860, 1720, 1460, 1355, 1175, 1110, 1015; ^1H NMR ($CDCl_3$, 60 MHz) δ 1.28 (q, 3H, J = 12 Hz, axial ring $C\underline{H}_2$-), 2.14 (s, 9H, CO-$C\underline{H}_3$), 3.41 (d of t, 3H, J = 12, 4 Hz, equatorial ring -$C\underline{H}_2$-), 3.27 (t of t, 3H, J = 12, 4 Hz, ring -$C\underline{H}$-), 4.08 (s, 6H, arm O-$C\underline{H}_2$-CO); ^{13}C NMR ($CDCl_3$, 22.5 MHz) δ_c 26.34, 37.59, 73.68, 73.88, 206.54; Mass Spectrum, m/z (Relative intensity) 300(M^+, 13) 153(56), 97(25), 95(46), 86(20), 85(23), 81(53), 80(20), 79(85), 75(58), 71(16), 69(23), 67(21), 60(44), 58(17), 57(100), 56(25), 55(29).

Methyl 3,4,5-Tris-(1,4-dioxapentyl)-benzoate (20)

A 1 L 3-neck round bottom flask was equipped with a reflux condenser with a N_2 inlet tube, a mechanical stirrer, and a 250 mL pressure equalizing addition funnel. Anhydrous K_2CO_3 (39.50 g, 0.2857 mol) and dry DMF (250 mL) were added and methyl 3,4,5-trihydroxybenzoate (16.27 g, 88.35 mmol) was added to the stirred suspension, which was then heated briefly to 80°C. After the suspension had cooled to 30°C, a solution of 1,4-dioxapentyl tosylate **9** (63.34 g, 275.1 mmol)

in 200 mL of dry DMF was added dropwise over a period of 6 h. The reaction mixture was stirred for 12 h before it was heated briefly to 110°C and allowed to cool again to room temperature. The supernatent DMF solution was decanted from the solids and suction filtered. The filtrate was concentrated to a brown residue by rotary evaporation. The solid salts in the reaction flask were washed with acetone (1000 mL total) and the washings were filtered and added to the brown residue to give a brown solution with a light brown crystalline precipitate. The acetone supernatant was decanted and filtered along with additional acetone washings of the precipitate. The combined filtrates were concentrated by rotary evaporation to yield a brown, opaque, viscous liquid. This was dissolved in 100 mL CH_2Cl_2 and extracted twice with H_2O (100mL, 50 mL). The aqueous layers were combined and back extracted with CH_2Cl_2. The combined organic extracts were concentrated and residual solvent was removed under high vacuum to yield a dark brown oil (28.99 g, 92% crude yield) that eventually solidified to give a low melting wax. A portion of crude **2** (2.30 g) was kugelrohr distilled (154-171°C, 0.03 mm Hg) to yield pure product **20** , a clear colorless oil that quickly solidified into a white/light pink wax (2.13 g, 93% recovery, 85% calculated total yield): IR (NaCl, neat) 2970, 2930, 2880, 2810, 1715, 1585, 1495, 1430, 1360, 1330, 1210, 1115, 1030, 860, 755 cm^{-1}; ^1H NMR ($CDCl_3$, 60 MHz) δ 3.44 (s, 9H), 3.77 (m, 6H), 3.85 (s, 3H), 4.20 (m, 6H), 7.30 (s, 2H); ^{13}C NMR (22.5 MHz) δ_c 52.02, 58.72, 58.98, 68.93, 71.01, 71.86, 72.31, 109.32,

125.05, 142.87, 152.43, 166.41; Mass Spectrum, m/z (Rel. Intensity) 358(M^+, 21) 210(11), 59(100); Anal. Calcd. for $C_{17}H_{26}O_8$: C, 56.97; H, 7.31. Found: C, 57.27; H, 7.44.

Physical Organic Procedures

^{1}H NMR Complexation Experiments Employing $CDCl_3$ as Solvent

Typically about 20-40 mg of the host compound (tripodand, or crown ether) was weighed into a 1-dram vial before being transferred into a Wilmad #507 PP 5mm NMR tube with several $CDCl_3$ washings (Total vol. 0.5-1.0 mL). The final volume in the NMR tube was measured by visual comparison to a known volume of solvent placed (with a Drummond1000 uL pipet) into an identical tube. The sample tube was sealed with a teflon cap and parafilm. After the spectrum of the host solution was obtained, the guest salt (0.5, 1.0, or >1.0 equiv.) was added directly to the NMR tube with the aid of a glassine paper funnel. The host-guest solution was usually shaken to speed the equilibration process. Heating or sonicating tended to increase significantly the rate of sample decomposition. The NMR spectrum of the solution was then recorded along with multiple proton integrations of host and guest resonances. For salts containing protons (eg. $NaBPh_4$), it is possible to calculate the fraction of total host complexed (FTHC) from the relative integrations according to the general formula given below.

$$FTHC = \frac{\left[\frac{I_{(guest)}}{\#\ H's/(guest)}\right]}{\left[\frac{I_{(host)}}{\#\ H's/(host)}\right]} \qquad (1)$$

where: FTHC = Fraction Total Host Complexed

I = Integration (proton)

#H's = number of Hydrogens in molecular formula

The FTHC values reported represent the averages of the values calculated from each set of integrations. One standard deviation was used as an estimate of error.

^{13}C NMR Complexation Experiments Employing $CDCl_3$ as Solvent

The same samples prepared for the ^{1}H NMR experiments were used to obtain the limiting ^{13}C chemical shifts for the complexed hosts. A similar sample was prepared for ^{13}C NMR analysis if the original ^{1}H NMR experiment sample was not available.

^{13}C NMR Titration Experiments

Sample preparation: A desired amount of the host, cis,cis-1,3,5-tris-(1,4-dioxapentyl)cyclohexane (3) or cis,cis-1,3,5-tris-(1,4,7-trioxaoctyl)cyclohexane (11), was weighed into a 1-dram vial and transferred to either a Wilmad #507-PP 5 mm or a #513-PP 10 mm NMR tube with acetone-d_6 washings (total vol. 0.5-2.0 mL). The final volume in the NMR tube was measured by visual comparison to a known volume of solvent placed (with a Drummond 1000 uL pipet) into an identical NMR tube. The sample tube was sealed with a teflon cap and parafilm. After the ^{13}C NMR spectrum of the host solution was obtained, small aliquots of guest salt ($NaBPh_4$ or $KBPh_4$) were added directly to the sample NMR tube with the aid of a glassine paper funnel. After each addition the tube was capped and then shaken until all salt dissolved before a new volume was measured and ^{13}C NMR spectrum was recorded.

Additions of salt were made until the solubility limit for the host/guest solution was reached, at which point the titration experiment was terminated. The number of additions made (titration points taken) for each experiment varied from 4-23 and was determined in part by the size of the salt aliquots.

Data workup: The observed ^{13}C NMR chemical shift change, $|\delta_{obs}-\delta_L|$ (for C-2,4,6 resonances) was plotted versus the ratio $[M^+]_T/[L]_T$. The apparent stability constant (K_{obs}) and the limiting chemical shift change ($|\delta_{ML}-\delta_L|$) were obtained from curve fitting the data using equation **(8)**.

$$|\delta_{obs}-\delta_L| = 0.5B\{(1+A+X)-[(1+A+X)^2-4X]^{1/2}\} \qquad (8)$$

where: $A = \dfrac{1}{K[L]_T}$ $\quad B = |\delta_{ML}-\delta_L|$ $\quad X = \dfrac{[M^+]_T}{[L]_T}$

$[L]_T$ = Total ligand conc.

$[M^+]_T$ = Total metal ion conc.

The fitting procedure was carried out on a Digital Equipment VAX-780 computer using the iterative Marquadt-Levenberg least-squares method supplied in the RS/1 software package (Version 12.00, BBN Research Systems, 1983).

Derivation of Equations: [90] Equation (27) can be rearranged to give the expression (28) for the ^{13}C NMR chemical shift change monitored during the titration experiment.

$$\delta_{obs} = ([ML^+]/[L]_T)(\delta_{ML} - \delta_L) + \delta_L \qquad (27)$$

$$\Delta\delta_{obs} = (\delta_{obs}-\delta_L) = ([M^+]_T/[L]_T)\ (\delta_{ML}-\delta_L) \qquad (28)$$

The equilibrium expression for this complexation is given by equation (29).

$$K = [ML^+]/\{([L]_T - [ML^+])[M^+]\} \qquad (29)$$

Solving equation (29) for $[ML^+]/[L]_T$ gives the titration function, T (equation 30)[158].

$$[ML^+]/[L]_T = T = 0.5\{(1+A+X) - [(1+A+X)^2 - 4X^{1/2}\} \qquad (30)$$

Substitution of this function into equation (28) gives equation (8) which was used in the curve fitting procedure.

^{13}C NMR Competition Experiments

For the 1:1:1 competition stoichiometry, typically about 20-40 mg of each of two ligands was transferred to a Wilmad #507-PP 5 mm NMR tube with $CDCl_3$ washings (total volume 0.5-1.0 mL). The solid $NaBPh_4$ salt was added with the aid of a glassine paper funnel. The sample tube was sealed with a teflon cap and parafilm. The final volume in the NMR tube was measured by comparison to a known volume of solvent placed (with a Drummond 1000 uL pipet) into an identical tube. The host-guest solution was usually shaken to speed the equilibration process. Competition samples were found to be particularly sensitive to heating or sonication, which increased the rate of sample decomposition. The ^{13}C NMR spectrum was recorded only for a homogeneous sample and usually immediately after complete dissolution of the solid salt.

Unless indicated otherwise, estimates of error are based on propagation of the point-to-point error ($\pm$0.06551 ppm for 6002 Hz spectral width) associated with ^{13}C chemical shift measurements.

T_1(^{13}C NMR) Relaxation Experiments

Sample preparation: The sample of uncomplexed ligand was prepared by transferring the tripodand 3 (0.0460g, 0.150 mmol) into a Wilmad Taperlok #507-SJ-8 5 mm NMR sample tube with $CDCl_3$ washings. The final volume in the NMR tube was measured by visual comparison to a known volume of solvent placed (with a Drummond 1000 uL pipet) into an identical tube. The sample tube was sealed by closing the Taperlok. The sample of complexed material was prepared in a similar fashion by first transferring tripodand 3 (0.0460g, 0.150 mmol) into the sample tube, followed by addition of slightly more than one equivalent of solid $NaBPh_4$ (0.0520g, 0.152 mmol, 1.01 equiv.) with the aid of a glassine paper funnel. After sealing the sample tube it was carefully shaken (so as not to splash sample against the greased Taperlok) until all but one or two crystals of the salt had dissolved. The final volumes and concentrations for each of the samples (of 3 & Na^+-3) were, 0.66 & 0.65 mL and 0.227 M & 0.231 M, respectively. Similar studies with lariat ethers indicated no concentation dependence of T_1 values for the concentration range of 0.1-0.7 M [124]. Possible error in the T_1 values introduced by incomplete complex formation for Na^+-3 should be negligible since in $CDCl_3$ the K_{obs} > 1.61×10^7 [159, 160]. All glassware was cleaned by successive washing with acetone, ethanol, distilled water, and the solvent $CDCl_3$ to remove paramagnetic impurities.

Each sample was carefully degassed by at least 4 freeze-pump-thaw cycles and sealed under vacuum by closing the Taperlok and securing it with Parafilm. The sample tubes were then stored in a N_2 atmosphere (to prevent O_2 from reaching the samples in case the Taperloks leaked) until the NMR measurements could be made.

Measurement of T_1^{DD}'s: The ^{13}C NMR measurements were conducted at 22.5 MHz on a JEOL FX90Q spectrometer. The relaxation times (T_1's) were obtained using a standard inversion-recovery technique with proton-noise-decoupling conditions [143]. For the pulse sequence;

$$(180^{\circ} - PI - 90^{\circ} - t_w)_n$$

where: PI= Pulse Interval (which is varied)

t_w= Total waiting time between cycles

90°= Pulse width measured by phase error detection method.

180°= 2 X (90° pulse)

t_w was at least five times the longest T_1 (note-except for the $T_1(CH_3)$ in the uncomplexed material [161]). Six pulse intervals (PI = 0.175, 0.25, 0.50, 1.0, 2.0, and 4.0 s) were used in addition to PI_i (infinity value, = 60.0 s) to give a total of seven points from which to calculate each T_1. A good signal-to-noise ratio was secured by taking 500 pulses

for each PI value. The two run times were approximately 23 and 38 hours (for uncomplexed and complexed ligand samples). Thus a Digital Equipment VAX-780 computer using Marquadt-Levenberg least-squares method supplied in the RS/1 software package (version 12.00, BBN Research Systems, 1983) was used to curve fit the experimental data.

Since the T_1's were only measured once an estimate of the standard deviation was not possible, but a reasonable approximation is $\pm$ 8%, based on experiments conducted on lariat ethers under similar conditions [124].

Measuring NOE: All NOE measurements were made by comparison of fully decoupled and gated decoupled ^{13}C spectra. The percent enchancement (% NOE) was calculated using equation 31;

$$\% \text{ NOE} = (100)\ \frac{\text{NOE}_{(obs)}}{\text{NOE}_{(max)}} \qquad (31)$$

where: NOE_{obs}= Observed Nuclear Overhauser Enhancement

NOE_{max}= 2.98 (Theoretical maximum for ^{13}C-NOE)

Attempts to measure NOE's (with a 6002 Hz spectral width (SW), at 22.5 MHz) using the JEOL FX90Q were unsuccessful due to large deviations ($\pm$ 20 for % NOE) for

single measurements. Instead of conducting multiple measurements on the FX90Q (which would improve the accuracy of the data by statistical averaging), a higher field instrument (with better precision) was used. The complete results from the NOE measurements with the Bruker AM360 (with 10,204 Hz SW; at 91 MHz) [162a] of the degassed T_1 samples for uncomplexed and complexed **3** in $CDCl_3$ are included in Appendix E. The estimate of error is $\pm$ 5% for % NOE calculated for a single run [162b].

APPENDICES

APPENDIX A.

Data Tables, Titration Plots, and Curve Fits

1.) Tables of Data from ^{13}C NMR Titration Experiments

Table 32: ^{13}C NMR Titration with **11** and $NaBPh_4$ in Acetone-d_6.

$[11]_{initial} = 0.2688$ M

addition #	C-2,4,6 (ppm)	$-\Delta\delta_C$ (ppm)	$[NaBPh_4]/[11]$
0	0.0000	0.000	0.000
1	38.758	0.585	0.125
2	38.173	1.170	0.250
3	37.522	1.821	0.375
4	37.002	2.341	0.500
5	36.417	2.926	0.625
6	35.832	3.511	0.750
7	35.376	3.967	0.875
8	34.856	4.487	1.000
9	34.466	4.877	1.125
10	34.206	5.137	1.250
11	33.881	5.462	1.375
12	33.751	5.592	1.500
13	Lost	-----	1.625
14	33.425	5.918	1.750
15	33.360	5.983	1.875
16	33.360	5.983	2.000
17	33.230	6.113	2.250
18	33.230	6.113	2.500
19	33.100	6.243	2.750
20	33.165	6.178	3.000
21	33.100	6.243	3.500

Table 33: ^{13}C NMR Titration with **11** and $NaBPh_4$ in Acetone-d_6.

$[11]_{initial}$ = 0.2813 M

addition #	C-2,4,6 (ppm)	$-\Delta\delta_C$ (ppm)	$[NaBPh_4]/[11]$
0	39.279	0.000	0.000
1	36.417	2.861	0.542
2	34.922	4.357	0.866
3	34.141	5.138	1.113
4	33.621	5.658	1.386
5	33.230	6.049	1.948
6	33.100	6.179	2.618
7	33.036	6.243	3.434

Table 34: ^{13}C NMR Titration with **3** and $NaBPh_4$ in Acetone-d_6.

$[3]_{initial}$ = 0.2690 M

addition #	C-2,4,6 (ppm)	$-\Delta\delta_C$ (ppm)	$[NaBPh_4]/[3]$
0	39.278	0.000	0.000
1	38.563	0.715	0.125
2	37.783	1.495	0.250
3	36.937	2.341	0.375
4	36.157	3.121	0.500
5	35.441	3.837	0.625
6	34.791	4.487	0.750
7	34.141	5.137	0.875
8	33.556	5.722	1.000
9	33.100	6.178	1.125
10	32.645	6.633	1.250
11	32.385	6.893	1.375
12	32.125	7.153	1.500
13	31.995	7.283	1.625
14	31.930	7.348	1.750
15	31.800	7.478	1.875
16	31.735	7.543	2.000
17	31.605	7.673	2.250
18	31.540	7.738	2.500
19	31.475	7.803	2.750
20	31.410	7.868	3.000
21	31.279	7.999	3.500
22	31.149	8.129	4.000
23	31.084	8.194	4.500

Table 35: ^{13}C NMR Titration with **3** and $NaBPh_4$ in Acetone-d_6.

$[3]_{initial}$ = 0.2898 M

addition #	C-2,4,6 (ppm)	$-\Delta\delta_C$ (ppm)	$[NaBPh_4]/[3]$
0	39.279	0.000	0.000
1	36.873	2.406	0.349
2	34.662	4.617	0.683
3	32.840	6.439	1.051
4	32.060	7.219	1.411
5	31.735	7.544	1.834
6	31.540	7.739	2.197
7	31.345	7.934	2.884

Table 36: ^{13}C NMR Titration with **3** and $NaBPh_4$ in Acetone-d_6.

$[3]_{initial}$ = 0.4805 M

addition #	C-2,4,6 (ppm)	$-\Delta\delta_C$ (ppm)	$[NaBPh_4]/[3]$
0	39.213	0.000	0.000
1	36.938	2.275	0.317
2	34.011	5.202	0.704
3	Lost	-----	1.036
4	31.800	7.413	1.246
5	31.540	7.673	1.575
6	31.345	7.868	1.886

2.) Plots and Curve Fits: ^{13}C NMR Titration Experiments

A) $[11]_{initial}$ = 0.2688 M (Data from Table 32)

^{13}C resonance = C-2,4,6
Solvent = Acetone-d_6

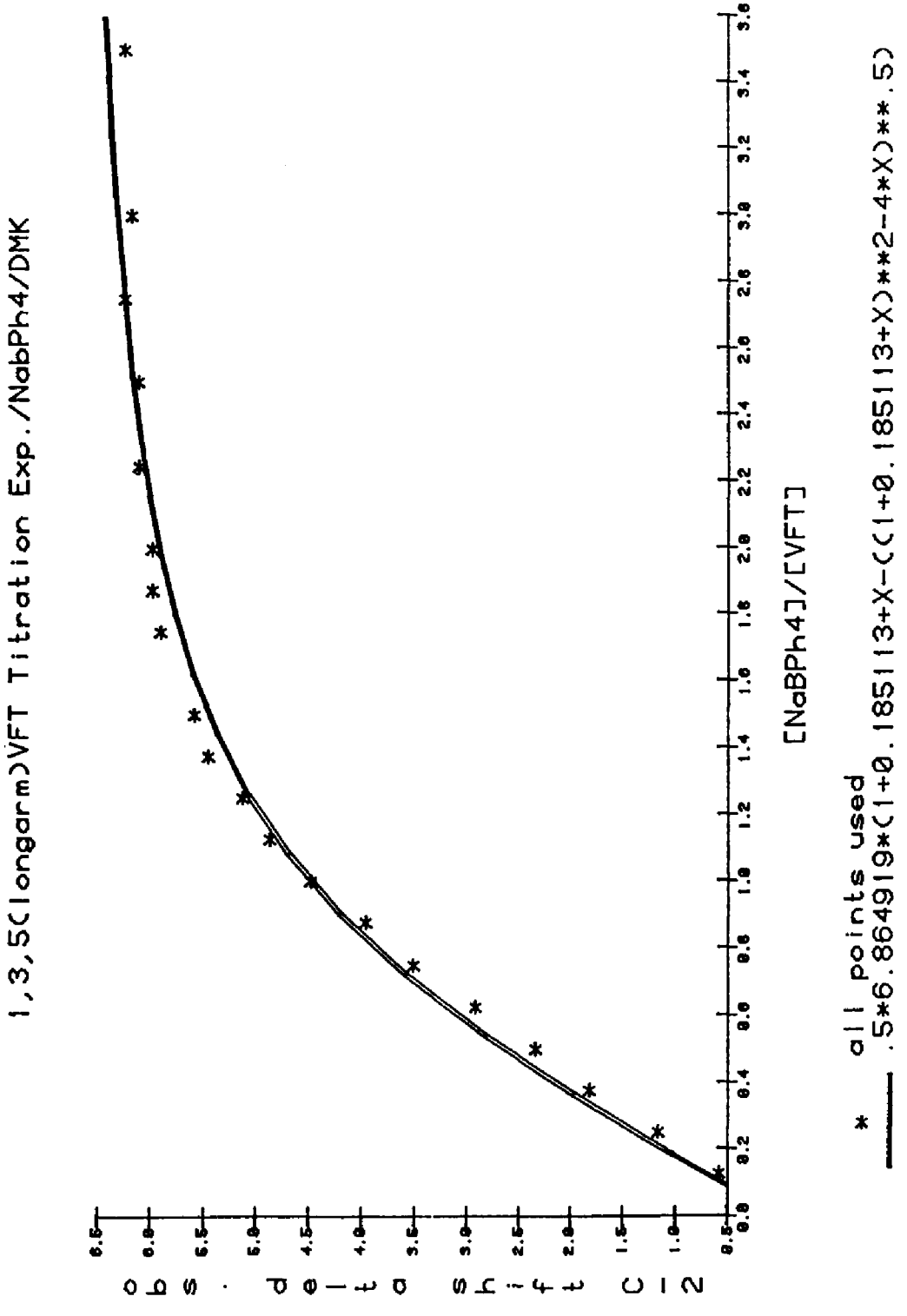

B) $[11]_{initial}$ = 0.2813 M (Data from Table 33)

^{13}C resonance = C-2,4,6
Solvent = Acetone-d_6

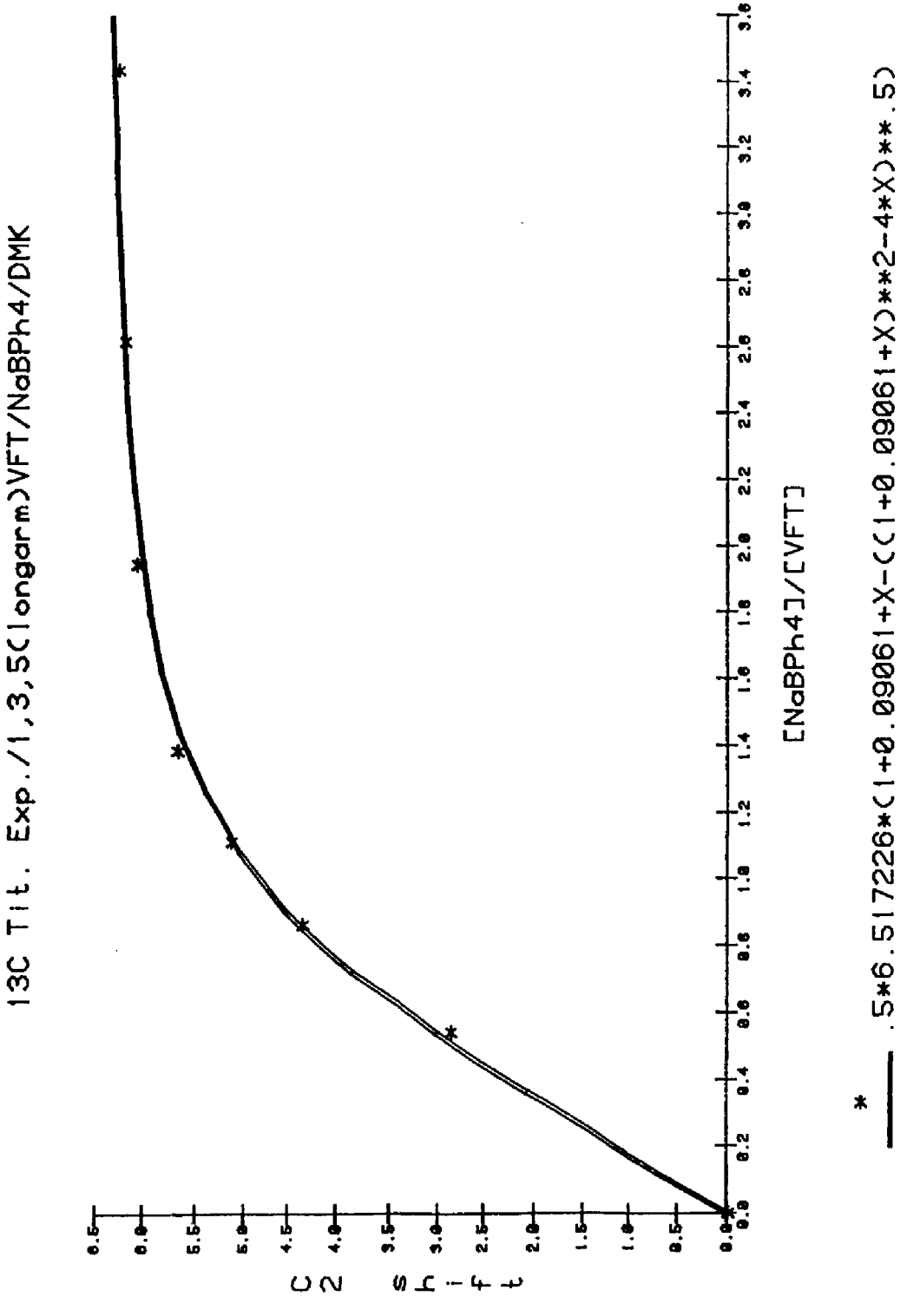

C) $[3]_{initial}$ = 0.2690 M (Data from Table 34)

^{13}C resonance = C-2,4,6
Solvent = Acetone-d_6

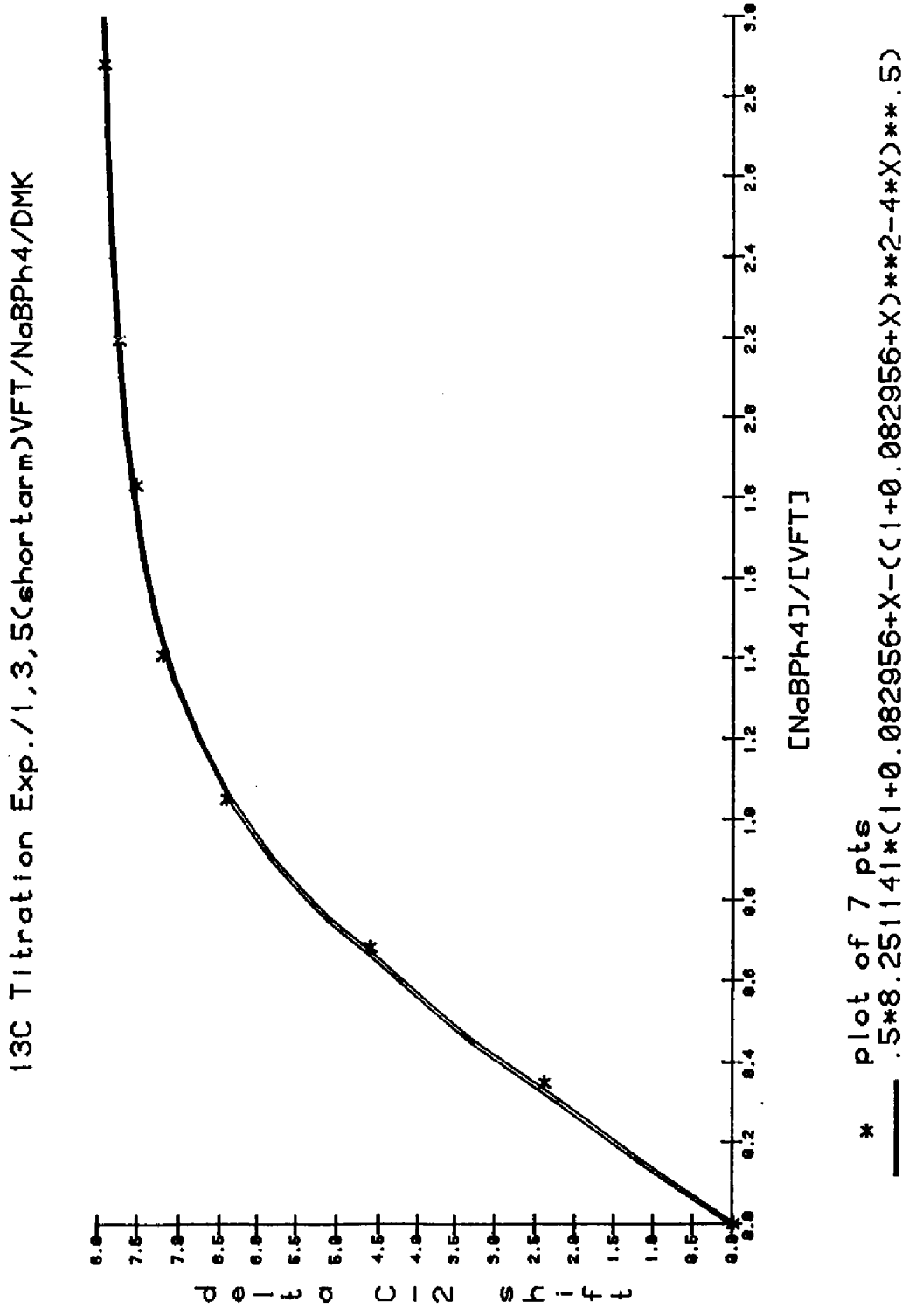

D) $[3]_{initial}$ = 0.2898 M (Data from Table 35)

^{13}C resonance = C-2,4,6
Solvent = Acetone-d_6

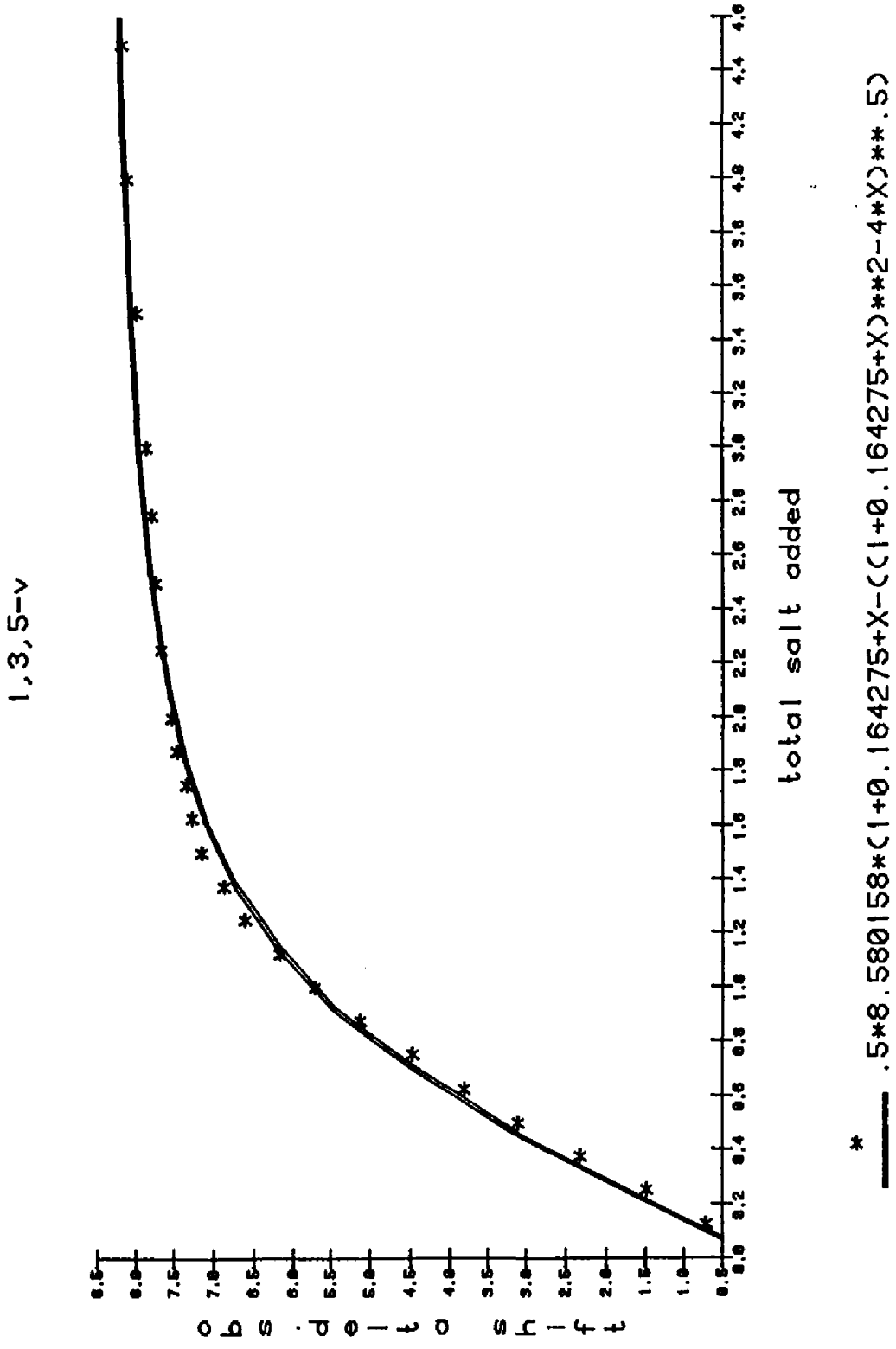

E) $[3]_{initial}$ = 0.4805 M (Data from Table 36)

^{13}C resonance = C-2,4,6
Solvent = Acetone-d_6

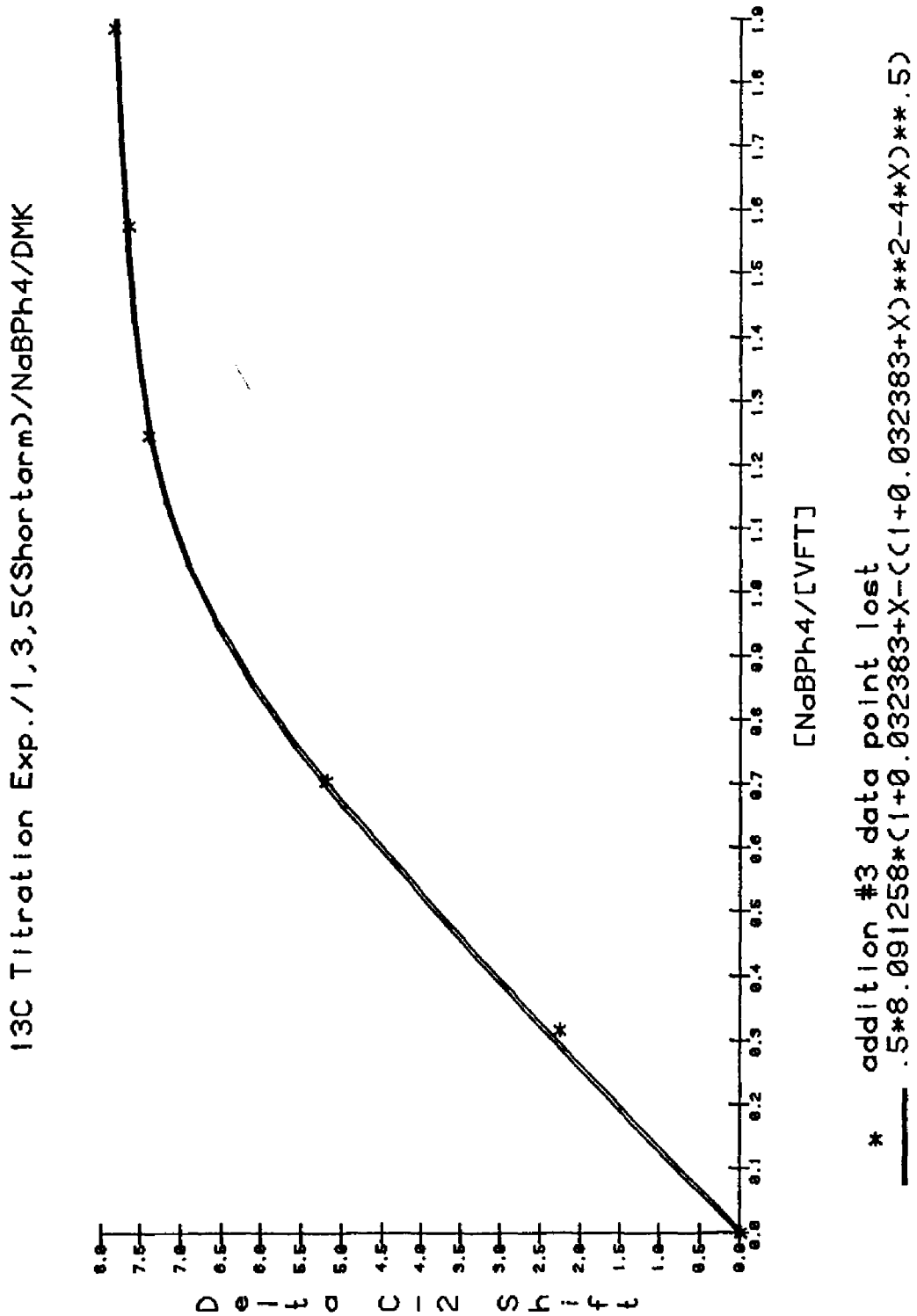

APPENDIX B.

Derivation of Equations for Competition Experiments

Definition of terms: K = stability constant or equilibrium constant; $[(ML^+)X^-]$, [L], $[M^+X^-]$ = conc. for complex ion pair, free ligand, and salt ion pair respectively; ip = (ion-paired); FTHC = Fraction Total Host Complexed.

Derivation of Equation (16):

By definition the equilibrium constant, K_{1-2}^{ip} for competition reaction (13) is:

$$K_{1-2}^{ip} = \frac{[(ML_1^+)X^-][L_2]}{[(ML_2^+)X^-][L_1]} \qquad (14)$$

Let K_{rel} represent the relative complexing ability for ligands, L_1 and L_2 interms of the complex stability constants K_1 and K_2 respectively:

$$K_{rel} = \frac{K_1}{K_2} \qquad (32)$$

The stability constants K_1 and K_2 for the complexation reactions (11) and (12) are:

$$K_1^{ip} = \frac{[(ML_1^+)X^-]}{[L_1][M^+X^-]} \qquad (33)$$

$$K_2^{ip} = \frac{[(ML_2^+)X^-]}{[L_2][M^+X^-]} \qquad (34)$$

Substitution of the above K's into equation (32) and canceling like terms yields equation (35):

$$K_{rel} = \frac{K_1}{K_2} = \frac{[(ML_1^+)X^-][L_2]}{[(ML_2^+)X^-][L_1]} \qquad (35)$$

Thus, the K_{1-2}^{ip} for the competition reaction can be equated to the relative stability constants for the components by equation (16).

$$\mathbf{K_{1-2}^{ip} = K_{rel} = \frac{K_1}{K_2}} \qquad \mathbf{(16)}$$

Derivation of Equation (17):

The free energy of competition, ΔG^o_{1-2}, is related to the K_{1-2}^{ip} by equation (15).

$$\Delta G^o_{1-2} = -RT \ln K_{1-2}^{ip} \qquad (15)$$

Substitution of K_{1-2}^{ip} using equation (16) gives:

$$\Delta G^o_{1-2} = -RT \ln \frac{K_1}{K_2} \qquad (36)$$

Separation of K terms and rearangement gives:

$$\Delta G^{\circ}_{1-2} = (-RT \ln K_1) - (-RT \ln K_1) \qquad (37)$$

By definition the free energies of complexation for ligands, L_1 and L_2 are:

$$\Delta G^{\circ}_{1} = -RT \ln K_1 \qquad (28)$$

$$\Delta G^{\circ}_{2} = -RT \ln K_2 \qquad (39)$$

Thus the free energy of competition can be expressed in terms of the component free energies of complexation by equation (17).

$$\Delta G^{\circ}_{1-2} = \Delta\Delta G^{\circ}_{1-2} = \Delta G^{\circ}_{1} - \Delta G^{\circ}_{2} \qquad (17)$$

Derivation of Equation (23)and (24):

The ratio of complexed to uncomplexed material (obtained from equation (22)) for ligands, L_1 and L_2 are:

$$\frac{[(ML_1^{+})X^{-}]}{[L_1]} = \frac{FTHC_1}{(1 - FTHC_1)} \qquad (40)$$

$$\frac{[(ML_2^{+})X^{-}]}{[L_2]} = \frac{FTHC_2}{(1 - FTHC_2)} \qquad (41)$$

Substitution of the above ratios into equation (14) gives (42):

$$K_{1-2}^{ip} = \frac{FTHC_1}{(1 - FTHC_1)} \cdot \frac{(1 - FTHC_2)}{FTHC_2} \qquad (42)$$

The FTHC for each ligand (in a 1:1:1 competition) is related by difference to the other host component (also see equation (21)).

$$FTHC_1 = (1 - FTHC_2) \qquad (43)$$

$$FTHC_2 = (1 - FTHC_1) \qquad (44)$$

Appropriate substitution of the above FTHC's into (42) gives:

$$K_{1-2}^{ip} = \frac{FTHC_1}{FTHC_2} = \frac{FTHC_1}{FTHC_2} \qquad (45)$$

Thus, the K_{1-2}^{ip} for a 1:1:1 competition can be calculated directly from the FTHC values for each host.

$$\mathbf{K_{1-2}^{ip} = \frac{(FTHC_1)^2}{(FTHC_2)^2}} \qquad \mathbf{(23)}$$

From equation (45) it is evident that:

$$\frac{FTHC_1}{FTHC_2} = \frac{[(ML_1^+)X^-]}{[L_1]} = \frac{[L_2]}{[(ML_2^+)X^-]} \qquad (46)$$

Thus, the K^{ip}_{1-2} can also be calculated directly from the ratio of complexed and uncomplexed material for a single ligand component in the competition.

$$K^{ip}_{1-2} = \left| \frac{[(ML_1^+)X^-]}{[L_1]} \right|^2 = \left| \frac{[L_2]}{[(ML_2^+)X^-]} \right|^2 \qquad (24)$$

APPENDIX C.

Tabulated Data for Competition experiments

Table 37: Peak area data for ^{13}C NMR competition experiments with $NaBPh_4$ and $CDCl_3$.

Compet.	Ligand (#)	S.W.[a] (Hz)	Carbon (#)	Peak Areas[b] ML^+	L	$[ML^+]$ / [L]
25 vs 3 (1:0.5)	25	6000	gem-Me	2.820	1.000	2.82
(1:1)	25	6000	gem-Me	1.923	1.000	1.92[c]
(1:1.5)	25	6000	gem-Me	1.107	1.000	1.11
		1400	gem-Me	1.116	1.000	1.12[d]
(1:1)	25	6000	gem-Me	1.544	1.000	1.54
		1400	gem-Me	1.471	1.000	1.47[d]
		600	gem-Me	1.480	1.000	1.48[d]
25 vs 4	3	6000	2,4,6	1.857	1.000	1.86
		6000	gem-Me	1.861	1.000	1.86

a: Spectral width
b: Peak areas were obtained from digital integration of the indicated carbon resonance.
c: The inconsistant result from this experiment was probably due to human error and did not appear in the repeat experiment.
d: Measurements were complicated by peak fold-over at narrower spectral width.

Table 38: Chemical shift data for ^{13}C NMR Competition experiments with $NaBPh_4$ and $CDCl_3$.

Compet.	Ligand (#)	Carbon (#)	δ_L (A)	δ_{ML^+} (B)	δ_{obs} (C)	$\Delta\delta_{max}$ (B-A)	$\Delta\delta_{obs}$ (C-A)
25 vs 3	25	gem-Me	(USED PEAK HEIGHTS/AREAS)				
26 vs 3	26	2,4,6	38.17	31.60	38.17	-6.57	0.00
21 vs 4	4	1,3	80.31	74.44	74.98	-5.87	-5.33
		4,6	25.4	26.4	26.40	-1.0	-1.00
		5	20.55	13.54	14.05	-7.01	-6.50
25 vs 4	4	1,3	80.31	74.44	74.54	-5.87	-3.77
		4,6	25.4	26.4	25.88	-1.0	-0.48
		5	20.55	13.54	---[a]	-7.01	
	25	gem-Me	(USED PEAK HEIGHTS/AREAS)				
		2,4,6	(USED PEAK HEIGHTS/AREAS)				
12 vs 4	4	1,3	80.3	74.4	---[a]	-5.9	
		4,6	25.4	26.4	26.27	-1.0	-0.87
		5	20.5	13.5	---[a]	-7.0	
	12	2,4,6	38.37	---[b]	38.43	-2.40[c]	+0.06
12 vs 3 (1:1)	12	2,4,6	38.37	---[b]	37.98	-2.40[c]	-0.39
(3:1)	12	2,4,6	38.37	---[b]	38.24	-2.40[c]	-0.13
12 vs 6 (3:1)	12	2,4,6	38.37	---[b]	38.37	-2.40[c]	-0.00
	6	1,3	77.06	75.11	75.24	-1.95	-1.76
		2	38.89	36.35	36.55	-2.54	-2.27
		4,6	31.80	27.64	27.83	-4.16	-3.91
		5	20.81	13.72	13.98	-7.09	-6.76
(6:1)	12	2,4,6	38.37	---[b]	38.27	-2.40[c]	-0.10
	6	1,3	77.06	75.11	75.16	-1.95	-1.90
		2	38.89	36.35	36.42	-2.54	-2.47
		4,6	31.80	27.64	27.71	-4.16	-4.09
		5	20.81	13.72	13.79	-7.09	-7.02

a: Not observed.
b: Chemical shift for 100% 1:1 complex not obtainable.
c: Observed shift for 2:1 ligand/salt ratio.

APPENDIX D.

Data Tables, Plots, and Curve Fits for ^{13}C-T_1 Measurements

Seven data points, (PI, Ln Z) were obtained for each ^{13}C nucleus in tripodand 3. The preset PI (pulse interval) times are plotted versus the observed ln Z (natural log of the fraction magnitization existing after a given PI). Curve fitting the data gives a straight line defined by equation 47.

$$\ln Z = -(1/A)t + B \qquad (47)$$

where:

$$Z = \frac{(M_o - M_t)}{(2M_o)}$$

The fraction of magnitization existing after time "t".
M_o = magnetization at $t = PI_1$ (PI_1 = infinite pulse delay)
M_t = magnetization at some time, t = PI

t = PI (pulse interval)

A = T_1 (the spin-lattice relaxation time)

B = value of ln Z at t = 0 (ideally B = 0)

1.) Tables of Data from ^{13}C NMR T_1^{DD} Experiments

Table 39: ^{13}C Relative Peak intensities for each Pulse Interval (PI) for Uncomplexed **3** in $CDCl_3$.

Data Point	PI (sec)	Peak 1 C-1,3,5	Peak 2 C-2'	Peak 3 C-1'	Peak 4 C-3'	Peak 5 C-2,4,6
1	60.00	7346	7022	9652	9644	8700
2	0.175	-4429	-4484	-6920	-7646	-3498
3	0.250	-3803	-4058	-6744	-7442	-1905
4	0.500	-1965	-2907	-4700	-6707	1695
5	1.00	1094	-1077	-1064	-5228	5645
6	2.00	4710	2277	3922	-2988	8350
7	4.00	6831	5148	8559	767	8831

Table 40: ^{13}C Relative Peak intensities for each Pulse Interval (PI) for Fully Complexed **3** with $NaBPh_4$ in $CDCl_3$.

Data Point	PI (sec)	Peak 1 C-1,3,5	Peak 2 C-2'	Peak 3 C-1'	Peak 4 C-3'	Peak 5 C-2,4,6
1	60.00	4519	7833	5059	7985	5292
2	0.175	-2755	-4588	-2664	-6254	-1929
3	0.250	-2620	-3831	-2310	-6169	-1403
4	0.500	-1837	-1722	-933	-5422	-340
5	1.00	-267	1471	1117	-4201	1059
6	2.00	2814	5162	3041	-2036	2661
7	4.00	3681	7347	4628	850	3387

2.) Plots and Curve Fits for ^{13}C-T_1 Data (for uncomplexed 3)

$[3]_{Total}$ = 0.227 M in $CDCl_3$

A) Plot of ln Z vs PI for C-1,3,5 in Uncomplexed 3

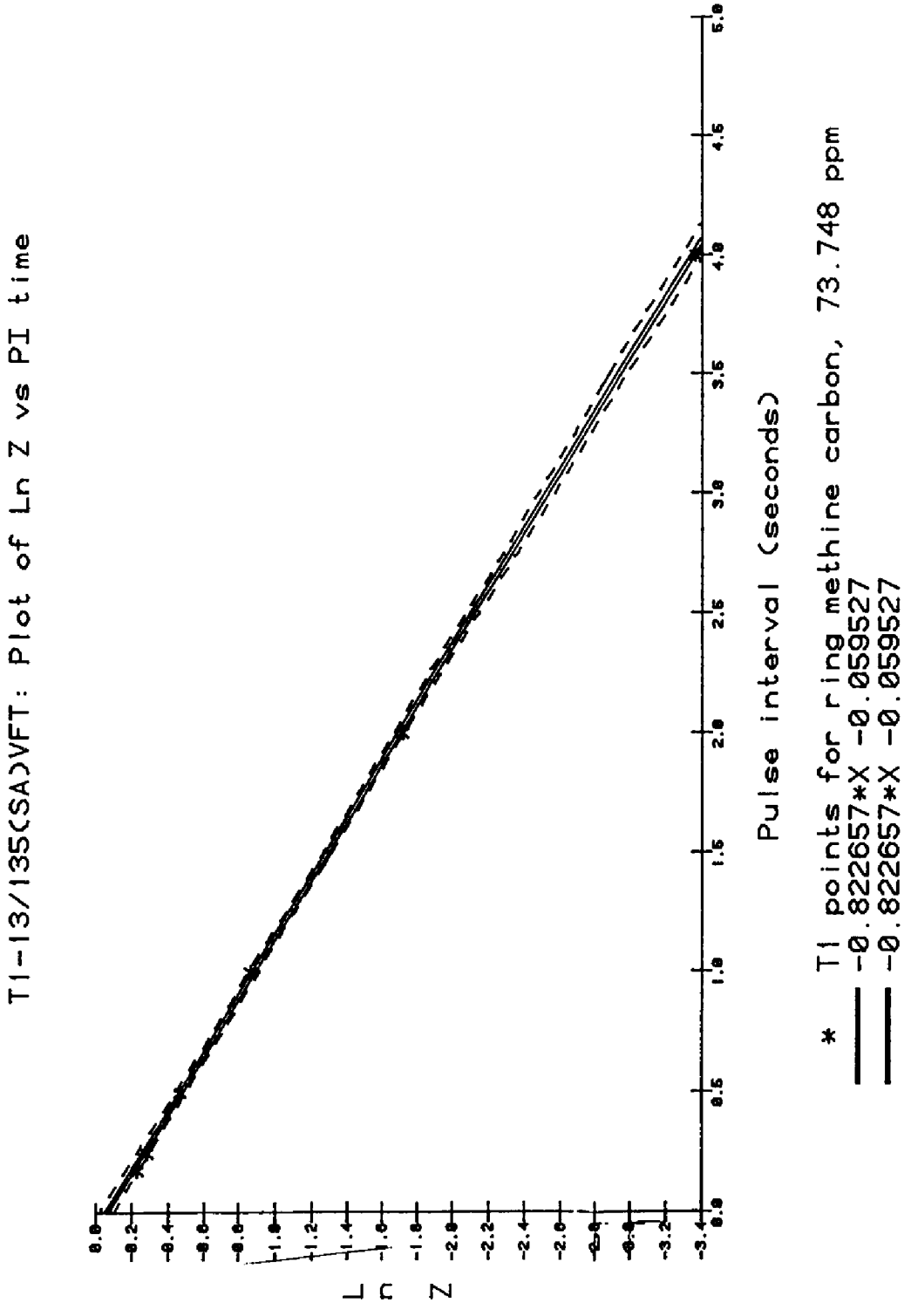

B) Plot of ln Z vs PI for C-2,4,6 in Uncomplexed 3

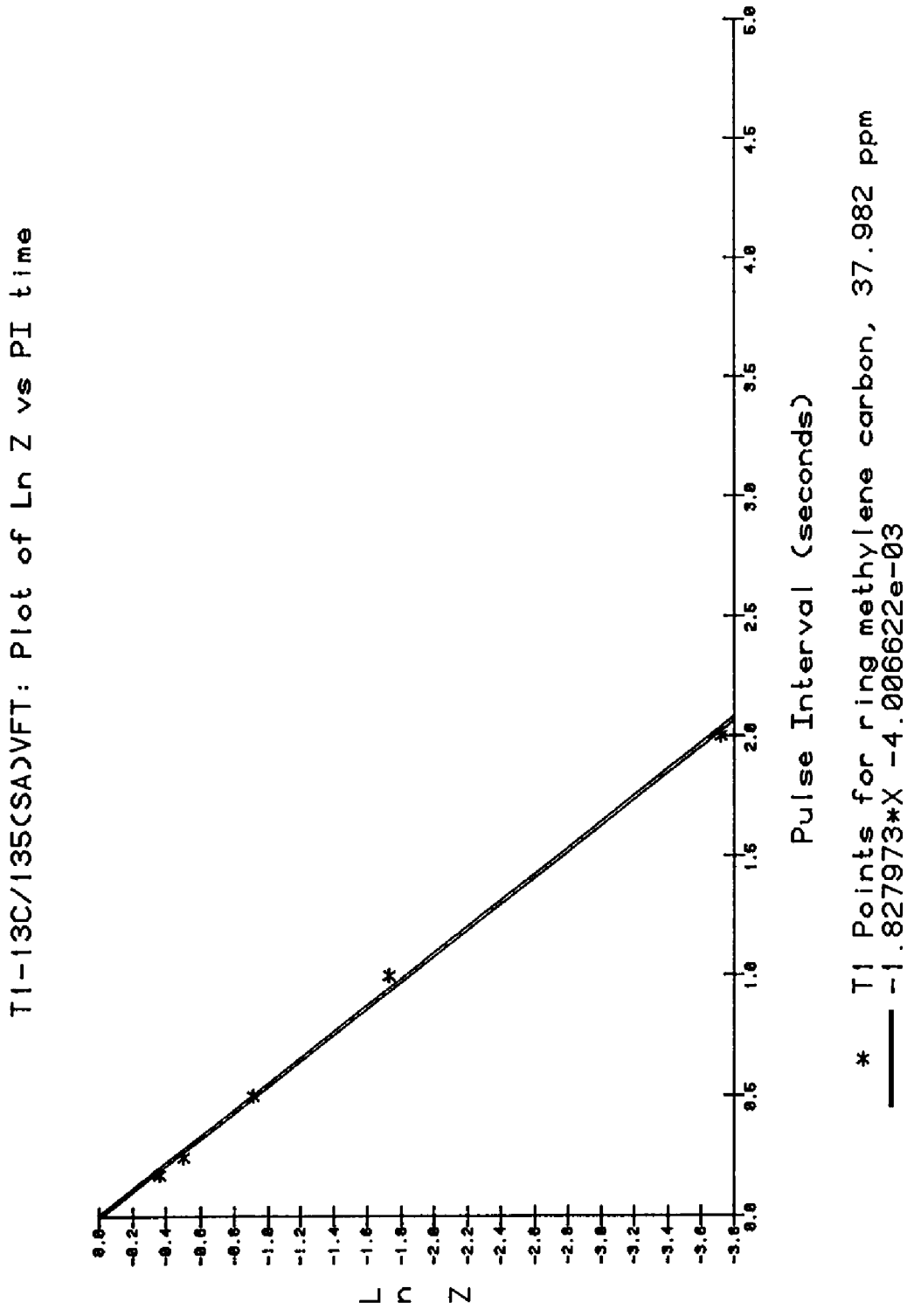

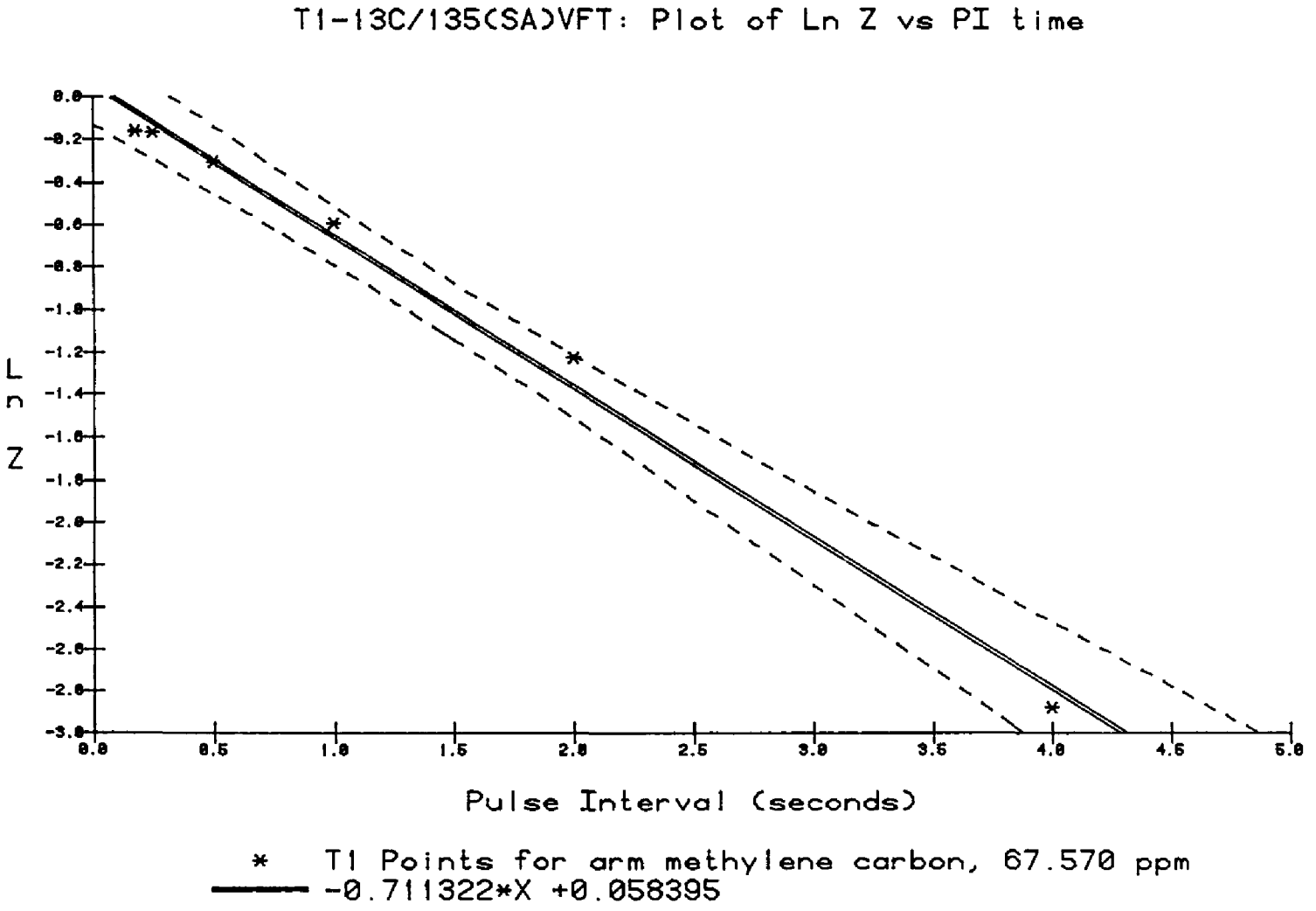

C) Plot of ln Z vs PI for C-1' in uncomplex 3

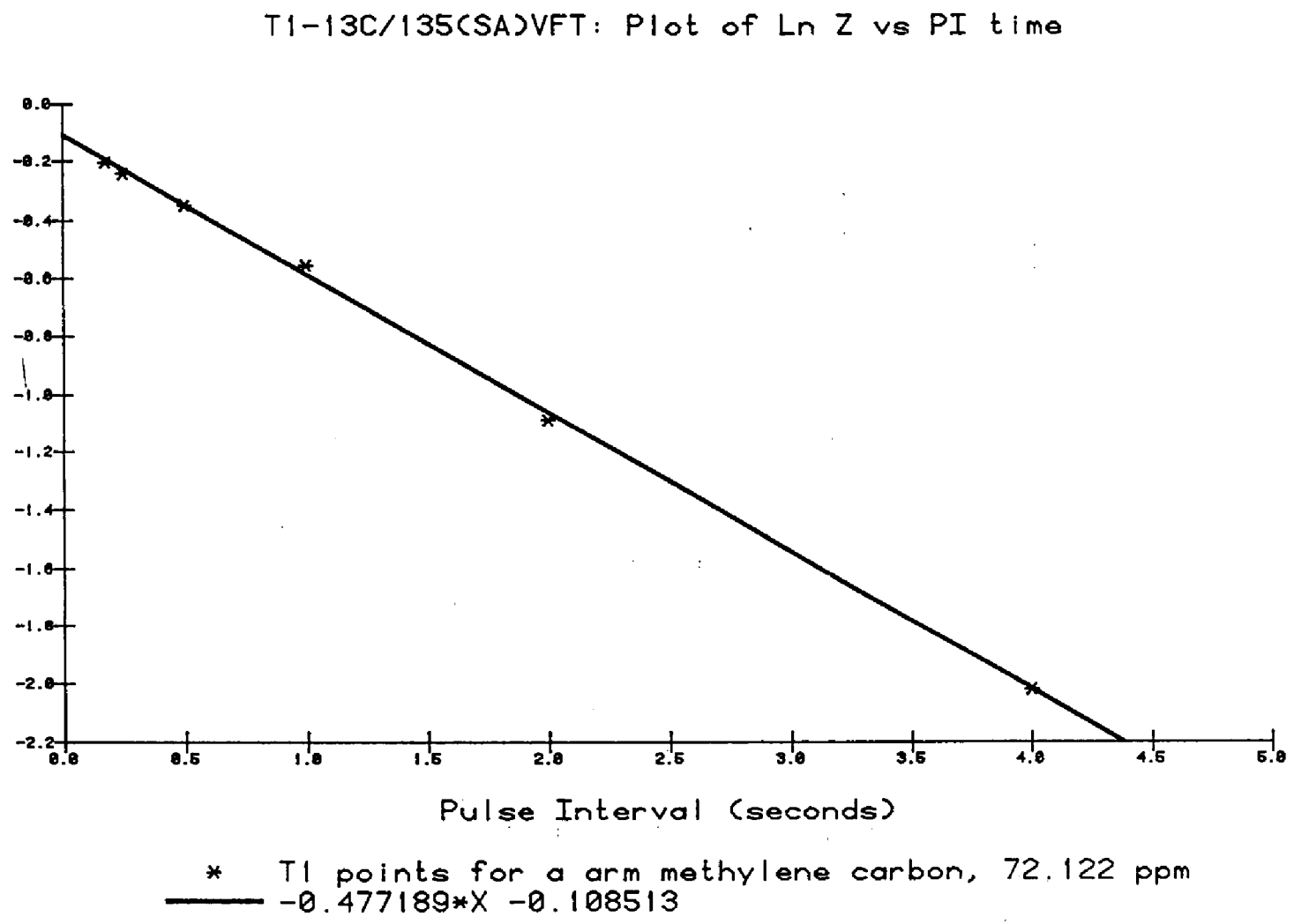

D) Plot of ln Z vs PI for C-2' in Uncomplexed 3

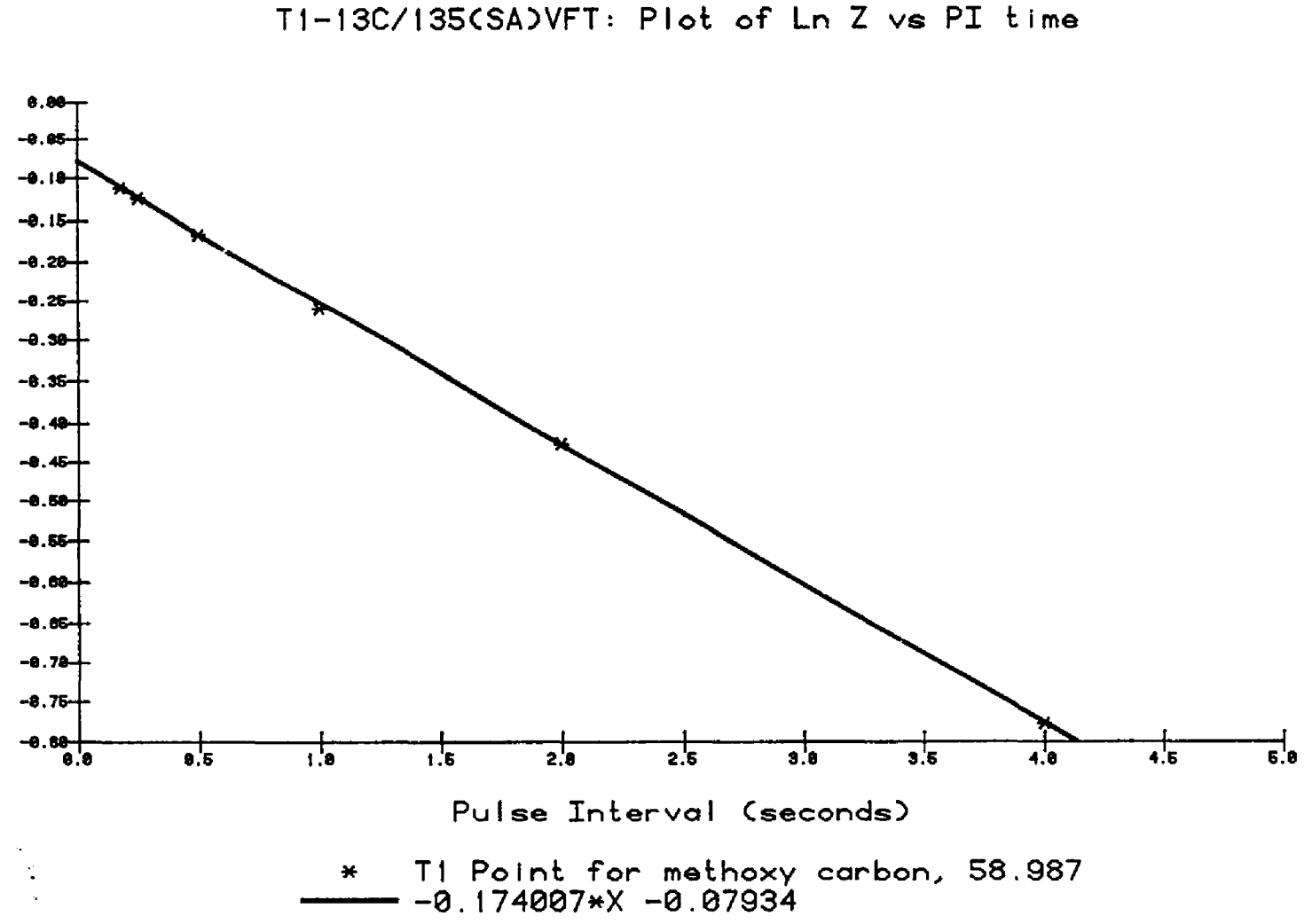

E) Plot of ln Z vs PI for C-3' in Uncomplexed 3

3.) Plots and Curve Fits for ^{13}C-T_1 Data (for complexed 3)

$[3]_{Total}$ = 0.231 M in $CDCl_3$ (with slight xs $NaBPh_4$)

A) Plot of ln Z vs PI for C-1,3,5 in complexed 3

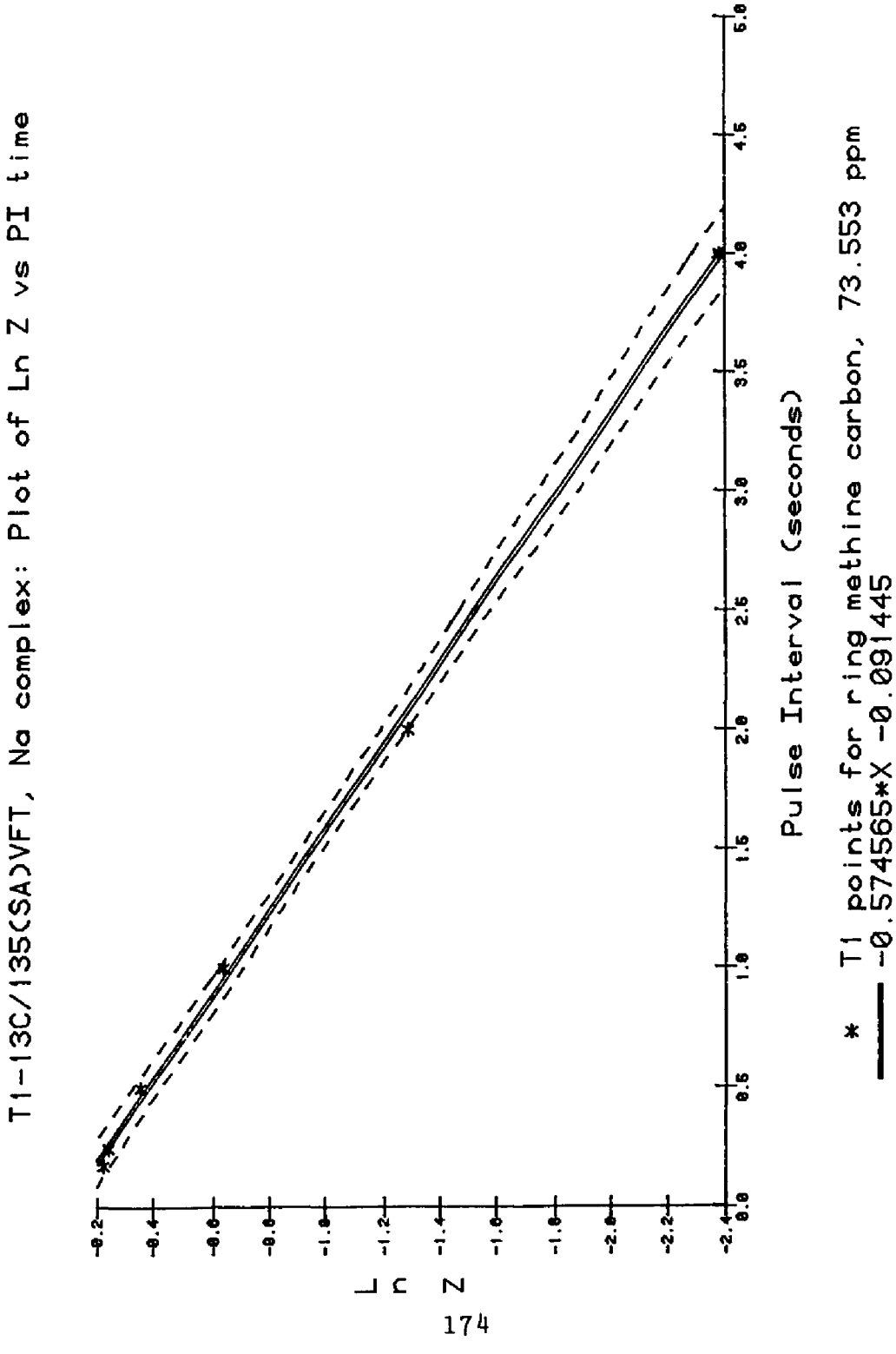

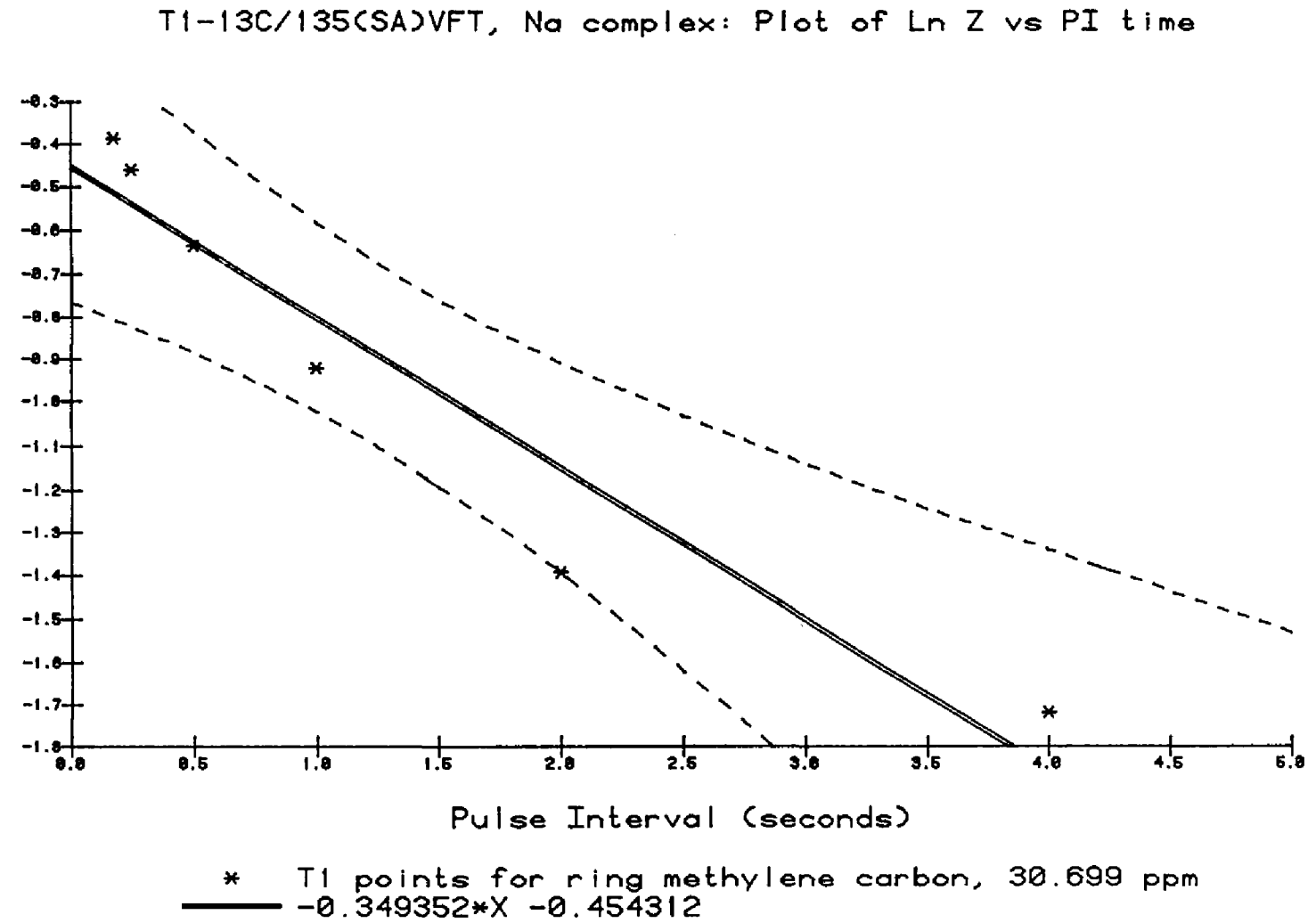

B) Plot of ln Z vs PI for C-2,4,6 in complexed 3

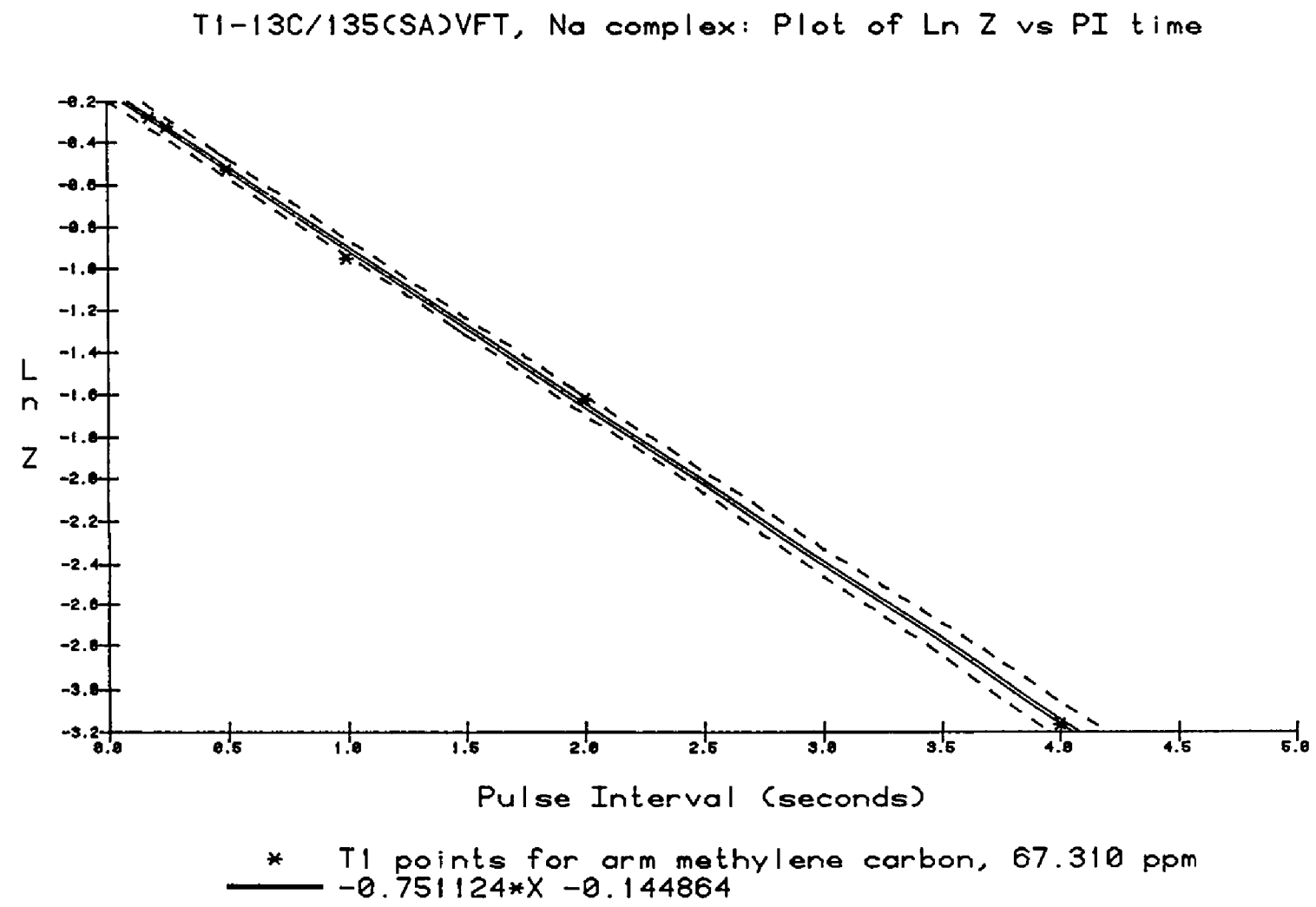

C) Plot of ln Z vs PI for C-1' in complex 3

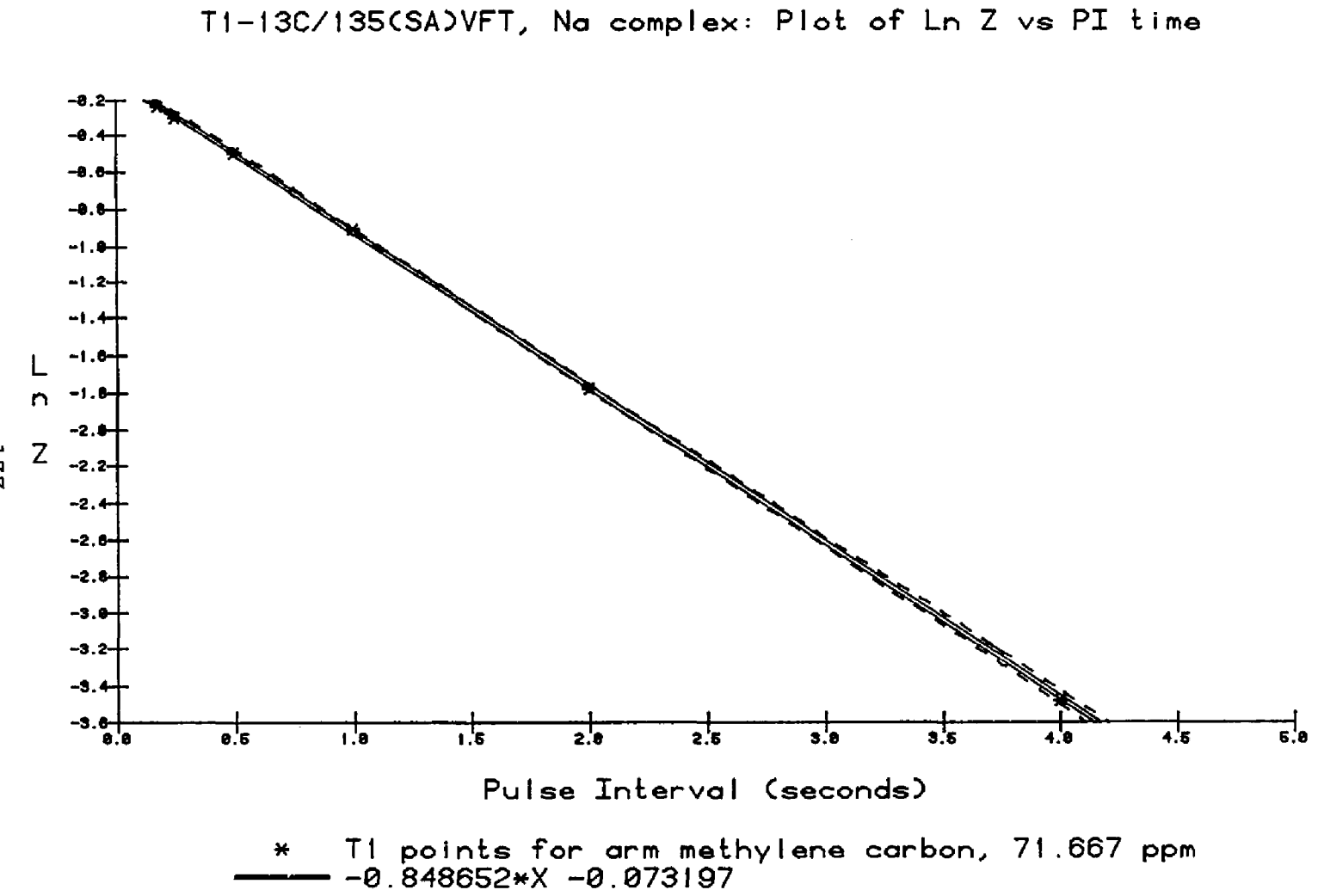

D) Plot of ln Z vs PI for C-2' in complexed 3

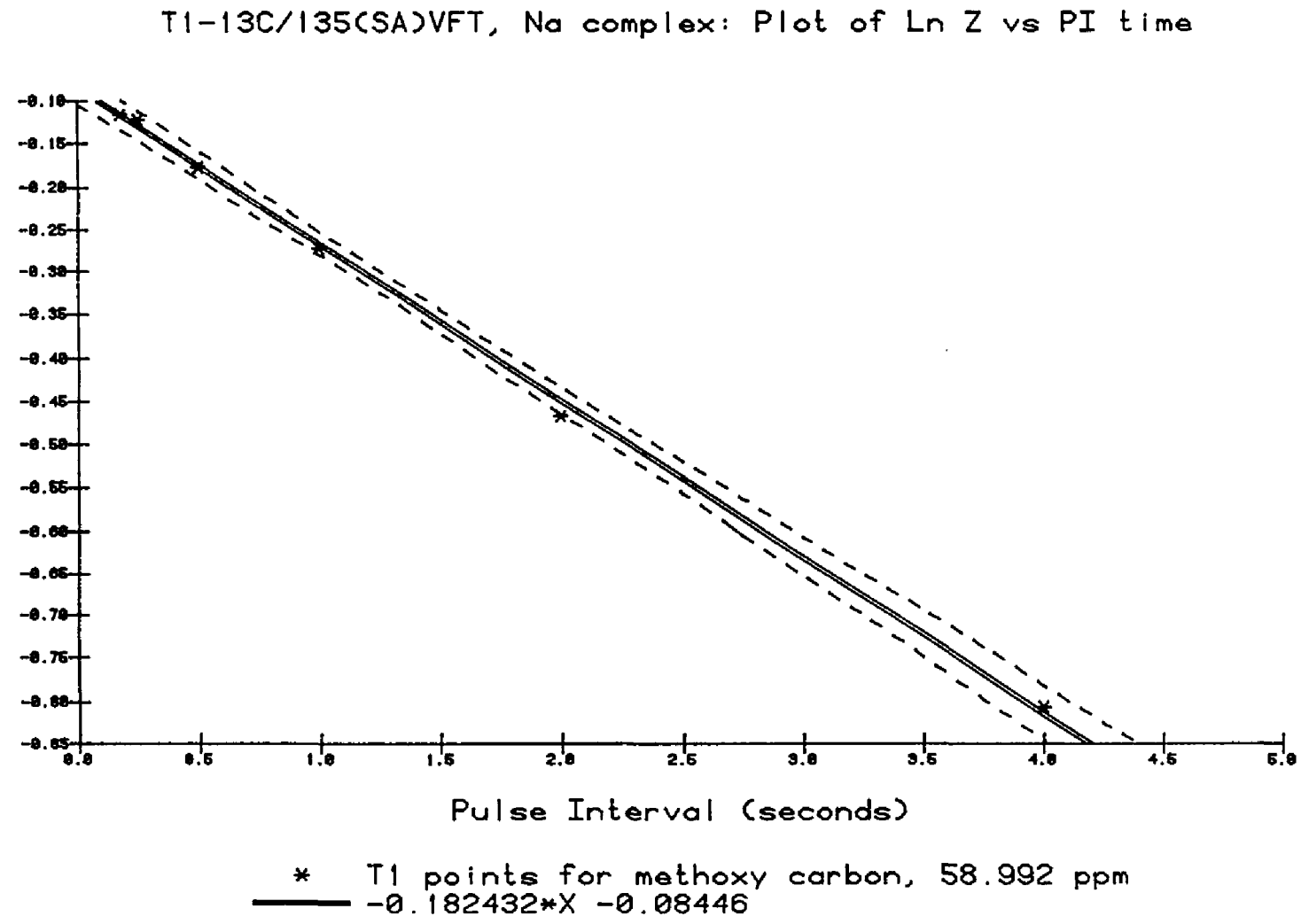

E) Plot of ln Z vs PI for C-3' in complexed 3

APPENDIX E.

Tabulated Results for NOE Measurements

(at 91 MHz, using a Bruker AM360 spectrometer)

Table 41: ^{13}C-NOE Results for T_1 sample of Uncomplexed 3 in $CDCl_3$.

Carbon #	^{13}C Shift (ppm)	Fully Coupled Intensity	Inverse Gated Intensity	NOE[a]	% NOE
C-1,3,5	74.11	143.7	50.5	2.85	96
C-2,4,6	38.28	133.3	48.5	2.75	92
C-1'	72.48[b]	147.7	48.7	3.03	102
C-2'	67.93[b]	147.7	48.2	3.06	103
C-3'	59.37	148.1	49.6	2.98	100

a- Theoretical maximum = 2.98 for ^{13}C nucleus.
b- Chemcial shift assignments tentative.

Table 42: ^{13}C-NOE Results for T_1 sample of Complexed 3 with $NaBPh_4$ in $CDCl_3$.

Carbon #	^{13}C Shift (ppm)	Fully Coupled Intensity	Inverse Gated Intensity	NOE[a]	% NOE
C-1,3,5	74.11	11.12	4.13	2.69	90
C-2,4,6	31.18	9.52	3.84	2.48	83
C-1'	72.20[b]	10.75	3.90	2.75	92
C-2'	67.83[b]	11.09	4.03	2.75	92
C-3'	59.50	10.82	3.96	2.73	92

a- Theoretical maximum = 2.98 for ^{13}C nucleus.
b- Chemcial shift assignments tentative.

APPENDIX F.

Tentative ^{13}C NMR Chemical Shift Assignments for C-1' and C-2' in Ligand 3

The tentative chemical shift assignments [163] of the C-1' and C-2' positions have been made based on equations and parameters [164] developed for calculation alkane ^{13}C shifts. The oxygen effects have been neglected. The theoretical chemical shift difference was obtained by adding the proper number of alpha, beta, and gamma substituent effects for each carbon position (equation 47) and finding the net difference, $^{\Delta}\delta_{C'(1-2)}$ using eq 48.

$$\delta_C = -2.1 \text{ ppm} + (9.1)A + (9.4)B + (-2.5)Y \qquad (47)$$

Where: A = # Alpha substituents
B = # Beta substituents
Y = # Gamma substituents
Substituent effects reported in ppm's

For C-1' A = 2 (1 carbon, 1 oxygen)
B = 2 (1 carbon, 1 oxygen)
Y = 3 (3 carbons)

For C-2' A = 2 (1 carbon, 1 oxygen)
B = 2 (1 carbon, 1 oxygen)
Y = 1 (1 carbon)

$$^{\Delta}\delta_{C'(1-2)} = \delta_{C-1'} - \delta_{C-2'} \qquad (48)$$

Thus there are two more gamma substituent effects for the C-1' position relative to C-2', and should be shifted upfield, -5 ppm and correspondes nicely with the experimentally chemical shift difference.

Calculated: $^{\Delta}\delta_{C'(1-2)} = 2(-2.5 \text{ ppm}) = -5.0 \text{ ppm}$

Experimental: $^{\Delta}\delta_{C'(1-2)} = 67.57 \text{ ppm} - 72.12 \text{ ppm}$
$= -4.55 \text{ ppm}$

The same rational was used to tentatively assign C-1' and C-2' in the sodium complex (Na^{+}-3).

APPENDIX G.

Spectra for Compounds

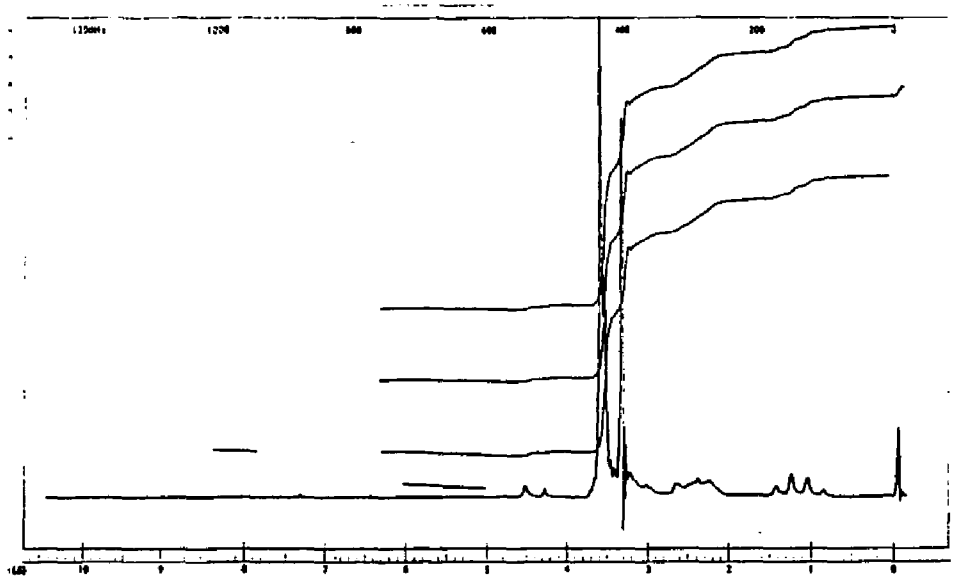

^{1}H NMR ($CDCl_3$)

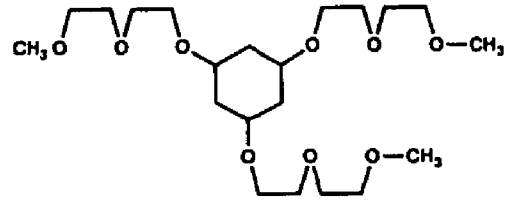

^{13}C NMR ($CDCl_3$)

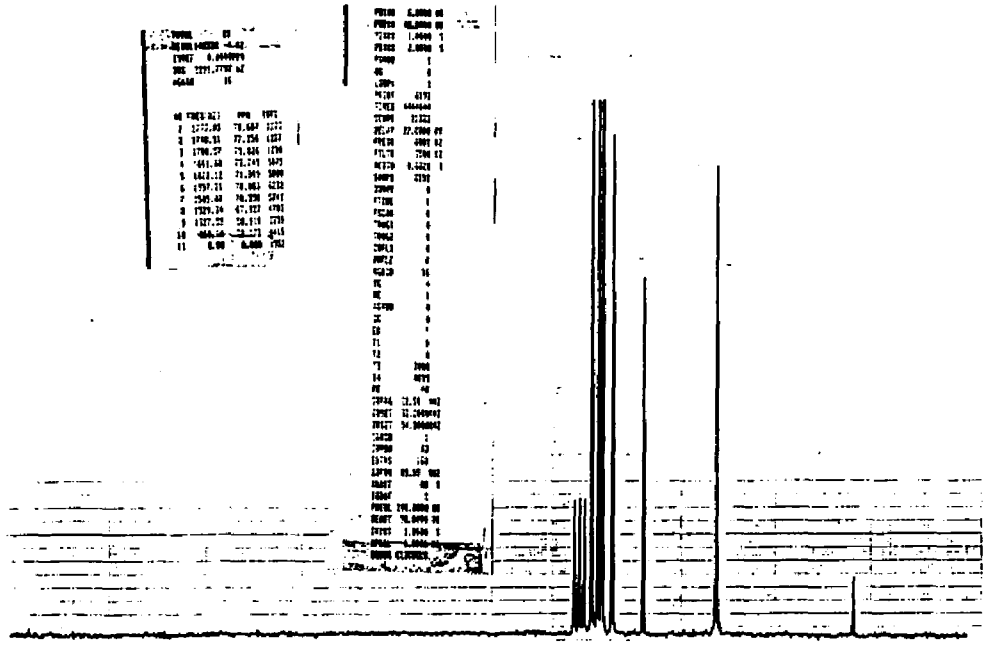

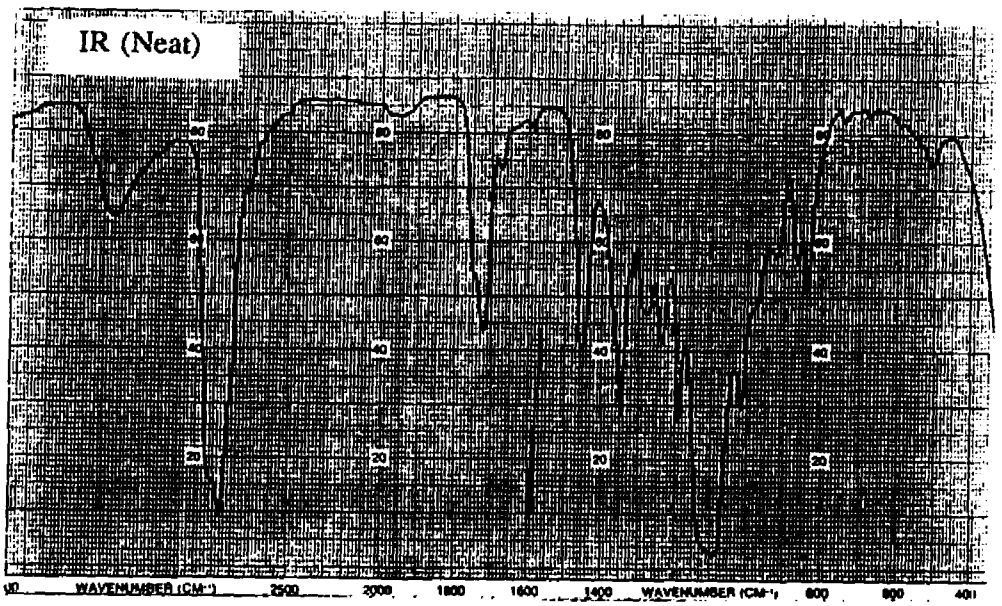
IR (Neat)
WAVENUMBER (CM⁻¹)
2500
2000
1800
1600
1400
WAVENUMBER (CM⁻¹)
800
600
400

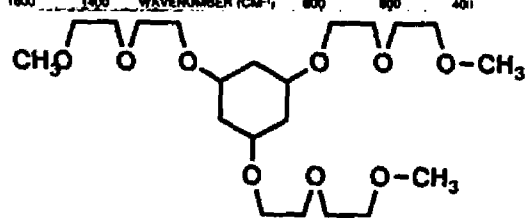
CH3O
O
O
O
O
O
O-CH3
O
O
O-CH3

Mass Spec.

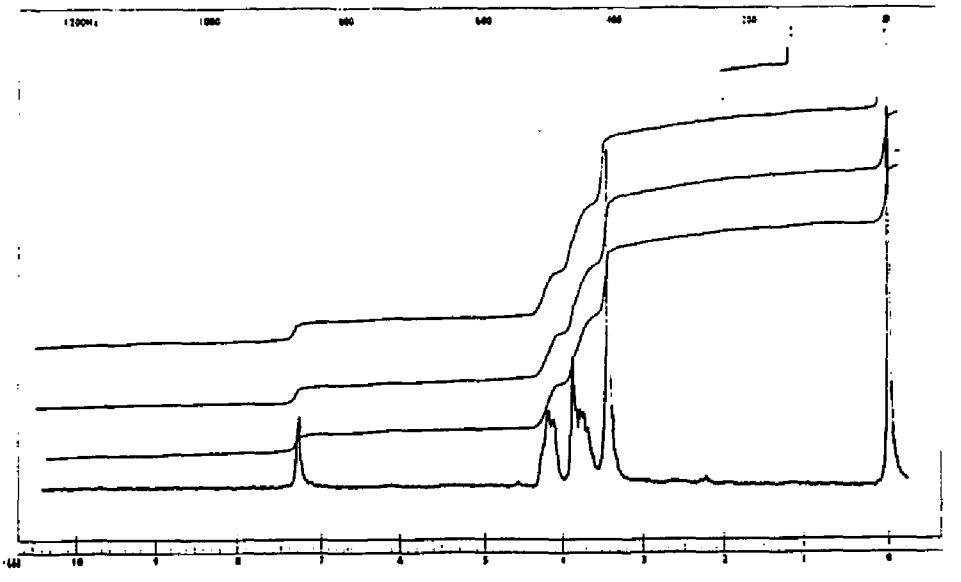

^{1}H NMR ($CDCl_3$)

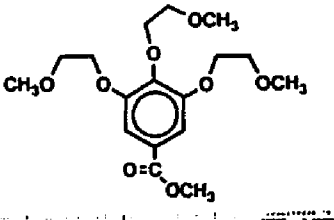

^{13}C NMR ($CDCl_3$)

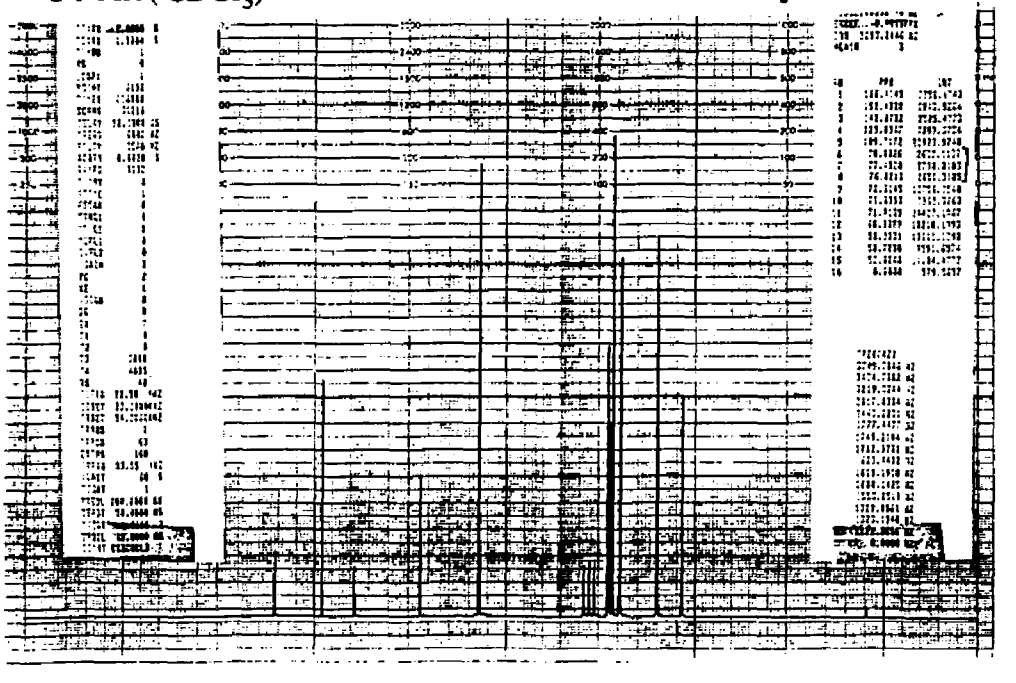

Mass Spec.

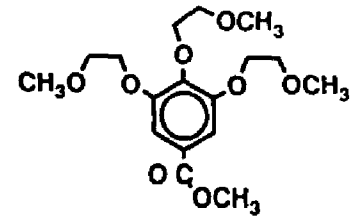

M/Z	REL INT
58	39
59	1000
60	46
66	11
69	10
152	11
165	14
179	17
184	50
195	19
198	13
210	107
211	17
242	30
268	15
300	71
314	13
327	20
358	214

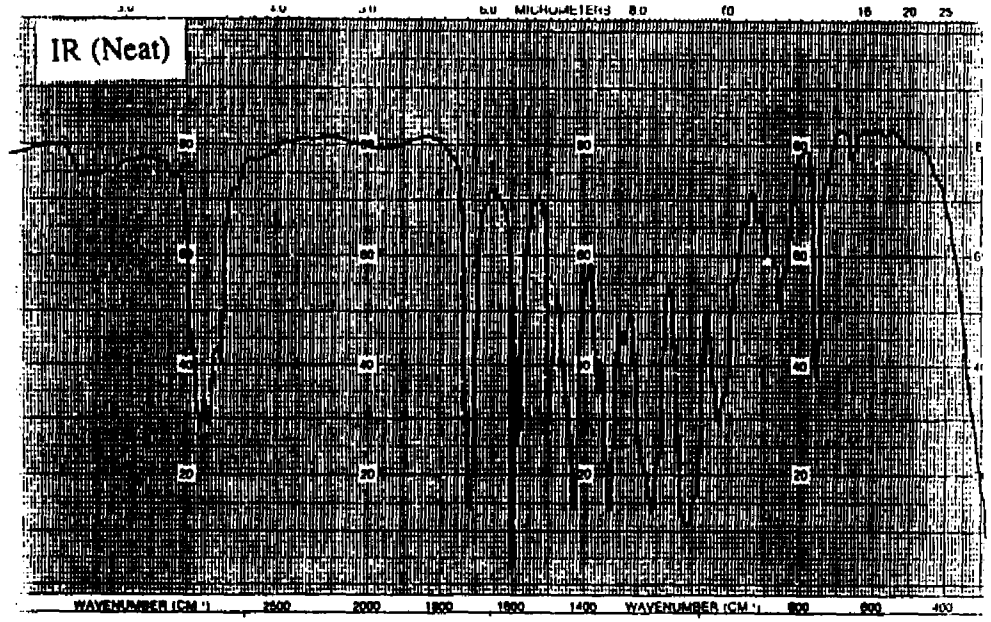

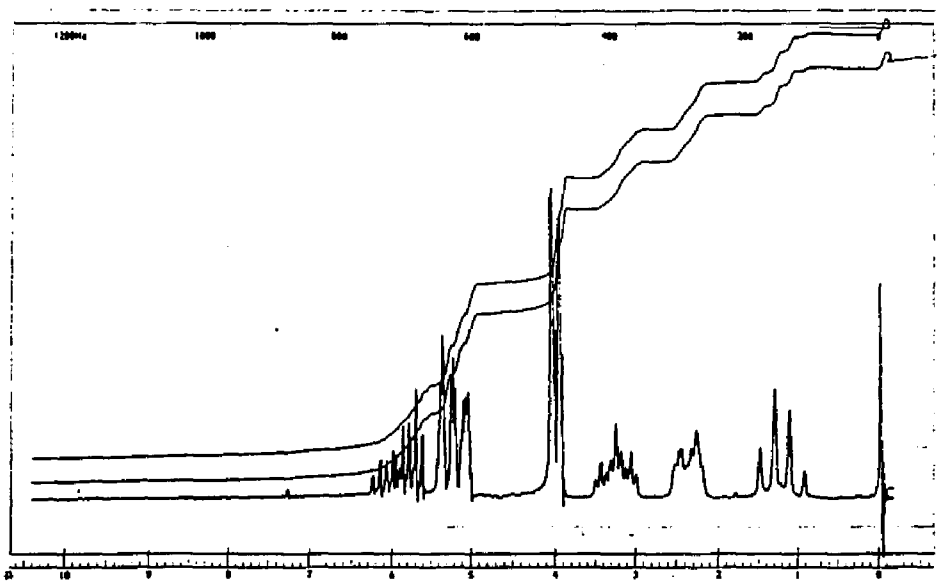

^{1}H NMR ($CDCl_3$)

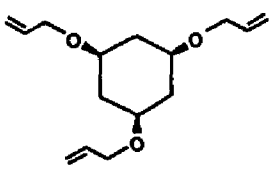

^{13}C NMR ($CDCl_3$)

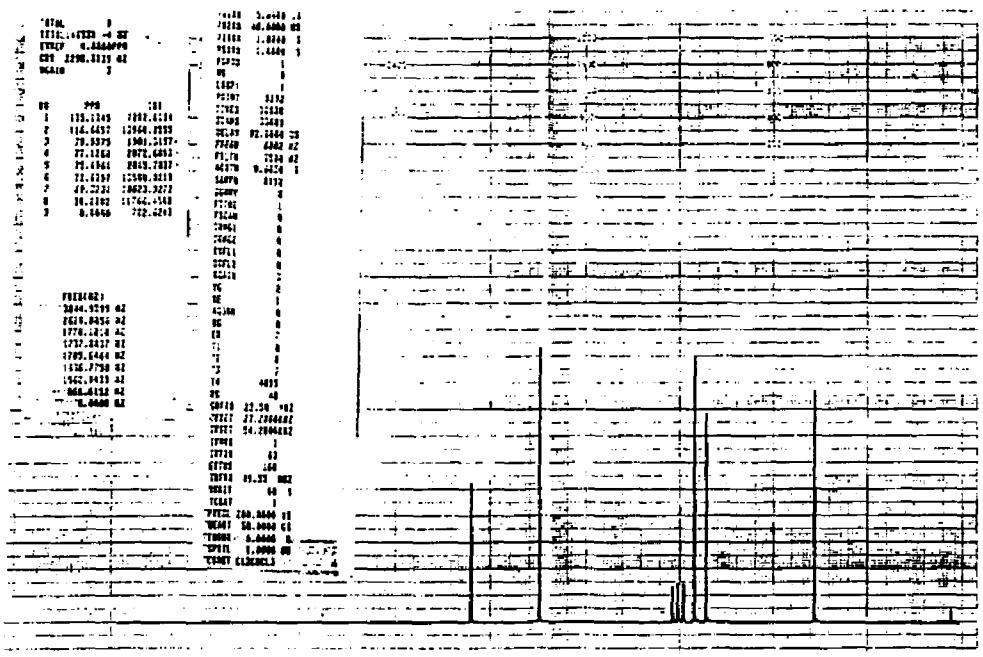

IR (Neat)

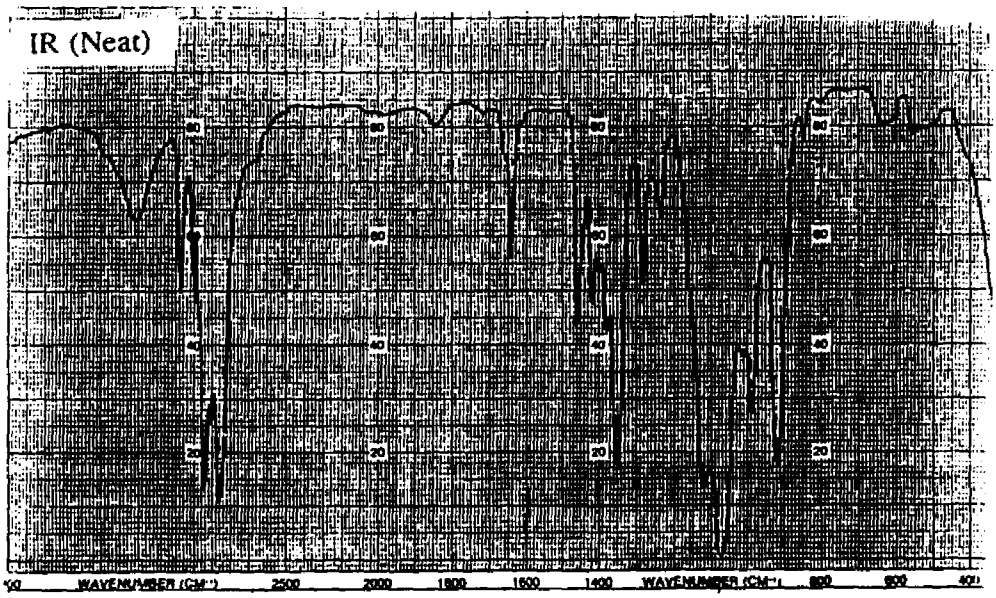

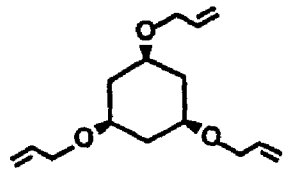

Mass Spec.

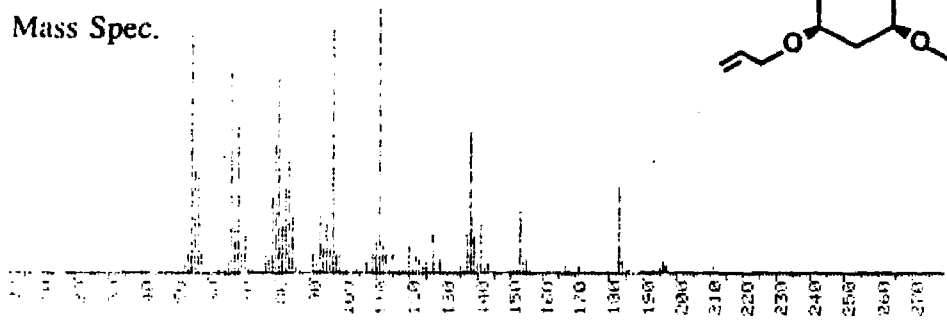

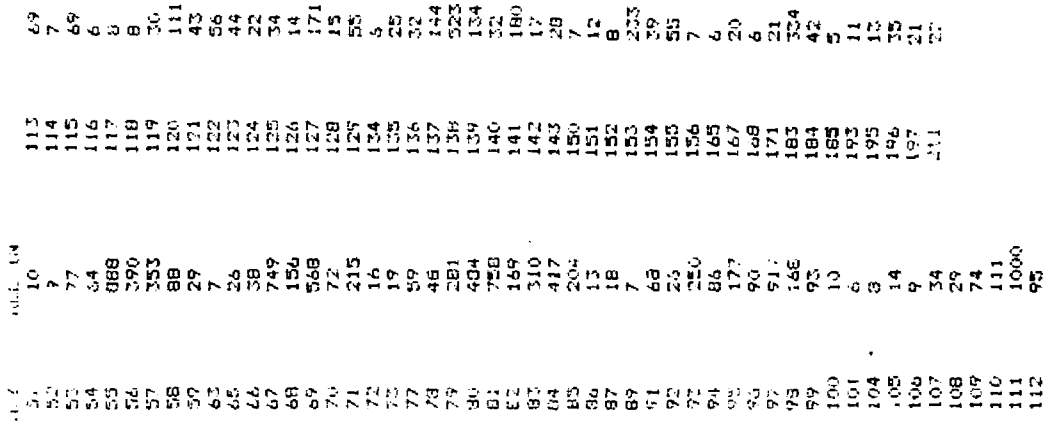

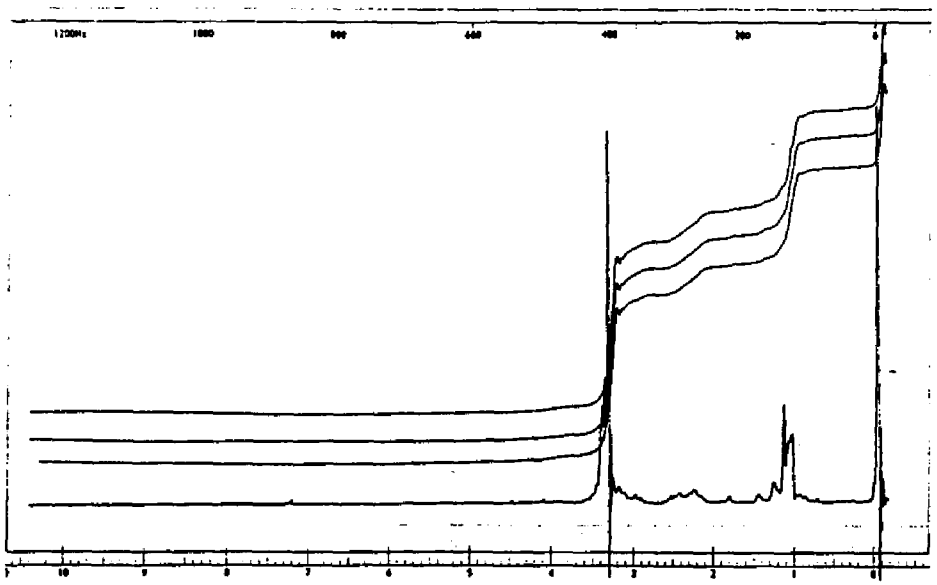

^{1}H NMR ($CDCl_3$)

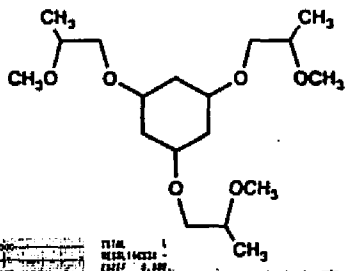

^{13}C NMR ($CDCl_3$)

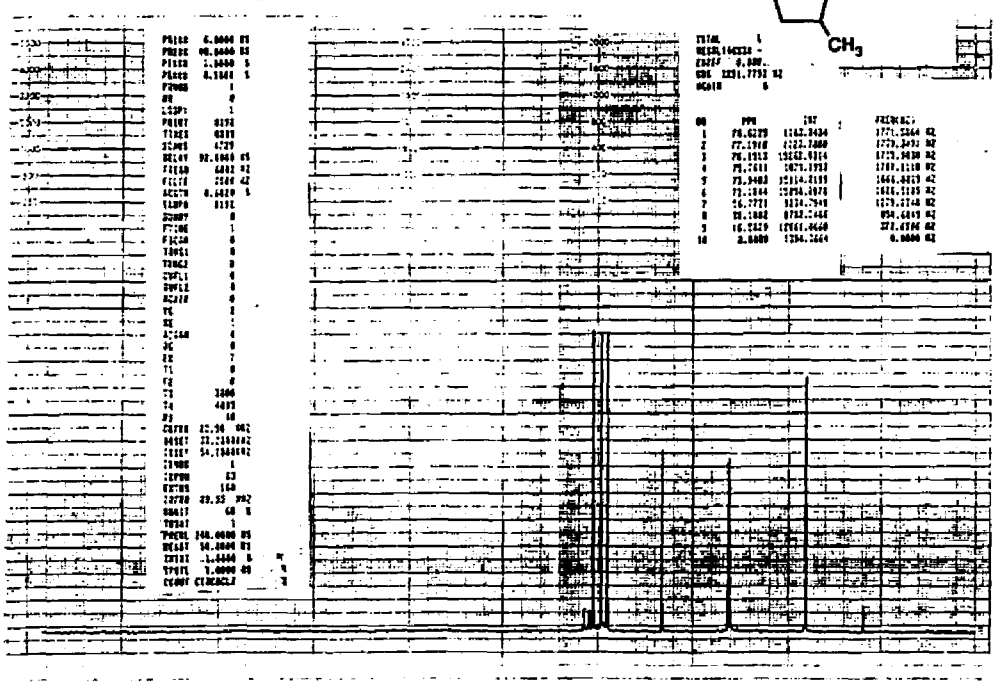

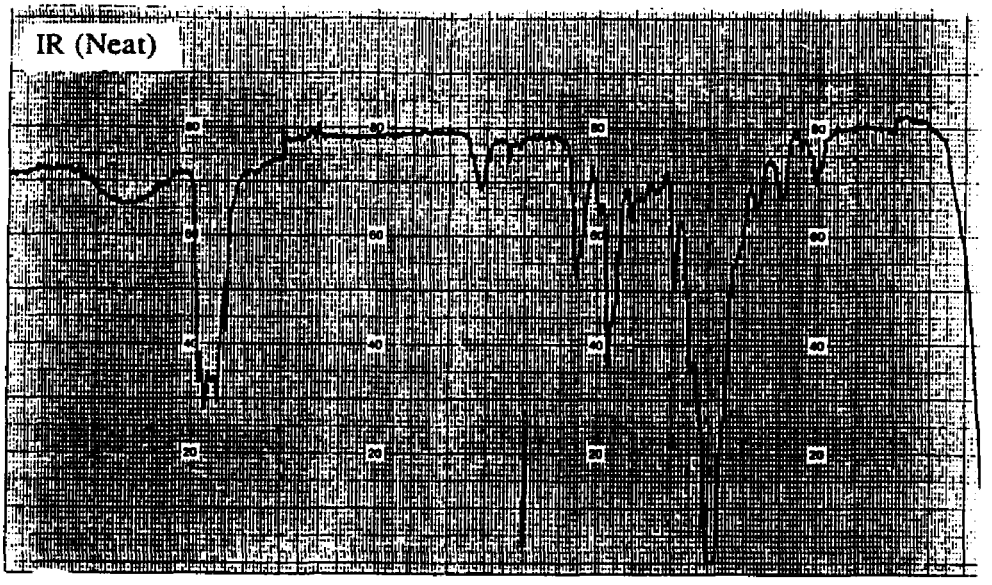

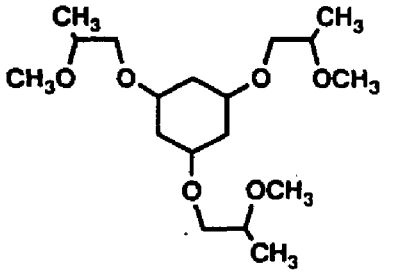

Mass Spec.

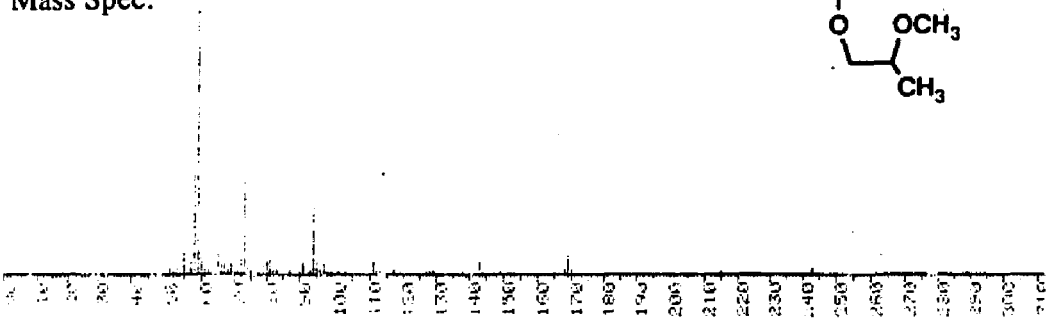

M/Z	REL INT
51	20
52	7
53	25
54	8
55	81
56	17
57	83
58	371
59	1000
60	56
61	16
62	13
63	16
64	16
65	71
66	72
67	37
68	18
69	35
70	7
71	20
72	67
73	351
74	25
75	17
76	6
77	10
78	6
79	38
80	51
81	52
82	13
83	20
84	22
85	18
86	12
87	6
90	66
91	18
93	252
94	44
95	13
96	35
97	9
98	6
99	7
101	10
105	46
111	7
112	10
113	12
117	11
119	8
127	11
128	12
129	16
138	54
143	6
144	8
149	7
153	18
168	66
169	12
170	6
215	20
243	7
289	

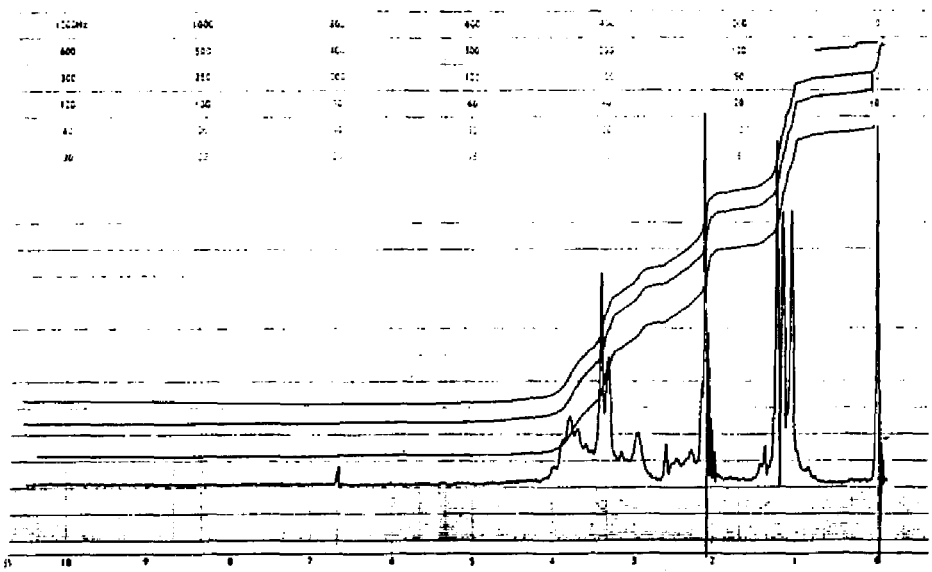

^{1}H NMR (DMK-d_6)

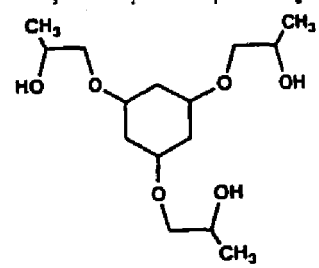

^{13}C NMR (DMK-d_6)

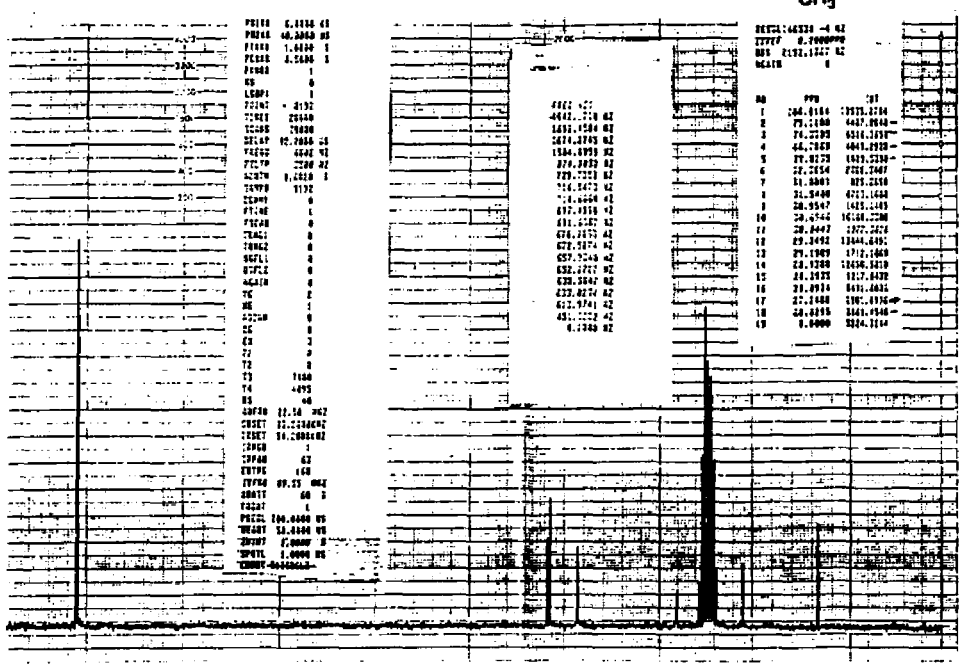

IR (Neat)

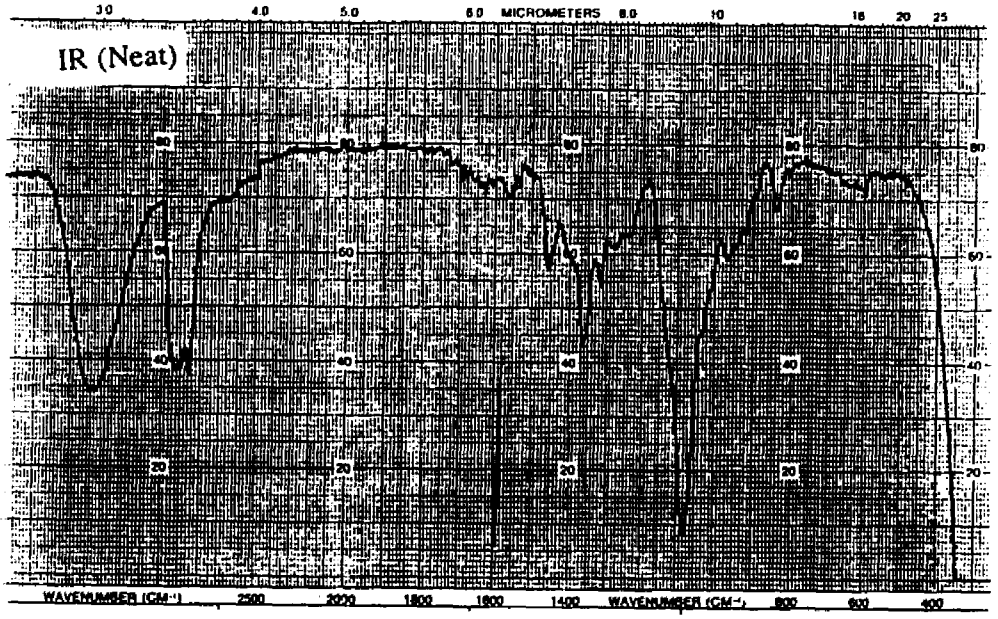

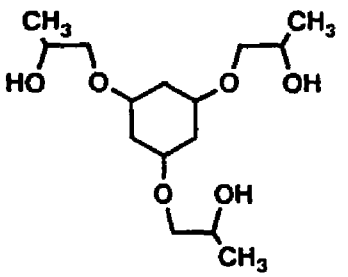

Mass Spec.

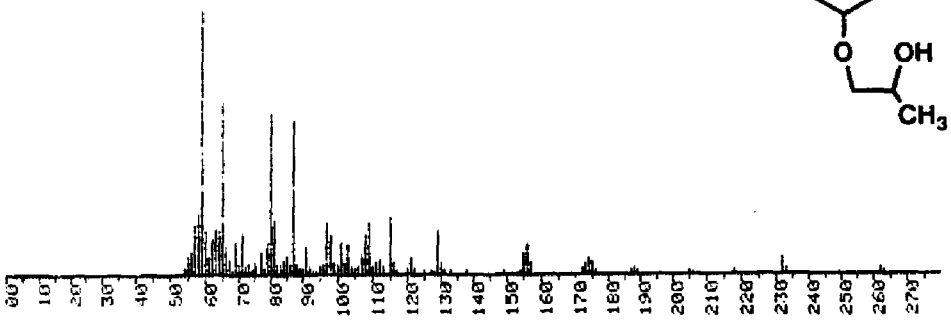

M/Z	REL INT
54	19
55	85
56	83
57	186
58	231
59	1000
60	164
61	70
62	133
63	168
64	164
65	651
66	102
67	55
68	18
69	122
70	39
71	158
72	26
73	36
74	12
75	48
77	78
78	22
79	121
80	604
81	209
82	37
83	40
84	49
85	65
86	35
87	582
88	39
89	23
90	23
91	101
92	27
93	15
94	13
95	30
96	40
97	189
98	146
99	42
100	34
101	117
102	48
103	112
104	26
105	21
106	27
107	72
108	151
109	193
110	33
111	47
112	50
113	32
115	215
116	41
117	12
120	21
121	59
122	20
125	15
127	14
128	11
129	163
130	47
131	18
133	13
138	14
149	12
153	11
154	16
155	79
156	112
157	47
172	20
173	35
174	60
175	47
176	12
187	19
188	30
189	15
205	16
206	11
218	164
232	57
233	25
262	24
263	12

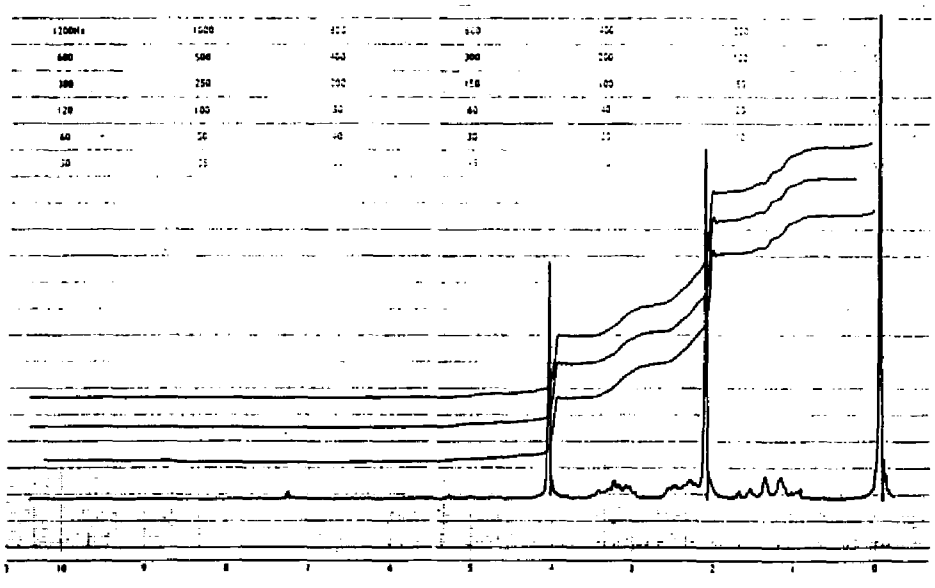

^{1}H NMR ($CDCl_3$)

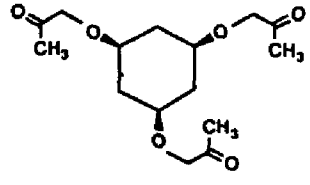

^{13}C NMR ($CDCl_3$)

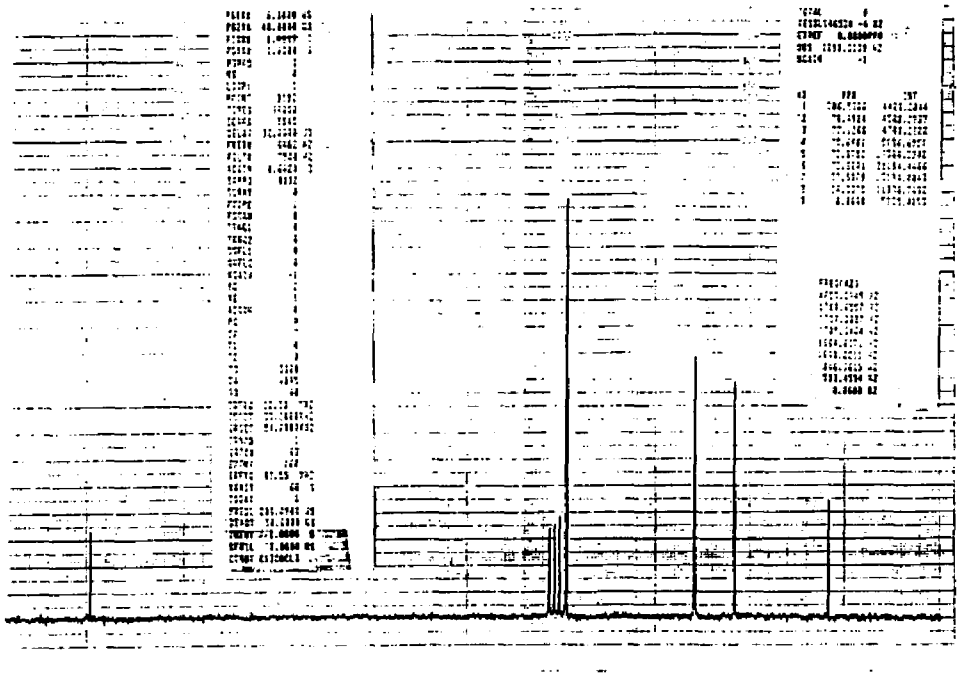

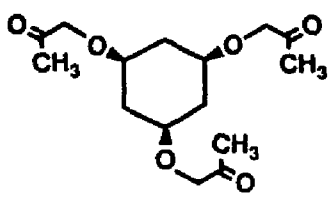

Mass Spec.

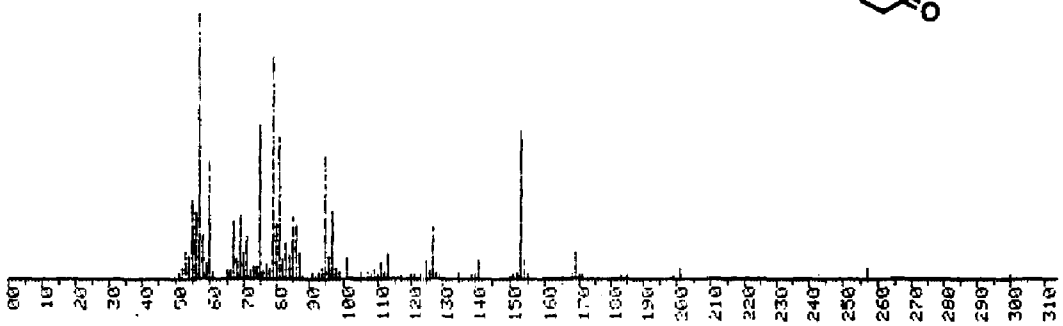

M/Z	REL INT
51	27
52	34
53	94
54	82
55	295
56	252
57	1000
58	165
59	59
60	444
61	22
65	30
66	26
67	213
68	77
69	234
70	93
71	155
72	29
73	43
74	45
75	501
76	30
77	54
78	36
79	846
80	205
81	534
82	77
83	136
84	86
85	223
86	202
87	75
88	11
91	22
92	11
93	24
94	38
95	360
96	79
97	251
98	40
99	24
101	74
105	19
107	24
108	18
109	29
110	14
111	60
112	24
113	92
117	11
119	11
120	14
121	16
123	16
125	67
126	27
127	193
128	20
129	12
139	22
139	14
146	15
141	70
150	11
151	15
152	19
153	555
154	68
155	12
168	16
169	99
170	14
171	12
183	17
185	13
199	11
201	76
243	15
257	35
300	13

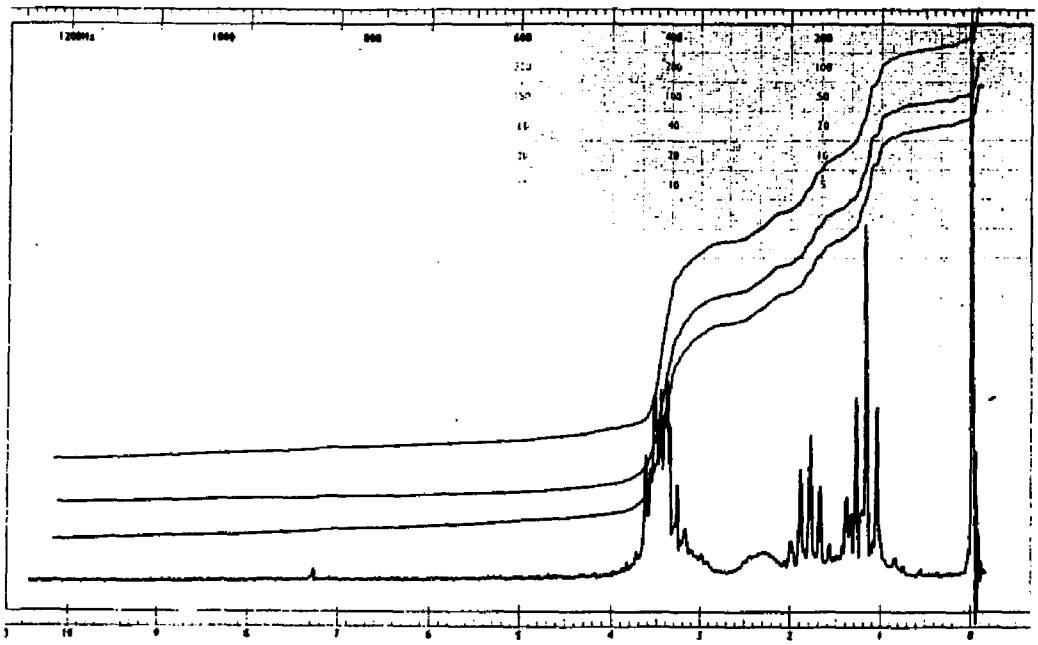

^{1}H NMR ($CDCl_3$)

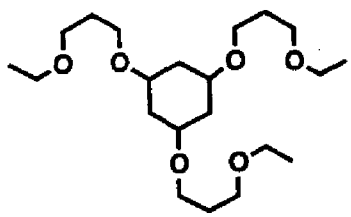

^{13}C NMR ($CDCl_3$)

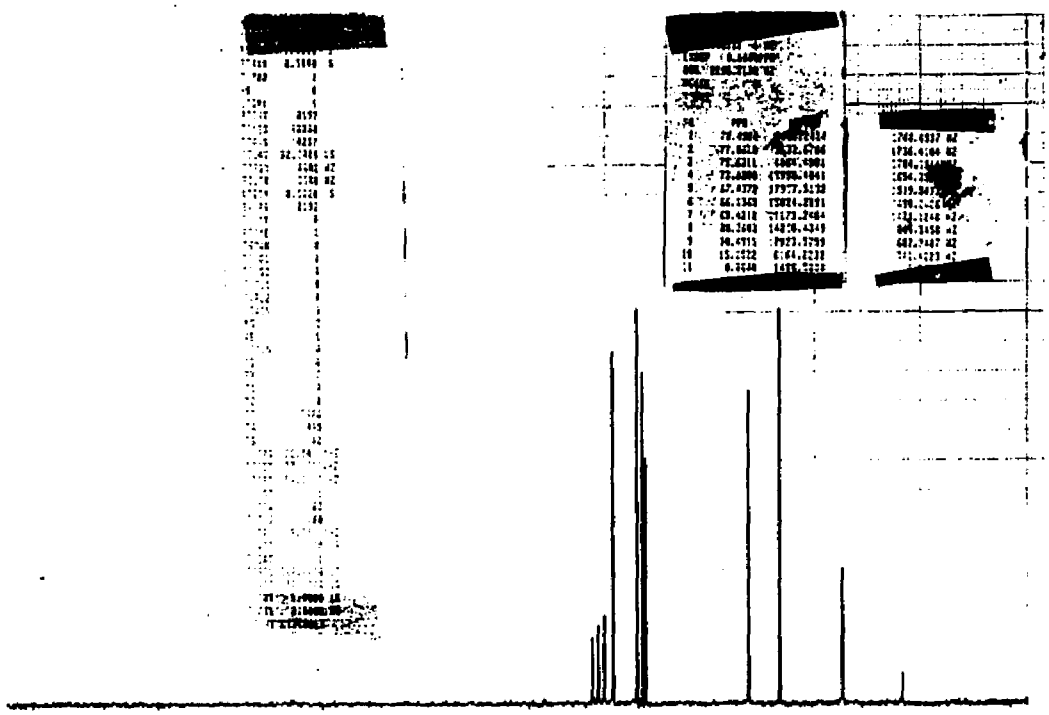

IR (Neat)

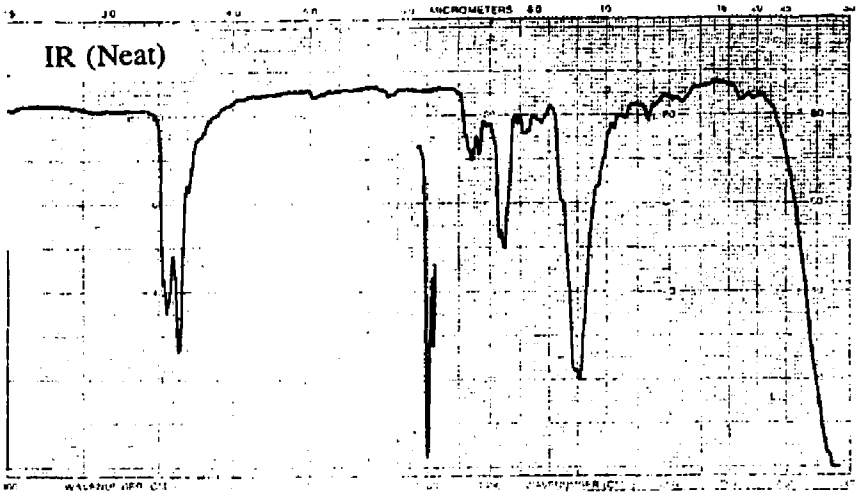

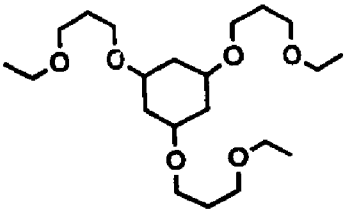

Mass Spec.

M/Z	REL INT
53	20
54	19
55	116
56	21
57	156
58	322
59	952
60	44
67	75
68	26
69	63
70	53
71	300
72	45
73	43
74	12
77	30
78	56
79	203
80	175
81	35
82	41
83	36
84	205
85	413
86	1000
87	258
88	33
89	15
91	16
92	37
93	294
94	294
95	197
96	38
97	45
98	24
101	155
102	543
103	30
104	12
105	13
106	34
111	74
113	52
115	15
117	20
124	14
126	19
127	18
130	16
131	48
135	21
137	16
138	77
139	15
141	17
143	422
144	42
149	13
153	21
155	19
156	14
157	127
158	16
161	14
162	135
163	67
181	58
185	26
186	12
199	74
200	13
201	14
203	35
245	20
284	15
288	83
289	17
305	102
306	28

APPENDIX H.

[1] NMR Complexation Experiment Spectra

^{1}H NMR / 51.0 mg

(0.00 Equiv. $NaBPh_4/CDCl_3$)

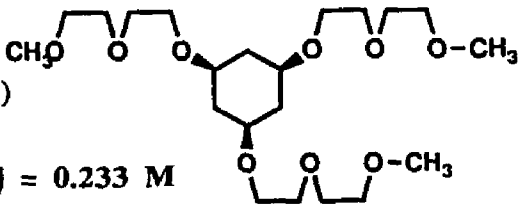

[L] = 0.233 M

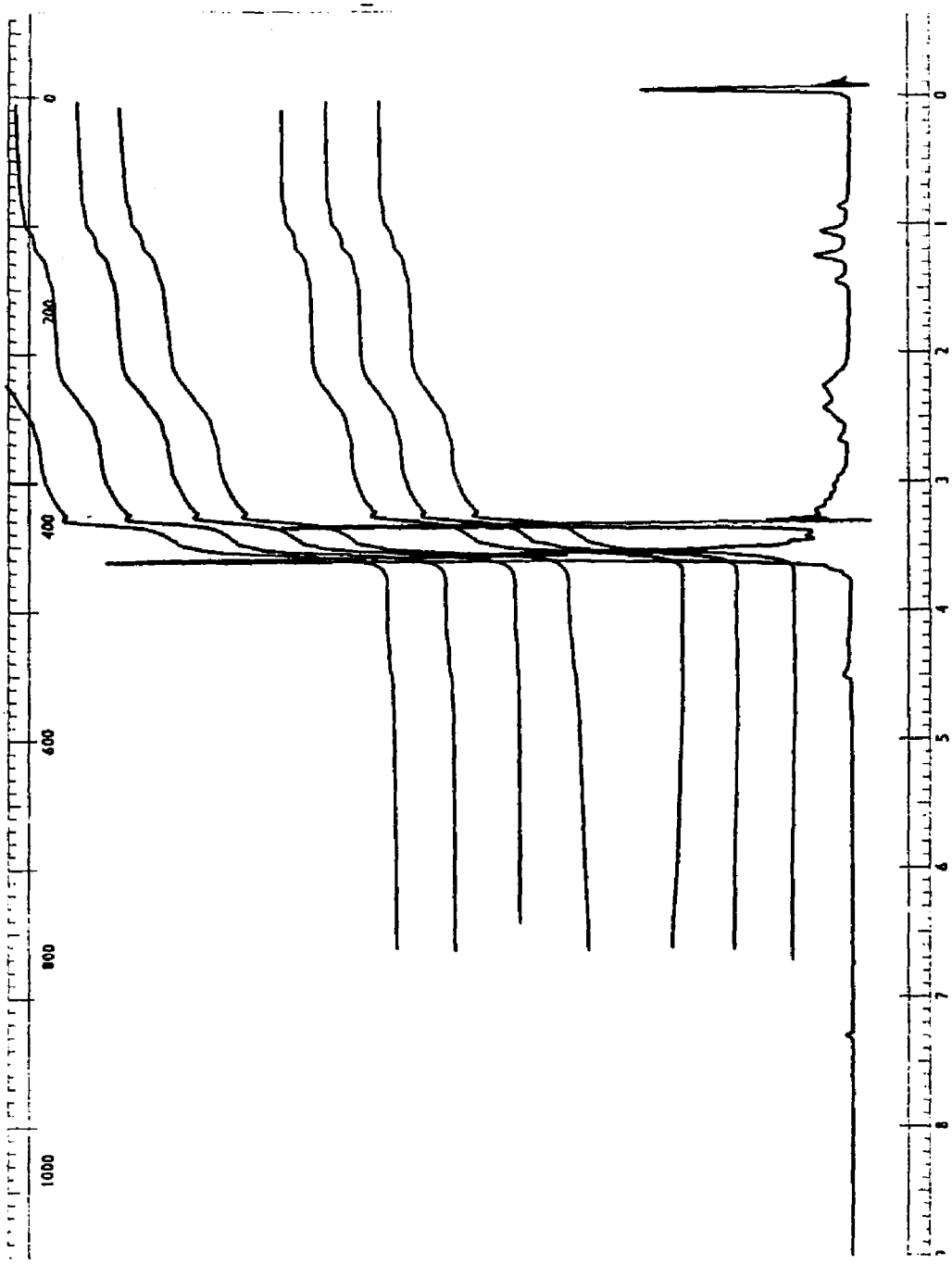

^{1}H NMR / 51.0 mg

(0.50 Equiv. $NaBPh_4/CDCl_3$)

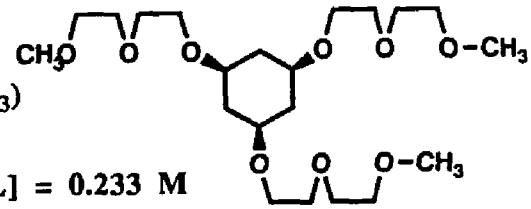

[L] = 0.233 M

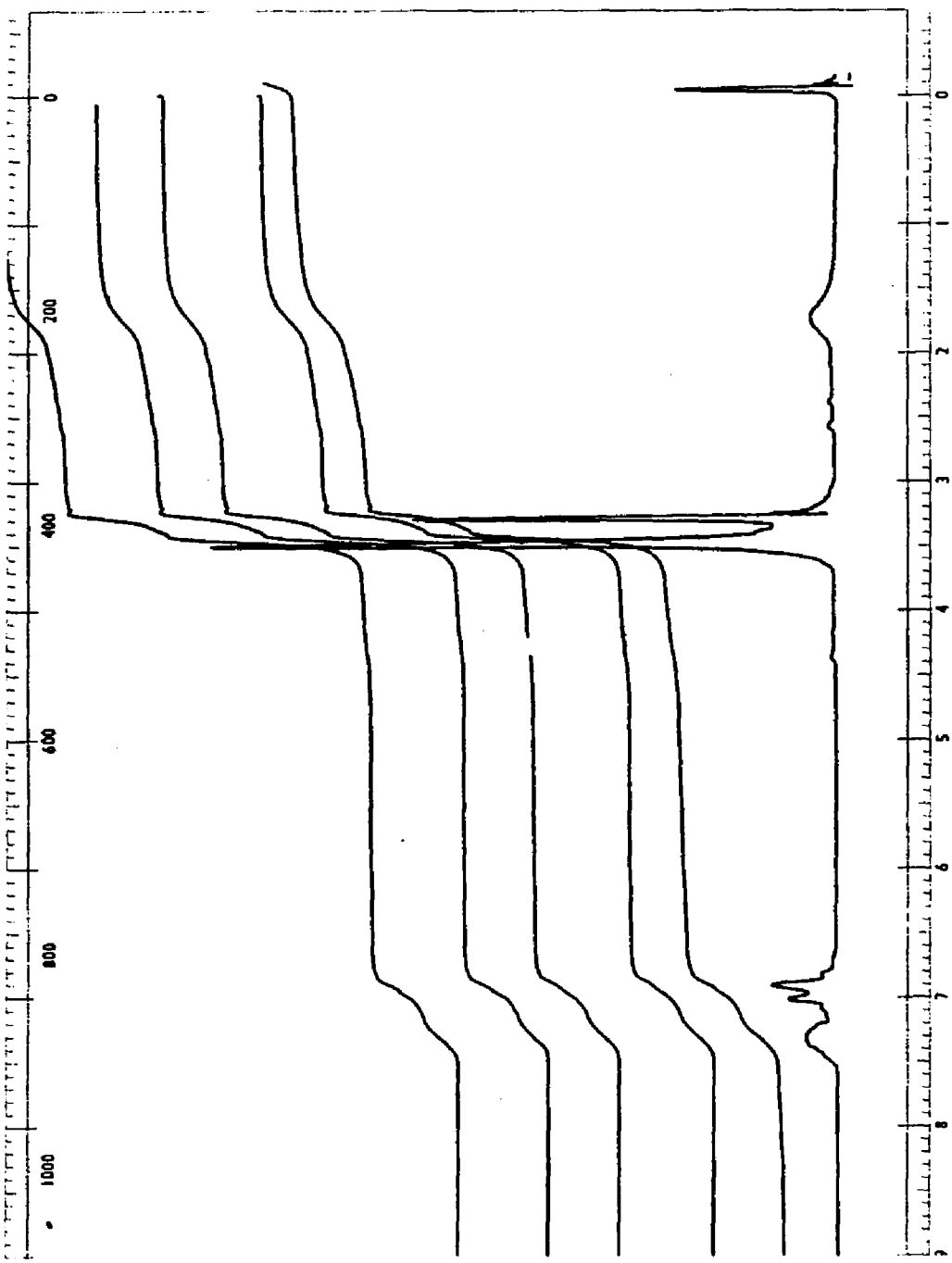

^{1}H NMR / 51.0 mg

(1.25 Equiv. $NaBPh_4/CDCl_3$)

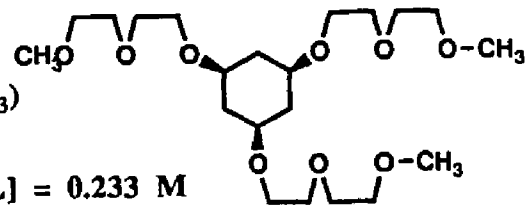

[L] = 0.233 M

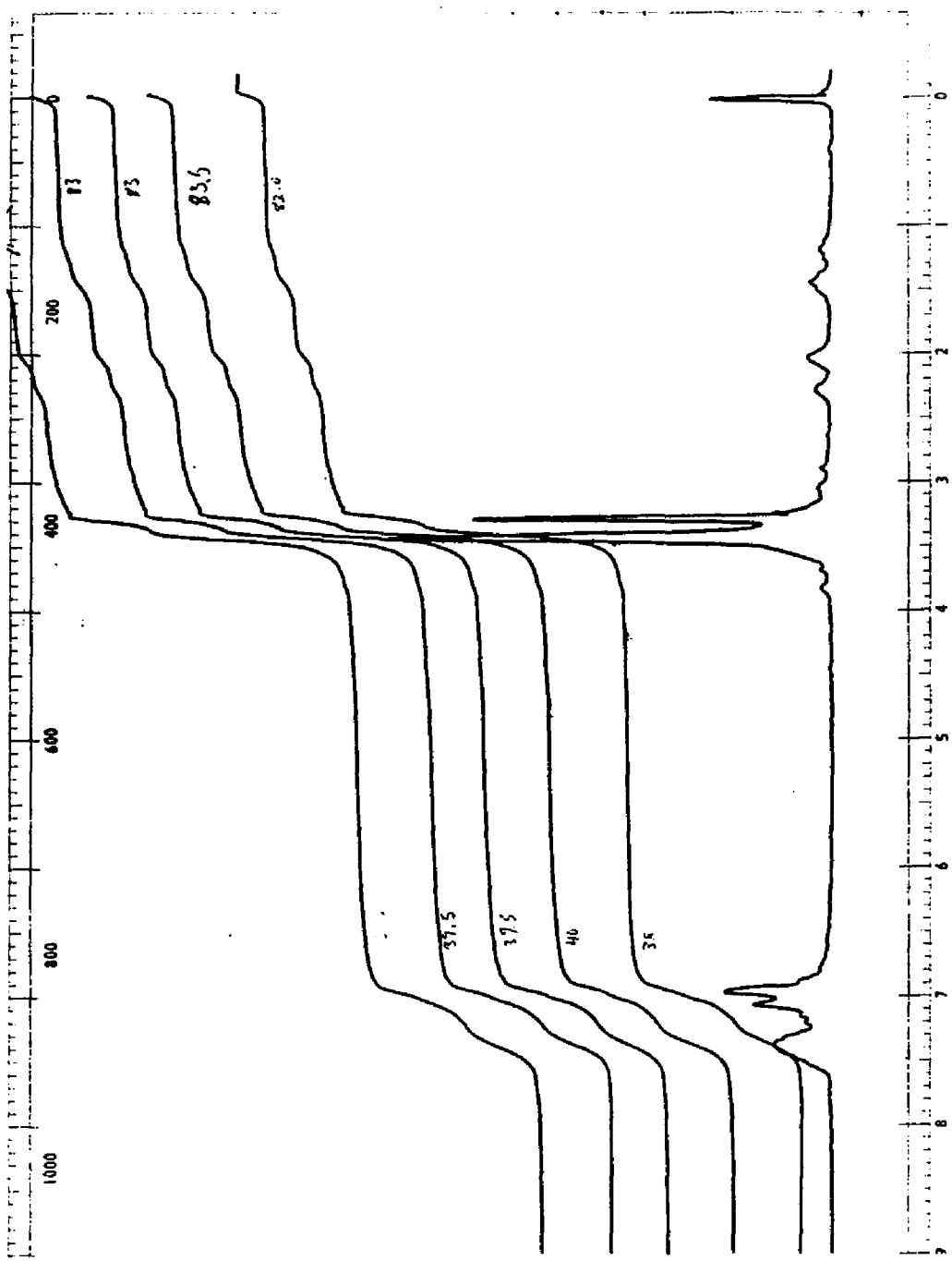

^{1}H NMR / 34.9 mg

(0.00 Equiv. $NaBPh_4/CDCl_3$)

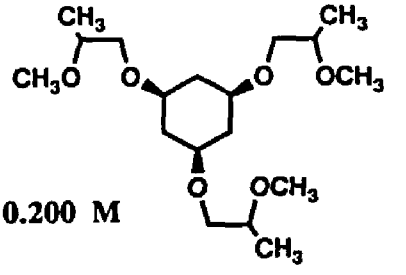

[L] = 0.200 M

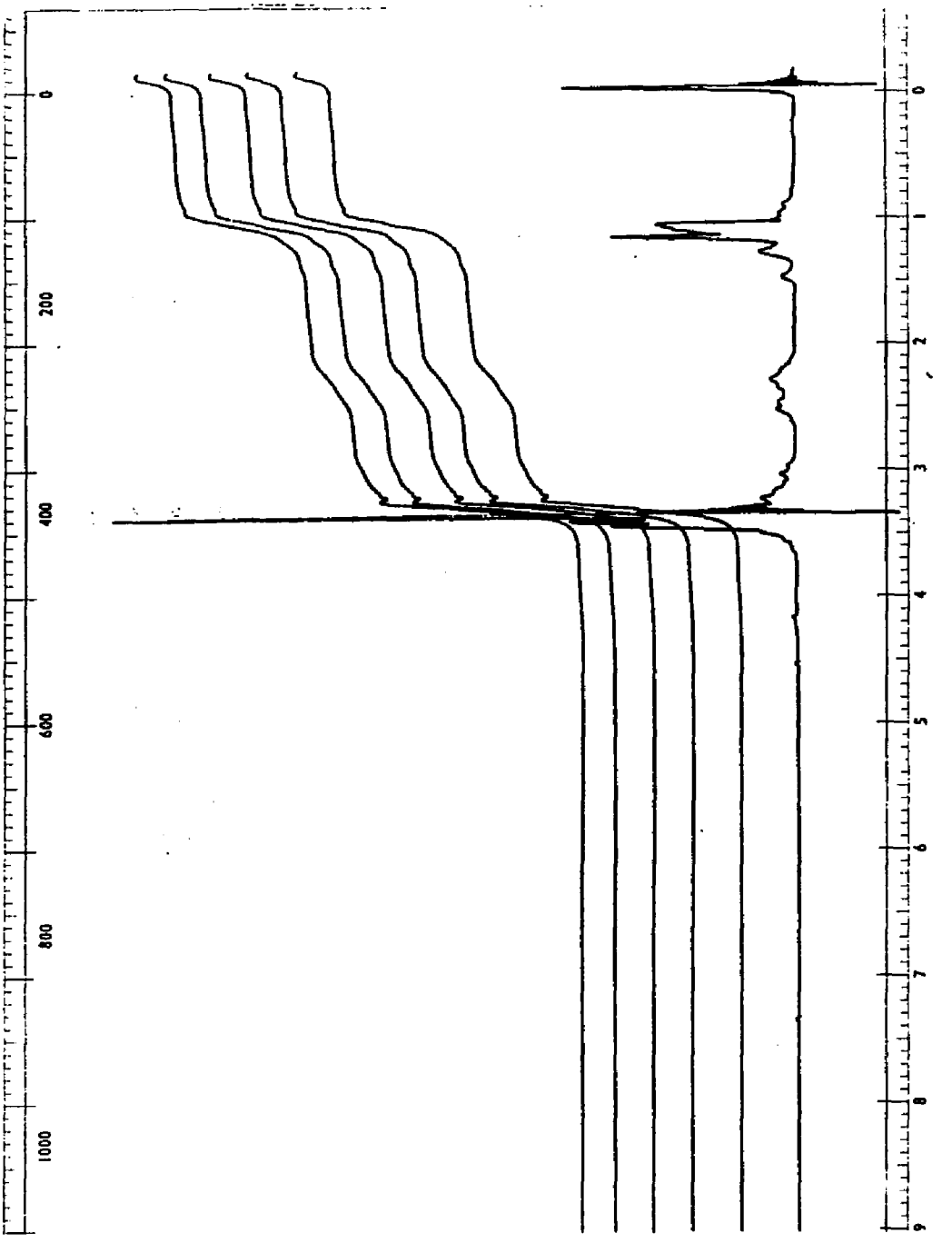

^{1}H NMR / 34.9 mg

(0.52 Equiv. $NaBPh_4/CDCl_3$)

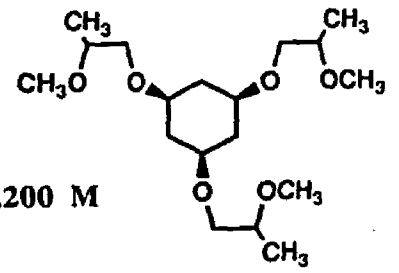

[L] = 0.200 M

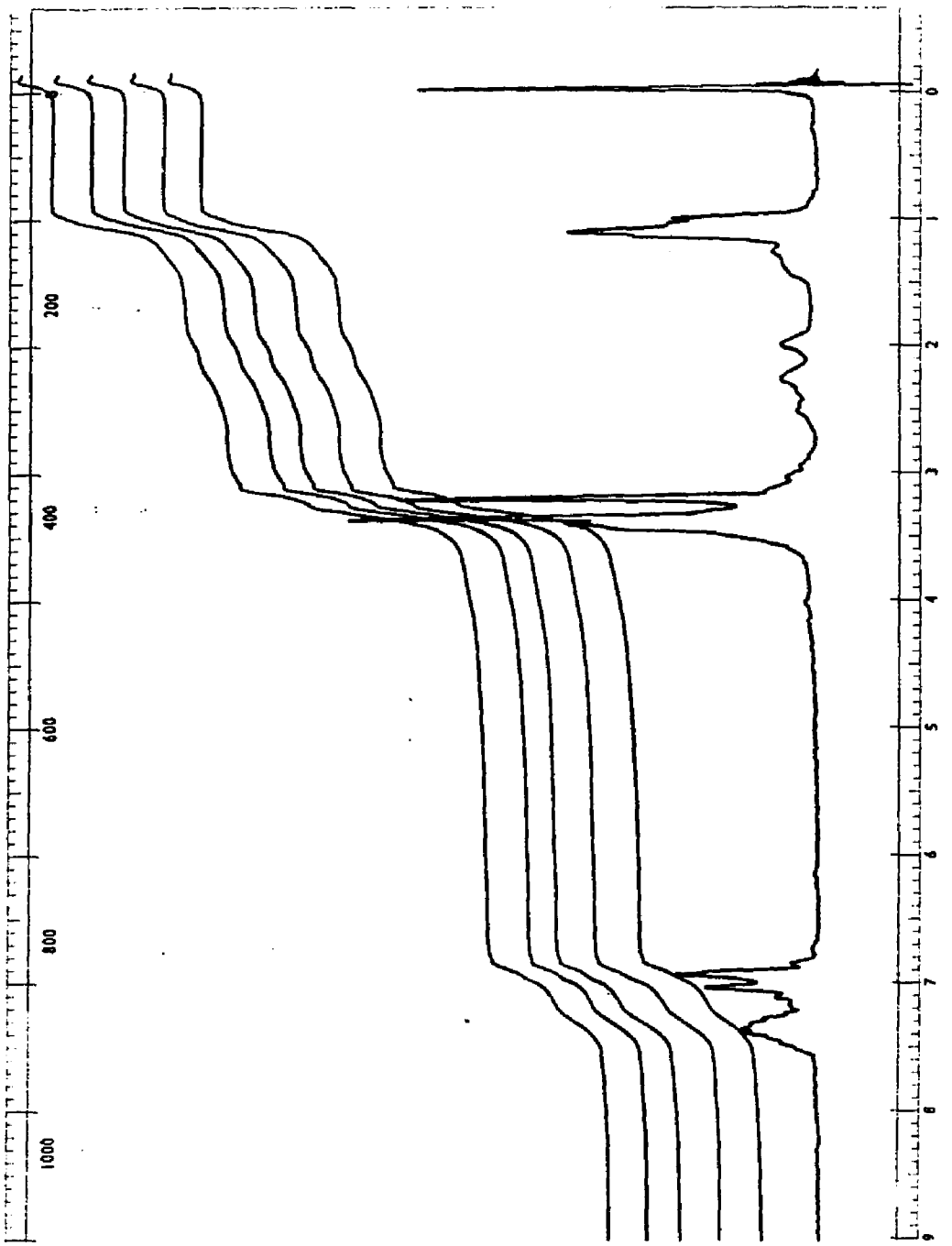

^{1}H NMR / 34.9 mg

(1.05 Equiv. $NaBPh_4/CDCl_3$)

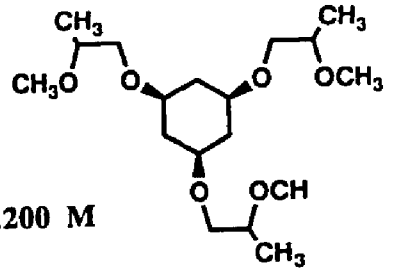

[L] = 0.200 M

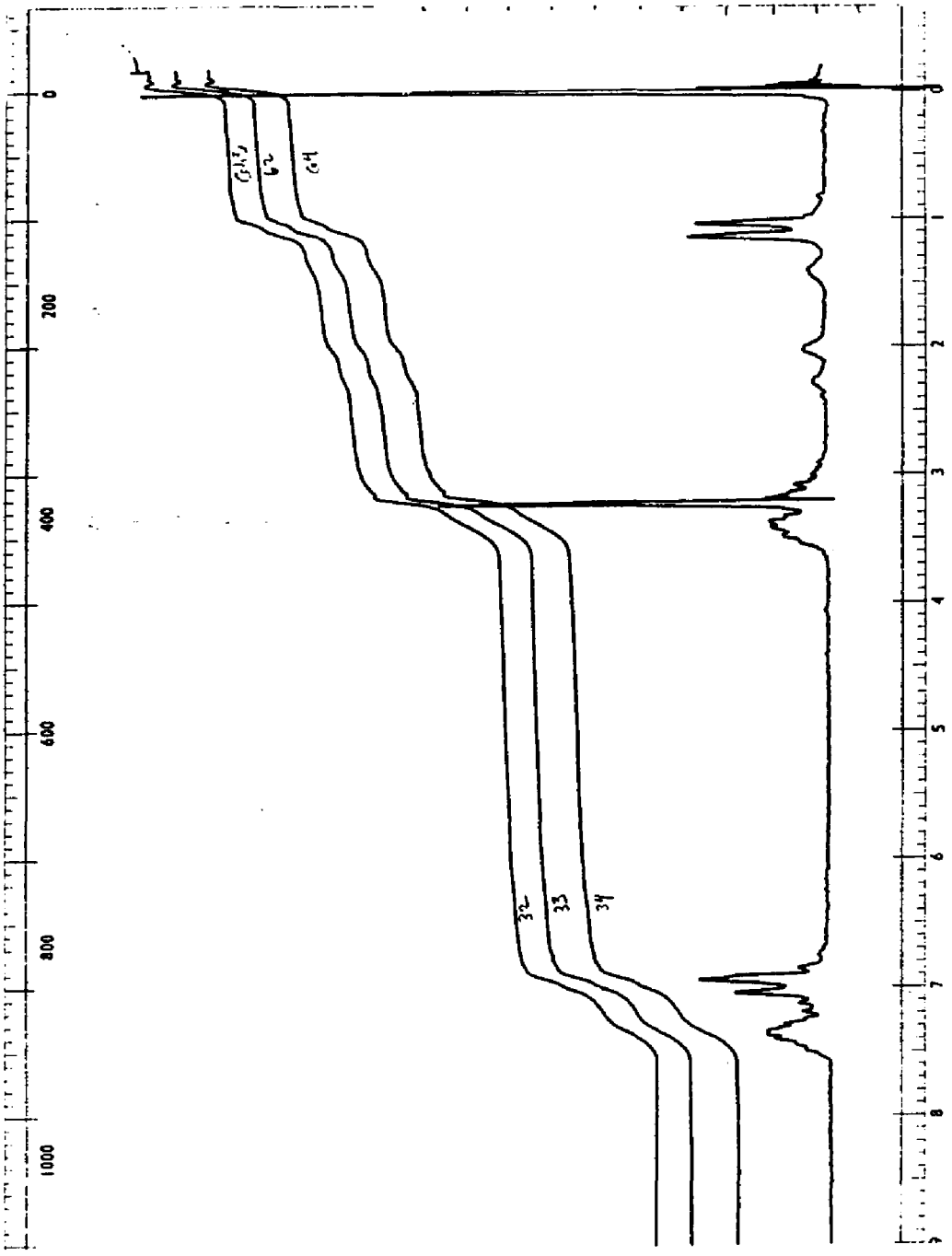

^{1}H NMR / 31.5 mg

(0.00 Equiv. $NaBPh_4/CDCl_3$)

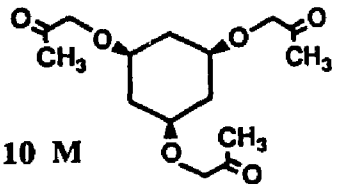

[L] = 0.210 M

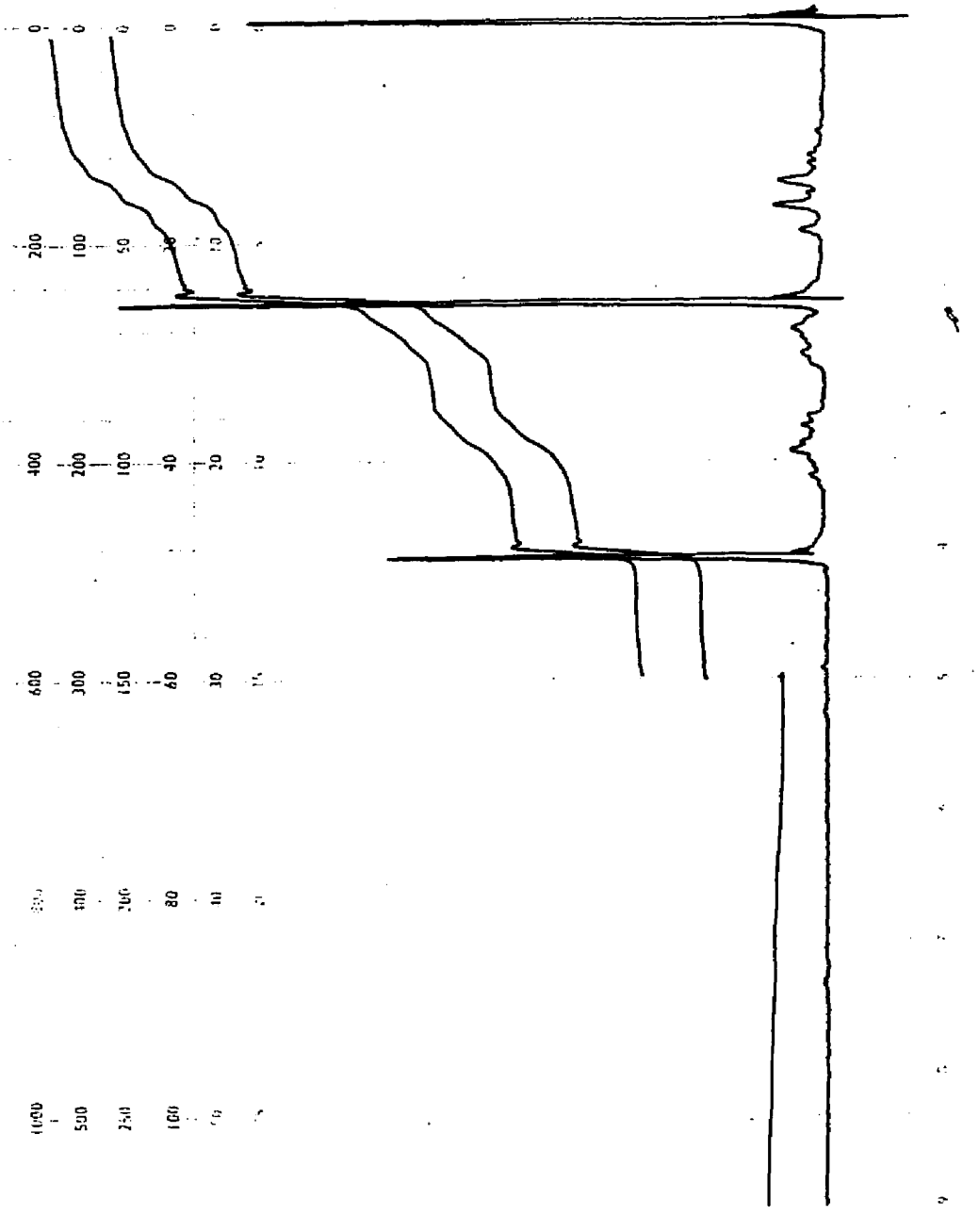

^{1}H NMR / 31.5 mg

(0.37 Equiv. $NaBPh_4/CDCl_3$)

[L] = 0.210 M

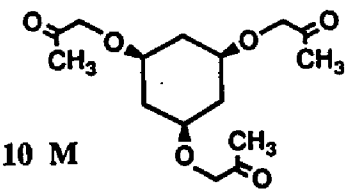

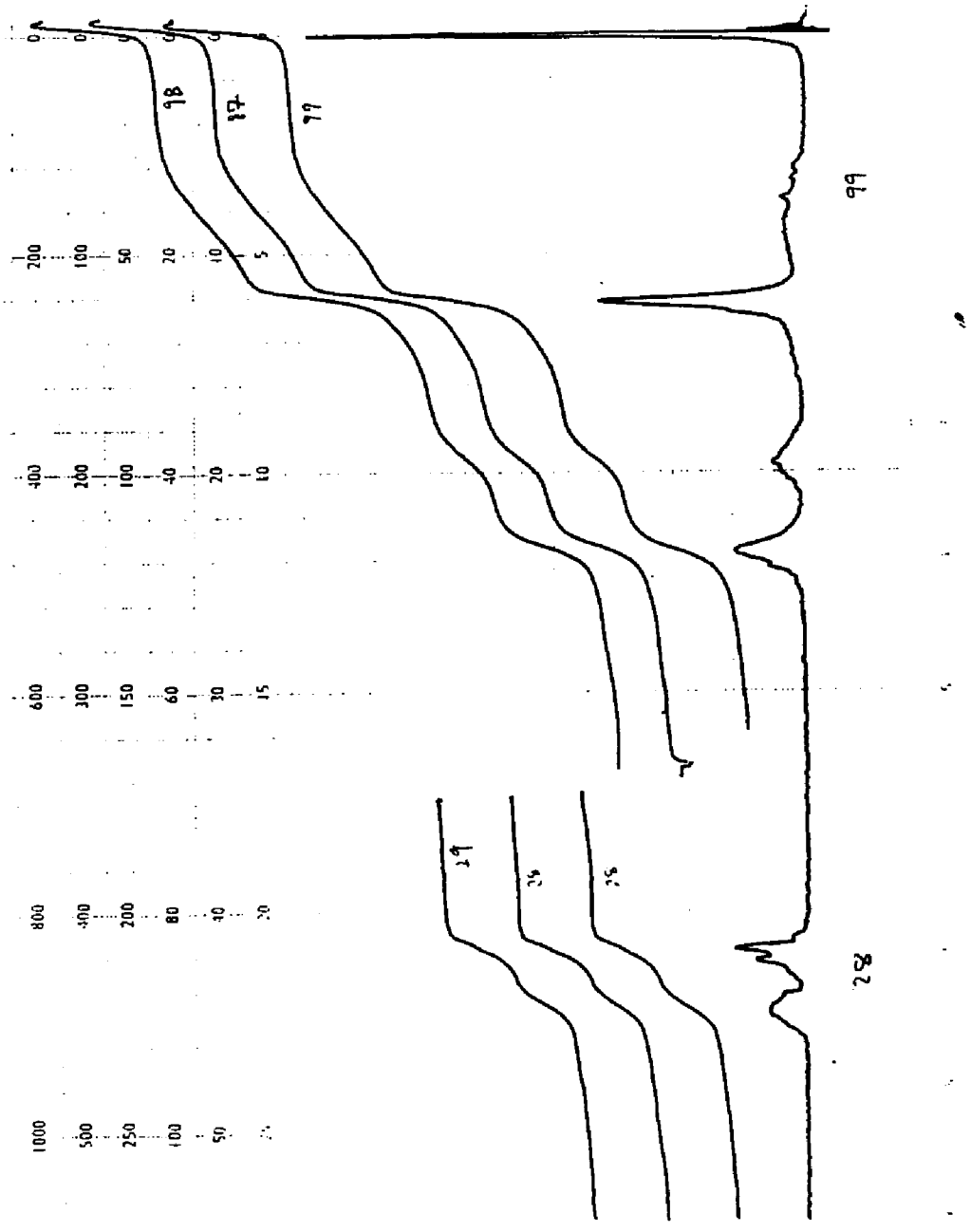

^{1}H NMR / 31.5 mg

(1.1 Equiv. $NaBPh_4/CDCl_3$)

(Precipitate formed in NMR tube)

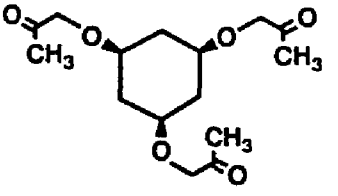

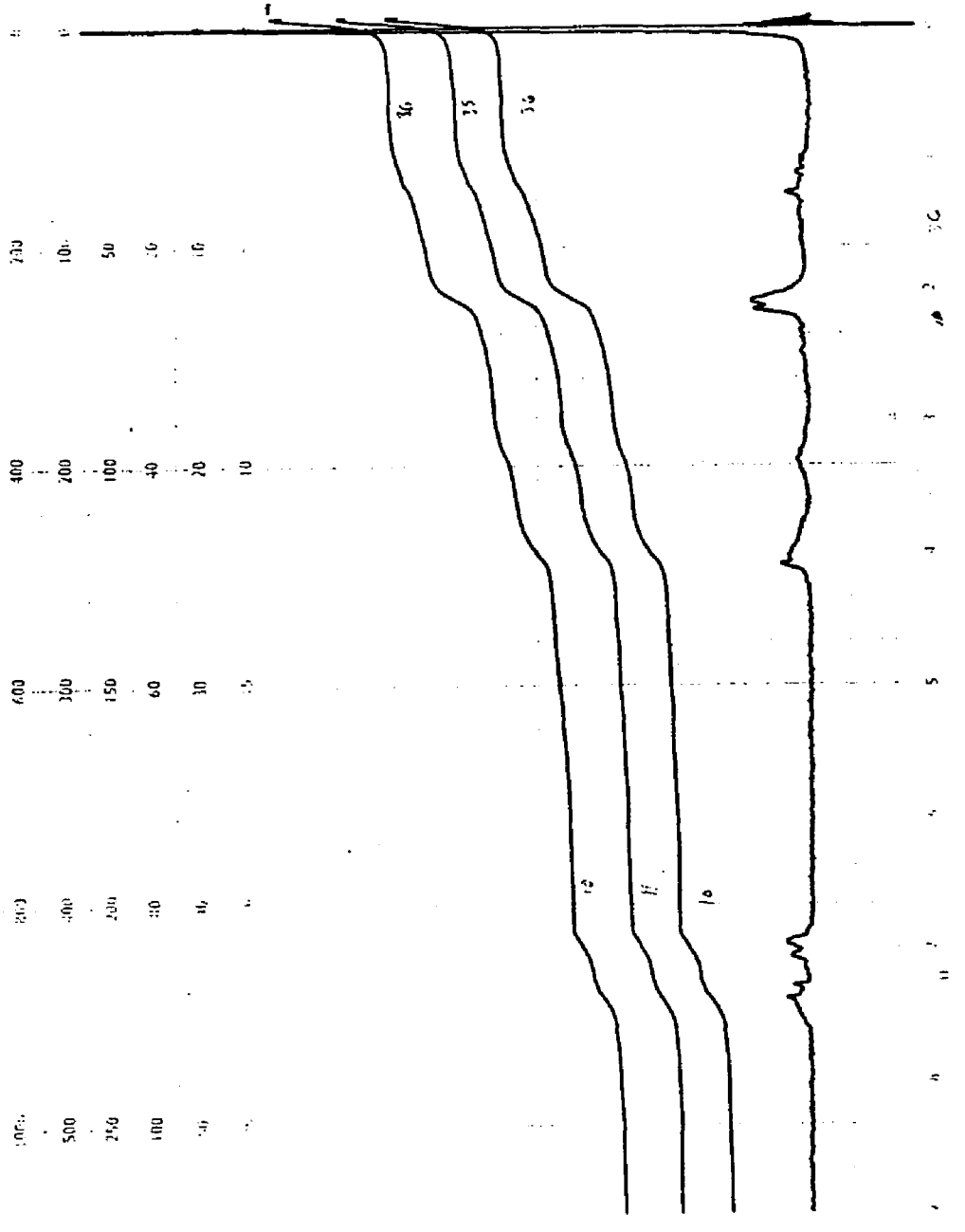

^{1}H NMR / 35.2 mg

(1.01 Equiv. $NaBPh_4/CDCl_3$)

(Large quantity of insoluble salt in sample)

[L] = 0.180

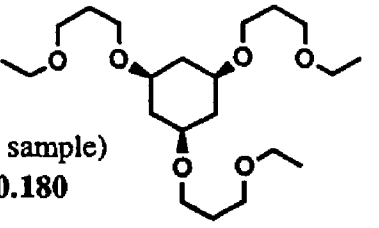

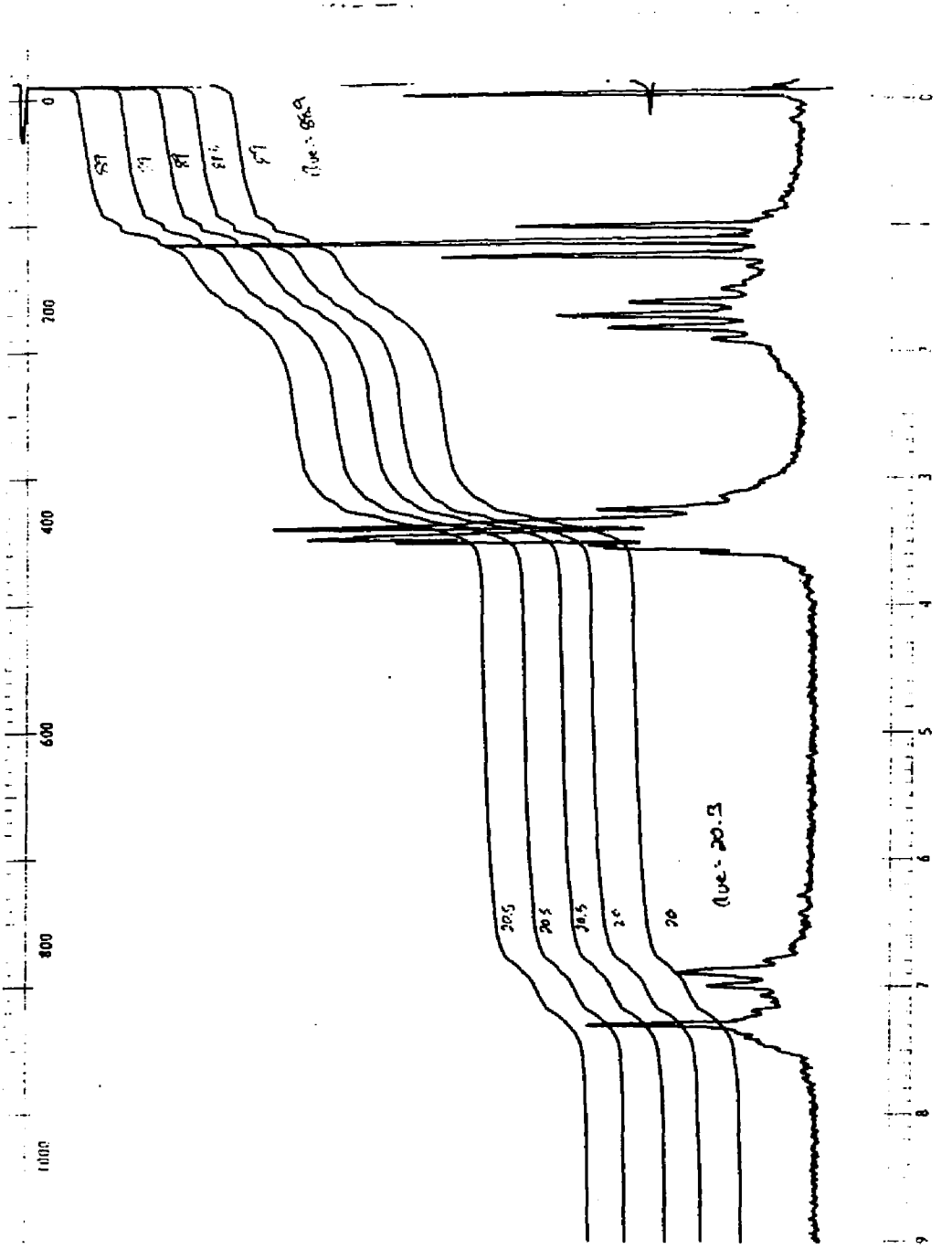

^{1}H NMR / 35.2 mg

(0.00 Equiv. $NaBPh_4/CDCl_3$)

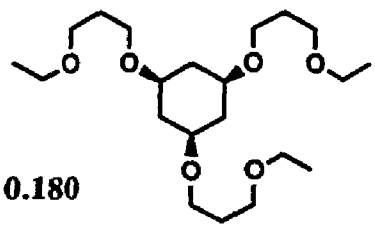

[L] = 0.180

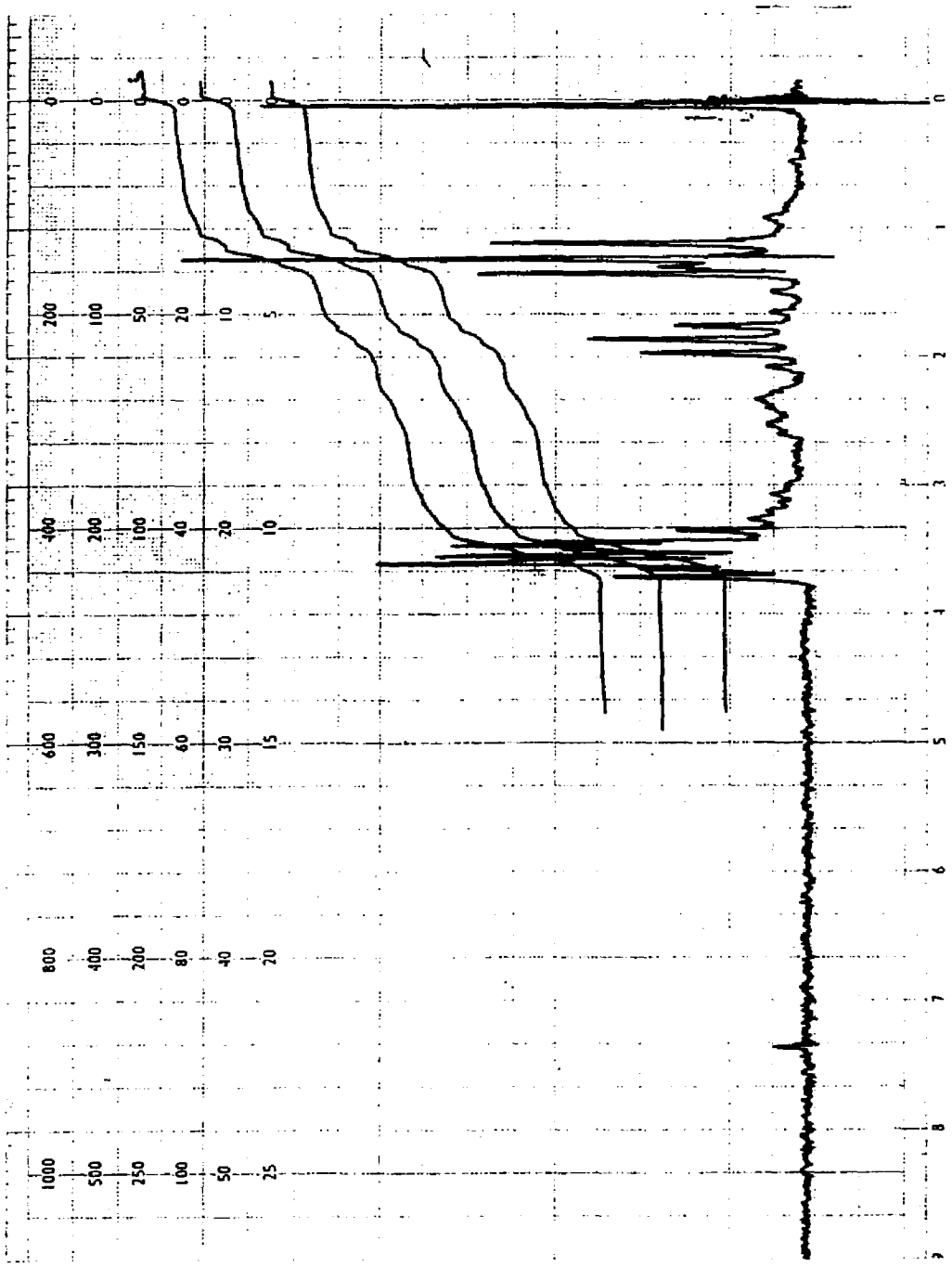

APPENDIX I.

^{13}C NMR Competition Experiment Spectra

^{13}C NMR
(1:1:0.5 Ratio)

(1.00 Equiv. $NaBPh_4$
$CDCl_3$)

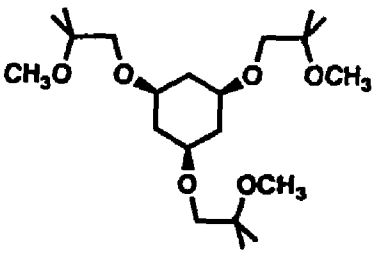

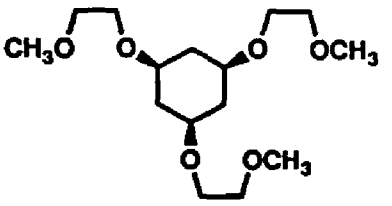

[Ligand] = 0.0977 M 0.0485 M

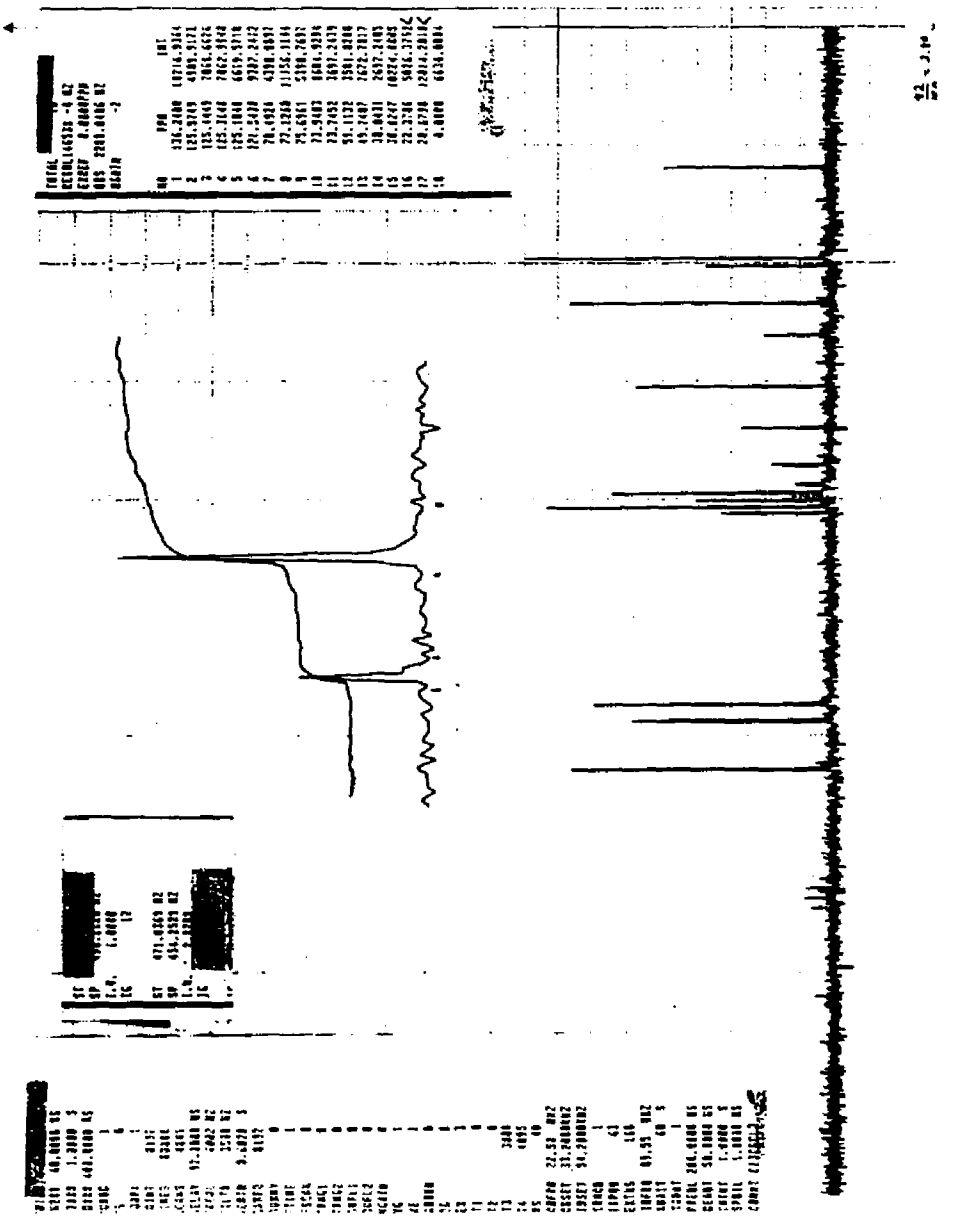

^{13}C NMR
(1:1:1 Ratio)

(1.00 Equiv. $NaBPh_4$
$CDCl_3$)

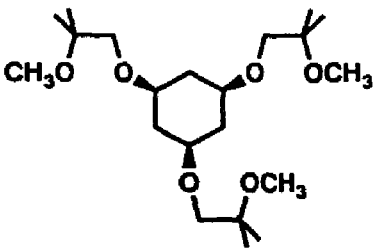

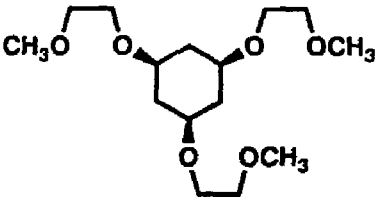

[Ligand] = 0.2103 M **0.2103 M**

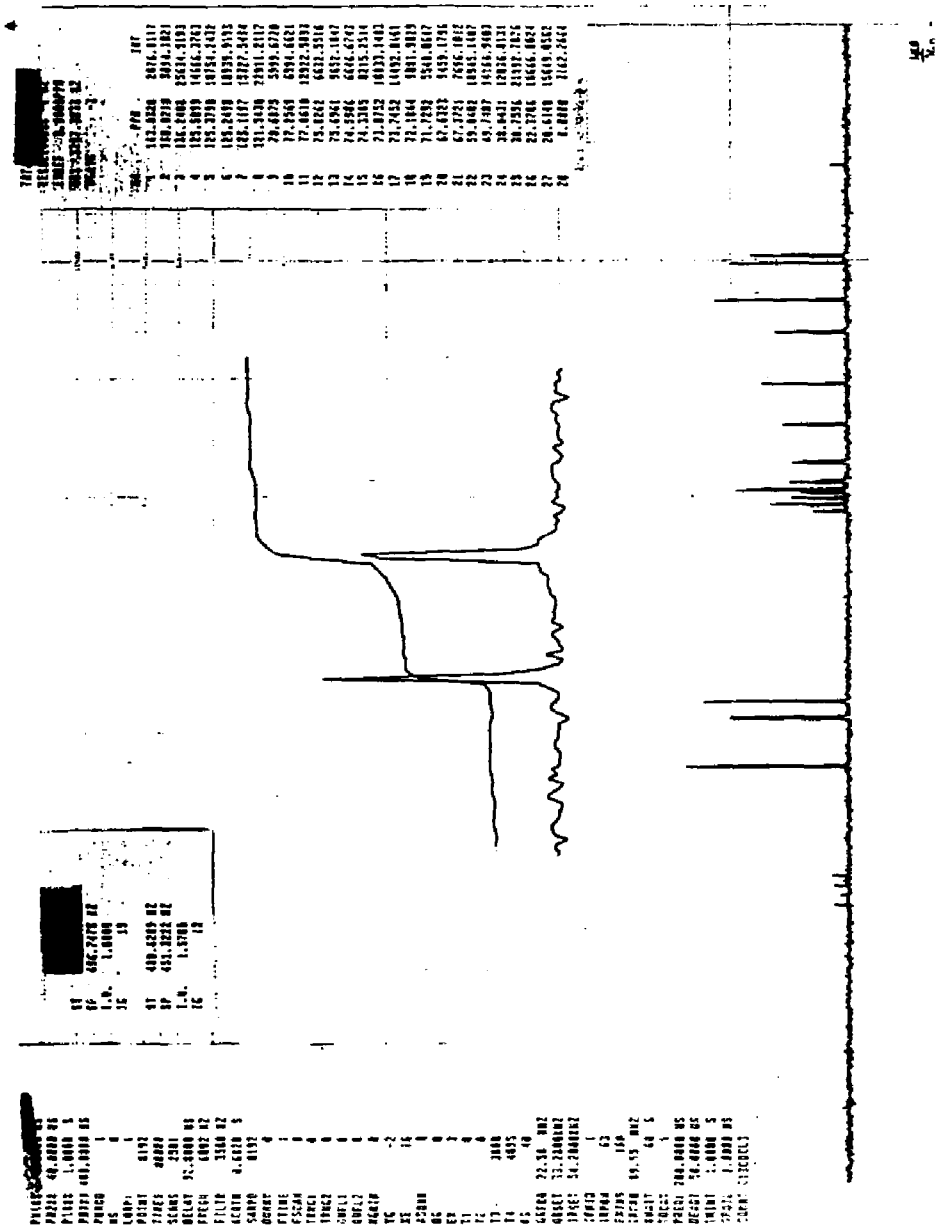

^{13}C NMR

(1:1:1.5 Ratio)

(1.00 Equiv. $NaBPh_4$ $CDCl_3$)

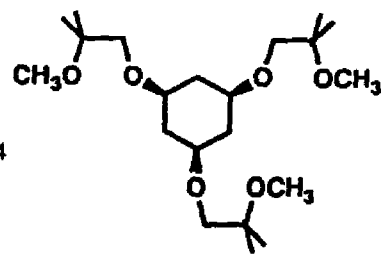

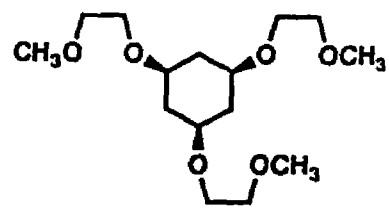

[Ligand] = 0.2040 M **0.3223 M**

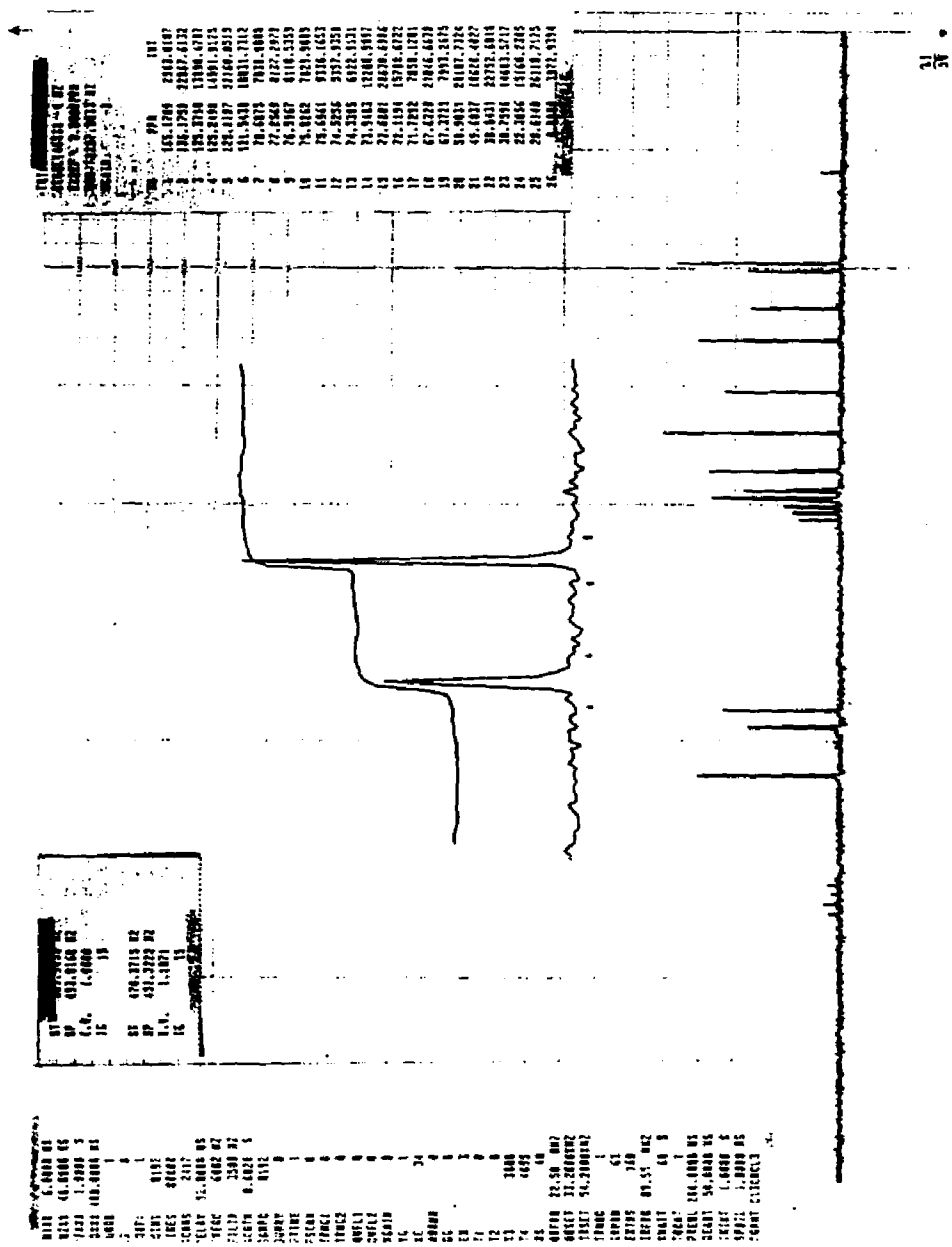

^{13}C NMR
(1:1:1 Ratio)

(1.00 Equiv. $NaBPh_4$
$CDCl_3$)

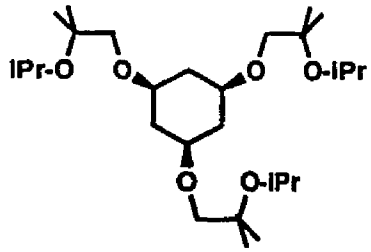

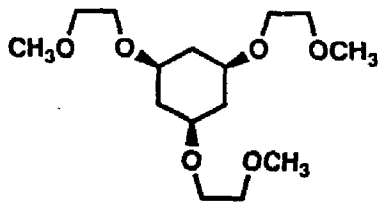

[Ligand] = 0.1682 M **0.1682 M**

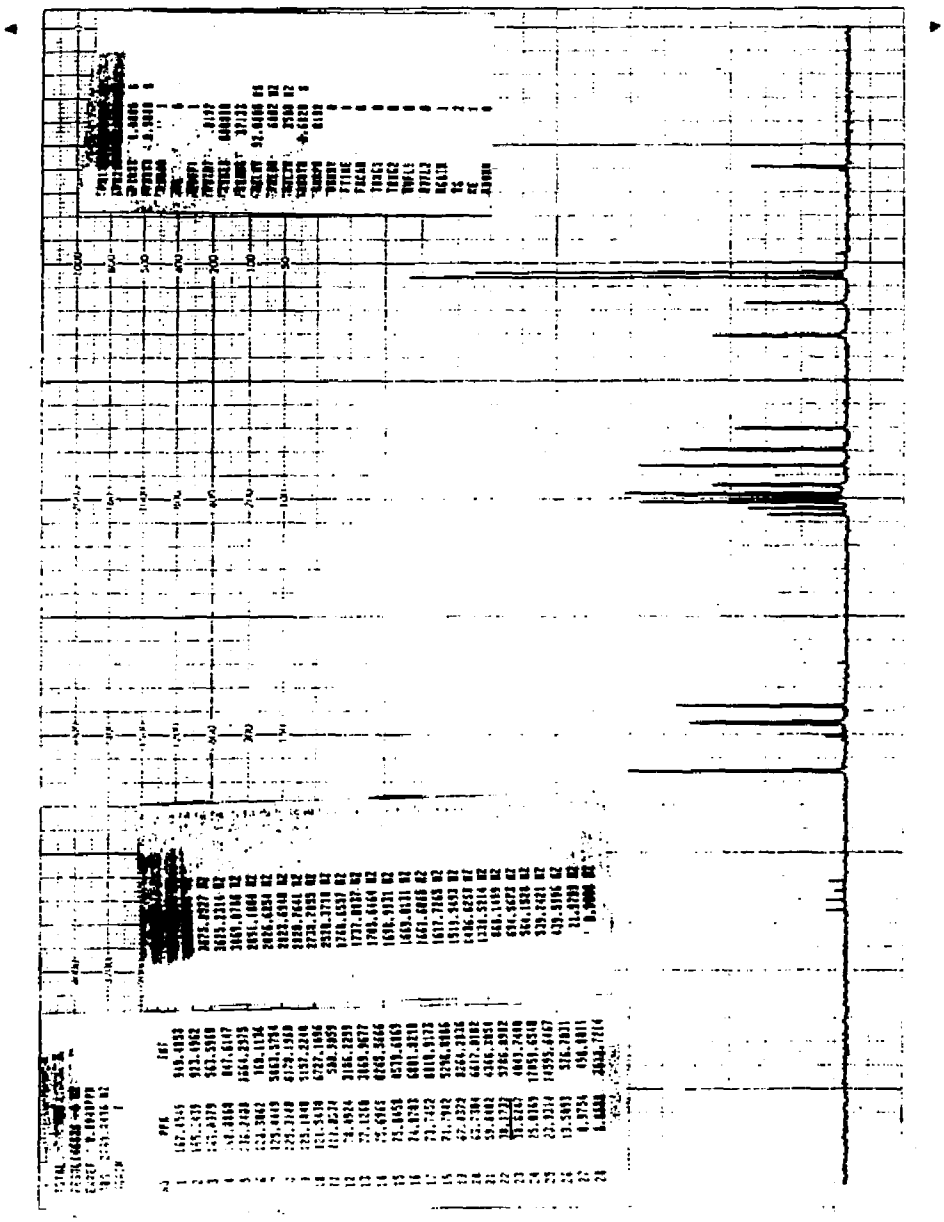

^{13}C NMR (1:1:1 Ratio)

(1.00 Equiv. $NaBPh_4$ $CDCl_3$)

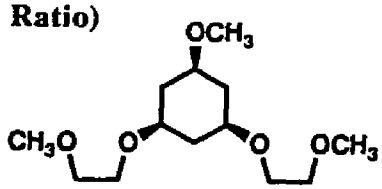

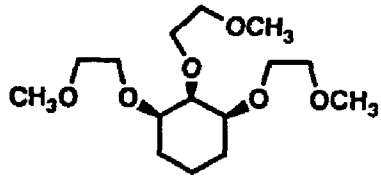

[Ligand] = 0.0995 M 0.0995 M

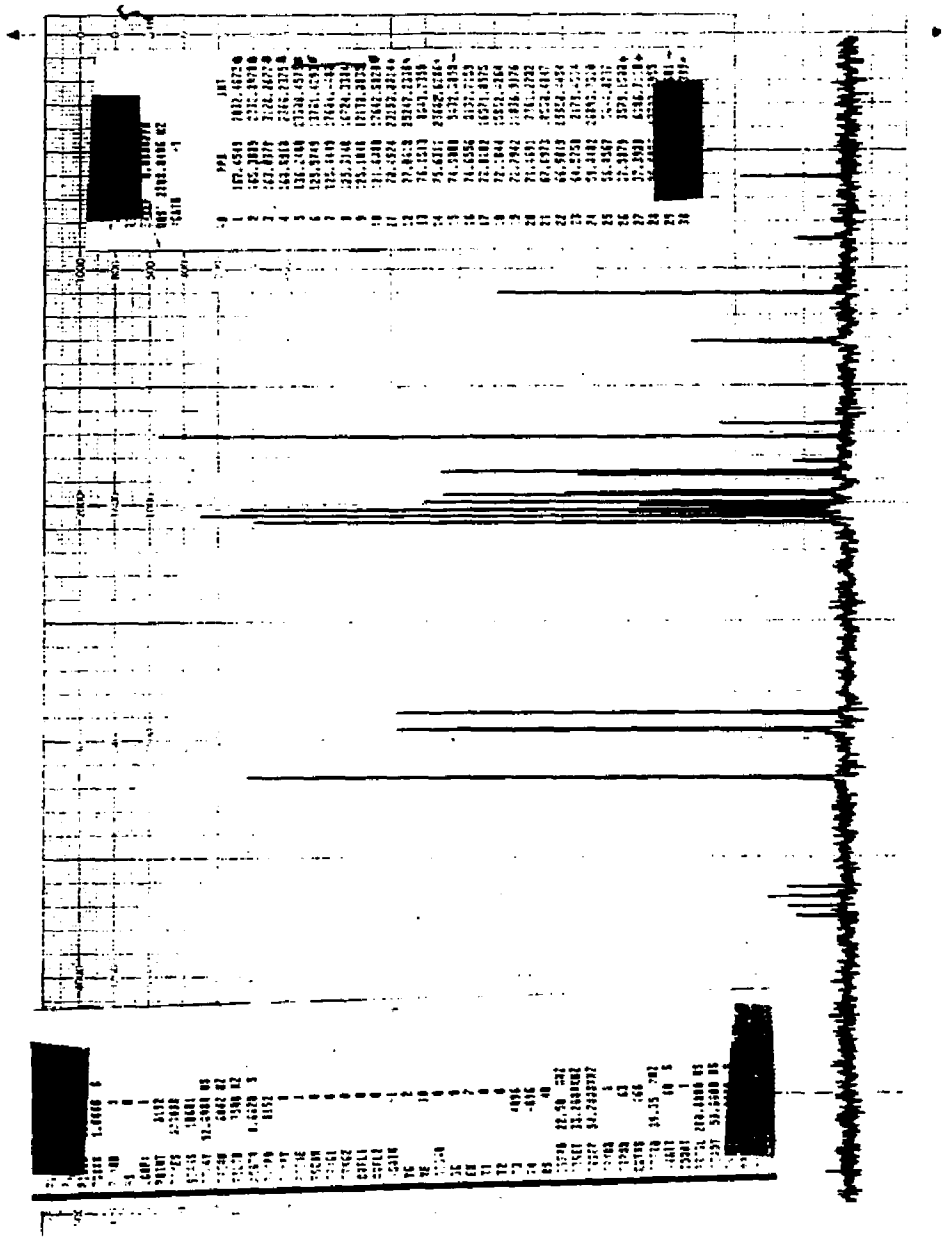

^{13}C NMR
(1:1:1 Ratio)

(1.00 Equiv. $NaBPh_4$
$CDCl_3$)

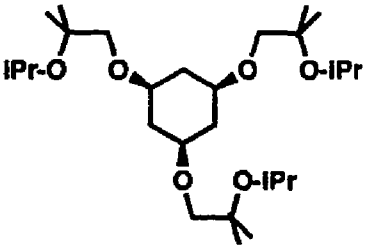

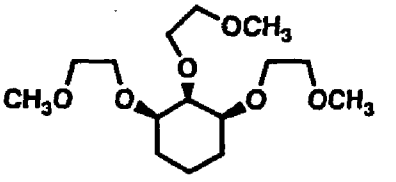

[Ligand] = 0.0406 M **0.0406M**

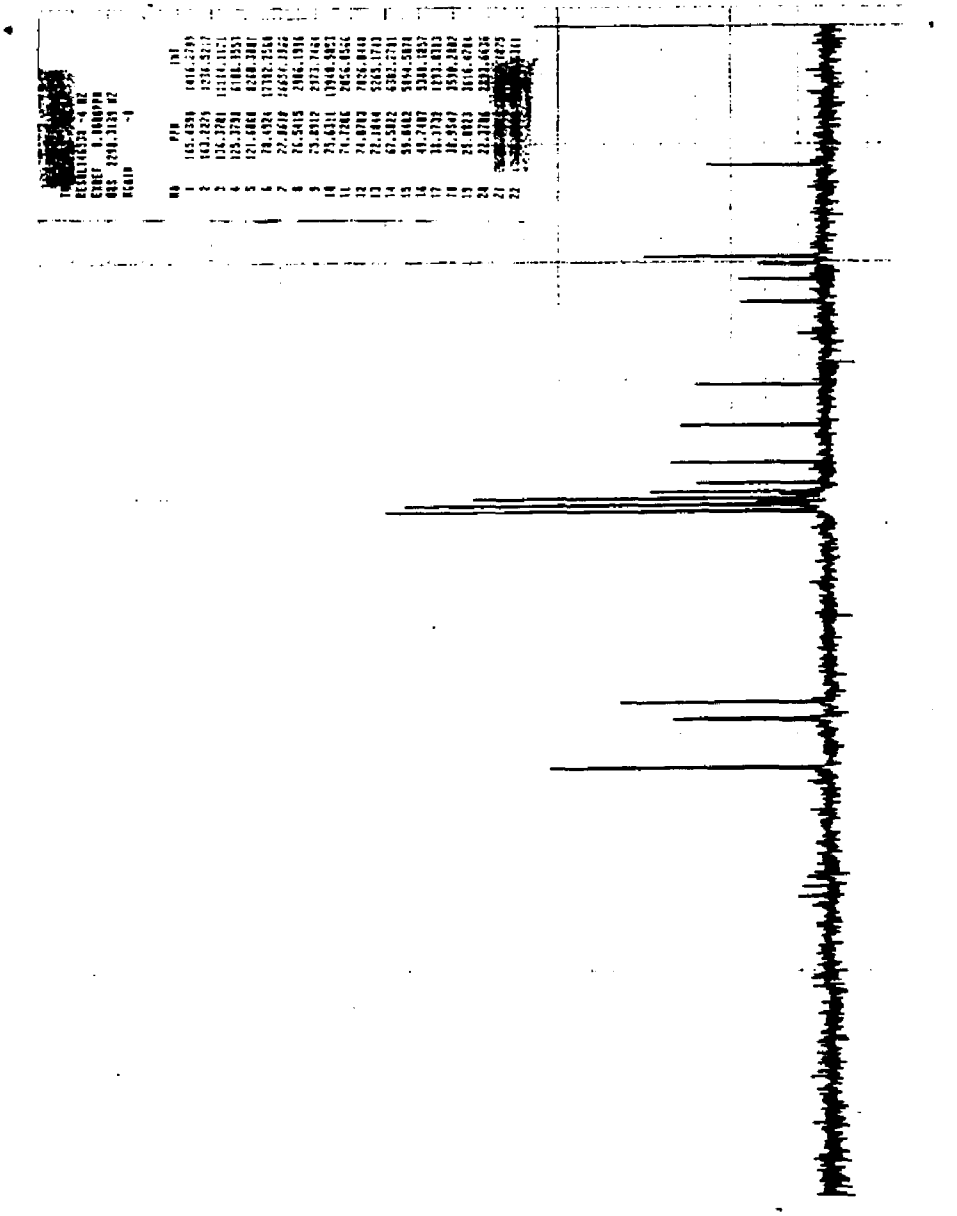

^{13}C NMR

(1:1:1 Ratio)

(1.00 Equiv. $NaBPh_4$ $CDCl_3$)

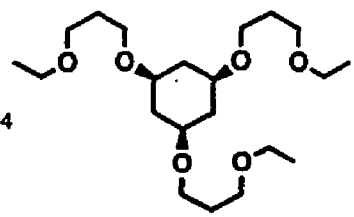

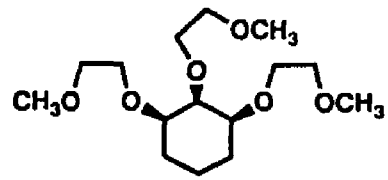

[Ligand] = 0.0765 M **0.0765 M**

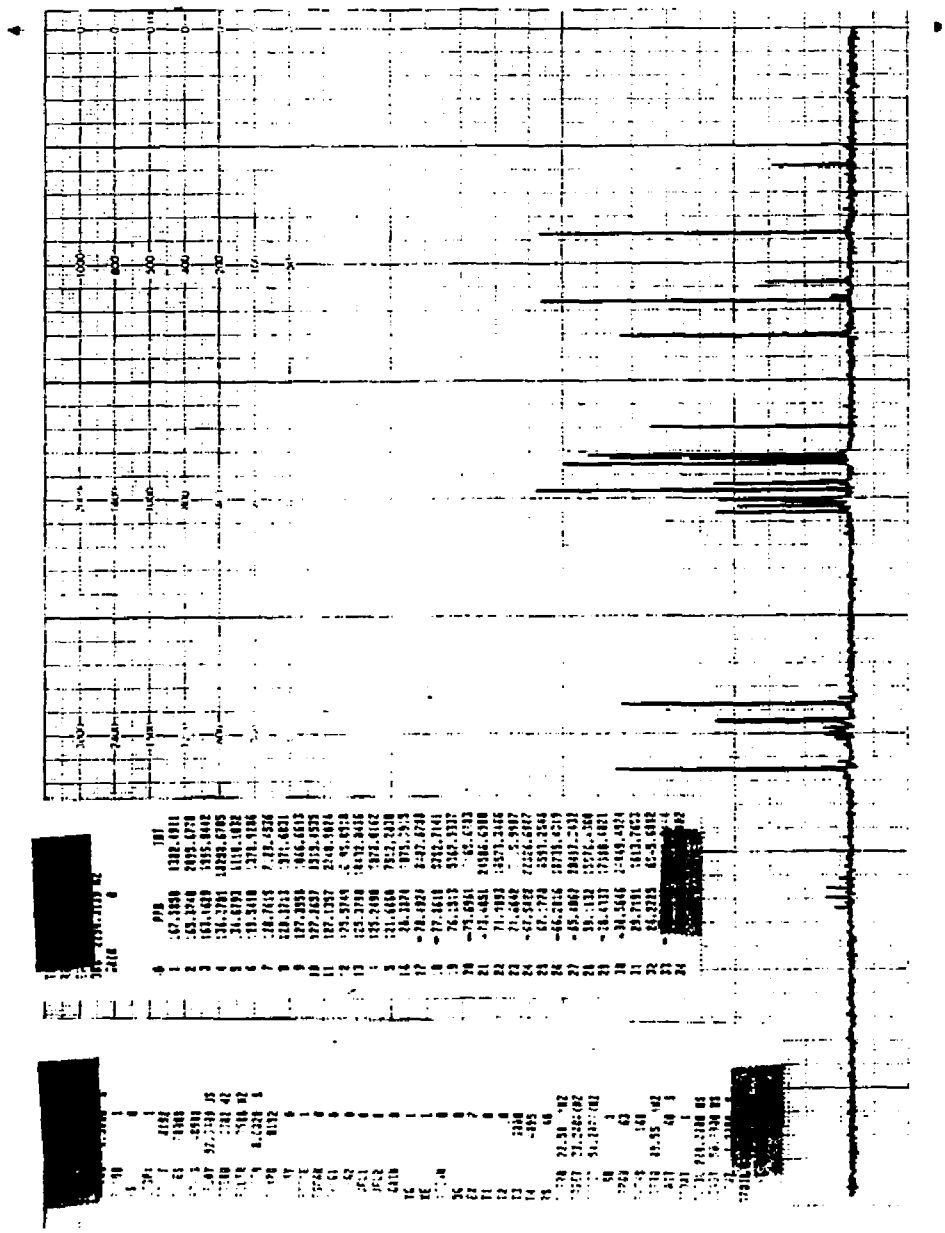

^{13}C NMR

(1:1:1 Ratio)

(1.00 Equiv. $NaBPh_4$ $CDCl_3$)

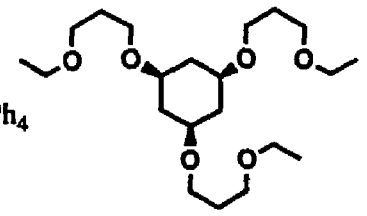

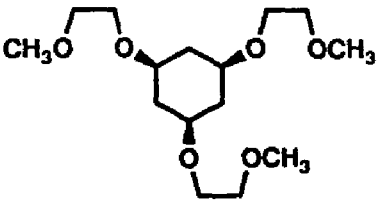

[Ligand] = 0.1170 M **0.1170 M**

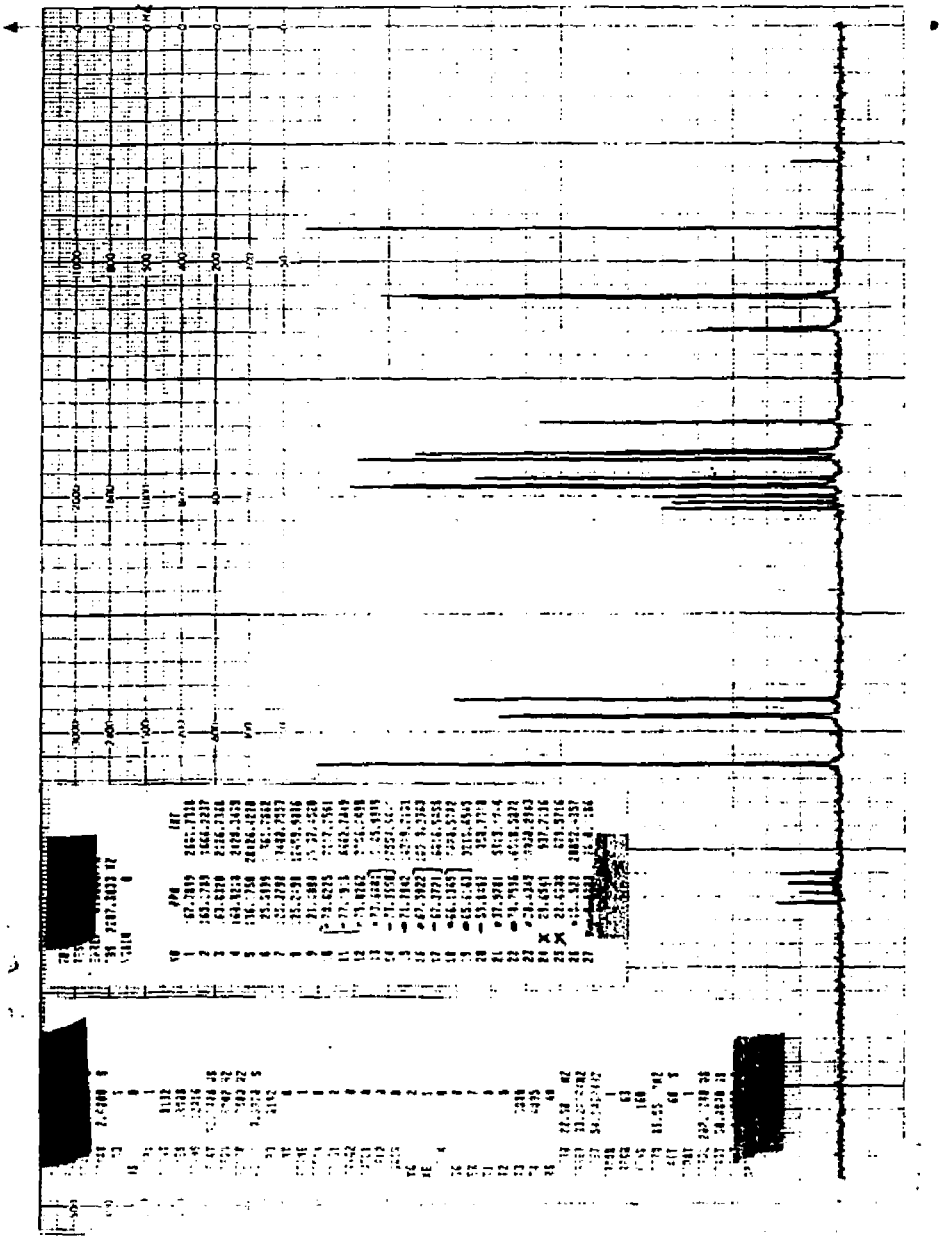

^{13}C NMR

(1:3:1 Ratio)

(1.00 Equiv. $NaBPh_4$ $CDCl_3$)

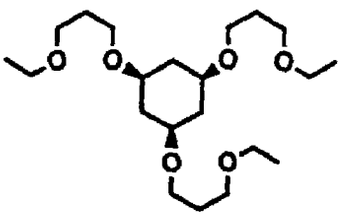

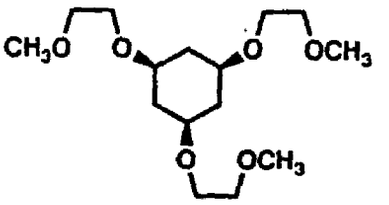

[Ligand] = 0.2585 M **0.0856 M**

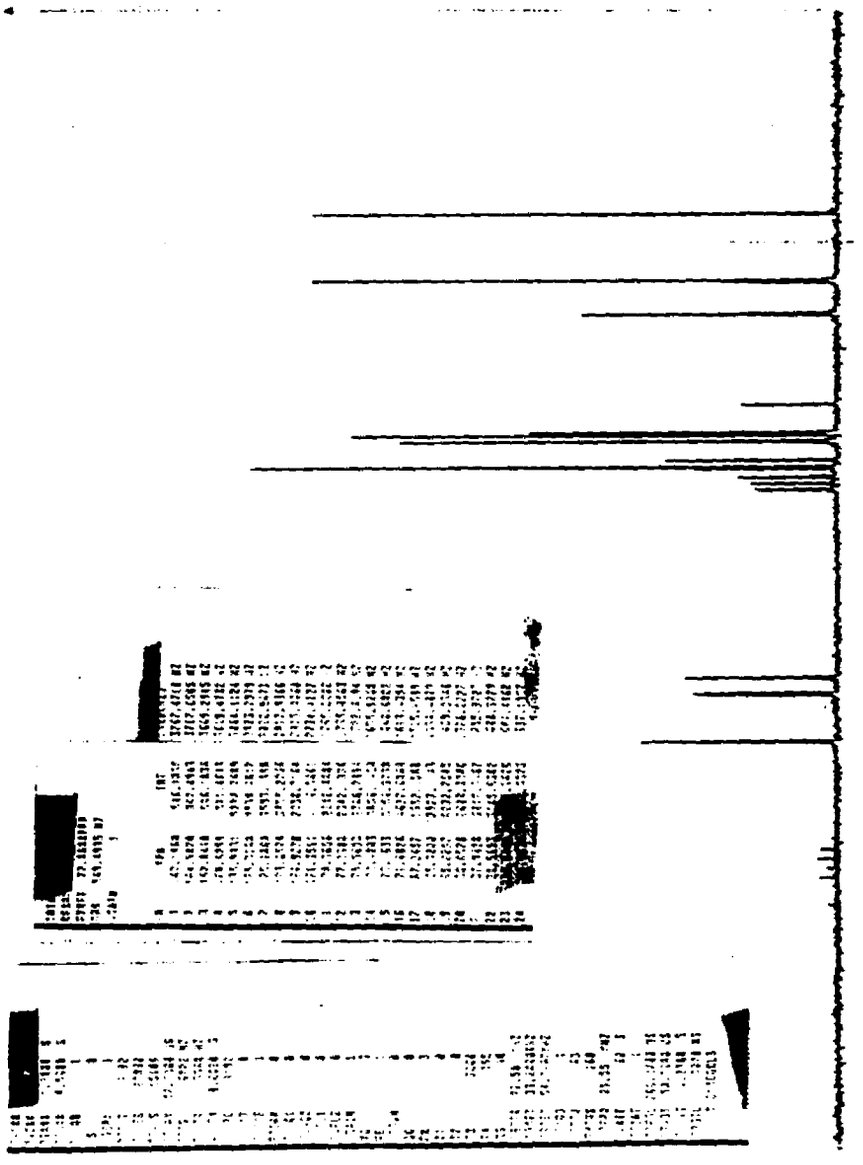

^{13}C NMR (1:1:3 Ratio)

(1.00 Equiv. $NaBPh_4$
$CDCl_3$)

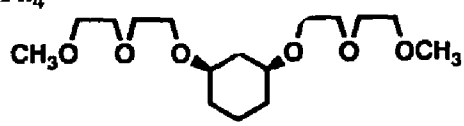

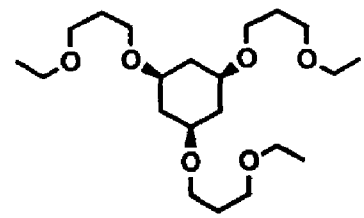

[Ligand] = 0.0814 M **0.2698 M**

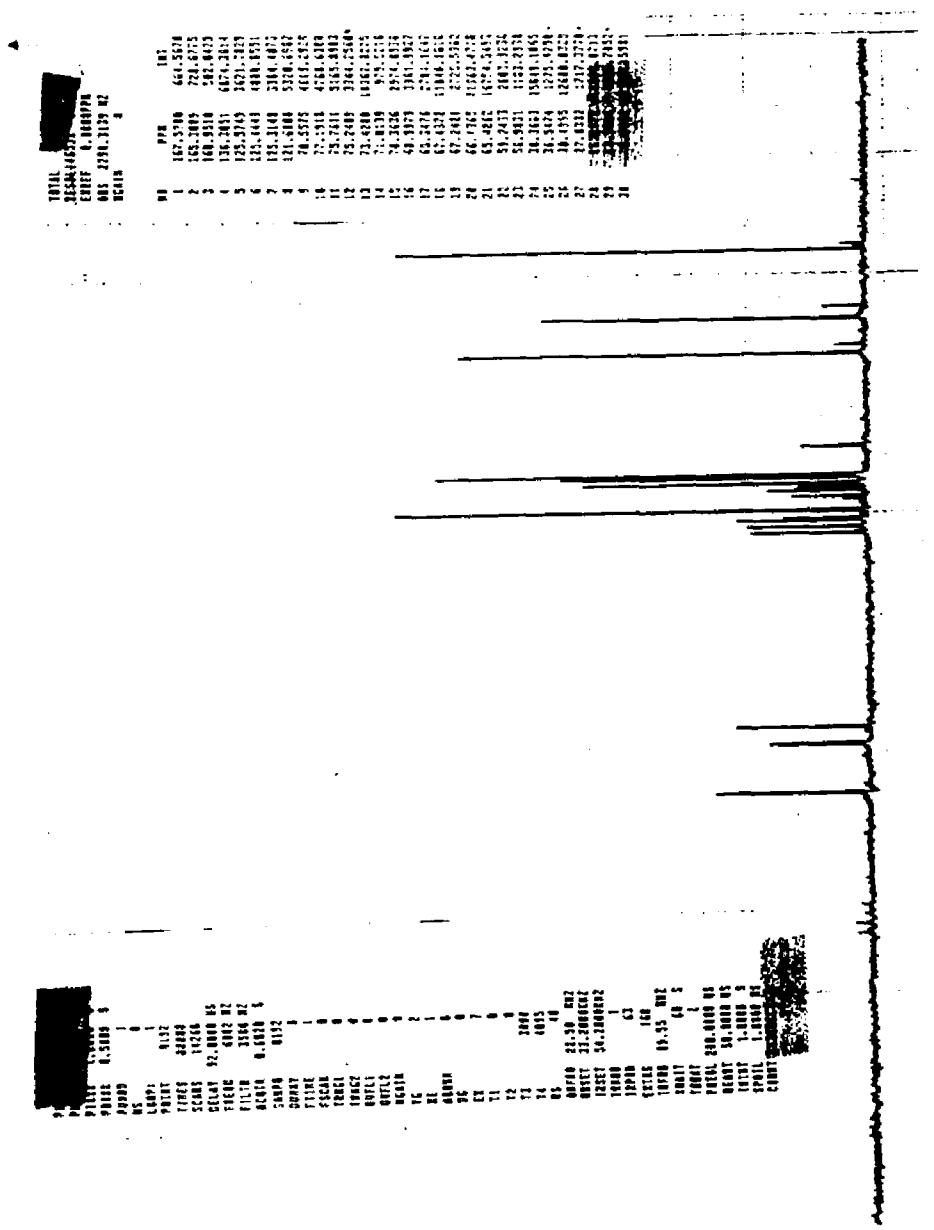

^{13}C NMR (1:1:6 Ratio)

(1.00 Equiv. $NaBPh_4$
$CDCl_3$)

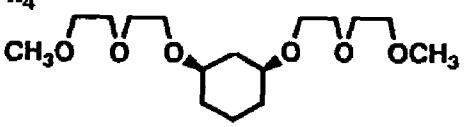

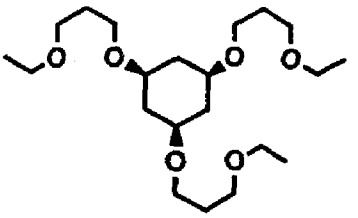

[Ligand] = 0.0728 M 0.4388 M

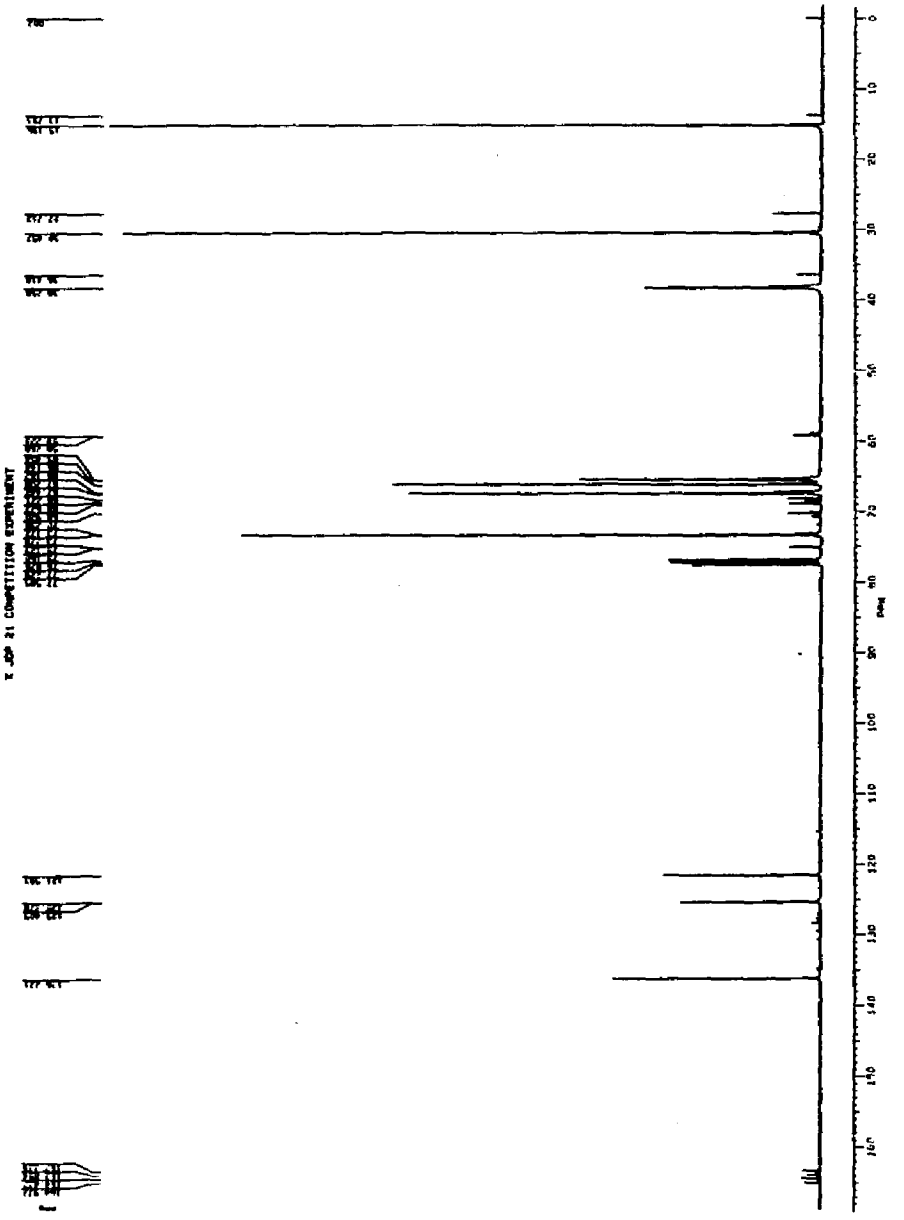

REFERENCES

[1] Cram, D.J. (Nobel Lecture), Science, R1988, 240, 760.

[2] Lehn, J.-M. (Nobel Lecture), Angew. Chem. Int. Ed. Engl., 1988, 27, 89.

[3] a) Pedersen, C.J. J. Chem. Am. Soc., 1967, 89, 2495.
b) Pedersen, C.J. J. Chem. Am. Soc., 1967, 89, 7017.
c) Pedersen, Nobel Address

[4] Izatt, R.M. and Christensen Progress in Macrocyclic Chemistry, (Eds.) John Wiley and Sons, NY, Vol. 1, 1979; Vol. 2, 1981; Vol. 3, 1987.

[5] Atwood, J.L.; Davies, J.E.; MacNicol, D.D. (Eds.) Inclusion Compounds, Academic Press, London, Vol. 1 (Structural Aspects...Inorganic and Organometallic Host Lattices), 1984; Vol. 2 (Structural Aspects... Organic Lattices), 1984; Vol. 3 (Physical Properties and Applications), 1984.

[6] "Host Guest Complex Chemistry", Topics in Current Chemistry Series, Voegtle, F.; Boschke, E.L., (Eds.) Springer-Verlag, Berlin, 1982-1984, Vols. 1 to 3.

[7] Kyba, E.P. et al. J. Am. Chem. Soc. 1977, 99, 2564.

[8] a) Lehn, J.-M. Struct. Bonding (Berlin), 1973, 16, 1.
b) Lehn, J.-M. Pure Appl. Chem. 1978, 50, 871.
c) Lehn, J.-M. Lecon Inaugurale, College de France, Paris 1980.

[9] Personal communication with G.R. Weisman.

[10] Pedersen, C.J.; Frensdorff, H.K. Angew. Chem. Int. Ed. Engl. 1972, 11, p 20.

[11] a) Gokel, G.W.; Dishong, D.M.; Diamond, C.J. J. Chem. Soc., Chem. Commun. 1980, 1053.
b) Dishong, D.M.; Diamond, C.J.; Cinoman, M.I.; Gokel, G.W. J. Chem. Am. Soc. 1983, 105, 586.

[12] Liesegang, G.W.; Eyring, E.M. "Synthetic Multidentate Macrocyclic Compounds"; Izatt, R.M., Christensen, J.J., Academic Press: New York, 1978; Chapter 5, p 245.

[13] a) Lehn, J.M. Struct. Bonding 1973, 16, 1.
b) Lehn, J.M. Acc. Chem. Res. 1978, 11, 49.

[14] a) Echegoyen, L.; Kaifer, A.; Durst, H.; Schultz, R.A.; Dishong, D.M.; Goli, D.m.; Gokel, G.W. J. Chem. Am. Soc. 1984, 106, 5100.
b) Kaifer, A.; Durst, H.D.; Echegoyen, L.; Dishong, D.M.; Schultz, R.A.; Gokel, G.W. J. Org. Chem. 1982, 47, 3195.

[15] a) Peacock, S.C.; Domeier, A.L.; Gaeta, F.C.A.; Helgeson, R.C.; Timko, J.M.; Cram, D.J. J. Am. Chem. Soc., 1978, 100, 8190.
b) Peacock, S.C.; Walba, D.M.; Gaeta, F.C.A.; Helgeson, R.C.; Cram, D.J. J. Am. Chem. Soc., 1980, 102, 2043.

[16] a) Dietrich, B. Lehn, J.-M.; Sauvage, J.-P. Tetrahedron Lett. 1969, 2885.
b) Diertrich, B. Lehn, J.-M.; Sauvage, J.-P. Tetrahedron Lett. 1969, 2889.

[17] Trueblood, K.N.; Knobler, C.B.; Maverick, E.; Helgeson, R.C. Brown, S.B.; Cram, D.J. J. Am. Chem. Soc. 1981, 103, 5594.

[18] Cram, D.J. Angew. Chem. Int. Ed. Engl. 1986, 25, 1039.

[19] Cram, D.J. and Lein, G.M. J. Am. Chem. Soc. 1985, 107, 3657.

[20] Voegtle, F. and Weber, E. "Multidentate Acyclic Neutral Ligands and Their Complexation", Angew. Chem. Int. Ed. Eng., 1979, 18, 753.

[21] a) Hancock, R.D. and Martell, A.E. "The Chelate, Cryptate, and Macrocyclic Effects", Comments Inorg. Chem. 1988, 6, (5-6), 237-84.
b) Cabbiness, D.K.; Margerum, D.W. J. Am. Chem. Soc. 1969, 91, 6540.

[22] a) Vananzi, C.A., "Computational Analysis of Molecular Recognition by Artificial Enzymes" in "Environmental Influences and Recognition in Enzyme Chemistry" Joel F. Liebman and Arthur Greenberg, (Eds.), VCH, 1988.
b) Wipff, G.; Kollman, P. Lehn, J.-P. J. Mol. Struct. 1983, 93, 153.
c) Ranghino, G.; Romano, S. Lehn, J.-M.; Wipff, G. J. Am. Chem. Soc. 1985, 107, 7873.
d) Wipff, G.; Kollman, P. Nouv. J. Chim. 1985, 9, 457.
e) Lifson, E.; Levit, M. "Structure and Dynamics of Macromolecules" (Isr. J. Chem. 1986, 27, No. 2).

[23] Angyal, S.J. Tetrahedron, 1974

[24] Curtis, W.D.; Stoddart, J.F.; Jones, G.H. J. Chem. Soc. Perkin I, 1977, 785.

[25] Weisman, G.R., Proposal to the National Science Foundation, University of New Hampshire, personal communication.

[26] Weisman, G.R.; Ho, S.C.-H.; Gash, D.; Caywood, G.A.; Perry, A.E. "Abstracts of Papers", 12th Northeast Regional Meeting of the American Chemical Society, Burlington, Vt., June, 1982; American Chemical Society, Washington, D.C.; **1982**; ORGN 177.

[27] a) Stoddart, J.F. Chem. Soc. Rev., **1979**, 8, 85.
b) Riddell, F.G. "The Conformational Analysis of Heterocyclic Compounds"; Academic: London, **1980**, 28.

[28] Petillo, P.A. Bachelors Thesis, The University of New Hampshire, Durham N.H., **1985**.

[29] Raven, P.H.; Evert, R.E.; Curtis, H. "Biology of Plants"; (2nd Ed.), Worth: New York, 1976; p 510, 550.

[30] Pascarella, T.A. Masters Thesis, The University of New Hampshire, Durham N.H., **1986**.

[31] a) Shirodkar, S.M. Ph.D. Dissertation, The University of New Hampshire, Durham N.H., **1987**.
b) Shirodkar, S.M. and Weisman, G.R. J. Chem. Soc., Chem. Commun., **1989**, 4, 236.

[32] Raban, M.; Hortelano, E.; Qiun, J. III; King, N.; Koch, J.J. Chem. Soc. Commun. **1985**, 1557.

[33] Caywood, G. B.S. Thesis, University of New Hampshire, Durham, NH, 1981.

[34] Steinacker, K.H. and Stetter, H. Ber. **1952**, 85, 451.

[35] Kyba, E.P.; Helgeson, R.C.; Madan, K.; Gokel, G.W.; Tarnowski, T.L.; Moore, S.S.; Cram, D.J. J. Am. Chem. Soc. **1977**, 99, 2564-2571.

[36] Arndt, H.C.; Carroll, S.A. Synthesis **1979**, 3, 202-4.

[37] Brown, H.C.; Rei, M.H. J. Am. Chem. Soc. **1969**, 91, 5646.

[38] Brown, H.C.; Geoghegan; P.,Jr. J. Am. Chem. Soc. **1967**, 89, 1522.

[39] Holum, J.R. J. Org. Chem. **1961**, 26, 4814.

[40] Collins, J.C.; Hess, W.W.; Frank, F.J. Tetrahedron Lett. **1968**, 30, 3363.

[41] a) Dauben, W.G.; Lorber, M.; Fullerton, D.S. J. Org. Chem. **1969**, 34, 3587.
b) Sisler, H.H.; Accountius, C.E. J. Am. Chem. Soc. **1948**, 70, 3827.

[42] Ref. [30].

[43] Burgstahler, A.L.; Bithos, Z.J. J. Am. Chem. Soc. **1960**, 82, 5466.

[44] Riddick, J.A. and Toops, E.E. Jr., "Organic Solvents", 2nd Ed., Vol. 7, of Weissberger, A. Ed., "Techiniques of Organic Chemistry, Interscience, N.Y. 1955; p 270.

[45] Pascarella, T. Master's Thesis, The University of New Hampshire, Durham, NH. 1986, p. 63.

[46] Ref.[45], p. 15.

[47] Reinhoudt, D.N.; Gray, R.T.; DeJong, F.; Smit, C.J. Tetrahedron **1977**, 33, 563-571.

[48] S. Patai (Ed.), "The Chemistry of Ethers, Crown Ethers, Hydroxyl Groups, and Their Sulfur Analogues", Supplement E of The Chemistry of Functional Groups, Part1, John Wiley and Sons, Chichester, 1980, chapter 2, p. 91.

[49] Ref. [30].

[50] Ref.[30], p. 17.

[51] a) Weisman, G.R., Proposal to the National Science Foundation, University of New Hampshire, personal communication.
b) Weisman, G.R.; Ho, S.C.; Gash, D.; Caywood, G.A.; Perry, A.E. "Abstracts of Papers," 12th Northeast Regional Meeting of the American Chemical Society, Burlington, Vermont, June, 1982; American Chemical Society: Washington, D.C.; 1982; ORGN 177.

[52] Wilson, N.K.; Stothers, J.B. In "Topics in Stereochemistry"; Eliel, E.L.; Allinger, N.L., Eds.; Wiley: New York, 1974, 8, 1.

[53] a) Dale, J. Tetrahedron **1974**, 30, 1683.
b) Dale, J. Israel J. Chem., **1980**, 20, 3.

[54] Duddeck, H. In "Topics Stereochemistry"; Eliel, E.J.; Wilen, S.H.; Allinger, N.L. Eds.; Wiley: New York, 1986, 16, 219.

[55] Ref.[54]

[56] a) Schneider, H.J.; Hoppen, V. Tet. Lett. **1974**, 7, 579.
b) Booth, H.; Everett, J.R.; Fleming, R.A.; Org. Mag. Res. **1979**, 12, 63.

[57] Roberts, J.D.; Weigert, F.J.; Kroschwitz, J.I.; Reich, H.J. J. Am. Chem. Soc. **1970**, 92, 1338.

[58] Grover, S.H.; Stothers, J.B. Can. J. Chem. **1974**, 52, 870.

[59] Ref.[54], p. 241

[60] Ref.[56a]

[61] Ref.[57]

[62] Schwenzer, G.M. J. Org. Chem. **1978**, 43, 1079.

[63] Whitsell, J.K. and Minton, M.A. J. Am. Chem. Soc. **1987**, 109, 225.

[64] Ref.[56a]

[65] a) Cheney, B.V.; Grant, D.M. J. Am. Chem. Soc. **1967**, 89, 5319.
b)Grant, D.M.; Cheney, B.V. J. Am. Chem. Soc. **1967**, 89, 5315.

[66] Ref.[57]

[67] Ref.[56a]

[68] a) Beierbeck, H.; Saunders, J.K. Can. J. Chem. **1976**, 54, 2985.
b) Beierbeck, H.; Saunders, J.K. Can. J. Chem. **1982**, 22, 48.

[69] a) Shirodkar, S. Doctoral Thesis, University of New Hampshire, Durham, NH. 1987, p. 33
b) Grover, S.H.; Guthrie, J.P.; Stothers, J.B.; Tan, C.T. J. Mag. Reson. **1973**, 10, 227.
c) Ayer, W.A.; Browne, L.M.; Fung, S.; Stothers, J.B. Org. Mag. Reson. **1978**, 11, 73.

[70] Ref.[54], p. 254

[71] Ref.[56a]

[72] a) Ref.[54], p. 257
b) Eliel, E.L.; Bailey, W.F.; Kopp, L.D.; Willer, R.L.; Grant, D.M.; Bertrand, R.; Christensen, K.A.; Dallling, D.K.; Duch, M.W.; Wenkert, E.; Schnell, F.M.; Cochran, D.W. J. Am. Chem. Soc. **1975**, 97, 322.

[73] Ref.[58]

[74] Ref.[69b], [58]

[75] Ref.[68]

[76] Dorman, D.E.; Angyal, S.J.; Roberts, J.D. J. Am. Chem. Soc. **1970**, 92, 1351.

[77] a) Eggert, H.; VanAntwerp, C.L.; Bhacca, N.S.; Djerassi, C. J. Org. Chem. **1976**, 41, 71.
b) Ref.[62]

[78] a)Ref. [33]
b) Ref. [30].
c) Ref. [69a].

[79] Ref. [30b]

[80] Ref. [69a], p. 37

[81] Gronbeck. D. Experimental work conducted by, (1986).

[82] Ref. [30].

[83] a) McMurry, J.E.; Haley, G.J.; Matz, J.R.; Clardy, J.C.; Mitchell, J. J. Am. Chem. Soc. **1986**, 108, 515.
b) Buschmann, H.J. Chem. Ber. **1985**, 118, 4297 (Ger).
c) Spiess, B.: Arnaud-Neu, F.; Schwing-Weill, M.J. Inorg. Nucl. Chem. Lett. **1981**, 17, 253.
d) Ferra, J.D.; Djebli, A. Tessier-Youngs,C.; Youngs, W.J. J. Am. Chem. Soc. **1988**, 110, 647.

[84] Tsukube. H.; Takagi, K.; Higashiyama,T.; Iwachido, T.; Hayama, N. J. Chem. Soc., Perkin Trans. I **1987**, (8), 1697.

[85] See section starting on p.66 for a background discussion of competition experiments.

[86] Ref. [30].

[87] Hartley, F.R.; Burgess, C.; Alcock, R.M. "Solution Equilibria", Ellis Horwood: Chichester, U.K., 1980, p. 150

[88] Rossotto, F.J.C.; Rossotti, H. "The Determination of Stability Constants in Solution", MaGraw-Hill: New York, 1961, p. 291

[89] Creswell, C.J; Allred, A.L. J. Phys. Chem., **1962**, 66, 1469-1472.

[90] Ref. [30].

[91] a) Groves, P.D.; Huck, P.J.; Homer, J. Chem. and Ind. **1967**, 915-97.
b) Huggins, C.M.; Pimentel, G.C.; Shoolery, J.N. J. Chem. Phys. **1955**, 23, 1244.
c) Gutowsky, H.S.; Saikia, A. J. Chem. Phys., **1953**, 21,1688-1694.
d) Ref. [87] and [90].
e) Shirodkar, S.H.; Doctoral Thesis, The University of New Hampshire, Durham, NH. 1987

[92] Measurements also made by T. Pascarella, Ref. [30], p. 39.

[93] a) Chaput, G.; Juillard, J. Can. J. Chem. **1975**, 53, 2240-2246.
b) Tümmler, B.; Maass, G.; Voegtle, F.; Sieger, H.; Heimann, U.; Weber, E. J. Am. Chem. Soc. **1979**, 101, 2588-2598.

[94] Gutmann, V. "The Donor-Acceptor Approach to Molecular Interactions", Plenum Press: New York, 1978

[95] a) Mayer, U.; Gutmann, V., Adv. Inorg. Chem. Radiochem., **1975**, 17, 189.
b) Ref. [94], p. 168.

[96] a)Schneider, H.; Strehlow, H. von Ber. Bunsenges. Phys. Chem., **1965**, 69, 674.
b) Ref. [94], p. 139.

[97] a) Strehlow, H. von; Schneider, H. J. Chim. Phys., **1969**, 66, 118.
b) Ref. [94], p. 139.

[98] a) Schlosser, M. "Struktur und Reaktivität polarer Organometalle", Springer, Berlin/Heidelberg/New York, 1973.
b) Ref. [94], p. 33.

[99] ($^{o}_{max}$ value obtained from other complexation studies)

[100] a) No special precautions for obtaining the data were necessary. Quantitative analysis of ^{13}C resonances often requires special NMR experimental conditions that account for different relaxtion times and NOE's [100b].
b) Wehrli, F. W. and Wirthlin, T. W., "Interpretation of ^{13}C NMR Spectra", p264.

[101] Ref. [30], p. 63.

[102] Pascarella, T.A. Masters Thesis, The University of New Hampshire, Durham N.H., **1986**, p. 35.

[103] Shirodkar, S.M. Ph.D. Dissertation, The University of New Hampshire, Durham N.H., 1987, p.42.

[104] Personal communication G.R. Weisman (also see reference [106]).

[105] a) Lowry, T. H. and Richardson, K. S. "Mechanism and Theory in Organic Chemistry"; 2nd Ed.; Harper and Row: New York, 1981, pp 197-8.
b) Hammond, G. S. J. Am. Chem. Soc. 1955, 77, 334.

[106] Ref. [30], p. 34

[107] Ref. [30].

[108] a) Dale, J., "Stereochemistry and Conformational Analysis" Verlag Chemie, N.Y., 1978.
b) Dale, J. Tetrahedron, 1974, 30, 1683.
c) Dale, J. Israel J. Chem., 1980, 20, 3.

[109] Ref. [31a].

[110] Personal communication with G.R. Weisman and T.A. Pascarella.

[111] Ref. [31a].

[112] Wehrli, F.W.; Wirthlin, T. "Interpretation of Carbon-13 NMR Spectra"; Heyden: London, 1976.

[113] Cooper, J.W.; "Spectroscopic Techniques for Organic Chemists"; Wiley-Interscience: New York, 1980.

[114] Levy, G.C.; Lichter, R.L.; Nelson, G.L. "Carbon-13 Nuclear Magnetic Resonance Spectroscopy"; Second Edition, Wiley-Interscience: New York, 1980.

[115] Neuhaus, D.; Williamson, M.P. "The Nuclear Overhauser Effect in Structural and Conformational Analysis"; VCH: New York, 1989.

[116] Lyerla, J.R., Jr.; Levy, G.C. "Carbon-13 Nuclear Spin Relaxation" In "Topics in Carbon-13 NMR Spectroscopy", Levy, G.C., Ed.; Wiley-Interscience: New York, 1974, Vol. 1, Chapter 3.

[117] Wright, D.A.; Axelson, D.E.; Levy, G.C. "Physical Chemical Applications of 13-C Spin Relaxation Measurements" In "Topics in Carbon-13 NMR Spectroscopy", Levy, G.C., Ed.; Wiley-Interscience, New York, 1979, Vol. 3, Chapter 2.

[118] Craik, D.J.; Levy, G.C. "Factors Affecting Accuracy in 13-C Spin-Lattice Relaxation Measurements" In "Topics in Carbon-13 NMR Spectroscopy", Levy, G.C.,

Ed.; Wiley-Interscience, New York, 1984, Vol. 4, Chapter 9.

[119] Fedarko, M.C. J. Mag. Reson. **1973**, 12, 30.

[120] a) Elbasyouny, A.; Brugge, H.J.; von Deuten, K.; Dickel, M.; Knochel, A.; Koch, K.U.; Kopf, J.; Melzer, D.; Rudolph, G. J. Am. Chem. Soc. **1983**, 105, 6568.

b) Grootenhuis, P.D.J.; van Eerden, J.; Dijkstra, P.J.; Harkema, S.; Reinhoudt, D.N. J. Am. Chem. Soc. **1987**, 109, 8044.

[121] Grandjean, J.; Laszlo, P.; Offerman, W.; Rinaldi, P.L. J. Am. Chem. Soc. **1981**, 103, 1380.

[122] Grace, D.S.; Krane, J.; J. Chem. Res., Synop. **1983**, 162.

[123] a) Fedarko, M.C. J. Mag. Reson. **1973**, 12, 30.
b) Live, D.; Chan, S.I. J. Am. Chem. Soc. **1976**, 98,3769.
c) Wehrli, F.W. J. Mag. Reson. **1977**, 25, 575.
d) Popov, A.I.; Smentana, A.J.; Kintzinger, J.P.; Nguyen, T.T.-T. Helv. Chim. Acta **1980**, 63, 668.
e) Bisnaire, M.; Detellier, C.; Nadon, D. Can. J. Chem. **1982**, 60, 3071.
f) Stover, H.D.H.; Maurice, L.J.; Delville, A.; Detellier, C. Polyhedron **1985**, 4, 1091.
g) Erk, C. Spectrosc. Lett. **1985**, 18, 723.
h) Eliasson, B.; Larsson, K.M.; Kowaleski, J. J. Phys. Chem. **1985**, 89, 258.
i) Stover, H.D.H.; Delville, A.; Detellier, C. J. Am. Chem. Soc. **1985**, 107, 4167.
j) Richter, H.; Zeidler, M.D. Mol. Phys. **1985**, 55, 49.
k) Erk. C. Appl. Spectrosc. **1986**, 40, 100.
l) Ozkan, E.; Erk, C. Spectrosc. Lett. **1986**, 19, 693.
m) Grooenhuis, P.D.; van Eerden, J.; Sudholter, J.R.; Reinhoudt, D.N.; Roos, A.; Harkema, S.; Feil, D. J. Am. Chem. Soc. **1987**, 109, 4792.

[124] Echegoyen, L.; Kaifer, A.; Durst, H.; Schultz, R.A.; Dishong, D.M.; Goli, D.M.; Gokel, G.W. J. Am. Chem. Soc. **1984**, 106, 5100.

[125] a) Kintzinger, J.-P.; Lehn, J.-M. J. Am. Chem. Soc. **1974**, 96, 3313.
b) Kintzinger, J.-P.; Kotzyba-Hilbert, F.; Lehn, J.-M.; Pagelot, A.; Saigo, K. J. Chem. Soc., Chem. Commun. **1981**, 833.
c) Schmidt, E.; Tremillon, J.M.; Kintzinger, J.-P.; Popov, A.I. J. Am. Chem. Soc. **1983**, 105, 7563.
d) Neurohr, K.J.; Drakenberg, T.; Forsen, S.; Lilja, H. J. Mag. Reson. **1983**, 51, 460.

e) Echegoyen, L.; Kaifer, A.; Durst, H.D.; Gokel, G.W. J. Org. Chem. **1984**, 49, 688.

[126] Kuhlmann, K.F.; Grant, D.M.; Harris, R.K. J. Chem. Phys. **1970**, 52, 3439.

[127] The relaxation rate can be defined as $(1/T_1)$.

[128] Ref. [114], p. 216.

[129] Ref. [112], p. 13

[130] "Sometimes t_c is defined as the average time required for a molecule to rotate through an angle of one radian." (See reference [112], p. 131.)

[131] Ref. [112], p. 247.

[132] Ref. [116]

[133] Ref. [116], p. 117.

[134] Kaifer, A; Durst, H.D.; Echegoyen, L.; Dishong, D.M.; Schultz, T.A.; Gokel, G.W., J. Org. Chem. **1982**, 47, 3195.

[135] Ref. [112], p. 257.

[136] Woessner, D.E. J. Chem. Phys. **1962**, 37, 647.

[137] Ref. [112], p. 259.

[138] Ref. [112], p. 254.

[139] Ref. [116], p. 116.

[140] Ref. [114], p. 238.

[141] Ref. [114], p. 229.

[142] Ref. [112], p. 260.

[143] Vold, R.L.; Waugh, J.S.; Klein, M.P.; and Phelps, D.E. J. Chem. Phys. **1968**, 48, 3831.

[144] Fully coupled (NOE) and gated decoupled (No NOE) ^{13}C NMR spectra obtained by K.S. Gallagher (UNH instramentation).

[145] From personal communication with G.R. Weisman: (See Appendix Section for a discussion the tentative chemical shift assignments C-1' and C-2' in 3 based on Grant Parameters.)

[146] Ref. [114], p. 221.

[147] It has been proposed that minor paramagnetic impurities (contained in the commercially prepared $NaBPh_4$) could be preferentially enhancing nuclear relaxation rates in the ligand. If this were the case lower than normal T_1's should be the result but in fact the opposite is observed.

[148] Ref. [114], p. 215.

[149] Ref. [112], p. 137.

[150] Ref. [33].

[151] Steinacker, K.H.; Stetter, H. Ber. 1952, 85, 451.

[152] Ref. [35].

[153] a) Pascarella, T.A. Masters Thesis, The University of New Hampshire, Durham N.H., 1986, p.50-60.
b) ibid., p.60.

[154] Shirodkar, S.M. Ph.D. Dissertation, The University of New Hampshire, Durham N.H., 1987, p.87.

[155] Dauben, W.G.; Lorber, M.; Fullerton, D.S. J. Org. Chem. 1969, 34, 3587.

[156] Tipson, R.S., J. Org. Chem. 1944, 9, 235.

[157] Sterling Drug Inc. Brit. Patent 869,083, 1961, Chem. Abstr. 1962, 56, 4684f.

[158] Tümmler, B.; Maass, G.; Voegtle, F.; Sieger, H.; Heimann, U.; Weber, E. J. Am. Chem. Soc. 1979, 101, 2588.

[159] Weisman, G.R., Proposal to the National Science Foundation, University of New Hampshire, personal communication.

[160] Ref. [26].

[161] The t_w wasincreased after obtaining the first T_1 values for uncomplexed ligand, so that t_w would be greater than five times the longest T_1 in the complex.

[162] a) High field spectra (91 MHz) run by K.S Gallagaher on a Bruker AM360 NMR spectrometer (Dept. Chem. Instrumentation, University of New Hampshire).
b) Personal communication with K.G. Gallagaher.

[163] From personal communication with G.R. Weisman.

[164] Grant, D.M. and Paul, E.G. J. Am. Chem. Soc. 1964, 86, 2984.

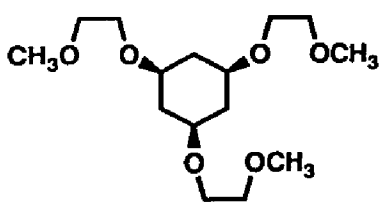

3

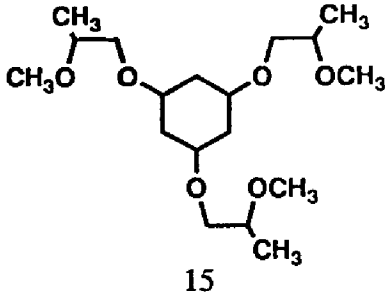

15

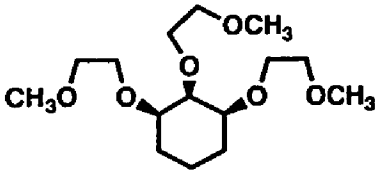

4

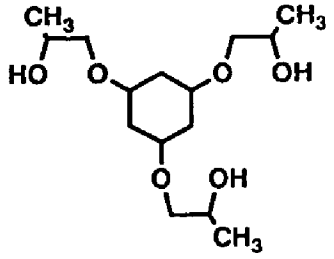

16

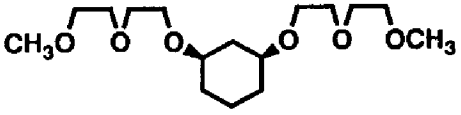

6

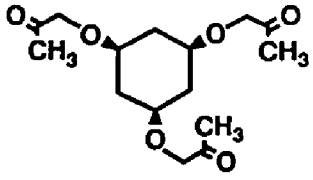

17

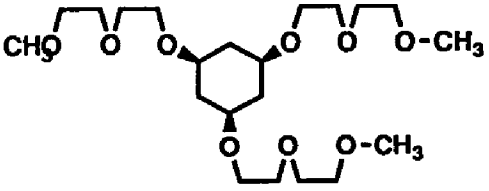

11

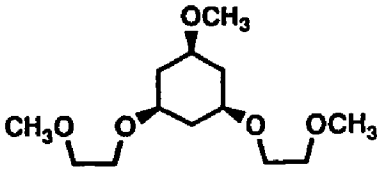

21

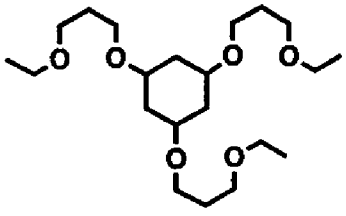

12

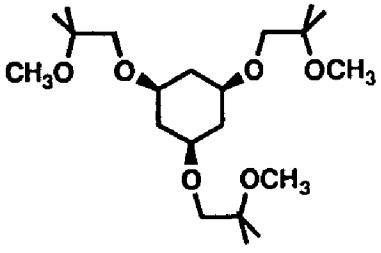

25

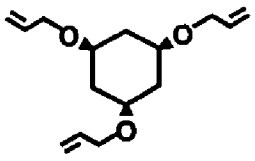

13

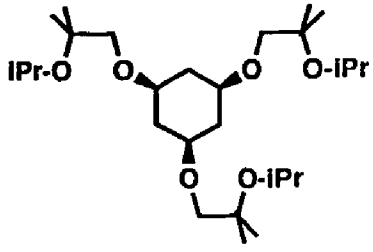

26